DEVELOPMENT AND OPTIMIZATION OF CONTROLLERS FOR MITIGATION OF SEISMIC VIBRATIONS

Ph.D. THESIS

by

GAURAV KUMAR

DEPARTMENT OF EARTHQUAKE ENGINEERING
INDIAN INSTITUTE OF TECHNOLOGY ROORKEE
ROORKEE - 247667 (INDIA)
SEPTEMBER, 2018

DEVELOPMENT AND OPTIMIZATION OF CONTROLLERS FOR MITIGATION OF SEISMIC VIBRATIONS

A THESIS

Submitted in partial fulfilment of the requirements for the award of the degree

of

DOCTOR OF PHILOSOPHY

in

EARTHQUAKE ENGINEERING

by

GAURAV KUMAR

DEPARTMENT OF EARTHQUAKE ENGINEERING
INDIAN INSTITUTE OF TECHNOLOGY ROORKEE
ROORKEE - 247667 (INDIA)
SEPTEMBER, 2018

TO BE USED IN FINAL SUBMISSION

INDIAN INSTITUTE OF TECHNOLOGY ROORKEE

CANDIDATE'S DECLARATION

I hereby certify that the work which is being presented in the thesis entitled **Development & Optimization of Controllers for Mitigation of Seismic Vibrations** in partial fulfillment of the requirements for the award of the Degree of Doctor of Philosophy and submitted in the Department/Centre of Earthquake engineering of the **Indian Institute of Technology Roorkee** is an authentic record of my own work carried out during a period from **03/01/2013** to **24/09/2018** under the supervision of **Prof. Ashok Kumar** & **Dr. Ravi S. Jakka**, Associate Professor.

The matter presented in the thesis has not been submitted by me for the award of any other degree of this or any other Institute.

Signature of the Candidate

This is to certify that the above statement made by the candidate is correct to the best of our knowledge.

Signature of Supervisor (s)

The Ph. D. Viva-Voce Examination of **Gaurav Kumar**, Research Scholar, has been held on **08/02/2019**.

Chairperson, SRC

8/2/19

Signature of External Examiner

This is to certify that the student has made all the corrections in the thesis.

Signature of Supervisor (s)
Dated: 08/02/19

8 Feb 2019

Head of the Department

ABSTRACT

Seismic vibrations induce additional stresses to the structures, which are harmful to their health. During the last three decades especially, since the introduction and unparalleled improvement of deployable computer systems, researchers and practicing engineers have studied the use of control technology to reduce the potential damage caused to these civil structures, particularly tall buildings by earthquakes. The motive of the structural control is to reduce the seismic vibration by supplying adequate counterforce by means of changing the stiffness, and/or altering the damping with the help of external active, passive or semi-active devices. In this study, semi active control scheme is considered due to its advantages over the other schemes. Semi active control schemes use lesser power and yet provide performance at par with the active control schemes and stability of passive control schemes.

Magnetorheological dampers (MR damper) are commonly used devices among the various available external semi active control devices. The MR damper can deliver a high level performance in the mitigation of seismic vibrations if an appropriately designed controller is utilized. Therefore, it is an interesting problem to design an efficient and effective controller which can take the advantage of MR damper while implementing the semi-active control scheme. In this thesis, new control algorithms are developed in this direction.

Proper selection of a controller dependent on the type of non-linearity present in the semi-active device, the available feedback measurements or the number of devices to be implemented in the structure. To gauge the difficulty level in the selection and development of appropriate controller, some previously used controllers are implemented initially. These controllers are the Passive ON/OFF, Double output feedback polynomial controller (DOFPC), the simple passive controller (SPC), the Lyapunov controller, the clipped-optimal LQR/LQG controller, Quasi bang bang controller, modified Quasi bang bang controller and the classic PID controller. These controllers are formulated for use with MR damper and evaluated for the best performance for a prototype three storey structure. It is observed that the controllers like Passive ON/OFF, Lyapunov, QBB, MQBB, SPC and DoFPC do not consider the feedback from the MR damper. These controllers continuously provide input command signal (electrical signal), based on the structural response, to the MR damper without considering its maximum capability whereas the controllers like clipped optimal LQR/LQG take the feedback from the MR damper and compare it with the desired force calculated by the control algorithm. Based on this comparison, the input signal is provided to the MR damper. Thus, clipped optimal LQR/LQG (CO-LQR/LQG)

controllers have better control over the actuator`s (MR damper) input and therefore it is further studied in this work.

In theory optimal controllers like LQR/LQG have a cost function which is to be minimized for the best performance. This cost function has constant weighting matrices namely state weighting matrix **Q** and control weighting matrix **R**. Control weighting matrix **R** indicates the force to be imparted to the structure. In conventional LQR/LQG theory, it is customary to note that the values of these design parameters are decided at the time of designing the controller and cannot be subsequently altered. During an earthquake event, the response of the structure may increase or decrease, depending the quasi-resonance occurring between the structure and the earthquake. In this case, it is essential to modify the value of the design parameters of the conventional LQR/LQG controller to obtain optimum control force to mitigate the vibrations due to the earthquake. A few studies have been done to sort out this issue but in all these studies it was necessary to maintain a database of the earthquake. To solve this problem and to find the optimized design parameters of the LQR/LQG controllers in real time two approaches namely PSO-FFT and PSO-τ_p^{max} are proposed to modify the control weighting matrix **R** for better control action at the quasi resonance. In PSO-FFT based approach, fast Fourier transform (FFT) is utilized to find the quasi resonance where the amplitude of the vibrations will be the maximum and the particle swarm optimization (PSO) is utilized to find the best value of control weighting matrix **R** to counter the effect of this quasi resonance. Two new controllers are developed based on PSO-FFT approach namely PSO-FFT-modified-LQR and PSO-FFT-modified-LQG.

Similarly, in PSO- τ_p^{max} based approach, the maximum dominant period (τ_p^{max}) approach is used to find the quasi resonance and PSO is utilized to find the best value of control weighting matrix **R** to counter the effect of this quasi resonance. Unlike in PSO-FFT approach where dominant frequency is estimated in frequency domain, PSO- τ_p^{max} approach works totally in time domain and is faster. The controllers developed based on the PSO-τ_p^{max} approach are PSO- τ_p^{max} -modified-LQR and PSO- τ_p^{max} -modified-LQG. These controllers are evaluated on a three storey prototype structure for various conditions. For a robust evaluation of the proposed controllers, many conditions are considered. A detailed study is carried out for each condition. These studies are discussed below.

To assess the performance of the developed controllers in the different seismic environment, the prototype structure is subjected to several recorded earthquake time histories. The analysis is carried out for the modified LQR/LQG controllers developed for both PSO-FFT and PSO- τ_p^{max} approaches. The responses of the structure are analyzed and compared with the

conventional clipped optimal LQR/LQG. Further, to make the evaluation consistent, the same conditions are considered as in [1]. The author established the supremacy of CO-LQR controller over the other controllers used in their research. Following the same methodology, the result analysis of current study demonstrates that the performance of the proposed modified LQR controller is superior than the CO-LQR controller. Similarly, proposed modified LQG controller performs better than the conventional CO-LQG controller.

To find the best location for the placement of MR damper within the structure if only one MR damper is available. The performance analysis of the proposed controllers is carried out keeping the MR damper at first, second and the third floor respectively. Further, an analytical study is presented for the assessment of the performance of the developed controllers if power vanishes at the peak of the seismic event. It is very likely to happen amid the seismic activity. To assess the performance of the developed controller for the structures in different soil conditions, a study is also carried out by subjecting the prototype structure to an earthquake recorded in different soil conditions (i.e. hard, medium and soft soil). Further, to check the suitability of the proposed controllers for higher modes, a similar analysis is carried out for a five-storey structure as carried out for the three storey structure.

Based on the analysis carried out in this thesis work, it is shown that the developed controllers based on the proposed two approaches (PSO-FFT and PSO-τ_p^{max}) deliver better performance for three storey as well as five storey structure as compared to conventional CO-LQR/LQG controllers.

Apart from these studies, a separate study has been carried out to develop PSO-modified quasi-bang bang controller to improve the performance of the modified quasi bang-bang controller which give command signal to actuator directly without considering the feedback from the MR damper. This controller is evaluated for the three DOF test structure subjected to several near-fault earthquake excitations and earthquake recorded in different soil conditions. It is shown that the PSO-modified quasi bang bnag controller performs better that the modified quasi bang bang controller. Moreover, a prototype hardware is also developed for this controller using ESP series microcontroller and three ADXL-435 accelerometers. For ease of the analysis a GUI is also developed using MATLAB.

ACKNOWLEDGEMENT

I would like to express my thanks of gratitude to my supervisors Prof. Ashok Kumar and Dr. Ravi. S. Jakka Associate Professor, Dept. of Earthquake Engineering, who gave me the golden opportunity to do the PhD thesis on the topic "DEVELOPMENT AND OPTIMIZATION OF CONTROLLERS FOR MITIGATION OF SEISMIC VIBRATIONS". I am thankful to them for their advice, encouragement, and support throughout my time at the Indian Institute of Technology. The experience and insight I gained in IIT, would be one of the most valuable assets for the rest of my life.

I sincerely appreciate the efforts of my committee members, Prof. Yogendra Singh (H.O.D, Dept. of earthquake engineering) Prof. S.P Singh, (Dept. of Electrical Engineering). Their comments and suggestions have enriched my dissertation while keeping it grounded and accessible to a wider audience. I owe a very special thanks to the Dr. Yogesh V. Hote Associate Professor, Dept. of Electrical engineering, for his valuable suggestions and constant encouragement to pursue my research work. I would also thankful to Professor Kulbir Singh and Dr. Sanjay Kumar, Associate Professor, Dept. of ECE, TU Patiala, Punjab, India for their best wishes.

I would like to thank my friends Dr. Roshan Kumar (Zhejiang University, mainland China), Dr. Upendra Kumar, Dr. Vikash Singh (Yokohama National University, Japan) and Mr. Rahul Ranjan (Sr. Engineer, John Deere, India), Mr. Manpreet Singh (Sr. engineer, R&D division, Saraswati Dynamics, Roorkee, India) for their untiring support and encouragement during this work. I have had the pleasure of interacting with all the Shake Table Laboratory (STL) members. I would like to appreciate their support and friendship throughout my research at the IIT Roorkee. I had a great time to study and work with them.

Especially, I would like to thank my colleagues, Dr. Rajeev Sachdeva, Dr. Dheeraj Raj and Mr. Govind (Research scholar) their advice and support during my research. This research is made possible through the MHRD Fellowship for research provided by the Ministry of Human Resource and Development (MHRD), Govt. of India. I am extremely grateful and honored to receive this funding.

It is beyond my literary capability to thanks my family for their ever-increasing love, support and instilling in me the importance of hard work, persistence.

Finally, I am thankful to almighty GOD for everything.

(GAURAV KUMAR)

CONTENTS

ABSTARCT…….. V

ACKNOWLEDGEMENTS…… VIII

CONTENTS…… IX

LIST OF FIGURES…… XIII

LIST OF TABLES…… XVII

LIST OF ACRONYMS AND SYMBOLS …… XVII

CHAPTER 1: INTRODUCTION…… **1-4**

1.1 Preamble…… 1

1.2 The objectives of the research work……... 3

1.3 Chapter organization in the thesis……... 3

1.4 Flow chart of the research work…… 4

CHAPTER 2: LITERATURE SURVEY…… **5-22**

2.1 Introduction…… 5

2.2 The control of the structures……... 5

2.3 Passive control scheme……... 6

2.4 Active control scheme…… 7

2.5 Semi-active control scheme…… 8

2.6 Review on control algorithms……. 9

2.6.1 Passive ON/OFF controllers…… 10

2.6.2 Quasi-bang-bang controller……. 10

2.6.3 The proportional-integral-derivative ……. 10

2.6.4 H∞ Controller……. 11

2.6.5 Sliding Mode Controller……. 14

2.6.6 Neural Network Controller... ……..... 16

2.6.7 Fuzzy Logic Controller ……..... 17

2.6.8 LQR/LQG controller……... 18

CHAPTER 3: FUNDAMENTALS OF SEMI ACTIVE CONTROL THEORY 23-42

3.1 Introduction……. 23

3.2 Semi-active control scheme…… 23

3.3 Mathematical modeling of the prototype structure……. 24

3.4 Semi-active control devices and magnetorheological material…… 26

3.4.1 Magneto rheological damper (MR damper)……. 27

3.4.2 Mathematical modelling of the MR damper…… 28

3.5 Theoretical & mathematical background of some previously used controllers…… 31

3.5.1 Passive ON/OFF……. 32

3.5.2 PID controller…….. 32

3.5.3 Lyapunov stability theory-based controller…….. 33

3.5.4 Quasi-bang-bang controller…….. 34

3.5.5 Modified quasi-bang- bang controller…….. 35

3.5.6 Simple passive controller (SPC) 35

3.5.7 Decentralized output feedback polynomial control (DOFPC)……. 36

3.5.8 Clipped optimal LQG/LQR controller……. 37

3.6 Comparative analysis……... 37

Summary……. 42

CHAPTER 4: DEVELOPMENT OF MODIFIED LQR/LQG CONTROLLERS USING PSO-FFT and PSO- τ_p^{max} APPROACH……. 43-108

4.1 Introduction……. 43

4.2 Development of modified LQR/LQG controllers using PSO-FFT approach……. 44

4.2.1 Development of modified LQR controller using PSO-FFT approach……. 44

4.2.2 The particle swarm optimization……. 46

4.2.3 Results and discussion on the performance of PSO-FFT-modified-LQR controller…… 48

(i) Using different earthquake time histories……. 48

(ii) Using an earthquake recorded in different soil conditions ... 54

(iii) Effect of placing MR damper at different floors……... 58

(iv) Effect of the power cut off at the peak of the earthquake…. 62

4.2.4 Development of modified LQG controller using PSO-FFT approach……... 64

4.2.5 Results and discussion on the performance of PSO-FFT-modified-LQG controller……. 65

(i) Using different earthquake time histories……. 65

(ii) Using an earthquake recorded in different soil conditions… 69

4.3 Development of modified LQR/LQG controller using PSO- τ_p^{max} approach……. 74

4.3.1 Development of modified LQR controller using PSO- τ_p^{max} approach……. 74

4.3.2 Results and discussion based on the performance of the PSO-τ_p^{max}-modified-LQR…… 76

(i) Using different earthquake time histories……. 76

(ii) Using an earthquake recorded in different soil conditions… 80

4.3.3 Results and discussion on the performance of PSO- τ_p^{max}-modified-LQG controller……. 84

(i) Using different earthquake time histories……. 84

(ii) Using an earthquake recorded in different soil conditions… 88

4.4 Applicability of the proposed algorithms on a five-storey structure ……. 92

4.4.1 Performance analysis of PSO-FFT-modified-LQR …… 93

4.4.2 Performance analysis of PSO-FFT-modified-LQG …… 97

4.4.3 Performance analysis of PSO- τ_p^{max}-modified-LQR ……... 101

4.4.4 Performance analysis of PSO- τ_p^{max}-modified-LQG…… 105

Summary……. 108

CHAPTER 5: DEVELOPMENT OF ADAPTIVE QUASI BANG BANG CONTROLLER USING PSO…… 109-123

5.1 Introduction……. 109

5.2 Evolution of the controller……..... 109

5.2.1 Quasi bang-bang controller……. 109

5.2.2 Modified quasi bang-bang controller……. 110

5.3 Formulation of adaptive quasi bang-bang controller using PSO……. 110

5.5 Result analysis and discussion……. 112

5.6 Development of a prototype hardware and graphic user interface (GUI). 120

5.6.1 The development of the hardware…… 120

5.6.2 Development of graphic user interface (GUI)……. 122

Summary…… 123

CHAPTER6: SUMMARY AND CONCLUSIONS……. 124-128

6.1 Summary & conclusions …… 124

6.2 Limitation of this research work and future studies …… 128

BIBLIOGRAPHY……. 139-142

PUBLICATIONS FROM THE WORK……. 143

LIST OF FIGURES

Figure 1.1	Flowchart of the research work	4
Figure 3.1	Block diagram of semi-active control scheme	23
Figure 3.2	The three story prototype structure	25
Figure 3.3	(a) Small-scale MR damper (b) Cross-section	27
Figure 3.4	(a) Simple Bouc-wen model (b) Modified Bouc-wen model of the MR damper	29
Figure 3.5	(a) Force generated in MR Damper at different input voltages due to a sine wave having amplitude 1.5cm and frequency 2.5Hz (b) Force-displacement diagram (c) Force-velocity diagram	31
Figure 3.6	Response of the prototype structure subjected to El-Centro earthquake for different controllers (a) Relative displacement (b) Interstorey drift (c) Absolute acceleration	39
Figure 3.7	Response of the prototype structure subjected to Chile earthquake for different controllers (a) Relative displacement (b) Interstorey drift (c) Absolute acceleration	40
Figure 3.8	Response of the prototype structure subjected to Uttarkashi earthquake for different controllers (a) Relative displacement (b) Interstorey drift (c) Absolute acceleration	41
Figure 3.9	Comparison of the uncontrolled and controlled displacement response time history of the third floor of the structure subjected to El-Centro earthquake for (a) Passive ON/OFF (b) PID (c) CO- LQR (d) CO-LQG (e) Lyapunov (f) Quasi bang-bang and Modified quasi bang-bang (g) SPC (h) DOFPC	42
Figure 4.1	Development of modified LQR controller using FFT-PSO approach	45
Figure 4.2	Flowchart representation of PSO algorithm	47
Figure 4.3	N–S component of time histories (a) 1940 earthquake at El-Centro site USA (b) 1999 Chi-Chi Nantou County Taiwan earthquake (c) 1999 Gebze Turkey earthquake.	49
Figure 4.4	Structural responses for the structure subjected to the 1940 El-Centro earthquake using PSO-FFT-modified-LQR	50
Figure 4.5	Structural responses for the structure subjected to 1999 Chi-Chi earthquake using PSO-FFT-modified-LQR	53
Figure 4.6	Structural responses for the structure subjected to 1999 Gebze earthquake using PSO-FFT-modified-LQR	53
Figure 4.7	Structural responses for the structure subjected to hard soil earthquake using PSO-FFT-modified-LQR	54
Figure 4.8	Structural responses for the structure subjected to medium soil earthquake using PSO-FFT-modified-LQR	56
Figure 4.9	Structural responses for the structure subjected to soft soil earthquake using PSO-FFT-modified-LQR	57

Figure 4.10	Percentage reductions in the structural responses using PSO-FFT-modified-LQR in the structure subjected to El-Centro earthquake by placing MR damper at different floors	59
Figure 4.11	Percentage reductions in the structural responses using PSO-FFT-modified-LQR in the structure subjected to Chi-Chi earthquake by placing MR damper at different floors	60
Figure 4.12	Percentage reductions in the structural responses using PSO-FFT-modified-LQR in the structure subjected to Gebze earthquake by placing MR damper at different floors	61
Figure 4.13	Performance analysis of PSO-FFT-modified-LQR for El-Centro time history, considering a situation if power vanishes during the peak (at 2 sec) of the earthquake	63
Figure 4.14	The Block diagram of LQG controller	65
Figure 4.15	Structural responses for the structure subjected to the 1940 El-Centro earthquake using PSO-FFT-modified-LQG	66
Figure 4.16	Structural responses for the structure subjected to 1999 Chi-Chi earthquake using PSO-FFT-modified-LQG	68
Figure 4.17	Structural responses for the structure subjected to 1999 Gebze earthquake using PSO-FFT-modified-LQG	68
Figure 4.18	Structural responses for the structure subjected to hard soil earthquake using PSO-FFT-modified-LQG	70
Figure 4.19	Structural responses for the structure subjected to medium soil earthquake using PSO-FFT-modified-LQG	72
Figure 4.20	Structural responses for the structure subjected to soft soil earthquake using PSO-FFT-modified-LQG	72
Figure 4.21	Flow chart of the development of adaptive LQR controller using PSO-τ_p^{max}approach	75
Figure 4.22	Structural responses for the structure subjected to the 1940 El-Centro earthquake using PSO-τ_p^{max}-modified-LQR	77
Figure 4.23	Structural responses for the structure subjected to 1999 Chi-Chi earthquake using PSO-τ_p^{max}-modified-LQR	79
Figure 4.24	Structural responses for the structure subjected to 1999 Gebze earthquake using PSO-τ_p^{max}-modified-LQR	79
Figure 4.25	Structural responses for the structure subjected to hard soil earthquake using PSO-τ_p^{max}-modified-LQR	80
Figure 4.26	Structural responses for the structure subjected to medium soil earthquake using PSO-τ_p^{max}-modified-LQR	82
Figure 4.27	Structural responses for the structure subjected to soft soil earthquake using PSO-τ_p^{max}-modified-LQR	83
Figure 4.28	Structural responses for the structure subjected to the 1940 El-Centro earthquake using PSO-τ_p^{max}-modified-LQG	85
Figure 4.29	Structural responses for the structure subjected to 1999 Chi-Chi earthquake using PSO-τ_p^{max}-modified-LQG	87
Figure 4.30	Structural responses for the structure subjected to 1999 Gebze earthquake using PSO-τ_p^{max}-modified-LQG	87
Figure 4.31	Structural responses for the structure subjected to hard soil earthquake using PSO-τ_p^{max}-modified-LQG	88
Figure 4.32	Structural responses for the structure subjected to medium soil earthquake using PSO-τ_p^{max}-modified-LQG	90

Figure 4.33	Structural responses for the structure subjected to soft soil earthquake using PSO- τ_p^{max}-modified-LQG	91
Figure 4.34	Structural responses for five structure subjected to the 1940 El-Centro earthquake using PSO-FFT-modified-LQR	94
Figure 4.35	Comparison of the percentage reduction in peak values of fifth floor of the structure due to CO-LQR and proposed controller for El-Centro earthquake	95
Figure 4.36	Structural responses for five structure subjected to the 1999 Chi-Chi earthquake using PSO-FFT-modified-LQR	96
Figure 4.37	Comparison of the percentage reduction in peak values of fifth floor of the structure due to CO-LQR and proposed controller for 1999 Chi-Chi earthquake	96
Figure 4.38	Structural responses for five structure subjected to the 1940 El-Centro earthquake using PSO-FFT-modified-LQG	97
Figure 4.39	Comparison of the percentage reduction in peak values of fifth floor of the structure due to CO-LQG and proposed controller for El-Centro earthquake	98
Figure 4.40	Structural responses for five structure subjected to the 1999 Chi-Chi earthquake using PSO-FFT-modified-LQG	100
Figure 4.41	Comparison of the percentage reduction in peak values of fifth floor of the structure due to CO-LQG and proposed controller for 1999 Chi-Chi earthquake	100
Figure 4.42	Structural responses for five structure subjected to the 1940 El-Centro earthquake using PSO-τ_p^{max}-modified-LQR	102
Figure 4.43	Comparison of the percentage reduction in peak values of fifth floor of the structure due to CO-LQR and proposed controller for El-Centro earthquake	102
Figure 4.44	Structural responses for five structure subjected to the 1999 Chi-Chi earthquake using PSO-τ_p^{max}-modified-LQR	103
Figure 4.45	Comparison of the percentage reduction in peak values of fifth floor of the structure due to CO-LQR and proposed controller for 1999 Chi-Chi earthquake	104
Figure 4.46	Structural responses for five structure subjected to the 1940 El-Centro earthquake using PSO-τ_p^{max}-modified-LQG	106
Figure 4.47	Comparison of the percentage reduction in peak values of fifth floor of the structure due to CO-LQG and proposed controller for El-Centro earthquake	106
Figure 4.48	Structural responses for five structure subjected to the 1999 Chi-Chi earthquake using PSO-τ_p^{max}-modified-LQG	107
Figure 4.49	Comparison of the percentage reduction in peak values of fifth floor of the structure due to CO-LQG and proposed controller for 1999 Chi-Chi earthquake	107
Figure 5.1	Response of the third floor of the structure subjected to El-Centro and Hachinohe earthquake time-history	113
Figure 5.2	Comparison of displacement response and Force of the third floor of the structure subjected to an earthquake recorded in (a) hard soil (b) medium soil (c) soft soil.	116
Figure 5.3	Force-displacement curve	117
Figure 5.4	Electrical (voltage) signal given to the MR damper by the different controllers when structure subjected to (i) El-Centro-earthquake (ii) Hachinohe Earthquake and earthquake recorded in different soils	118

Figure 5.5	Power and response spectra for different controllers for the structure subjected to El-Centro earthquake	119
Figure 5.6	Prototype hardware for the proposed controllers	120
Figure 5.7	Calibration of the prototype hardware using 10 Hz sine wave	121
Figure 5.8	Graphic user interface with the (a) List of controllers and uncontrolled structure(b) List of controllers uncontrolled and controlled structure	122

LIST OF TABLES

Table 2.1	Classification of the structural control	6
Table 2.2	Summary of the controllers	21
Table 3.1	Parameters of the generalized MR damper	30
Table 4.1	Peak responses of structure using PSO-FFT-modified-LQR and CO-LQR controller for various earthquake time histories.	51
Table 4.2	Classification of the soil based on shear wave velocity (v_s)	54
Table 4.3	Peak responses of structure using PSO-FFT-modified-LQR and CO-LQR controller for earthquake recorded in different soil conditions.	55
Table 4.4	Peak responses of structure using PSO-FFT-modified-LQG and CO-LQG controller for various earthquake time histories.	67
Table 4.5	Peak responses of structure using PSO-FFT-modified-LQG and CO-LQG controller for earthquake recorded in different soil conditions.	71
Table 4.6	Peak responses of structure using PSO- τ_p^{max}-modified-LQR and CO-LQR controller for various earthquake time histories.	78
Table 4.7	Peak responses of structure using CO-LQR controller and PSO- τ_p^{max}-modified-LQR controller subjected to earthquake recorded in different soil conditions	81
Table 4.8	Percentage change in peak responses of structure due to conventional CO-LQG controller and PSO-τ_p^{max}-modified LQG controller	86
Table 4.9	Peak responses due to CO-LQG and PSO-FFT-modified LQG for structure the subjected to earthquake recorded in different soil conditions	89
Table 5.1	Parameters used in PSO algorithm	112
Table 5.2	Peak values of the responses of the structure subjected to different earthquakes	115

LIST OF ACRONYMS AND SYMBOLS

AMD	Active mass damper
AWGN	Additive white Gaussian noise
DWT	Discrete Wavelet Transform
EPD	Elastoplastic damper
FLC	Fuzzy logic controller
FFT	Fast Fourier Transform
GA	Genetic algorithm
LQR	Linear quadratic regulator
LQG	Linear quadratic Gaussian
LVDT	Linear variable differential transformer
NN	Neural network
MR	Magnetorheological
MQBB	Modified quasi bang bang
PSO	Particle swarm optimization
QBB	Quasi bang bang
SMC	Sliding mode controller
STFT	Short time Fourier transform
TLD	Tuned liquid damper
VD	Viscous damper

LIST OF SYMBOLS

A, B, C, D	State space parameter of the structure
β, γ, n and A	Hysteresis parameter for the MR damper
C_a	Damping matrix

K_a	Stiffness matrix
M_a	Mass matrix
Vs	Pseudo wave velocity
Vmax	Maximum voltage
Vmin	Minimum voltage
Q	State weighting matrix
R	Control weighing matrix
τ_p^{max}	Maximum dominant period

1.1 Preamble

Structural response to seismic shaking has been a major area of research for the scientists across the globe. In the last two decades, several deadly earthquakes occurred having magnitude between 5.0 to 9.1. These resulted in the irreparable loss of thousands of people lives and great monetary loss to the world. On April 25, 2015, an earthquake hit Nepal's eastern district Lamjung having magnitude 7.8, killed around 9,000 people and obliterated old landmarks, including UNESCO legacy site Basantapur Durbar Square in Kathmandu. The catastrophe likewise set off a torrential slide on Mount Everest and the Langtang valley.

Similarly, on May 12, 2008, an earthquake of 7.8 magnitude in Sichuan province of China, was responsible for the death of about 87,600 people. These earthquakes occurred in the regions where the infrastructures have no to very little earthquake resistive measures. On the contrary, 7.1 magnitude Loma Prieta earthquake on October 17, 1989, caused only 62 casualties despite the high population density of the San Francisco Bay area because the infrastructures there had better earthquake resistive measures. These and several other appalling consequences of the strong earthquakes have compelled the practising engineers and the researchers to find some viable solutions to make the infrastructures safer. One of the possible solutions is structural vibration control. The structural control may be helpful in saving millions of lives and reducing the damage to the strategic infrastructures.

The notion of seismic vibration control of the structures was given by Yao in 1972, since then this field has emerged by leaps and bounds [2]. The vibrations in the structure can be kept in control by altering its stiffness, providing extra damping and applying appropriate counterforce, however, its dynamic material properties ought to remain unaltered [2]. Further, the structural control can be broadly classified in the three categories i.e. Passive, active and semi active. The passive control scheme is the simplest and incorporates some good features like it does not require any external power to operate, easy to implement and it does not alter the stability of the structure. But, being non-adaptive to the changes in the external excitation and its poor performance at low-frequency vibrations forced the researchers to look for other alternatives. The other alternative was the active control scheme. The active control scheme was adaptive to the external changes and delivers excellent performance for a range of vibration frequencies, but it relies on the large power source to operate which is difficult to ensure during seismic activity.

Additionally, the active control scheme may destabilize structure. Therefore, the semi active control scheme was proposed which incorporates the good features of the passive control scheme and the active control scheme. It requires very less power to operate (a few watts) and shows performance at par with the active control scheme. Moreover, it also does not subvert the stability of the structure because the energy of the vibration will only be engrossed without imparting any additional energy to the structure. Thus, the semi active control methodology is an intelligent choice for structural vibration control.

Though there are several devices those could be employed as an actuator in the semi active control scheme, none is as successful as a magnetorheological damper (MR damper) in semi active control scheme owing to its rheological properties [3]–[5]. The MR dampers absorb energy which is being produced due to vibrations in the structure by responding to its motion. Further, the experiments conducted by the researchers on a scaled three-story prototype structure having MR damper fixed at the ground floor demonstrated that the effectiveness of the semi active control scheme very much relies on the control algorithm (controller) used. Hence, with the rapid advancement in the robust control theory, the direction of the current research is focused to find out the better control algorithms to enhance the performance of the semi active control scheme. The commonly used controllers for the semi active control scheme are Liner Quadratic Regulator (LQR) controller, Sliding Mode Controller (SMC), Linear Quadratic Gaussian (LQG)/H2 controller, Quasi bang-bang controller, Simple Passive Control (SPC) and many more [6]–[9]. Moreover, the phenomenal growth of the signal processing techniques and the advent of the highly efficient digital signal processors facilitates the deployment of the complete control system on a single silicon chip. This helped to reduce the risk of possible damage to the installations due to any seismic activity.

This research work is focused on the development of modified LQR/LQG control algorithm for the semi active control scheme to attain better performance in reducing the relative displacement, inter-story drift and the absolute acceleration in real time. In these modified LQR/LQG algorithms the quasi resonance between the earthquake and the structure where the magnitude of the vibration will be larger have been determined using fast Fourier transform (FFT) and maximum dominant time (τ_p^{max}) approaches. In quasi resonance situations, a larger force would be required to counter these large magnitude vibrations. Therefore, suitable modifications have been made in the LQR/LQG controller to enable them to respond appropriately in quasi resonance situations.

1.2 The objectives of the research work

The development of new adaptive LQR/LQG controllers using FFT and τ_p^{max} approach for attaining the increased performance of the semi active control scheme is the main objective of this research work. Additionally, the development of the optimized quasi bang-bang controller using particle swarm optimization (PSO) is also carried out. Various other subtasks carried out in the research work are enumerated as follows:

1. A comparative study of some prevalent control algorithms used for the semi active control scheme is carried out.
2. Comprehensive performance analysis of the proposed controllers is carried out by comparing of the structural responses (i.e. relative displacement, interstorey drift and the absolute acceleration) achieved by them and the corresponding conventional controllers under following listed conditions.
    i. Using different earthquake time histories.
    ii. Using time histories recorded in different soil conditions.
    iii. Putting the MR damper on different floors.
    iv. Considering a situation, if power is lost at the peak of the earthquake
3. An assessment of the suitability of the adaptive LQR/LQG controllers by applying them to a prototype five-story structure.
4. A small workable prototype microcontroller-sensor assembly hardware

1.3 Chapter organization in the thesis

This thesis report focuses on the development of the controller for a semi active control strategy for reducing the structural response and to show that the newly developed modified LQR/LQG controllers are better than their conventional counterpart for semi active control strategy. The organization of the thesis is as follows: -

Chapter 1 introduces the semi active control scheme and the objectives of the research work.

Chapter 2 presents a detailed literature survey of the preceding research pertaining to this dissertation is presented.

Chapter 3 develops the necessary technical background for this thesis. The mathematical modelling of the MR damper along with the prototype three-story structure used in this

dissertation is discussed. Further, a comparative parametric study is also presented to lay the foundation of this research work

Chapter 4 explains the development of the new modified control algorithms based on FFT/ τ_p^{max} approach and particle swarm optimization (PSO) for the semi active control scheme. Subsequently, the performance of the proposed controllers is numerically assessed on the three-story prototype model under various conditions. Besides this, the suitability of the proposed controllers is numerically tested on the prototype five story structure.

Chapter 5 explains the development of optimized modified quasi bang bang controller with use of the PSO algorithm to make the modified quasi bang-bang controller more efficient. Moreover, the development of prototype hardware for this controller is presented.

Chapter 6 Summarizes the research presented in this dissertation. The limitations of the research work and the scope for future studies are discussed.

1.4 Flow chart of the research work

The approach to accomplish this research work is briefly described in a flowchart shown in Figure 1.1.

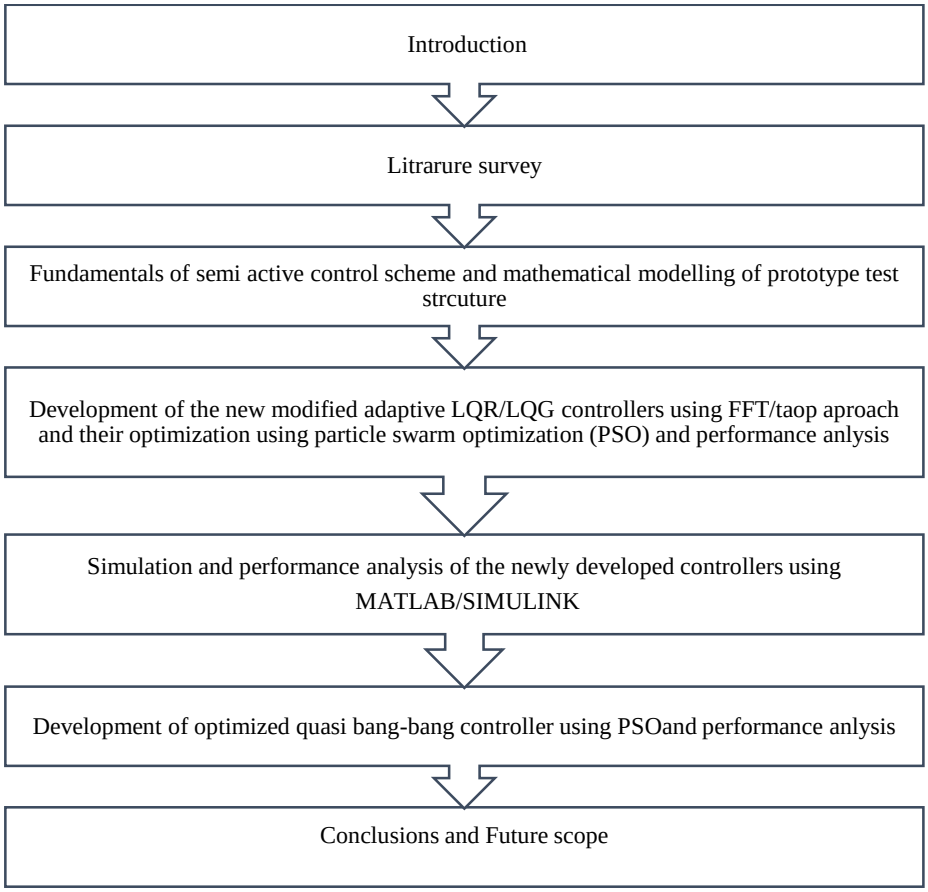

Figure 1.1 Flowchart of the research work

2.1 Introduction

This chapter provides a review of the different control algorithms used in the structural control. Many crucial issues arise while designing the controller for a semi active control scheme for structural control [10]. Some of these are dependent on the modelling of the structure, performance in the uncertain and noisy environment, stability, feedback planning (centralized/decentralized) and non-linearities present in the structure. The organization of the review is very complicated in the field of structural control because these issues can combine differently for different control problems

An attempt is made to present a review of the control methods used in semi active and active structural control. First, a review of passive and active control scheme is presented briefly. Second, a detailed review of the semi active control scheme with a focus on the control algorithms is presented. A summary of the control algorithm is also presented in Table 2.2.

2.2 The control of the structures

The seismic vibrations put unnecessary stress on the structure and are considered as harmful for their health. Therefore, the need for the technical remedies for the vibrations arises. One of the most adopted technical solutions is the control of the structure. Since 1972, it has been a very lucrative research area for the researchers and the engineers worldwide. The motive of the structural control is to reduce the seismic vibration by supplying adequate counterforce, by varying the stiffness, and/or by altering the damping with the help of external devices i.e. passive, active and semi active devices. The brief description of these external devices is presented in Table 2.1.

Housner *et al*. [2] presented a comprehensive review of the control of the structure. The authors investigated the possibilities of the application of control theory in the mitigation of the seismic vibrations. This landmark work proved a boon for those who wanted to apply the multidisciplinary approach to the structural control. They also explored the many actuating devices and sensors needed for feedback purposes. The traditional approaches for seismic vibration mitigation are, to plan structures with adequate strength, having the ability to deform in a yielding manner and to use smart materials in the construction. Though, these approaches are successful but are not up to the expectations in the seismic environment. As an alternative, some contemporary approaches have been proposed in the last two decades of the nineteenth

century. These approaches can be classified as passive, active, hybrid and semi active for structural control. The acceptance of these approaches is growing day by day. A general classification of the structural control schemes based on their characteristics and example devices is presented in Table 2.1.

Table 2.1 Classification of the structural control

S. No.	Classification	Characteristics	Example devices
1.	Passive control	Requires no additional energy	Tuned mass damper (TMD), TLCD, friction dampers, VEDs, VFDs.
2.	Active control	Uses external energy to apply to restore force	Active mass damper (AMD), active tendons.
3.	Hybrid control	Consists of continuous and discrete systems	Hybrid mass damper (HMD).
4.	Semi active control	i. It requires very less power to operate. ii. Can only produce dissipative forces.	Semi active TMD, stiffness control devices, Magneto rheological dampers (MR dampers), Electro rheological dampers (ER dampers).

The control of the structures has been widely explored by the researchers and in present work, three main categories (i.e. passive, active and semi active) are discussed. [11].

2.3 Passive control scheme

Passive control scheme uses the external damping devices which are sensitive to the movement of the structure. These external damping devices are known as supplemental devices and generate counterforce utilizing the motion of the structure itself. Thus, the passive control scheme may be defined by the process that dissipates the external energy caused by a seismic event without an external power source. The passive control mechanism is reviewed comprehensively by [12]. The supplemental devices used in passive control mechanisms are such as elastoplastic dampers (EPDs), tuned liquid dampers (TLDs), tuned mass damper (TMD) and viscous dampers (VD) [13]. The working of these supplemental devices is dependent on their construction. These devices boost the stiffness and the quality of the structure to which these are joined. Base isolation is another popular technique that also falls into the passive control

category. Some researchers have presented some state of the art survey on the base isolation [14]–[18].

The passive control strategy, including base isolation systems, is very well acknowledged and widely employed as an effective tool to mitigate the seismic vibrations. However, these methods are unable to acclimatize to the alterations in the structure during the seismic event. The performance of passive control scheme has been found to be poor at low frequencies whereas the effectiveness of base isolation is limited to a narrow bandwidth. Also, the performance of passive control poor for the near-fault earthquakes [19].

2.4 Active control scheme

On the contrary, the active control scheme is adaptive and provides highly improved performance over the passive control scheme [20]–[24]. As a matter of fact, the active control scheme needs a larger external power source to drive the actuators to produce the control force required for the reduction of the seismic vibrations. The active control scheme is characterised as a multidisciplinary approach which utilizes the modern control theory [25] and the response of the structure measured through the appropriately placed sensors as feedback to improve upon the passive control scheme [26]–[33].

The adaptive control forces are generated by the special designed active control actuators using the feedback from the sensors. These actuators may be electro-hydraulic or electro-mechanical in their construction. Sometimes feedforward data from the external loading may also be used in addition to the feedback from the sensors to generate the more appropriate control force from the actuators for mitigation of the vibrations. The feedback and/or the feedforward information is continuously monitored by a controller. The controller based on its control algorithm determines the necessary control input to the actuator in the form of an electrical signal to produce the adaptive control force. In 1989, the Kajima cooperation was the first to implement the full scale active control system in its 11-storey Kyobashi centre building in Tokyo [34]. The control system installed in this building consists of two active mass dampers (AMD) of different capacity. The first was of 4t mass to reduce motion in the transverse direction and the second was of 1t to reduce motion in a torsional direction. The authors also presented a comprehensive survey on structural control and listed the structures having structural control mechanism located especially in Japan and USA.

Since its first installation, the active control scheme was employed in various structures and bridges especially in Asia [35]. Several control algorithms were used in the active control

scheme. The control algorithms were developed that employed absolute acceleration [30]. It is observed that absolute acceleration is easier to measure instead of velocity or displacement during the seismic event. Consequently, it led to a quicker response from the control system to reduce the vibrations. The non-linear control algorithms were considered to explore the full potential of the active control scheme. Neural based control algorithms were proposed to increase the adaptability of the active control scheme [36]. A detailed survey of active control scheme is presented in the literature [37].

The active control scheme has not become very successful because of the following reasons.

i. The active control algorithm requires power typically tens of kW for small scale structures and large power of the order of megawatts for large structures to operate which is very difficult to ensure amid a seismic event.
ii. The structure may get destabilize due to energy imparted externally by the active control strategy.
iii. The measurement of structural responses for feedback should accurate and accurate measurement is a herculean task amid the seismic event.

2.5 Semi active control scheme

A new class of control of the structure has been developed by making a simple trade-off between active and passive control strategies. This is known as a semi active control scheme [38]–[41]. Semi active control strategy keeps up the consistency of the passive control scheme while exploiting the adaptable features of an active control scheme. Semi active control scheme allows the adjustment of mechanical properties similar to the passive control scheme. These adjustments are allowed based on the feedback from the measured responses through the sensors just like the active control scheme. Therefore, semi active control scheme has features of passive control (e.g. stability) and effectiveness of active control [42]. Many semi active supplemental devices are listed in Table 2.1. Any of these can be used in this control scheme but owing to many qualities, the magnetorheological dampers (MR dampers) played a vital role in the overall success of the semi active scheme. The MR damper absorbs energy generated due to vibrations in the structure. The rheological materials used in MR dampers can vary their physical appearance proactively. A small power, approximately 10 watts, is required to operate the semi active control scheme because the energy is required only to alter the properties (stiffness and damping) of the semi active device [43].

An electrical control signal required to generate the control force in this scheme is due to the predetermined algorithm. Like the active control scheme, this predetermined control algorithm utilizes a different kind of structural responses (i.e. relative displacement, interstorey drift, and absolute acceleration) as its feedback input. This controlling force is a counter force in nature which opposes the structural movement, so, the stability of the structure is confirmed unlike the case of the active control scheme.

2.6 Review of control algorithms

A wide range of control algorithms has been utilized in the control of structures from the seismic and wind loadings [44]. These control algorithms are successful for specific sort of structures and deficient for another type of structures. The reason behind this assortment of control methodologies is the distinctive kind of premises and presumptions made at the designing phase of the controller, for example, the prior knowledge of the structure and its mathematical modelling, nature of the uncertainties and the elements of the utilized actuators etc. This has been discussed by many authors in the literature [45]–[48]. Some state of the art surveys on semi active control schemes were published which endorse the remarkable success of semi active control scheme in many directions related to the control of the structures [11], [25]. Though the research in the field of the semi active control scheme has reached to advance stage, still there are some areas like to determine suitable control algorithms which require more attention. To dispense the appropriate electrical control signal in a semi active control scheme, it is necessary to develop a controller which must be realizable, simple, fault tolerant, optimal and most importantly robust. The following section reviews some common and reliable control laws used in the semi active control scheme. These controllers were used and tested previously by many authors in their work.

2.6.1 Passive ON/OFF controllers

Passive ON/OFF control algorithms are the simplest form of the controller. Passive ON is the case when the maximum voltage (V_{max} = 2.25V) is fed to the MR damper whereas supplying minimum voltage (V_{min} = 0) to the MR damper is known as Passive OFF. Although these controllers are very simple and practically implementable the problem here is that there is only one level of voltage whether the structure moving away from the centre or moving towards the centre [49].

Cha *et al.* (2014) [47] proposed two new methods namely simple passive control (SPC) and the decentralized output feedback polynomial control (DoFPC). The authors have used different structural responses as inputs to the controllers to find out the required control signal for

MR damper. It was observed that the DoFPC controller shows better performance as compared to Passive ON/OFF.

2.6.2 Quasi-bang-bang controller

In this control algorithm, the voltage to the MR damper is determined according to the two different rules. These rules depend on the reference position of the structure. There may be only two possibilities based on the reference position

i. If the structure is moving away from the centre (i.e. Reference position)
ii. If the structure is moving towards the centre

The comparison of quasi bang bang controller and sliding mode controller is also reported in the literature [50]. In the quasi bang-bang controller, the voltage levels between the centre and extreme are not considered which are important to consider. So, a modified Quasi bang bang controller approach was proposed in the literature [51]. In this approach, the author made use of the intermediate stages of the two extremes, i.e. (0, V_{max}) of the command voltages to the MR damper. The weights on the variables in this control law are like the fuzzy logic controller (FLC). These weights are constant and chosen by trial and error method. Therefore, It is difficult to find the optimized weights using trial and error method.

2.6.3 The proportional-integral-derivative (PID controller)

The proportional-integral-derivative (PID) and its variants like P (proportional), PI (proportional-integral), and PD (proportional-derivative) controllers have been widely used for practical and industrial applications. These controllers are especially useful for the lower order systems preferably one or two DOF. PID controller becomes very complex for multiple inputs and multiple outputs (MIMO) systems. It is insensitive to the parameter changes of the structure[52], [53]. Many researchers used PID family controllers for control of the structures and compared their performance with some advanced controller like SMC or FLC [20], [54], [55]. From various comparisons, it is observed that the PID controllers alone are not as useful as it is in hybrid form i.e. PID with SMC/FLC etc. Some contributions from the literature are listed as under.

Krishnan *et al.* carried out a simulation for a simple proportional (P) controller. This controller demonstrated satisfactory performance to reduce the displacement of the structure due to wind loading but found ineffective for seismic vibrations [56].

Guclu *et al*. a PID controller and a sliding mode controller (SMC) were designed to mitigate the vibration of a four degree of freedom structure. The efficiency of the PID controller

was compared with the sliding mode controller (SMC). The author considered the first and third floor for the comparison of the results using time histories namely Marmara earthquake Turkey (1999). The SMC controller performed superior to the PID controller[54].

Guclu *et al*. used two PD controllers for controlling two actuators installed in the first and top floor of a fifteen-storey structure model. A fuzzy logic controller (FLC) also designed for controlling the vibration of the same model. The performance of PD controllers was found substandard than the FLC controller [57].

Teng *et al*. used a proportional-integral (PI) controller to control an AMD to diminish the vibration of the structure due to the earthquake. However, the performance of the PID family controllers was found unsatisfactory because of proper tuning of the PID gain was very difficult to achieve. Furthermore, the stability analysis was not discussed in the above works. Despite having the clear physical significance of the variables in the PID controller, it was found unsuitable for the seismic vibration control for the MDOF structures due to increased complexity and inadequate gain tuning [58].

2.6.4 H∞ Controller

It is a fact that a mathematical model no matter how precisely defined, cannot accurately represent a real physical system. Generally, in classical control theory, the stability of the system was ensured in presence of the model uncertainties by the stability margin. But the issue here is, the model uncertainties are not accurately quantified. Similarly, the performance of the control system may not be considered in terms of the disturbance or noise. The classic approach to this problem from the 1960s was the Linear Quadratic Gaussian (LQG) theory. In LQG approach the uncertainty is modelled as a white noise Gaussian input. The major problem with this approach is that the uncertainty may not always be modelled as white noise. While designing a controller for the uncertain system like structure in the seismic event, irrespective of the variations in the structural dynamics within a fixed framework, a certain level of stability must be attained. Therefore, the following objectives were considered to design a controller to mitigate the seismic vibrations.

i. Stability of the controller
ii. Environmental disturbance rejection
iii. Handling of sensor (measurement) noise
iv. Robustness- the response of the structure should not exceed to beyond a predefined level if some changes occur due to the uncertainties in the model during the seismic activity.

To fulfil some of these objectives, the researchers worked on H∞ controller. The H∞ ("H-infinity") methods is used in control theory to synthesize controllers to achieve stabilization with guaranteed performance. H∞ is the Hardy space defined with the ∞-norm. The H∞ can be thought of as maximum gain of a function in any direction and at any frequency. This control method is one of the widely used linear robust controller in structural vibration control [59].

Gadewadekar *et al*. explained the method to use the H-infinity approach. According to the authors first, the control problem must be represented as a plane mathematical optimization problem. Then find a control law that solves this optimization problem. In this work, the authors implement a numerically efficient solution algorithm to solve the optimization problem. The authors also found that the performance of H∞ control algorithm for MIMO systems is excellent [60].

Park *et al*. represented a modified approach to design H∞ controllers namely pole shifting technique with H∞ control. The author employed a modified methodology which prescribes the use of decreasing the damping ratio instead of altering the stiffness of the structure. To track the roots of the characteristic equation in the design consideration H∞ controller, a bilinear transform is espoused where a relation between these closed loop poles and the bilinear transform parameters is determined in the form of a quadratic equation [61]. Most of the studies considered this controller reliable for the structural control but some authors observed that implementation of the H∞ controller usually results in complex higher order system which is difficult to implement and degrade the efficacy of the overall system. Some prominent works in this direction are discussed below.

Wu *et al*. worked on the reduction of the order of the system to make them implementable. In this work, the H∞ controller and the LQR controller are compared for both high order system and reduced order system. It was found that the performance of both the controller for reduced order system is comparable with the high order system [62].

Saragih *et al.* worked on a 4-story structure which has 30 states. In this work, the author reduced the order of the state up to 7^{th} order using balanced truncation. The author smartly chose only those states for truncation which are less controllable and less observable and consequently, important information about the system is saved. He compared the H∞ controller for both the cases and found that the performances are nearly the same [63]. In structural control time delay is inherent because of measurements from different sensors located at various places of the structure, the calculation time of the controller, command signal transmission time to the actuator to build up necessary control force. From the previous studies [64] it is observed that time delay

can cause the irreparable loss to the structure because the actuator may apply the force to the structure when it is not required [65]. Though there are other approaches are present in the literature to resolve the time delay problem, but some authors worked on hybrid approaches of control algorithms using an H∞ controller for this purpose. Some of them are discussed as under.

Lin *et al.* proposed a neural network-based hybrid approach for nonlinear structural systems. This approach combines the intelligent NN controller with the conventional H∞ controller [66]. The NN is utilized in this work to handle modelling errors of the nonlinear structure under the seismic excitation. The well-known Lyapunov stability theory is utilized in the form of LMI problem to check the stability of the hybrid controller. Efficacy of the controller was established through the numerical simulations on a four-storey structure.

Du *et al*. considered the time delay in their work while designing the H∞ controller for vibration mitigation. The authors make use of the powerful search capability of the genetic algorithm approach (GA) to find the feedback control gain and solving a set of LMIs. For evolution, the authors simulated the proposed controller by feeding the small as well as large time delay into the system [67].

Liu *et al.* considered varying time delay in their work. H∞ controller is designed using matrix inequality and parameter adjusting method [68]. It is worth to note here that the controller obtained using the H∞ norm method may not necessarily the best because this controller represents the optimal results according to the cost function. Only a few works in the literature demonstrate the non-linear constrictions such as saturation of the actuators while designing the controller. Moreover, this controller results in a higher order system. In this way, it becomes difficult to implement.

2.6.5 Sliding Mode Controller

The sliding mode control is viewed as a control algorithm suitable for nonlinear applications. It is a good choice for structural control because it is immune to model uncertainties and very robust. In linear optimal control, the constant parameters are chosen based on the various design conditions whereas the controller can change its constant parameters from one continuous state function to another within the given set of conditions whereas the sliding mode controller changes the dynamic properties of the nonlinear system using a set-valued control signal. This state feedback control law is not continuous in time and it switches its current state based on the current position in the state-space. Therefore, this control law is also known as variable structure control algorithm. In 1964, V A Taran was among the first who studied this

variable control structure algorithm [69]. Since then it became a popular robust controller for various application including control of the structure.

Utkin *et al.* presented an exclusive survey on sliding mode controller in form of tutorial. According to this tutorial, "the sliding mode control may also be defined as a switching control law used to drive the system's state trajectory onto a predetermined surface in the state-space and to maintain it in the subsequent time". The controller designed on this concept results in a stable system [69].

Adhikari *et al*. proposed a new approach to design the sliding mode control named as a modal space (MS-SMC) method. The modal reduction is achieved by two methods in this work namely spectral analysis and wavelet analysis of the structural response. The authors have devised a suitable mechanism to ignore the effect of the higher modes and designed the SMC based on a single-mode (first mode) reduced-order model [70].

Zhao *et al.* proposed two different hybrid control law namely "the constant plus proportional rate reaching law and the power rate reaching law based on discontinuous switching sliding mode control algorithm." They tested these control laws through simulations on an eight-storey shear building having base isolation under seismic loading [71].

Allen *et al*. presented an experimental study in which the first six modes of a large structure are considered. These first six modes were considered while designing the sliding surface using a quadratic criterion for the system. The results show that this type of SMC allows a dedicated control action in each mode to achieve better overall results [72].

Monajemi-Nezhad *et al.* proposed a decentralized approach of the control of the structure assuming a condition that the main control unit may lose its functionality amid the seismic event. Therefore, in their approach, the authors divided the large structure into several small substructures and proposed a separate standalone control unit devoted to each subsystem. Alternatively, the authors divided the whole control unit into many standalone subsystems that are being controlled locally by a separate control unit. These control units are based on SMC and reaching law. The authors demonstrated through numerical simulations that there is no significant difference In the efficacy of both the approaches [73].

Xiang *et al*. carried out a similar study on decentralization the control units. The authors proposed a full order decentralized SMC controller for tracking the uncertainty in the path of the unmanned aerial vehicles. But the performance was unsatisfactory due to the chattering effect of

SMC. In this work, the authors employed a low pass filter to obtain a chattering free SMC controller [74].

Guclu *et al*. reported a remedy to this chattering effect by using an averaging filter and proposed a new chattering free SMC. They compared the results of this proposed controller with the PID controller and found that new chattering free SMC is very attractive for the control of the structure [54].

Furthermore, some researchers used an intelligent control algorithm with the SMC to remove chattering effect and to achieve both robustness and adaptability in the control algorithm design for semi active control scheme.

Yakut *et al*. presented SMC based on neural network. It has the good features, like the robustness of SMC and the flexibility of the neural network. The authors tested this new controller through simulations on an eight-storey structure using many different external earthquake excitations. The neural network used to make the SMC chattering free. Moreover, the author optimized the parameters to obtain the minimum cost function using a genetic algorithm (GA). The controller thus obtained proved to be more successful than the simple SMC controller [75].

Li *et al*. presented another solution to get rid of this unwanted chattering effect of the conventional sliding mode control algorithm. This solution is based on RBF neural network control method using the fixed switch gain. The authors developed an RBF neural network control algorithm by adjusting the control gain parameter. The effectiveness of the newly developed adaptive SMC has been tested numerically on a three-story structure. it was found that the proposed algorithm was effective in reducing the structural responses as well as the chattering effect as compared to the conventional SMC [76].

Another intelligent controller namely Fuzzy logic controller (FLC) also has been used to avoid the chattering effect in SMC. The resulting controller is known as Fuzzy sliding mode controller (FSMC) as reported in literature [77]. The authors developed FSMC to reduce chattering effect from the SMC without compromising the robustness and insensitivity of the SMC towards the parameter changes. Furthermore, to attain lesser chattering some authors also used genetic algorithm (GA) in conjunction with the FSMC as reported in [78], [79].It is reported in the literature that the efficiency of the SMC controller is satisfactory but the chattering effect due to imperfections in the sliding surface due to high frequency switching may cause damage to the mechanical components i.e. actuators.

The chattering effect is a serious problem in the sliding mode control algorithm and it should be eliminated. In the light of reported literature, this can be done in two ways:

(i) By suitably smoothing the control force

(ii) By using continuous sliding mode control algorithm (SMC)

2.6.7 Neural Network Controller (NN controller)

Over the last decade, there has been a lot of research on the development and application of neural networks (NN). The control frameworks based on neural network (NN) are exceptionally prevalent, considering its capability of execution of various task simultaneously, the capacity to learn, and its ability to provide the solutions for still unsolved problems. Its capacity of learning inspired by the human brain makes it class apart from the conventional controller because the conventional controllers are designed to perform a precise task whereas NN controller learns to perform a task. This quality makes NN controller a versatile choice in control of the vibrations of structure and other nonlinear applications.

According to Ghaboussi *et al*. "The system's dynamics are defined through a set of rules for the propagation of the signals along the weighted connections. The result of the neural computation is a function of its connection weights. The knowledge acquired by a neural network is stored in its connection weights, which are adaptive and can change in response to outside stimuli" [80]. An increasing number of civil engineering applications of neural networks are also being reported in literature [81][82]–[84]. Ghaboussi *et al*. presented the neural network (NN) based approach for the control of the nonlinear single degree of freedom system in their landmark work [80]. In this work, the authors used two NN in the development of controller, one for reverse mapping and one for the emulator. Although the desired response can be set by some strategy, the selection of the desired response is not straightforward, and hence, may not be optimal.

An optimal control algorithm using neural networks was proposed by Kim *et al.* [85]. In this work, a training rule for the ANN is designed and developed to minimize the cost function to achieve the optimum results. For the simulation of the nonlinearity of the structure, a bilinear hysteric approach is considered. The controller suits both linear and nonlinear applications. The main advantages of this controller are summarized below.

i. The unknown dynamics of the structure is not the problem for this controller

ii. The external disturbances can be considered in the optimal control.

Morishian *et al.* proposed an adaptive NN controller for an MR damper. The proposed controller required batch training like the controller given in the literature [86]. The efficacy of the controller is tested on a three degree of freedom structure equipped with the MR damper.

Madan proposed a counter propagation neural network (CPN) approach which can learn from the control environment to compute the required control force to mitigate the earthquake induced vibrations in the building structure [83].

Cho *et al*. proposed a multilayer NN controller having a single hidden layer for control of the vibrations in a bridge. A critical aspect of their approach to design the controller is to determine the optimal number of hidden neurons. These are determined by trial and error method. The efficacy of the proposed control system was tested on a single degree of freedom and two DOF type bridge. The results of the tests established that the neural network controller is very effective to mitigate the vibrations [36].

Laflamme *et al.* proposed an adaptive neural network controller for a structure having an MR damper [87]. The authors have used Gaussian radial functions to map the properties of the structure. Connor *et al*. used wavelets in place of Gaussian radial functions which makes the controller more flexible. Further, the problem of instability due to time delay is not an issue for the NN controller [88]. The main advantage of using the intelligent controller like NN controllers is that they do not require an accurate modelling of the structure. The results of computer simulation and experiments in the time-domain and frequency-domain demonstrate the advantages of the NN controller over the other controller.

2.6.7 Fuzzy Logic Controller (FLC)

The fuzzy logic controller is also a model free approach for structural control like the NN approach. The designing of FLC involves the intelligent choice of the input, output variables, and data manipulation method, membership function, and rule base design [89]. The FLC became very popular in structural control owing to its simplicity, nonlinear mapping capability and stability. Mamdani defined a system in which a fuzzy law is used to control plant (a laboratory-built steam engine). This procedure was applied as a translator of a usual of instructions conveyed as fuzzy rules [90].

Ramaswamy *et al.* developed a fuzzy logic controller for active tuned-mass dampers (ATMD) to control the seismic vibrations [91]. Choi et al. presented a study having a semi active fuzzy control technique using an MR damper on the ground floor in a three-storey structure which resulted in seismic response decrease. The individual one obtainable controller creates openly

the anticipated knowledge voltage using fuzzy rule inference as the anticipated force required is various so which the actuator can create forces as close as likely to the anticipated forces [92]. Further, some researchers worked on the hybrid approach to design the controller using FLC [93]–[95].

Park *et al.* represented a decentred approach which has a fuzzy supervisory control. There is one higher level i.e. supervisory control and three sub controllers under this supervisory controller. These sub controllers are based on the optimal LQR control theory having three different weights for each. This fuzzy supervisor controller observers the performance of the sub controllers and tune them according to the current situation of the structure[96].

Choi *et al.* proposed a fuzzy logic controller (FLC) using the modern time domain control theory for mitigation of seismic vibrations of the structures. The observer capability of the Kalman filter is explored by authors for state estimation. Further, the authors used a low-pass filter for eliminating the spillover problem [97].

Das *et al.* proposed the FLC algorithm for the semi active control scheme. The authors did the fuzzification of the MR damper characteristics, that eliminates the need for mechanical modelling of the MR damper [98].

Though FLC is an intelligent controller like the NN controller as it requires a practical understanding of the system. However, the FLC has some disadvantages in the determination of parameters such as membership functions, control rules, and inadequate stability analysis. Also, The FLC and NN controller do not consider the feedback from the actuator (MR damper) and these controllers simply work upon the measurements of the structural response which difficult to get accurately amid the seismic event.

2.6.8 Linear Quadratic Regulator (LQR) and Linear Quadratic Gaussian (LQG)

The linear quadratic regulator (LQR) controller is a basic and popular controller across the control theory in general and well explored in the literature [99]. In optimal control theory, there is a cost function which needs to be minimized to achieve the desired or optimum results. This cost function is the function of the controller and the system parameters [100]–[103].

Krishnan *et al.* describes "the optimal control algorithms are based on the minimization of a quadratic performance index termed as a cost function while maintaining the desired system state and minimizing the control effort"[56].

Dyke *et al*. proposed the LQR controller in conjunction with the on-off switch-based controller to determine the control signal (voltage/current) to the MR damper. It is difficult to

maintain the relation between the input voltage and output force of the MR damper owing to the highly nonlinear nature of the MR damper which is difficult to model precisely. Therefore, most of the proposed control strategies modify the voltage through on–off rules without the use of a model. This controller became very famous in the structural control and popularly known as the clipped optimal controller. The authors developed a command signal (voltage) for the MR damper with the help of the LQR controller using damper`s force in feedback. The command signal (voltage) was set according to the clipped control law by comparing the desired force to the available damper`s force [9].

In the LQR control algorithm, the measurement noise or the sensor noise is not considered even though it remains present all the time. It is very difficult to measure owing to its nature but for the theoretical purpose, the researchers assumed this noise as a Gaussian white noise [102], [104]. In presence of this noise or otherwise, it is difficult to determine the states of the system for application of the control action. Therefore, an observer known as a Kalman filter is used to estimate the states of the system. The combination of the Kalman observer to the LQR controller is known as the Linear Quadratic Gaussian regulator (LQG) [102], [105]. A fuzzy logic approach to design LQG controllers is also reported in the literature [105].

Jansen *et al.* compared the performance of recently proposed controllers such as the Lyapunov controller, decentralized bang- bang controller, moderated homogeneous friction procedure, with the clipped optimal LQG controller used in semi active control scheme. The clipped optimal LQG/LQR controllers were found to be most effective in this study [106]. However, determining the appropriate weighting matrix for the optimum performance was still an area of research. In this direction, Panariello *et al.* proposed an algorithm based on carrying up-to-date weighting matrices for the gain of the LQR controller from a database of documented earthquake excitations. The need for an offline repository of known earthquakes is the limitation in the above studies [107].

Alavinasab *et al.* presents an energy-based approach to find the gain matrices for the LQR controller. The authors worked to eradicate the necessity of trial and error method to find the suitable gain matrices [108]. Different approaches to find the weighting matrix is presented in the literature [109], [110]. To overcome this shortfall, Basu *et al.* introduced modified time variable LQR (TVLQR) method by updating weighting matrices using a constant multiplier based on DWT analysis [111]. The value of this constant multiplier is decided by the energy content in the distinctive frequency groups over a period window and lies in the range from 0 to 1. Although in this method, weighting matrices vary at resonance condition, the constant

multiplier was determined offline. Therefore, offline data was still a requirement. For the solution of this problem, Amini presented a novel technique to find the best control forces for the active tuned mass damper. Three distinct procedures were used in this technique: discrete wavelet transforms (DWT), particle swarm optimization (PSO), and linear quadratic regulator (LQR) [112].

Further, as all the structural states are unobservable, a suboptimal control is used, where the system states are reduced using low-pass filters. The real problem in this controller was to determine the weighting matrices for optimum performances. To address this issue an LQR based on genetic algorithm (GA) was proposed, where the GA was employed to determine the weighting matrices [113].

Although many studies have been carried out to determine the weighting matrices appropriately, the area still requires more research. Based on the above discussion the following conclusion set the direction of the research in the field of structure control

i. The intelligent controllers like FLC and NN do not consider feedback from the MR damper and keep on applying counterforce based on the measurement of the structural responses. The SMC has the chattering problem and H infinity controller usually results in higher order system which is difficult to manage.
ii. The clipped optimal LQR/LQG controller consider the feedback from the MR damper and hence, these can determine the more accurate and optimum amount of counter force. Though LQR does not consider external noise and uncertainties present in the seismic environment, it is more popular controller because of its design simplicity and satisfactory results.
iii. A quick responsive method is required to determine the weighting matrix in real time for LQR/LQG controllers.

A summary of several controllers used in semi active and active control scheme is in Table 2.2 which summaries the important properties of the various controllers.

Table 2.2 Summary of the controllers

S.no.	Controller	Applications	Remarks
1.	Passive ON/OFF	Semi active control, Active control	Only one level of the voltage is available during the earthquake
2.	Quasi bang-bang controller	Semi active control	It has only two extreme levels of the voltage.
3.	Modified quasi bang-bang controller	Semi active control	1. It considers the intermediate stages of voltages between the two extremes with help of some constant weights. 2. There is a need to determine the optimal values of these constants.
4.	PID controller	The active and semi active control scheme	1. It requires position and velocity as an input which very difficult to measure accurately 2. It is not very suitable for multi-storey structure
5	H∞ controller	The active and semi active control scheme	1. It results in the higher order system 2. Difficult to implement 3. Order reduction is necessary 4. The resulting force may not be optimal
6.	Sliding mode controller (SMC)	The active and semi active control scheme	1. These controllers are very robust and stable. 2. The chattering effect degrades the performance of these controllers

7.	A neural network controller (NN controller)	The active and semi active control scheme	1. These controllers do not require the exact model of the structure and are highly effective. 2. Very well suited to the non-linearities of the structure. 3. Very helpful to overcome the time delay issue.
8.	Fuzzy logic controller (FLC)	The active and semi active control scheme	1. Like NN controllers the FLC also do not require the exact modelling of the structure. 2. Disadvantages in the determination of parameters such as membership functions, control rules, and inadequate stability analysis.
9.	Optimal controller (LQR)	The active and semi active control scheme	1. These require the structure modelling. 2. Easy to implement but the weighting matrices are fixed and not adaptive. 3. It does not take account of the uncertainties and noise inherently present amid the seismic event
10.	Optimal controller (LQG)	The active and semi active control scheme	1. Provide excellent result 2. It considers the uncertainty and noise present in the occurrence of the seismic activity. 3. It estimates the next state with the help of the KALMAN observer amid the seismic uncertainties.

3.1 Introduction

A semi active control scheme has both the reliability of the passive control scheme and the performance at par with the active control scheme. The performance of a semi active control scheme is largely dependent on the control algorithm used. Thus, the design of suitable control algorithms emerged as new multidisciplinary research interest in the field of control of the structure in the last two decades. With the advances in the field of control theory, it is now possible to design highly sophisticated control algorithms to attain better results in terms of the structural responses i.e. relative displacement, interstorey drift and the absolute acceleration. This chapter focuses on the fundamentals of the semi active control scheme. The mathematical models of the structure and the MR damper are presented. This chapter also discusses the theoretical background and the simulation results of previously used control algorithms in the semi active control strategy. These results are obtained using simulation on a three story test structure fitted with MR damper at the base. Furthermore, a comparative analysis of the performances of these controllers is carried out. This comparison lays a strong foundation for the proposed work.

3.2 Semi active control scheme

The semi active control scheme can be divided into three parts (i) Structure (ii) MR damper (iii) Control block as shown in Figure 3.1. Each of these shall be discussed in later sections of this chapter. The controller (control law) and the semi active control device (MR damper) are the main constituents of a semi active structural control system.

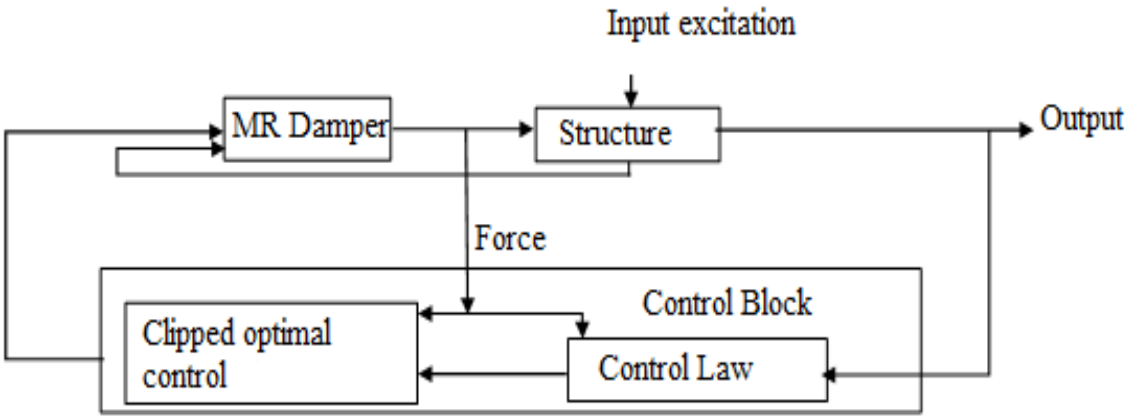

Figure 3.1 Block diagram of semi active control scheme

In a semi active control scheme, the seismic vibrations are reduced by applying adequate counterforce through MR damper by using a suitable control law. Once the suitable MR damper is determined and installed in the structure, the control algorithm is the only remaining variable to influence the efficacy of the overall scheme. The recent surveys suggest that the modern control theory is an essential part of active and semi active strategies [11]. The control theory is concerned with the control of processes with inputs and outputs. It is essential to know how the desired goal can be achieved by choosing available inputs from the structure. The first step in this direction is to determine a mathematical model describing the behaviour of the structure. The second step is to use mathematical tools to find suitable inputs for structure based on sensor measurements and then to develop an apt control law to achieve the desired results. However, it is evident that the mathematical model of the structure does not exactly replicate the behaviour of the structure. The mathematically obtained results may be significantly different from those obtained experimentally. Thus, the model usually kept simple (in the present study it is kept linear) for effective implementation of the control laws. Further, while designing a new control algorithm for the model, it is vital to understand the behaviour of the mathematical model, which will be different from the actual structure. This leads to the robustness analysis of the complete semi active control mechanism. The structure is effectively controlled by the counterforce generated by the MR damper utilizing the control signal from the developed controller. This control signal must be appropriately derived to provide the required control force.

3.3 Mathematical modelling of the prototype structure

The test structure shown in Figure 3.2 is employed in the present work which is a scaled model of the structure explored very well in the literature by many researchers [92], [114]. There is an MR damper, which is installed between the ground and the first floor rigidly.

The building frame is constructed of steel, with a height of 158 cm. The three floors have mass 98.3 kg each. “The first three modes of the model structural system are at 5.7 Hz, 17.3 Hz, and 28.3 Hz, with associated damping ratios given, respectively, by 0.33%, 0.23%, and 0.30%” as given in the literature [1]. The relative displacement of each floor with respect to the ground is x_1, x_2 and x_3 similarly, the absolute accelerations of the respective floors are denoted as x_{a1} x_{a2} and x_{a3} as shown in Figure 3.2.

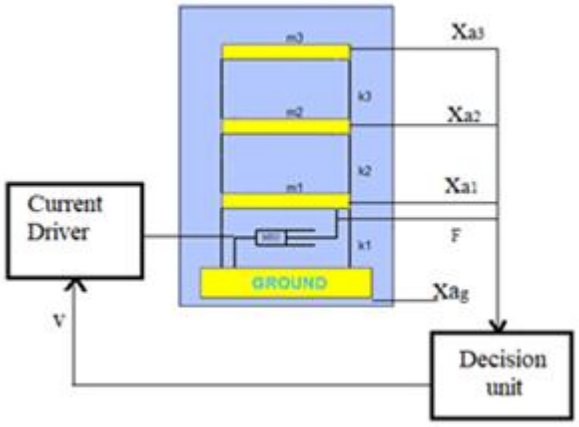

Figure 3.2 The three-story prototype structure [109]

Now, if the complete set up is a linear system, the equation of motion for the system is specified as in Eq. (3.1)

$$\mathbf{M_a\ddot{x} + C_a\dot{x} + K_a x = \Gamma f - M_a \Lambda \ddot{x}_{ag}} \tag{3.1}$$

$\mathbf{M_a}$, $\mathbf{K_a}$ and $\mathbf{C_a}$ have their usual meanings, i.e. the mass, stiffness and damping matrices of the structure respectively. In this work, the relative displacement response vector $\mathbf{x}$ has a dimension (3×1) due to the unidirectional excitation $\ddot{\mathbf{x}}_{\mathbf{ag}}$. The control force is represented by variable $\mathbf{f}$ and a column vector of ones is given by the variable $\mathbf{\Lambda}$. The parameter $\mathbf{\Gamma}$ fixes MR damper`s location in the structure which is the ground floor in this case. The parameter $\mathbf{\Lambda}$ fixes MR damper`s location in the structure which is the ground floor in this case. Since the MR damper is mechanically coupled at the ground floor as shown in Figure 3.1, the displacement of the lowest floor may be assumed the displacement of MR damper i.e. $x_{MR} = x_1$. The value of the mass, stiffness and damping matrices of the structure are given in Eqs. (3.2-3.4) [1]

$$\mathbf{M_a} = \begin{bmatrix} 98.3 & 0 & 0 \\ 0 & 98.3 & 0 \\ 0 & 0 & 98.3 \end{bmatrix} \text{kg} \tag{3.2}$$

$$\mathbf{C_a} = \begin{bmatrix} 175 & -50 & 0 \\ -50 & 100 & -50 \\ 0 & -50 & 50 \end{bmatrix} \text{N sec m}^{-1} \tag{3.3}$$

$$\mathbf{K_a} = \begin{bmatrix} 12 & -6.84 & 0 \\ -6.84 & 13.7 & -6.84 \\ 0 & -6.84 & 6.84 \end{bmatrix} \times 10^5 \text{ N m}^{-1} \tag{3.4}$$

The state space form of the equation of motion is determined by defining Eqs. (3.5-3.6).

$$\mathbf{\dot{z}_a = A\, z_a + B\, f + E\, \ddot{x}} \tag{3.5}$$

$$\mathbf{y_a = C\, z_a + D\, f} \tag{3.6}$$

Here the state vector is represented by the variable $\mathbf{z_a}$, measured output is represented by a vector $\mathbf{y_a}$, **v** is the noise vector whereas the MR damper's force is given by **f**. For n-DOF structure, these matrices may be found as in Eqs. (3.7-3.8).

$$\mathbf{A}=\begin{bmatrix} \mathbf{0_{n\times n}} & \mathbf{I_{n\times n}} \\ \mathbf{-M_a^{-1}K_a} & \mathbf{-M_a^{-1}C_a} \end{bmatrix} \qquad \mathbf{B}=\begin{bmatrix} \mathbf{0_{1\times n}} \\ \mathbf{-M_a^{-1}\Gamma} \end{bmatrix} \tag{3.7}$$

$$\mathbf{C}=\begin{bmatrix} \mathbf{-M_a^{-1}K_a} & \mathbf{-M_a^{-1}C_a} \\ \mathbf{I_{n\times n}} & \mathbf{0_{n\times n}} \\ \mathbf{0_{n\times n}} & \mathbf{I_{n\times n}} \end{bmatrix} \qquad \mathbf{D}=\begin{bmatrix} \mathbf{-M_a^{-1}\Gamma} \\ \mathbf{0_{2n\times n}} \end{bmatrix}, \quad \mathbf{E}=\begin{bmatrix} \mathbf{0_{1\times n}} \\ \mathbf{\Lambda} \end{bmatrix} \tag{3.8}$$

The sensor`s measurements are MR damper`s displacement and the absolute acceleration of all floors (i.e. = $[x_{a1}, x_{a2}, x_{a3}, x_{MR}]$) necessary to decide an appropriate control action. These structural measurements are readily available from the sensors. The linear variable differential transformer (LVDT) is normally used to measure the displacement and the high accuracy accelerometers are used to obtain the acceleration.

3.4 Semi active control devices and magnetorheological material

According to presently accepted definitions, a semi active control device is one which is not capable of injecting the mechanical energy into the controlled structural system (i.e. including the structure and the control device) but has properties that can be controlled to optimally reduce the responses of the system. Therefore, in contrast to active control devices, semi active control devices do not have the potential to destabilize (in the bounded input bounded output sense) the structural system. Preliminary studies indicate that appropriately implemented semi active systems perform significantly better than passive devices and have the potential to achieve, or even surpass, the performance of fully active systems, thus allowing for the possibility of effective response reduction during a wide array of dynamic loading conditions. Examples of such devices include variable-orifice fluid dampers, controllable friction devices, variable stiffness devices, adjustable tuned liquid dampers and controllable fluid dampers i.e. MR damper or ER dampers. The controllable fluid dampers are made of smart materials.

Smart materials are kind of designed materials whose properties are controllable with the application of external stimuli such as the magnetic field, electric field, stress, and heat. Smart materials whose rheological properties are controlled by an externally applied magnetic field are known as magneto-rheological materials. The essential characteristic of these controllable fluids is their ability to reversibly change from a free-flowing, linear, viscous fluid to a semi-solid in milliseconds when exposed to a magnetic field. MR fluids typically consist of micron-sized, magnetically polarizable particles dispersed in a carrier medium such as mineral or silicone oil.

In the last two decades, magneto-rheological materials have gained the great attention of researchers because of their salient controllable properties, its potential applications to various fields such as the automotive industry, civil environment, military sector and life sciences. They offer the versatility of active control scheme without requiring the related expansive power sources. As a matter of fact, it works on batteries, which is needful amid seismic occurrences when the primary power source to the structure may come up short.

Many researchers have carried out several pilot studies to assess the usefulness of MR dampers for seismic response reduction [115], [116]. In present work, the MR damper is used as a semi active device.

3.4.1 Magnetorheological damper (MR damper)

To have a deeper insight into the semi active control of the structure, the understanding of the magnetorheological damper (MRD) is essential. The MR dampers of different sizes and capacities are available. The appropriate MR damper is determined according to the requirement of the structure.

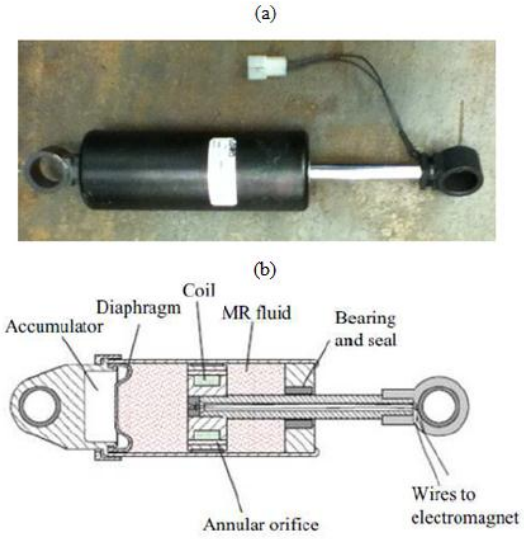

Figure 3.3 (a) Small-scale MR damper (b) Cross-section [117]

The MR damper considered in this study is 8.5-inch-long in its extended position, and the main cylinder is 1.5 inch in diameter. It has a stroke of ±1.0 inch and can generate forces up to about 3000N using very less power (<10 watts). The main cylinder of the damper accommodates the piston, the electromagnet, an accumulator, and 50 ml of MR fluid. Figure 3.3(a) shows the small-scale MR damper built by Lord corporation USA and the cross-section of this device is depicted in Figure 3.3(b). A small electromagnet located in piston head is sufficient to produce

the required magnetic field [39], [117]–[120]. However, a small-scale MR damper is considered for this study, but now it is possible for MR dampers to generate a force of 200 kN in 60 ms, with a 50W power input [121].

Since there are no moving parts, other than the cylinder itself, damping device that exploits controllable liquids are more robust than other semi active dampers considering electromechanical parts. Moreover, the MR damper is very modest to fabricate and work. Some primer tests by the researchers show that it can produce the required force for structural building applications [122], [123]. Nonetheless, semi active devices are inherently non-linear which makes its mathematical modelling difficult.

3.4.2 Mathematical modelling of the MR damper

To develop a control algorithm that could take maximum advantage of the unique features of the damper, a model of MR damper is required that can adequately characterize the damper's intrinsic nonlinear behaviour. Different static and dynamic models have been presented and reviewed in the literature [124]–[126]. An internal state, whose dynamics is governed by a nonlinear differential equation, captures the hysteretic behaviour of the MR damper. Other types of models such as the Bingham model, polynomial and tangent hyperbolic models have also been studied previously [117]. As these models are mathematical models, parameter identification is required to determine the corresponding values of the parameters for a given MR damper. The hysteretic behaviour of MR dampers is closely related to their frictional mechanics. The total MR damper effects are dominated by the magnetic and friction forces. Especially at low amplitude forces, the friction plays an important role in the overall resulting force. One model, which is numerically tractable and has been used extensively for modelling hysteretic systems is the Bouc-Wen model (Wen 1976). The Bouc-Wen model as shown in Figure 3.4 (a) is extremely versatile and can exhibit a wide variety of hysteretic behaviour [117], [127]. This model predicts the force-displacement behaviour of the damper and it possesses force-velocity behaviour that more closely resembles the experimental data. However, like the Bingham model, the nonlinear force-velocity response of the Bouc-Wen model does not roll-off in the region where the acceleration and velocity have opposite signs and the magnitude of the velocities are small [103]. Therefore, to predict the damper response better at small velocities, a modified version of the system shown in Figure 3.4(b) was proposed in literature [117]. Consider only the upper section of the model shown in Figure 3.4(b), to determine the governing equations for the MR damper model. The forces on either side of the rigid bar are equivalent.

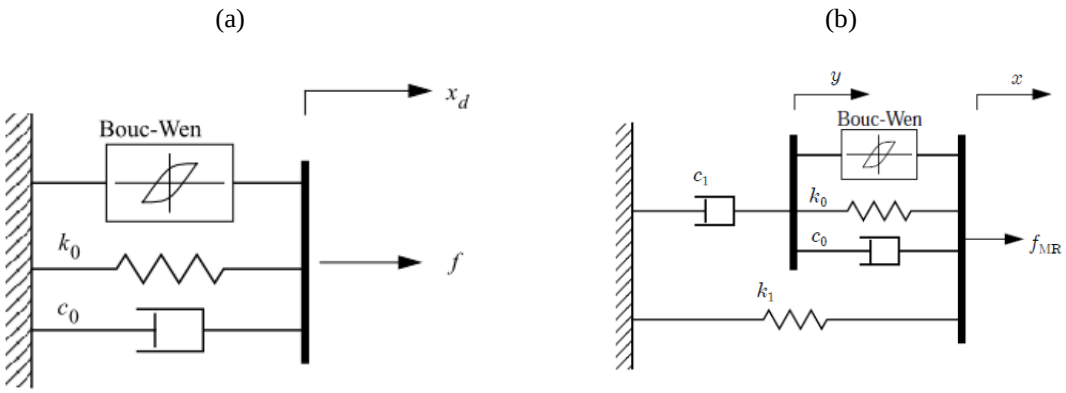

Figure 3.4 (a) Simple Bouc-wen model (b) Modified Bouc-wen model of the MR damper [117]

The damper force is a function of the damper displacement and velocity. The reason for considering modified Bouc-Wen model instead of the classic Bouc-Wen model because classic Bouc-wen model fails to predict the roll-off issue seen at low velocities. The equations used to simulate this model are given from Eqs. (3.9-3.15). This damper generates a force f as in Eq. (3.9) which is subject to the voltage applied to the damper. As can be seen from Eqs. (3.12-3.15) the variables α, c_0 and c_1 are linearly corresponding to the effective voltage "u".

$$f = c_1\dot{y}+k_1(x-x_0) \tag{3.9}$$

$$\dot{y} = \frac{1}{(c_0+c_1)}\{\alpha z+c_0\dot{x}+k_0(x-y)\} \tag{3.10}$$

$$\dot{z} = -\gamma|\dot{x}-\dot{y}||z|^{n-1}-\beta(\dot{x}-\dot{y})|z|^{n}+A(\dot{x}-\dot{y}) \tag{3.11}$$

$$\alpha=\alpha_a+\alpha_b u \tag{3.12}$$

$$c_0=c_{0a}+c_{0b}u \tag{3.13}$$

$$c_1=c_{1a}+c_{1b}u \tag{3.14}$$

$$\dot{u}=-\eta(u-v) \tag{3.15}$$

These variables link the mechanical properties of the MR damper to the command voltage and to ensure the working of the model is good in altering magnetic fields. The accumulator`s stiffness is shown by the variable k_1, the damping observed at large, and low velocities are shown here by two dashpots c_0 and c_1 respectively. The stiffness, at large velocities, is depicted by variable k_0 and the displacement x_0 of spring $k_1$demonstrate a small force of the accumulator. The adjustable parameters β, γ, n and A control the hysteresis curve for MR liquid. These parameters are used to shape the hysteresis curve and to control the non-linear

behaviour of the MR damper. The parameter z is an evolutionary variable, and it expresses the mechanism of the dependence of the response on history. The output of the first order filter given in Eq. (3.15) is used to drive the electromagnet in the MR damper. it helps to understand how the MR damper attains the rheological equilibrium [1]. Table 3.1 provides the parameters obtained using MATLAB (MATLAB, 2016) optimization toolbox which is very close to those obtained experimentally by the researchers in literature [9]. The MR damper with parameter given in Table 3.1, has been tested using a sine wave having an amplitude 1.5 cm and frequency 2.5 Hz through simulation and the results are shown in Figure 3.5.

Table 3.1 Parameters of the generalized MR damper [117]

Parameter	Value	Parameter	Value
c_{0a}	21.0 N. sec/cm	α_a	140N/cm
c_{0b}	3.50N.sec/cm. V	α_b	695 N/cm. V
k_0	46.9 N/cm	γ	363 cm-2
c_{1a}	283 N. sec/cm	β	363 cm-2
c_{1b}	2.95N.sec/cm. V	A	301
k_1	5.00 N/cm	n	2
x_0	14.3 cm	η	190 sec-1

These results are similar to those obtained by laboratory testing of the MR damper as represented in the work carried out by some authors in literature [1]. These results established that the mathematical models developed for present work are appropriate. Hence, these can be considered further for controller design. The presence of an accumulator in the MR damper (see Figure 3.3(b)) that is filled with nitrogen gas pressurized at some definite pressure level, does not allow the force to be cantered at zero. It means that there is an offset force even if there is no supply of power. Moreover, this accumulator can think of a spring in the damper and it prevents the cavitation in the MR fluid during the normal operation. Thus, to obtain an effective model of the MR damper, the stiffness associated with the accumulator must be considered. Other interesting features can be observed in the force-velocity responses shown in Figure 3.5(c). The upper branch of the force-velocity curve corresponds to decreasing velocities which means negative accelerations, and therefore positive positions for large positive velocities and the force in the damper varies linearly with this velocity. It is important to note that the force-velocity relationship is no longer linear and decreasing rapidly as the velocity decreases and before it becomes negative. This roll-off in the force at small velocities is due to bleed or blow-by of fluid

between the piston and the cylinder and is necessary to eliminate harshness from the subjective feel of the damper in vehicular applications. This type of behaviour is required in a prospective model of the MR damper.

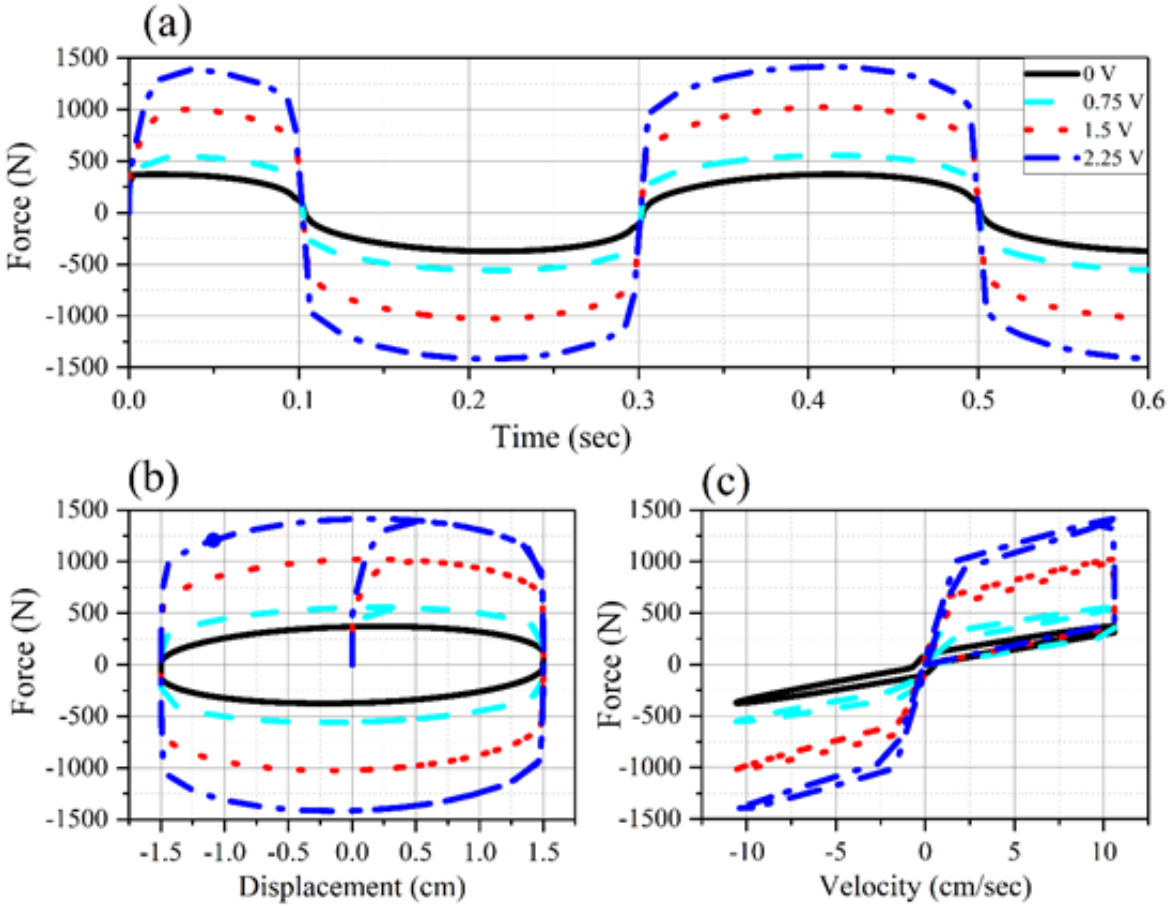

Figure 3.5 (a) Force generated in MR Damper at different input voltages due to a sine wave having amplitude 1.5cm and frequency 2.5Hz (b) Force-displacement diagram (c) Force-velocity diagram

3.5 Theoretical & mathematical background of some previously used controllers

The theoretical and mathematical backgrounds of some previously used controller are presented briefly in this section. The controllers are passive OFF/ON, clipped optimal LQR (CO-LQR), clipped optimal LQG (CO-LQG), Double output feedback polynomial controller (DOFPC), simple Passive controller (SPC), Lyapunov stability criteria-based controller (Lyapunov), quasi bang-bang (QBB), and modified quasi bang-bang controller (MQBB). These controllers are not only used for structural control but also used in several other applications like robotics, satellite communication, and automobile etc. The control algorithms are first numerically simulated for a closed loop semi active system on a three-storey structure as described in section 3.2, the results are compared based on their capability of reducing the structural response for all the floors.

3.5.1 Passive ON/OFF

These control laws are the simplest form of the controller. Passive ON is the case when the maximum voltage (Vmax = 2.25V) is fed to the MR damper whereas supplying minimum voltage (Vmin = 0) to the MR damper is known as Passive OFF. Although these controllers are very simple and practically feasible, the problem with this pair of controllers is that there is only one level of voltage whether the structure moving away from the center or moving towards the center. The mathematical representation of this controller pair is given in Eq. (3.16)

$$V_i = \begin{cases} V_{max} & \text{Passive ON} \\ 0 & \text{Passive OFF} \end{cases} \tag{3.16}$$

3.5.2 PID controller

The proportional-integral-derivative (PID) has been widely used for practical applications, especially for the systems with one or two DOF. For multivariable systems, this controller becomes complex, which makes it inapt for the applications like vibration control of MDOF flexible structures [128], [129]. This control law is given in Eq. (3.17)

$$u(t) = K_p[e(t) + \frac{1}{K_i}\int_0^t e(t)dt + K_d\frac{de(t)}{dt}] \tag{3.17}$$

where K_p and K_d are the proportionality constant and derivative gain and K_i is the integral gain. respectively, and e(t) is the position error. This controller has three variants that may be used depending on the requirement. There may be three possible combinations which are described as following.

(i) Proportional controller (P)

When there is a need to reduce the transient response, the P controller is used. The mathematical representation of the P controller is as following

$$u(t) = K_p[e(t)] \tag{3.18}$$

(ii) Proportional integral controller (PI)

This controller integrates the error signal over a period and then acts. An integral term increases action in relation not only to the error but also the time for which it has persisted. So, if the applied force is not enough to bring the error to zero, this force will be increased as time passes. A pure "I" controller could bring the error to zero, however, it would be both slow reacting at the start (because action would be small at the beginning, needing time to get significant), brutal (the action increases as long as the error is positive, even if the error has started to approach zero), and slow to end (when the error switches sides, this for some time will only reduce the strength of the action from "I", not make it switch sides as well), prompting overshoot and

oscillations. Moreover, it could even move the system out of zero error, remembering that the system had been in error, it could prompt an action when not needed. An alternative formulation of integral action is to change the electric current in small persistent steps that are proportional to the current error. Over time the steps accumulate and add up dependent on past errors. The control law is given in Eq. (3.19)

$$u(t)= K_p[e(t)+\frac{1}{K_i}\int_0^t e(t)dt] \tag{3.19}$$

(iii) Proportional derivative controller (PD)

A derivative term does not consider the error (meaning it cannot bring it to zero). A pure D controller cannot bring the system to its setpoint. It considers the rate of change of error. It tries to bring the rate of change of the error to the zero. It aims at flattening the error trajectory into a horizontal line, damping the force applied, and so reduces overshoot (error on the other side because of larger applied force). Applying too much force when the error is small and is reducing, will lead to overshoot. After overshooting, if the controller were to apply a large counterforce in the opposite direction and repeatedly overshoot the desired position, the output would oscillate around the setpoint in either a constant, growing, or decaying sinusoid. If the amplitude of the oscillations increases with time, the system becomes unstable. If they decrease, the system remains stable. If the oscillations remain at a constant magnitude, the system is marginally stable. The control law is given as in Eq. (3.20)

$$u(t)= K_p[e(t)+K_d\frac{d\,e(t)}{dt}] \tag{3.20}$$

A simulation is carried out for a simple PID controller, which can reduce the structure`s displacement for low to mild magnitude earthquake excitation but found to be less effective for strong earthquake excitation.

3.5.3 Lyapunov stability theory-based controller

It is possible to employ Lyapunov's direct approach to stability analysis in the design of a feedback controller especially for nonlinear applications [130], [131]. The approach to design a controller based on Lyapunov stability criteria requires the use of a Lyapunov function, V(z). The most important consideration for selecting this function V(z) that it must be a positive definite function of the states of the system, z. Now, assuming the origin as a stable equilibrium point, the Lyapunov stability theory states that if the rate of change of the Lyapunov function, V(z), is negative semi-definite, the origin will be stable. Thus, in developing the control law, the goal is to choose control inputs for each device that will result in making as negative as possible.

An infinite number of Lyapunov functions may be chosen, that may result in a variety of control laws. Leitmann *et al.* applied Lyapunov's direct approach to the design of a semi active controller [9]. In this approach, a Lyapunov function is chosen for the form of a function given in Eq. (3.21)

$$V(\mathbf{z}) = \frac{1}{2}\|\mathbf{z}\|_p^2 \tag{3.21}$$

where $\|z\|_p$ is the P-norm of the states defined by Eq. (3.22) and here, **P** is a real, symmetric and positive definite matrix.

$$\|z\|_p = [\mathbf{z}`\mathbf{P}\mathbf{z}]^{1/2} \tag{3.22}$$

In the case of a linear system, to ensure $\dot{V}$ is negative definite, the matrix **P** is found using the Lyapunov equation for a positive definite matrix is as in Eq. (3.23)

$$\mathbf{A}`\mathbf{P} + \mathbf{P}\mathbf{A} = -\mathbf{Q_p} \tag{3.23}$$

The derivative of the Lyapunov function for a solution of first state space equation is given in Eq. (3.24)

$$\dot{V} = -\frac{1}{2}\mathbf{z}`\mathbf{Q_p}\mathbf{z} + \mathbf{z}`\mathbf{P}\mathbf{B}f + \mathbf{z}`\mathbf{P}\mathbf{E}\,\ddot{x}_g \tag{3.24}$$

The only term which can be directly affected by a change in the control voltage is the middle term which contains the force vector. Thus, the control law which will minimize $\dot{V}$ is

$$v = V_{max} H(-\mathbf{z}`\mathbf{P}\boldsymbol{B_i} f_i) \tag{3.25}$$

where H (.) is the Heaviside step function, f_i is the measured force produced by the i^{th} MR damper, and $\mathbf{B_i}$ is the ith column of the **B** matrix in state space matrix. But in present work onl,y one MR damper is being considered. However, the selection of the appropriate matrix remains a challenge in the use of the Lyapunov algorithm.

3.5.4 Quasi-bang-bang controller

In this algorithm, the voltage to the MR damper is decided according to the two different rules. These rules depend on the reference position of the structure. The structure is assumed to be at rest position (static equilibrium) when there is no external loading, i.e. its center position. There may be only two possibilities based on the reference position

i. If the structure is moving away from the center (i.e. Reference position)

ii. If the structure is moving towards the center

The command voltage is selected as per control law in Eq. (3.26)

$$V_i = \begin{cases} V_{max} & \text{if moving away from the center} \\ 0 & \text{if moving towards the center} \end{cases} \quad (3.26)$$

Here, the quasi bang-bang controller is simple, effective and easy to implement a controller for the semi active control scheme. The major disadvantage of this controller is the undesirable control chattering near the origin of state-space due to high-frequency switching of control force often occurs and great care must be taken against spillover instability at higher modes.

3.5.5 Modified quasi-bang- bang controller

This is the control approach proposed by A.M. aly in 2013 [51]. In this approach, the author made use of the intermediate stages of the two extremes, i.e. (0, Vmax) of the command voltages to the MR damper. The weights, selected in this control law, are in like the fuzzy logic controller. These weights are constant and chosen by trial and error method. The control law is given as in Eq. (3.27)

$$V_i = \begin{cases} \alpha_1 V_{max} & (\text{if } \text{sign}(x)=1, \text{sign}(\dot{x})=1) \\ \beta_1 V_{max} & (\text{if } \text{sign}(x)=-1, \text{sign}(\dot{x})=-1) \\ \gamma_1 V_{max} & (\text{if } \text{sign}(x)=1, \text{sign}(\dot{x})=-1) \\ V_{max} & (\text{Otherwise}) \end{cases} \quad (3.27)$$

This is accomplished by assigning constant weights to the output. But these weights had been chosen randomly by trial and error in the range of 0 to 1. This random selection does not determine the optimized value of the command signal to the MR damper. It leads to the inferior performance of the controller and semi active control scheme.

Further, the modified quasi bang-bang controller uses the maximum available power which needs to be lower down. Using lesser electrical power is one of the main features of the semi active control method. A semi active control scheme is considered good only if the power consumption is as low as possible.

3.5.6 Simple passive controller (SPC)

A simple-passive control [47] (SPC) rule is based on the problems occurred by feeding a high voltage to the MR damper to generate a relatively large control force when the damped floor vibrates across its original position. It is evident from the dynamics of the MR damper that the high input voltage and large input velocity guarantee a large output force and maximized energy dissipation. Therefore, during the vibration of a damped structure, a relatively large control force will be generated to “catch” the structure when it vibrates across its original position. However, “keeping the MR damper working under high voltage (2.25V) for a long time (i.e. passive on)

will result in a floor lock-up, increase the absolute acceleration of the damped floors, and increase the drifts of the undamped floors" [9]. A simple controller known as simple passive control (SPC) is proposed to maximize the energy dissipation as well as avoid the floor lock-up. The control law is described as in Eq. (3.28),

$$v = \begin{cases} v_1 & |x|<x_1 \\ v_2 & x_1 \le |x| < x_1+x_2 \\ v_3 & (x_1+x_2 \le |x| < x_1+x_2+x_3) \\ 0 & x_1+x_2+x_3 \le |x| \end{cases} \quad (3.28)$$

where v is the control voltage x is the interstorey drift of the floor on which the MR damper is installed and x_1, x_2, x_3,v_1,v_2 and v_3 are the design parameters that can be determined by a multi-objective optimization for a structure subject to different earthquakes. A voltage of $v_1$will be input to the damper when the interstorey drift is within the range of $\pm x_1$.

When the floor swings away from its undeformed position beyond x_1, the control voltage drops to v_2 to avoid locking up of the floor. However, as the peak interstorey drift increases, the voltage will be increased to v_3 after the threshold drift x_1+x_2 so that the damper can act as a stiffness element to limit peak interstorey drift. Note that the voltage is dropped from v_3 to zero for $x_1+x_2+x_3 \le |x|$ since the high voltage v_3 cannot be applied for a long duration.

3.5.7 Decentralized output feedback polynomial control (DOFPC)

Based on two polynomial equations expressing a direct relationship between structural responses and the optimal control signal for MR damper, the decentralized output feedback polynomial control (DOFPC) was proposed for nonlinear highway bridges [47]. The control signal is formulated using the following Eq. (3.29)

$$v = \left|(a_0+a_1x+a_2x^2+a_3x^3)+\left(b_0+b_1\dot{x}+b_2\dot{x}^2+b_3\dot{x}^3\right)\right| \quad (3.29)$$

where x and $\dot{x}$ are the interstorey drift and the interstorey velocity of the structure and a_0,a_1,a_2,a_3,b_0,b_1,b_2 and b_3 are optimal coefficients of the polynomial equations for the control signal. These optimal coefficients can be investigated by any heuristic search method (e.g. genetic algorithm (GA), particle swarm optimization (PSO), adaptive particle swarm optimization (ADPSO)) or any machine-running method. The two polynomial equations can address the highly nonlinear hysteretic behaviour of the MR damper between the MR damper responses and the control signal. Therefore, this controller considers the non-linearities in the overall system.

3.5.8 Clipped optimal LQG/LQR controller

This controller is very effective and used with MR damper for semi active control strategy. It is one of the best available controllers that has shown the ability to diminish the vibrations effectively. A controller K_c, which is linear and optimal, is designed to estimate a desired control force fc based on measurement of structural responses **y,** and measured force f applied to the structure as given in Eq. (3.30)

$$f_c = L^{-1}\left\{K_c(s)L\begin{pmatrix} y \\ f \end{pmatrix}\right\} \tag{3.30}$$

Here L{–} is the Laplace transform. To determine the desired control force f from the MR damper, the command voltage v is selected as in Eq. (3.31)

$$v = v_{max} H\{(f_c - f)f\} \tag{3.31}$$

Where v_{max} is the maximum voltage can be given to the MR damper within its saturation limits and H (.) is the Heaviside step function. this rule consists in adjusting the voltage in such a way that the actual force supplied by the MR damper tracks a desired force in the best possible way under the restriction of the purely dissipative capacity of the device. This desired force is usually calculated by means of a feedback control algorithm, designed to achieve a control objective on the structure. This overall strategy has been popularized as 'clipped control' in the literature [114]. The idea behind this controller was that the desired force cannot be always generated because the force generated in the MR damper is dependent upon the structural measurements, but the input voltage can be altered according to the need of the system. In LQR, the linear gain is calculated using full state feedback in such a way that it minimizes the quadratic cost function. The LQR controller is very effective in reducing the structural response but it assumes that all the states are available and there is no measurement noise. However, this is not the practical case. Therefore, the clipped optimal LQG controller was introduced which considers the measurement noise present in the system and assumes this noise is Gaussian in nature. In the seismic event, the determination of the next state may be difficult due to noise. In this linear quadratic Gaussian (LQR) controller combines with the Kalman estimator which estimates the unknown states of the system. This combination of the LQR controller and the Kalman filter is known as a Linear quadratic Gaussian (LQG) control algorithm [102].

3.6 Comparative analysis

The theoretical background of some previously used controllers is discussed in section 3.5 of this chapter. In this section, the performance of these controllers is assessed through numerical simulations on a scaled three story structure (discussed in section 3.2) and a visual

(qualitative) and quantitative comparative study is presented. The three earthquake time histories are used for this study. El-Centro valley earthquake is taken for the study to validate the results with those presented in literature [49]. Further, two more earthquake time histories are considered only for the sake of robustness of the comparative analysis. The list of earthquake time histories is as following.

i. El-Centro valley earthquake
ii. Chile earthquake
iii. Uttarkashi earthquake

The peak values of the structural responses (i.e. relative displacement (X_n), inter-story drift (ID_n) and absolute acceleration (A_n)) of the test structure subjected to various earthquake time histories. Figures (3.6-3.8) show the comparison of the percentage reduction of the X_n, ID_n, and A_n for El-Centro, Chile and Uttarkashi earthquake time histories respectively.

Further, it is evident that the visual inspection is the most common way to judge the best performance of a control algorithm for a semi active control application. Especially, this approach is frequently used in the application of earthquake engineering where visually compares the plot of the displacement time history. This method is entirely based on human inspection. Alternatively, it is assumed that the visual approach is user dependent which requires proficiency of the person-in-charge. In the present study, for visual analysis, the time histories of the third-floor displacement of the test structure subjected to El-Centro earthquake time history for the first 5 seconds for different controllers are shown in Figure 3.9. This Figure shows the reduction in the third-floor displacement as compared with the uncontrolled structure.

First, the quantitative analysis of the results is carried out for El-Centro earthquake. The percentage reduction in relative displacement, interstorey drift and absolute acceleration for all the three floors are calculated with respect to the uncontrolled structure and plotted in Figures 3.6(a-c). A careful observation of Figure 3.6 (a) concludes that the maximum reduction (85% as compared with uncontrolled structure) in relative displacement for the first floor is achieved by three controllers namely Passive ON, Lyapunov and DOFPC controller. However, clipped optimal LQG (CO-LQG) controllers achieve the highest reduction (78%) for the third floor of the structure. The CO-LQG demonstrates the percentage reduction in the displacement of the first and second floor very similar (79% and 77% respectively) to the best performing Passive ON, Lyapunov, and DOFPC controllers. In this study, the reduction of the responses of the third floor of the structure is considered the main basis of the performance evaluation of the controller

(a)

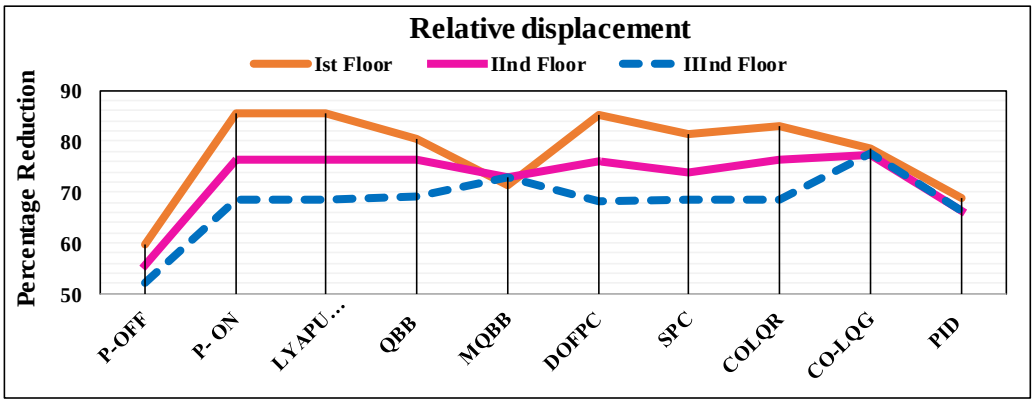

(b)

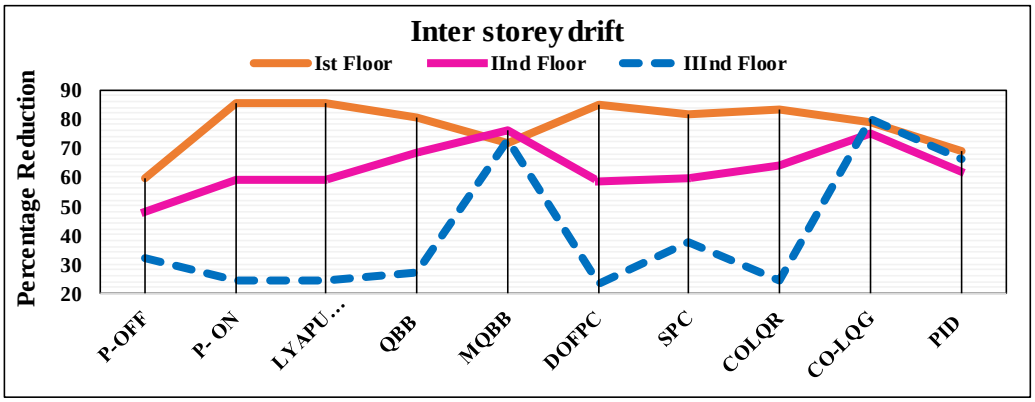

(c)

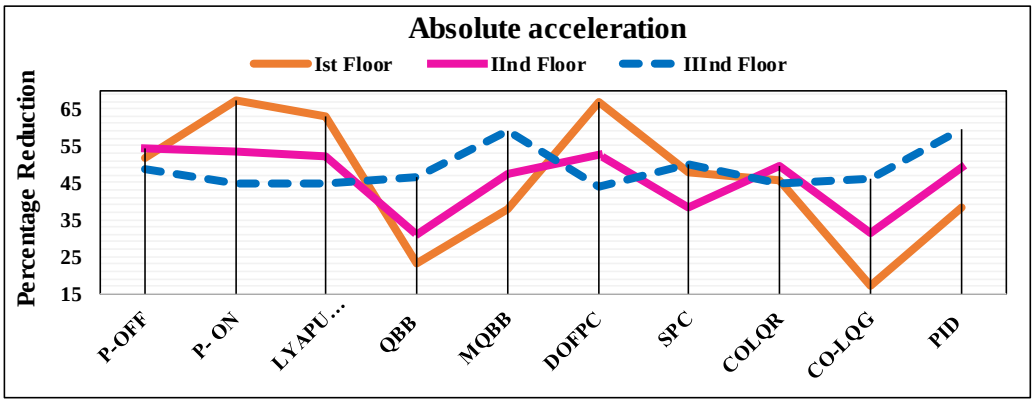

Figure 3.6 Response of the prototype structure subjected to El-Centro earthquake for different controllers (a) Relative displacement (b) Interstorey drift (c) Absolute acceleration

Therefore, on this basis, the CO-LQG controller can be declared as the best performing controller in reducing the relative displacement for the considered three-storey structure. Figure 3.6(b) gives the interstorey drift response of the structure due to various controllers. A careful examination of this Figure reveals that the modified quasi bang-bang (MQBB) (73%) followed by PID (66%) and CO-LQG (64%) controller are the best performing controllers in reducing the drift between second and the third floor of the structure.

(a)

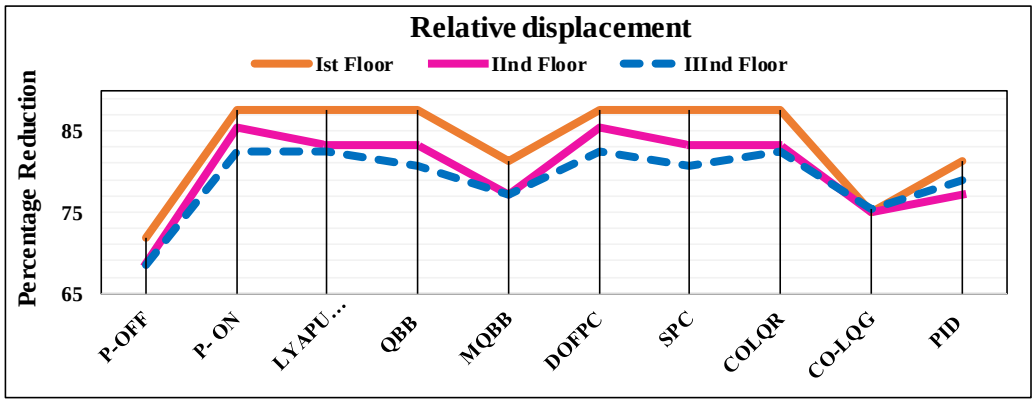

(b)

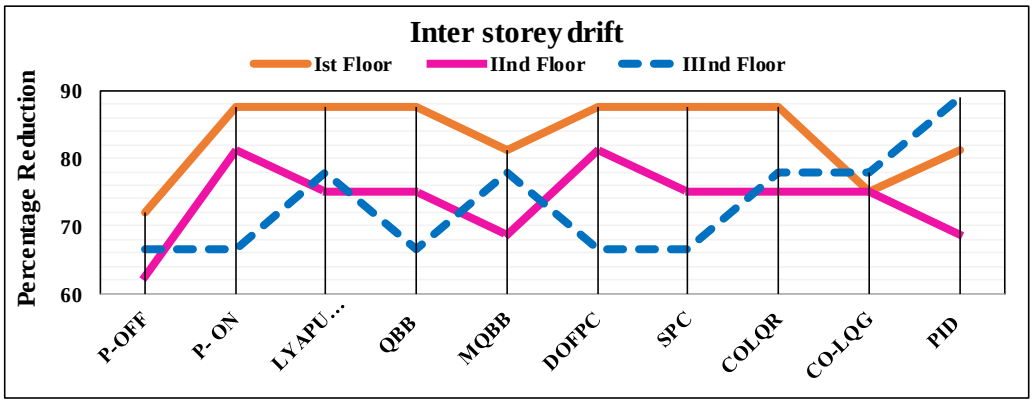

(c)

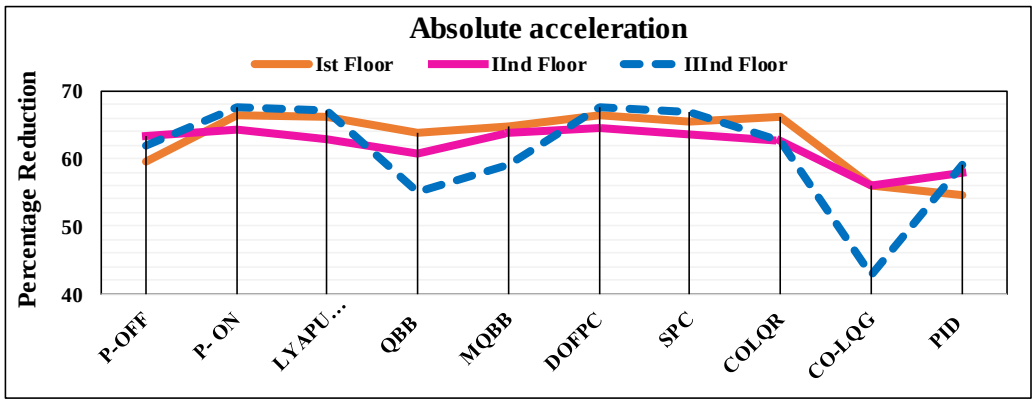

Figure 3.7 Response of the prototype structure subjected to Chile earthquake for different controllers (a) Relative displacement (b) Interstorey drift (c) Absolute acceleration

Now, the interstorey drift, the PID controller achieves the maximum percentage reduction (89%) followed by CO-LQR, MQBB and Lyapunov based controller (78%) as can be seen from Figure 3.7(b). Similarly, the maximum percentage reduction in the third-floor absolute acceleration is achieved by the Passive ON, DOFPC and the SPC (67%) and closely followed by CO-LQR (63%).

(a)

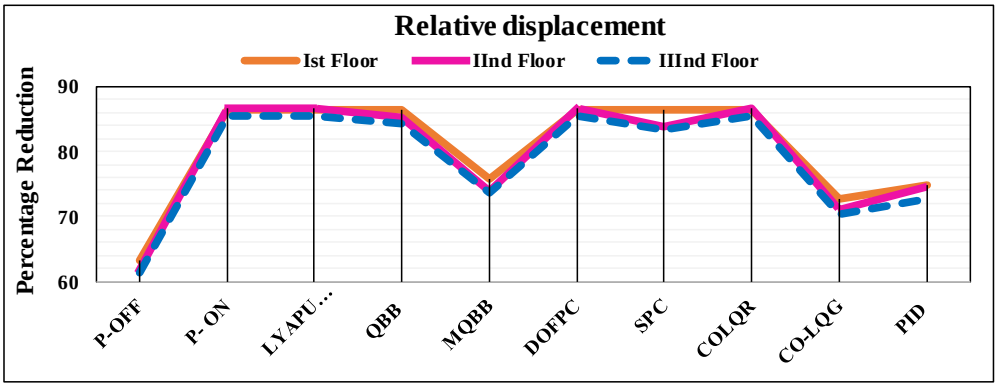

(b)

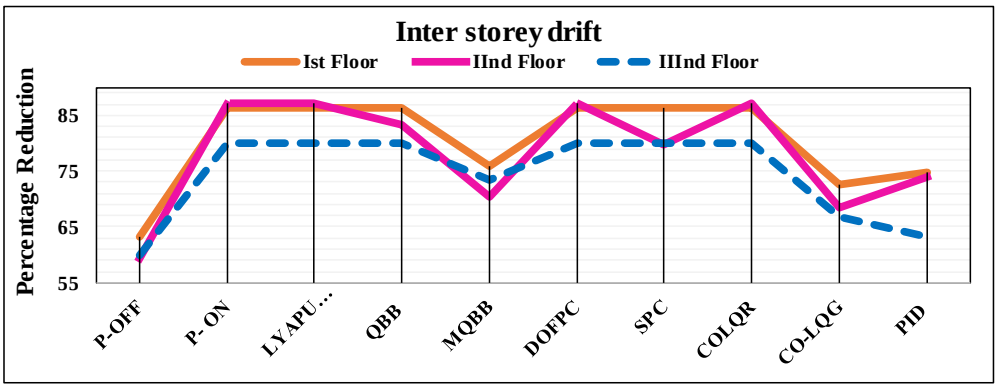

(c)

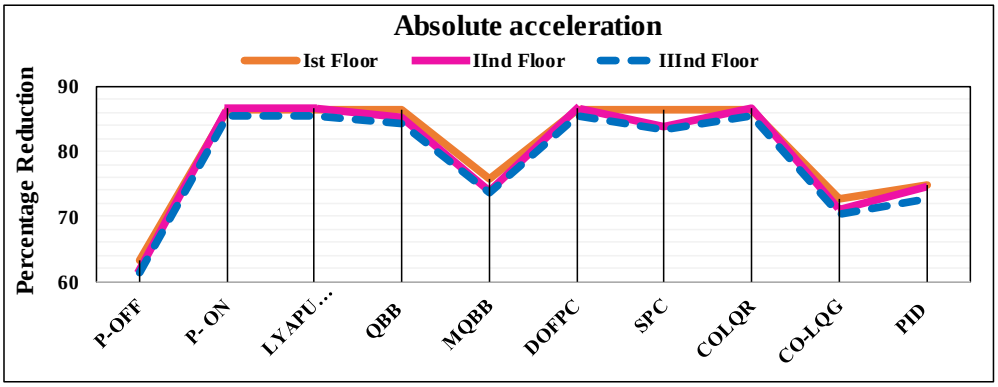

Figure 3.8 Response of the prototype structure subjected to Uttarkashi earthquake for different controllers (a) Relative displacement (b) Interstorey drift (c) Absolute acceleration

Further, the quantitative analysis is carried out for Uttarkashi earthquake occurred on 20 October 1991 in India. The percentage reduction in relative displacement due to various controllers is plotted in Figure 3.8(a). From this Figure, it is clearly seen that the maximum reduction in the third-floor displacement is achieved by Passive ON, Lyapunov, DOFPC and CO-LQR (85%) and closely followed by SPC and QBB (83%).

Similarly, the maximum percentage reduction in the absolute acceleration of the third floor as compared with the uncontrolled structure is achieved by using MQBB (59%) followed by simple passive control (SPC) (50%) and CO-LQG (46%) as seen from Figure 3.6(c). Further, for the

percentage reduction in the acceleration of the first floor is achieved by DOFPC (67%) and Passive ON (67%) and followed by Lyapunov based controller (63%). Further, the quantitative analysis is carried out for the Chile earthquake. Referring to Figure 3.7(a), the Passive ON, Lyapunov, DOFPC, and CO-LQR are the best performers achieving 82% reduction as compared with the uncontrolled structure in the relative displacement of the third floor. The maximum percentage interstorey drift reduction between the second-third floor is achieved by CO-LQR and Passive ON and DOFPC controller as can be seen in Figure 3.8(b). Likewise, the maximum percentage reduction in the third-floor acceleration is achieved by Passive ON and CO-LQR controller as shown in Figure 3.8(c).

Summary

This chapter is aim to provide the necessary fundamentals of the semi active control scheme. The mathematical modelling of the different blocks used in the semi active control scheme is presented. Because of the inherently nonlinear nature of the MR damper, one of the challenging aspects of utilizing this technology to achieve high levels of performance is in the development of appropriate control algorithms. Another purpose of this study is to evaluate a selection of control algorithms for use in single input semi active structural control systems.

Some recently proposed semi active control algorithms including the Passive ON/OFF DOFPC, SPC, the Lyapunov controller, the clipped-optimal LQR/LQG controller, QBB and the MQBB controller are discussed. These algorithms are formulated for use with MR damper and evaluated for the best performance for a three storey structure. The results showed comparable performance for controller group Passive ON/OFF MQBB, Lyapunov, SPC, and DOFPC as compared with the damper feedback controller group CO-LQR and CO-LQG.

However, the need for the damper feedback semi active controllers still exists because this kind of controllers is helpful for improvement in system capability. These controllers like QBB, MQBB and SPC etc. continuously provide input (electrical signal), based on the structural response, to the MR damper without considering its maximum capability whereas the damper feedback controllers like CO-LQR/LQG take the feedback from the MR damper and compare it with the desired force calculated by the control algorithm. Based on this comparison, the input signal is provided to the MR damper. Thus, the damper feedback controllers have better control over the actuator`s (MR damper) input.

CHAPTER 4: DEVELOPMENT OF MODIFIED LQR/LQG CONTROLLERS USING PSO-FFT AND PSO- τ_p^{max} APPROACHES

4.1 Introduction

The objective of applying semi active control system is to improve behaviour (i.e. response) of the structure by mitigating the effects of dynamic loadings such as an earthquake. This is an intricate task because of the nonlinear actuator dynamics, resonance conditions, dynamic coupling, uncertainties and measurement limitation. These issues can be handled by using an intelligent control algorithm in a semi active control scheme. Indeed, these challenges are the reasons, why developing a suitable control algorithm is still a very lucrative field of research.

The optimal control theory is used significantly in the control of the structures since decades by the researchers. The central idea of optimal control theory is to design a controller within defined constraints and boundary conditions to fulfil a certain criterion. Thus, the controller developed using optimal control theory tries to attain the best fit values of parameters required to fulfil the desired criterion within constraints. In seismic conditions, the controller needs to optimally adjust these parameters rapidly because the impulse-like excitations quickly send the system in a new set of states away from the initial states. Therefore, an aggressive optimization of the control parameter is advised at this time. It is, therefore, essential to understand the control objectives for structures to select appropriate parameters or weighting matrices of the optimal controller for the best results.

This chapter aims at the development of the modified LQR and LQG controllers modified using fast Fourier transform (FFT) and maximum dominant period (τ_p^{max}) approaches along with particle swarm optimization (PSO). Three main tasks are performed in this chapter. First, the development of adaptive LQR and LQG are carried out by modifying their parameters in real time using the PSO-FFT and PSO- τ_p^{max} approaches respectively. Second, the performance proposed controllers are investigated through numerical simulations on a scaled three story building fixed with an MR damper between ground and first floor. Simultaneously, the structural responses (i.e. relative displacement, interstorey drift and the absolute acceleration) produced by the widely employed LQR/LQG-based clipped-optimal controller are compared with the responses obtained using proposed controllers. Third, the effect of the higher modes on the performance of the proposed controllers is assessed on the five story structure. The conclusions obtained from this study are presented at the end of the chapter.

4.2 Development of modified LQR/LQG controllers using PSO-FFT approach

Development of modified LQR and modified LQG controller using PSO-FFT approach are carried out by modifying the control weighting matrix **R** in the conventional clipped optimal LQR and LQG controllers**.** These are explained subsequently in the following sections.

4.2.1 Development of modified LQR controller using PSO-FFT approach

In the Linear Quadratic Regulator (LQR) algorithm, the state weighting matrix **Q** and control weighting matrix **R** are determined only while designing the controller and the control effort depends on the components of the weighting matrix **R**. It is evident that earthquake signal is highly non-stationary having infinite frequency components. The frequencies in the earthquake excitation near to the natural frequency of the structure will cause quasi-resonance. Consequently, it results in higher structural responses that require higher control force for effective mitigation of structural responses. In conventional LQR controller, the matrices **Q** and **R** in the objective function given in Eq. (4.1) have global values and are not updated during the seismic occurrence to deliver larger control force required when quasi-resonance causes high structural responses. It is a serious drawback of this controller that need to be resolved appropriately. Therefore, to counter the effect of quasi-resonance, the conventional LQR must be amended by the intelligent choice of weighting matrices in real time. Moreover, this will also enhance the performance of the controller by saving the extra energy for non-resonant bands (i.e. no resonance between earthquake and structure).

The structural response reflects properties like the earthquake. Therefore, the entire duration of the response (0, t) is further divided into smaller time windows (t_w), with the i^{th} window being (t_{i-1}, t_i). Now, fast Fourier transform (FFT) is used to find the dominant frequency for each time window. This dominant frequency determines the quasi-resonance occurrences where the value of **R** is to be modified in real time during an earthquake. Here, it is appropriate to use the PSO algorithm to find the optimal value of **R** that gives the optimum structural response with lesser control effort. PSO algorithm helps to find weighting matrix **R** on the occurrences of quasi-resonance (i.e. quasi-resonant bands). It can be thought as the control weighting matrix **R** has a local solution instead of a global solution as in conventional LQR. The benefit of this specific local optimal solution is that it can change the estimation of matrix **R** at the frequency where the quasi-resonance occurs, unlike the conventional LQR which has a global value of **R** during an entire earthquake. The cost function to be minimized for this modified LQR problem

is formulated having state weighting matrix [$\mathbf{Q_i}$] and control weighting matrix [$\mathbf{R_i}$] for i^{th} window and it is given by Eq. (4.1).

$$J_i(x,u)=\int_0^t \left(x^T\mathbf{Q_i}\, x(t)+u^T\mathbf{R_i}\, u(t)\right) d(t) \tag{4.1}$$

The result of this modified optimal control problem with cost function J_i leads to a control law given by Eq. (4.2)

$$u = -[\mathbf{G_i}]\, x \tag{4.2}$$

The solution of the Ricatti matrix differential equation [111] for every windowed interval gives the gain matrix [$\mathbf{G_i}$] and the anticipated control force required to counter the effect of quasi-resonance can be found by applying this gain of the i^{th} window. The flow chart of the development of this adaptive LQR controller is shown in Figure 4.1.

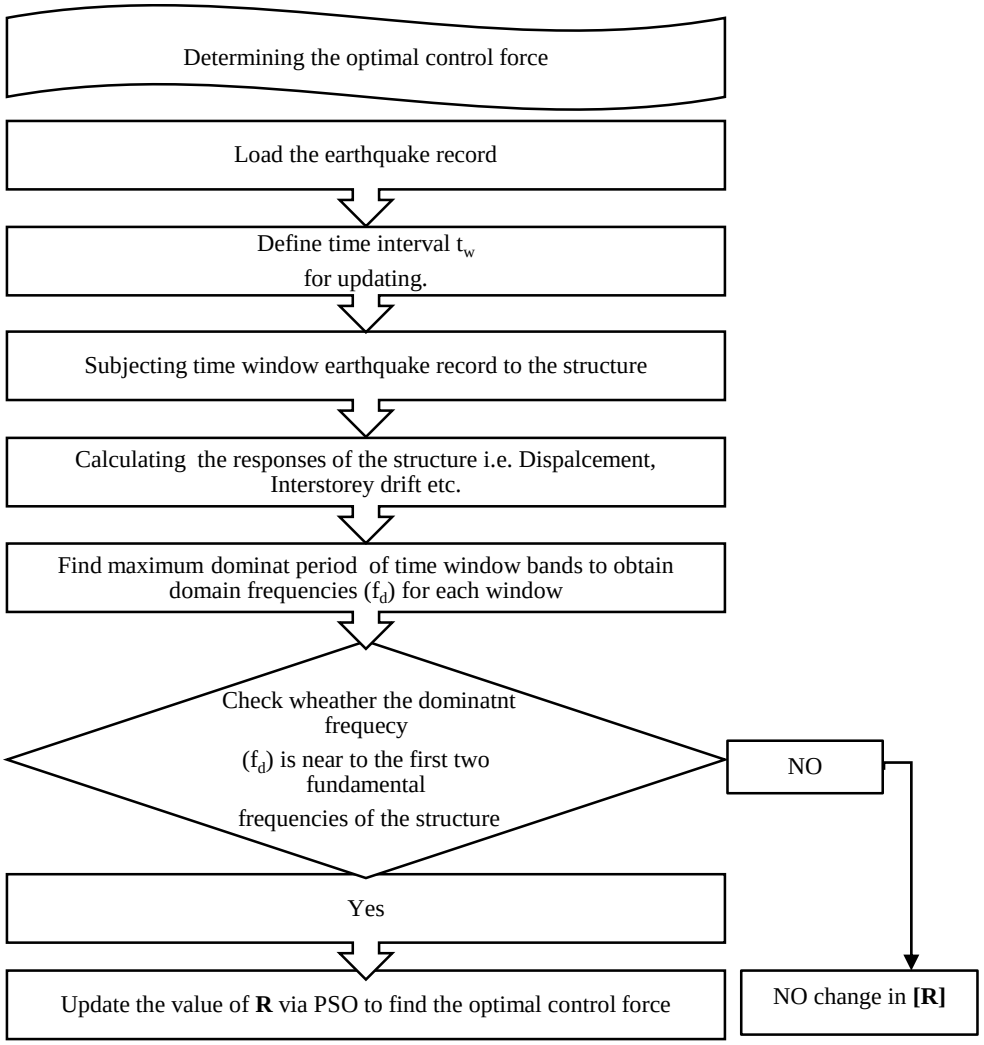

Figure 4.1 Development of modified LQR controller using FFT-PSO approach [141]

2.2 The particle swarm optimization (PSO)

The PSO algorithm was discovered in the 1990s by Kennedy and Eberhart. The PSO algorithm [132], [133] begins with an arbitrary populace (swarm) of people (particles) in the hunt space and chips away at the social conduct of the particles in the swarm. The position and the velocity of the k^{th} particle in the d-dimensional pursuit space can be symbolized as in Eqs. (4.3-4.4).

$$Q_k = \left[q_{(k,1)}, q_{(k,2),} q_{(k,3),} q_{(k,4),} \ldots\ldots q_{(k,d)}\right] \tag{4.3}$$

$$\dot{Q}_k = \left[\dot{q}_{(k,1),} \dot{q}_{(k,2),} \dot{q}_{(k,3),} \dot{q}_{(k,3),} \dot{q}_{(k,d),}\right] \tag{4.4}$$

Where Q and $\dot{Q}$ represent the position and velocity respectively of the particles. Every particle must have its own best position related to individual best objective value attained by now at time t. The global best particle (G_{best}) which characterizes the best particle found by this time in the entire swarm at the same time t [4], [134]. The updated velocity of each particle is given as in Eq. (4.5).

$$\dot{q}_{k,j}(t+1) = \partial \dot{q}_{k,j}(t) + a_1 b_1 + a_2 b_2 \left(G_{best}(t) - q_{k,j}(t)\right) \tag{4.5}$$

Here, j is a real positive integer and can have value j=1,2……d. where d is a natural number. Here, a_1 and a_2 are acceleration coefficients, ∂ is the inertia factor and b_1 and b_2 are two independent arbitrary numbers unvaryingly dispersed in the range of [0, 1]. The position update of each particle in each generation is given in Eq. (4.6).

$$q_{k,j}(t+1) = q_{k,j}(t) + \dot{q}_{k,j}(t+1) \tag{4.6}$$

The objective function of the PSO algorithm for each ground motion is dependent on the displacement of the structure and is represented as in Eq. (4.7) in terms of the displacement $x_k(t)$ of the k^{th} floor

$$J_{PSO} = \int_0^{t_i} \{x_{k+1}(t) - x_k(t)\}^2 \, dt \tag{4.7}$$

The control weighting matrix **R** decreases when the structure has higher displacement due to quasi-resonance. This lessening of weighting matrix **R** sets off the reduction of structural response without any loss. Therefore, the merit of the advised modified LQR method is that the gain matrices are ascertained adaptively by the PSO algorithm, unlike the time-varying LQR case described in the literature [111]. In the PSO algorithm, the solution obtained via meeting

the stopping criteria is considered the optimal solution. If the algorithm is going to execute maximum iteration, it may not be optimal solution. Going for the maximum iteration means the algorithm did not find the best optimal solution yet. To find an optimal solution now it is required to vary the parameter of the PSO algorithm and run the simulation again in the quest for an optimal solution via stopping criteria. It is shown by the flowchart in Figure 4.2.

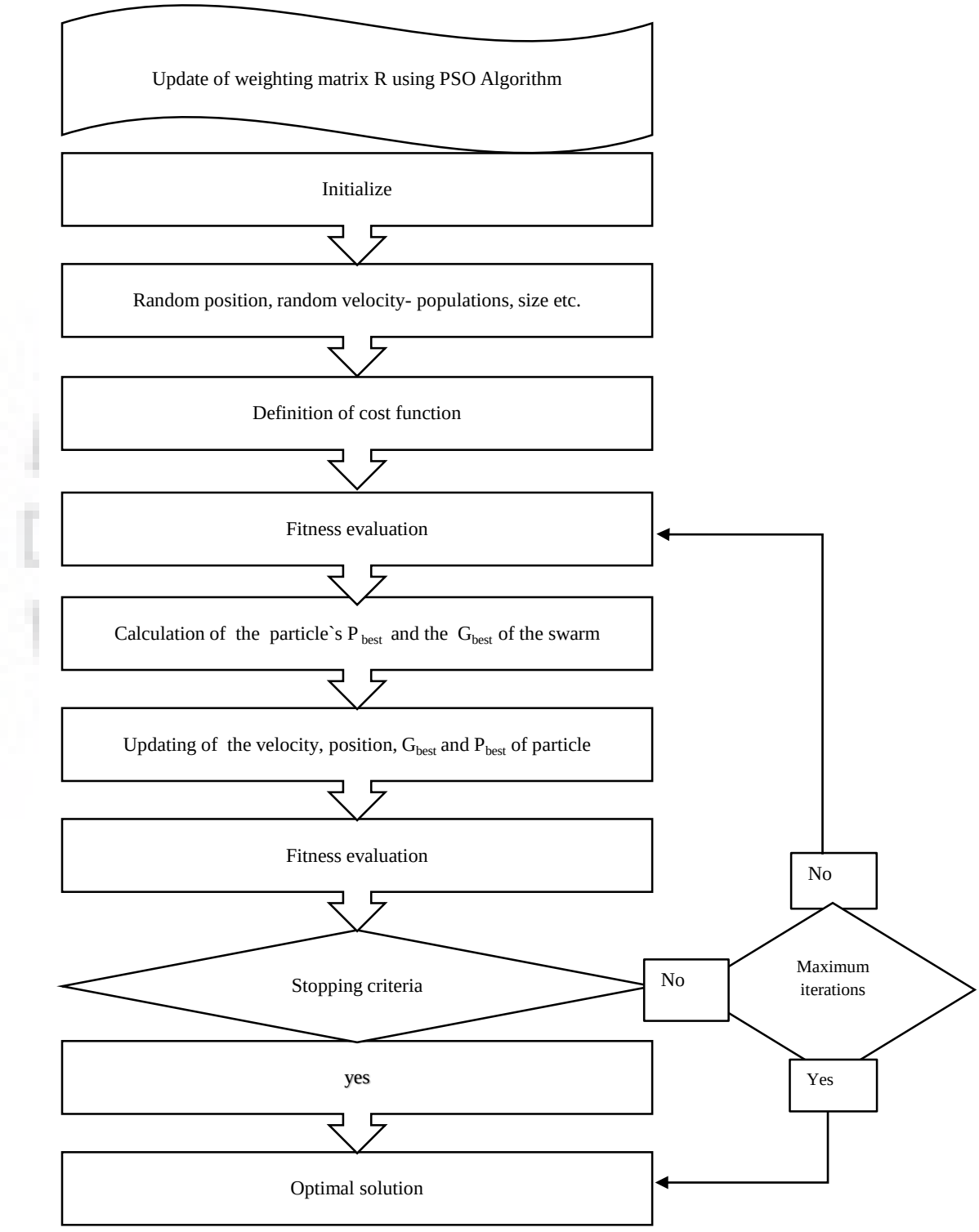

Figure 4.2 Flowchart representation of PSO algorithm [138]

Comprehensive performance analysis of the proposed controllers is carried out by comparing of the structural responses of the three storey test structure (see section 3.2) obtained using the proposed controllers and the corresponding conventional controllers under the following conditions as listed in section 1.3 of chapter 1.

(i) Using different earthquake time histories.

(ii) Using an earthquake recorded in different soil conditions.

(iii) Placing the MR damper on different floors.

(iv) Considering a situation, if power is lost at the peak of the earthquake

There exist two main regulatory control objectives in the structural control namely acceleration mitigation, and displacement mitigation. Acceleration mitigation is a serviceability criterion whereas displacement mitigation deals with structural integrity. The acceleration criterion allows higher robustness for the control algorithm due to lesser concern of structural integrity. Though acceleration mitigation is important, displacement mitigation is a prevalent concern during earthquake excitations because structural integrity is at stake. For structural integrity, it is essential to minimize stresses and strains in structural members. Therefore, in present discussion emphasis is given on the displacement mitigation. Further, a new parameter of the performance analysis, cumulative energy, confined in the displacement signal of the top floor is introduced. This parameter gives the magnitude of the disruptive energy content of the displacement signal. The cumulative energy (W) for any continuous time signal x(t), is given by following Eq. (4.8)

$$W = \int_0^t |x(t)|^2 \, dt \tag{4.8}$$

4.2.3 Results and discussion on the performance of PSO-FFT-modified-LQR controller

To scrutinize the effectiveness of the proposed adaptive LQR (PSO-FFT-modified-LQR) controller, the dynamic analysis of three storey test structure having an MR damper between the ground and the first floor is presented. The state weighting matrix **Q** is the same as in the clipped optimal LQR presented in [1] for every time window (t_w).

(i) Using different earthquake time histories

For analysis under this condition, following three earthquake time histories shown in Figure 4.3(a-c) are used.

(a) 1940 El-Centro Valley earthquake (c) 1999 Gebze Turkey earthquake

(b) 1999 Chi-Chi Nantou County Taiwan earthquake

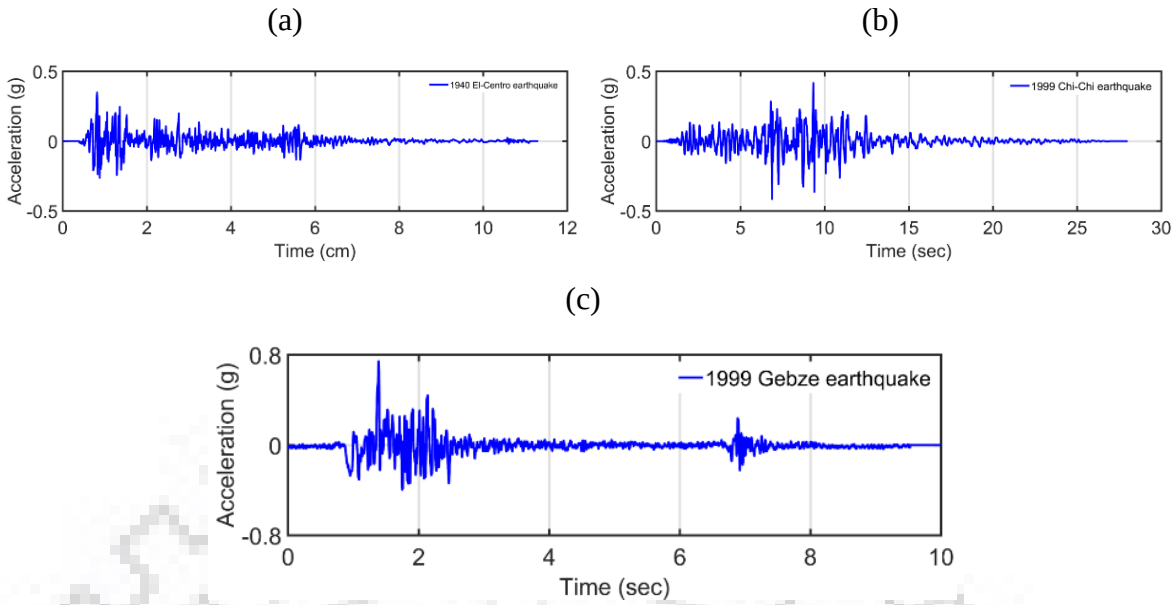

Figure 4.3 N–S component of time histories (a) 1940 earthquake at El-Centro site USA (b) 1999 Chi-Chi Nantou County Taiwan earthquake (c) 1999 Gebze Turkey earthquake.

The comparative analysis between the structural responses obtained using conventional LQR controller and proposed PSO-FFT-modified-LQR controller is carried out. Two popular methodologies can be employed to demonstrate the effect of the proposed controller on the structural responses. These are qualitative analysis and quantitative analysis. For qualitative analysis in the present study, the visual inspection of the time histories of the relative displacement responses of the third floor of the structure using PSO-FFT-modified-LQR and the clipped optimal-LQR (CO-LQR) is carried out. Whereas, for quantitative analysis, the comparison of the reduction in the peak values of the structural responses for all three floors of the structure using a proposed controller and the CO-LQR controller is carried out. The peak values of the structural responses (i.e. relative displacement (X_n), inter-story drift (ID_n) and absolute acceleration (A_n) of the test structure subjected to various earthquake time histories are presented in Table 4.1.

Initial 5 seconds of time histories of structural responses of the third floor of test structure subjected to El-Centro earthquake are shown in Figure 4.4. The reason is that the maximum energy is confined in the initial 5 seconds of the El-Centro earthquake. For a similar reason, the time histories of the structural responses due to the Chi-Chi and Gebze earthquake are shown for the initial 20 seconds in Figure 4.5 and 8 seconds in Figure 4.6 respectively.

For the structure subjected to El-Centro earthquake, the relative displacement response of the third floor of the uncontrolled structure is shown in Figure 4.4(a) whereas comparison of uncontrolled relative displacement response and relative displacement response due to CO-LQR

and the proposed controller is shown in Figure 4.4(b). From Table 4.1, this reduction in the peak values is 68% using CO-LQR and 82% using the PSO-FFT-modified-LQR.

Inspection of Figure 4.4(c) concludes that the displacement is reduced using the proposed controller throughout earthquake time history. From Table 4.1, the reduction in the peak values of relative displacement using the proposed controller is 23%, 19% and 24% for first, second and third floor respectively as compared with the CO-LQR. The change in the control weighting matrix **R** according to the occurrences of the quasi-resonance is shown in Figure 4.4(e). The value of **R** for the CO-LQR remains same through the seismic event whereas, for proposed algorithm, there are variations of in the value of **R** for each time window (t_w) according to the quasi-resonance between the domain frequency and first two fundamental frequency of the structure. It is to note that a larger value of **R** corresponds to lesser control force and a smaller value of **R** corresponds to the larger control force. The value of **R** changes in real time and determined optimally using the PSO algorithm. In this way the control force used to mitigate the seismic vibration is used intelligently, therefore, saving the precious power amid the seismic event. This is an advantage of the proposed algorithm over the CO-LQR.

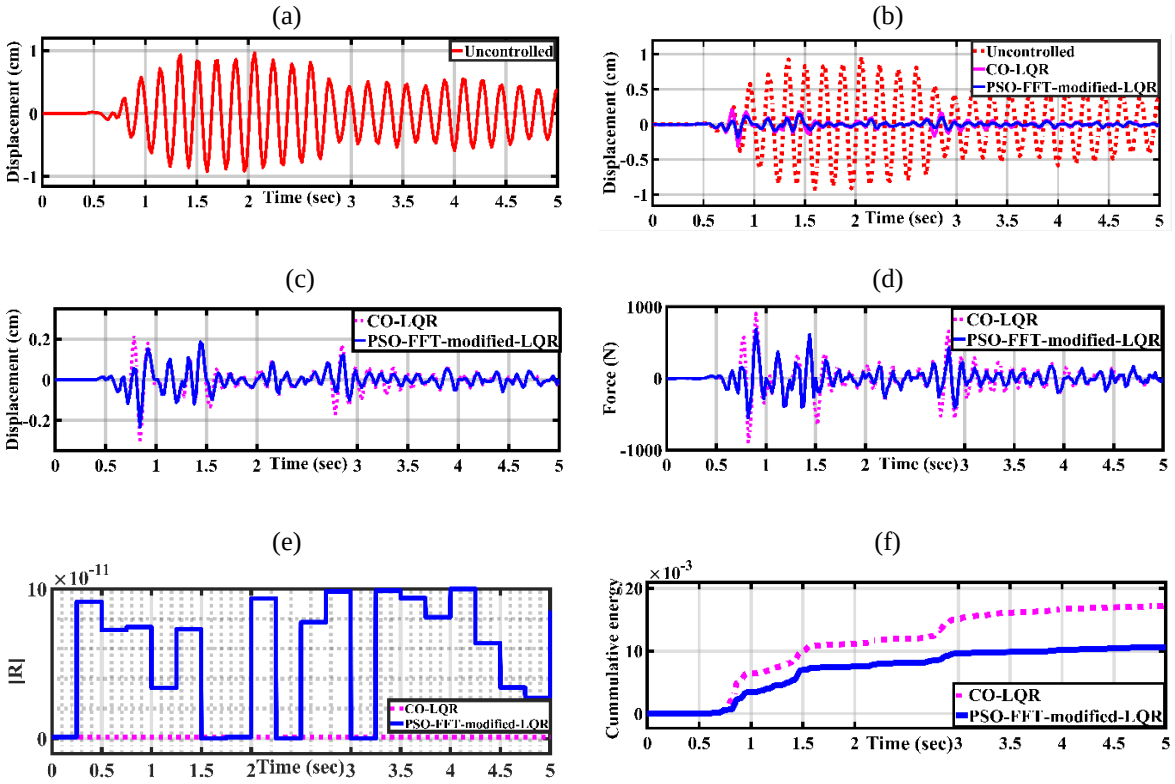

Figure 4.4 Structural responses for the structure subjected to the 1940 El-Centro earthquake (a) displacement response of third floor of uncontrolled structure (b) comparison of controlled responses of third floor using CO-LQR and PSO-FFT-modified-LQR algorithms (c) control forces for the CO-LQR and the PSO-FFT-modified-LQR algorithm (d) variation of **R** with time (e) comparison of cumulative energies of the third floor`s displacement by applying CO-LQR and PSO-FFT-modified-LQR

Additionally, the proposed control algorithm achieved the reduction in the peak values of the interstorey drift by 15% between the first-second floor and 33% between second-third floor as compared with the CO-LQR. The reduction in peak values of the absolute acceleration is also deduced from Table 4.1. Observations from Table 4.1 reveal that the proposed algorithm can reduce the peak values of the acceleration by 44% for the first floor, 14% for the second floor and 32% for the third floor as compared with the CO-LQR.

It is necessary to point out here that all these reductions in the structural responses are achieved using lesser control force as shown in Figure 4.4(d). The proposed controller utilizes 25% lesser force (peak value) to achieve the above-mentioned results as compared with the CO-LQR as can be seen from Table 4.1. Comparison of the energy confined in the signal of the relative displacement of the third floor due to CO-LQR and the PSO-FFT-modified-LQR controllers is shown in Figure 4.4(f). This comparison indicates that the displacement signal due to the proposed controller has the lesser energy for destruction as compared with the displacement signal due to the CO-LQR.

Table 4.1 Peak responses of structure using PSO-FFT-modified-LQR and CO-LQR controller for various earthquake time histories.

Control algorithm	El-Centro earthquake			Chi-Chi earthquake			Gebze earthquake		
	Uncontrolled	CO-LQR	PSO-FFT-modified LQR	Uncontrolled	CO-LQR	PSO-FFT-modified LQR	Uncontrolled	CO-LQR	PSO-FFT-modified LQR
Displacement (cm)	0.55	0.09	0.07	0.14	0.03	0.02	0.074	0.021	0.020
	0.83	0.20	0.16	0.22	0.05	0.03	0.117	0.032	0.030
	0.97	0.31	0.23	0.27	0.06	0.04	0.138	0.06	0.050
Inter story drift(i_d) (cm)	0.55	0.09	0.07	0.14	0.021	0.02	0.074	0.021	0.020
	0.29	0.10	0.09	0.08	0.02	0.01	0.042	0.017	0.010
	0.14	0.11	0.07	0.05	0.011	0.01	0.022	0.026	0.020
Acceleration (cm/s^2)	870	474	266	181	38	36	126	81	59
	1070	540	465	268	63	59	150	95	68
	1400	772	525	317	101	96	185	114	110
Force (N)	0	984	737	0	1398	1190	0	1080	1050

For Chi-Chi earthquake, referring to the Figure 4.5, the displacement response of the third floor of the uncontrolled structure is shown in Figure 4.5(a) whereas comparison of the uncontrolled displacement response and response due to CO-LQR and PSO-FFT-modified-LQR controller is shown in Figure 4.5(b). It can be seen in Figure 4.5(b) that the displacement response is reduced. For Chi-Chi earthquake, comparison of displacement response due to CO-LQR and PSO-FFT-modified-LQR is shown in Figure 4.5(c) whereas, for Gebze earthquake, the same is presented in Figure 4.6(c). It can be concluded from Figures 4.5(c) and 4.6(c) that the displacement is reduced using the proposed controller throughout the time history.

According to the Table 4.1, the reduction in the peak values of displacement using the proposed controller is 33%, 40% and 34% for first, second and third floor respectively for Chi-Chi earthquake and 5%,12% and 17% for first, second and third floor for Gebze earthquake as compared with the CO-LQR. For CO-LQR the value of **R** remains same through the seismic event whereas in the proposed algorithm the value of **R** changes according to the quasi-resonance between the domain frequency of each time window (t_w) and first two fundamental frequency of the structure. Variations of the control weighting matrix **R** are shown in Figure 4.5(e) for Chi-Chi earthquake whereas for Gebze earthquake it is shown in Figure 4.6(e).

In fact, the variations in the control weighting matrix **R** lead the PSO-FFT-modified controller to deliver better structural responses especially relative displacement and so, the interstorey drift. For the comfort of the occupant of the structure, the interstorey drift must be less. It is shown through the numerical analysis that the interstorey drift is reduced effectively using the proposed controller. From Table 4.1, for Chi-Chi earthquake, the proposed control algorithm achieved the reduction in interstorey drift by 50% between the first-second floor and 10% between second-third floor as compared with the CO-LQR. Similarly, for Gebze earthquake, the proposed controller achieved the reduction in the interstorey drift by 43% between the first-second floor and 22% between the second- third floor as compared with the CO-LQR.

The observations from Table 4.1 confirm that the proposed algorithm can reduce the peak values of the acceleration by 6%,6%,5% for Chi-Chi earthquake whereas for Gebze earthquake, reductions of 28%, 28%, 4% for the first, second and third floor respectively are achieved as compared with the CO-LQR. These reductions in the structural responses are achieved using lesser control force as shown in Figure 4.5(d) for Chi-Chi earthquake and in Figure 4.6(d) for the Gebze earthquake. It can be seen from Table 4.1 that the proposed controller utilised 15% lesser force (peak value) for Chi-Chi earthquake and 3% lesser force for Gebze earthquake to achieve the above-mentioned results. The comparison of the cumulative energies of the third floor`s displacement by applying CO-LQR and the PSO-FFT-modified-LQR is shown in Figure 4.5(f) for Chi-Chi earthquake and Figure 4.6(f) for Gebze earthquake. Figures 4.5(f) and 4.6(f) show that the cumulative energy of the third floor`s displacement applying the proposed algorithm is less than that of CO-LQR. This cumulative energy indicates that the controlled displacement response signal using the proposed controller has the lesser energy for the damage. The more is the energy, more will be damaging capability. Since this energy is in the displacement signal of the third floor obtained using the proposed controller, therefore, the structural integrity is

protected. In this way, the structural responses are reduced more effectively by employing a proposed adaptive LQR controller instead of conventional clipped optimal LQR controller.

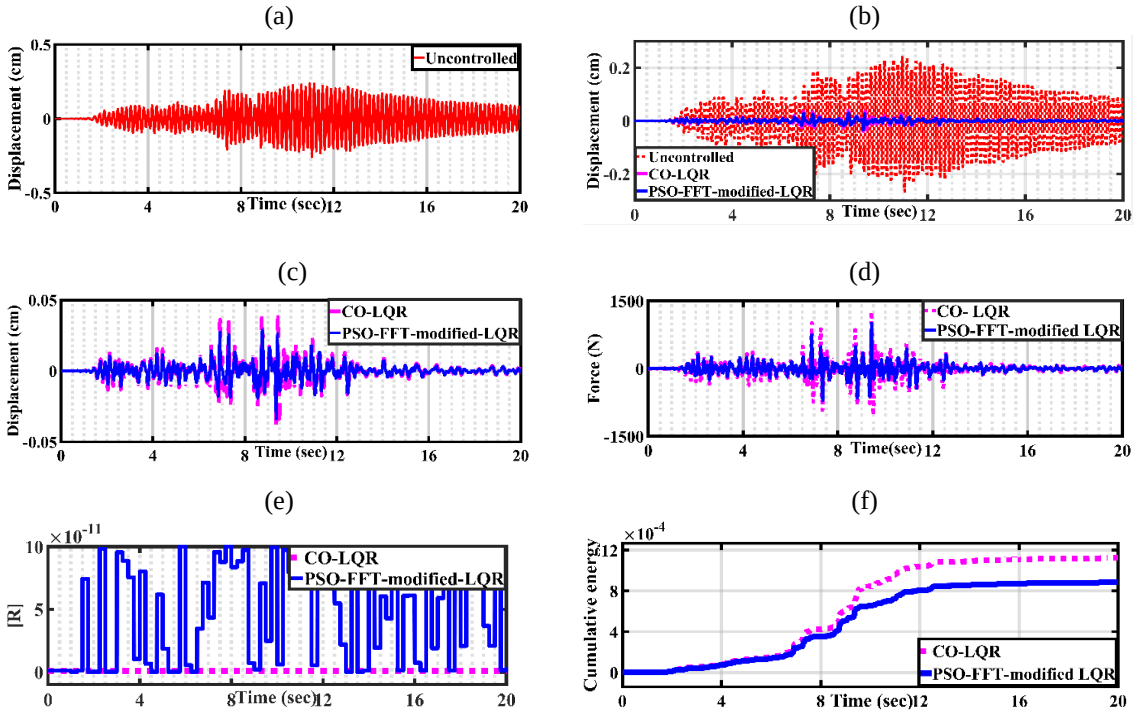

Figure 4.5 Structural responses for the structure subjected to 1999 Chi-Chi earthquake (a) displacement response of third floor of uncontrolled structure (b) comparison of controlled responses of third floor using CO-LQR and PSO-FFT-modified-LQR algorithms (c) control forces for the CO-LQR and the PSO-FFT-modified-LQR algorithm (d) variation of **R** with time (e) comparison of cumulative energies of the third floor`s displacement by applying CO-LQR and PSO-FFT-modified-LQR

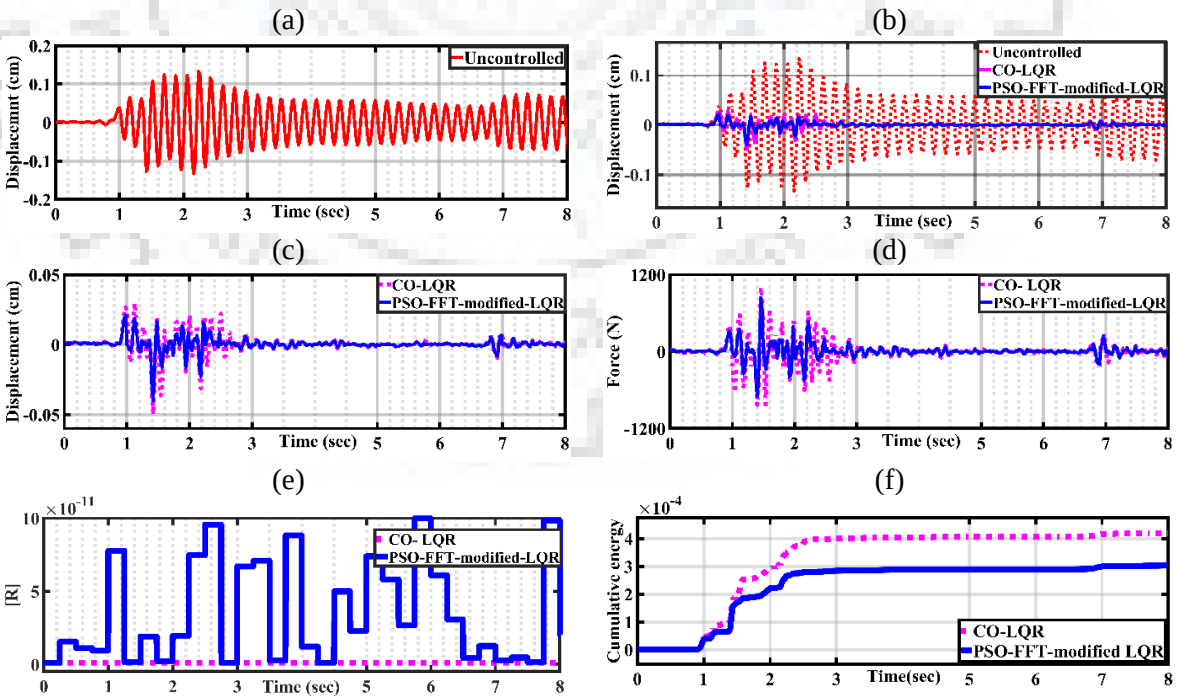

Figure 4.6 Structural responses for the structure subjected to 1999 Gebze earthquake (a) displacement response of third floor of uncontrolled structure (b) comparison of controlled responses of third floor using CO-LQR and PSO-FFT-modified-LQR algorithms (c) control forces for the CO-LQR and the PSO-FFT-modified-LQR algorithm (d) variation of **R** with time (e) comparison of cumulative energies of the third floor`s displacement by applying CO-LQR and PSO-FFT-modified-LQR

(ii) Using an earthquake recorded in different soil conditions

The soil conditions change the characteristics of ground motions significantly. All the three ground motion characteristics (viz. intensity, frequency and duration) are being modified by the soil conditions. The objective of the selecting ground motions recorded in different soil types is to check the effectiveness of the proposed controller in different soil conditions. For this purpose, an earthquake recorded in Japan (having the station names SAG001, SAG005 and SAG001) deployed in three different soil conditions (i.e. hard soil, medium soil and soft soil), is used. This earthquake record is taken from the Kyoshin network (K-NET). The soil type is determined according to the federal emergency management agency (FEMA)-356 based on the shear wave velocity (v_s) given in Table 4.2.

Table 4.2 Classification of the soil based on shear wave velocity (v_s) [135]

Serial number	Soil type	Shear wave velocity (v_s)
1.	Hard soil	>1500 m/s
2.	Medium soil	750 m/s < v_s <1500m/s
3.	Soft soil	180 m/s < v_s < 750 m/s

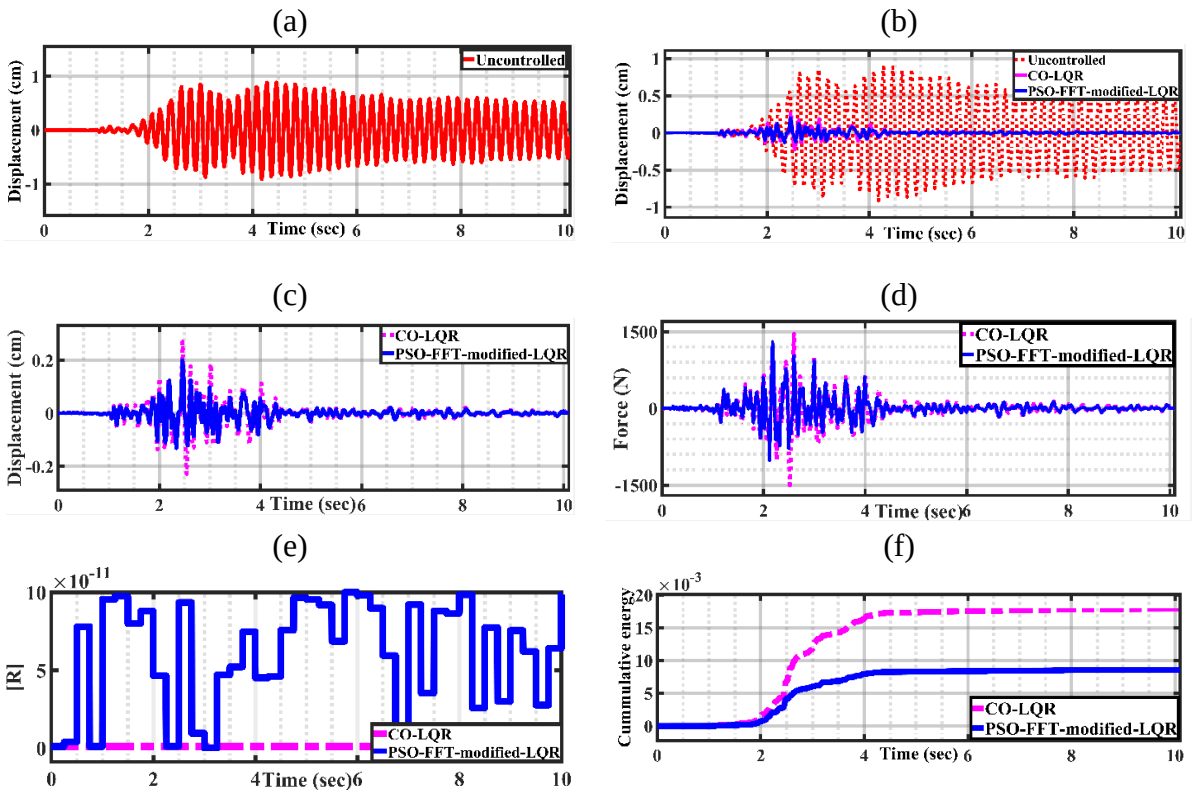

Figure 4.7 Structural responses for the structure subjected to hard soil earthquake (a) displacement response of third floor of uncontrolled structure (b) comparison of controlled responses of third floor using CO-LQR and PSO-FFT-modified-LQR algorithms (c) control forces for the CO-LQR and the PSO-FFT-modified-LQR algorithm (d) variation of **R** with time (e) comparison of cumulative energies of the third floor`s displacement by applying CO-LQR and PSO-FFT-modified-LQR

For the performance assessment in hard soil, the displacement response of the third floor of the structure is shown in Figure 4.7. Figure 4.7(a) shows the third floor`s displacement of the uncontrolled structure. To show the effectiveness of structural control, a comparison of the third floor`s displacement responses of the uncontrolled structure and semi-actively controlled structure using CO-LQR and PSO-FFT-modified-LQR control algorithm is shown in Figure 4.7(b). Figure 4.7(b) shows that the displacement response is reduced through seismic event effectively. The peak values of the structural responses are given in Table 4.4. From Table 4.3, the reduction in the peak value of the displacement response is 43% using CO-LQR and 80% using the proposed PSO-FFT-modified-LQR as compared with the uncontrolled structure.

Table 4.3 Peak responses of structure using PSO-FFT-modified-LQR and CO-LQR controller for earthquake recorded in different soil conditions.

Control algorithm	Earthquake (Hard Rock)			Earthquake (Medium soil)			Earthquake (Soft soil)		
	Uncontrolled	CO-LQR	PSO-FFT-modified LQR	Uncontrolled	CO-LQR	PSO-FFT-modified LQR	Uncontrolled	CO-LQR	PSO-FFT-modified LQR
Displacement (cm)	0.66	0.28	0.12	0.60	0.38	0.20	0.99	0.24	0.14
	0.80	0.42	0.16	0.93	0.45	0.27	1.26	0.50	0.38
	0.99	0.56	0.20	1.20	0.50	0.31	1.53	0.87	0.47
Inter story drift(i_d) (cm)	0.66	0.28	0.12	0.60	0.38	0.20	0.99	0.24	0.14
	0.14	0.14	0.04	0.33	0.08	0.06	0.27	0.26	0.22
	0.19	0.14	0.04	0.27	0.05	0.04	0.27	0.27	0.11
Acceleration (cm/s^2)	1167	501	293	830	621	526	852	576	525
	1287	527	304	1018	709	610	1217	757	625
	1356	570	328	1157	986	880	1299	890	806
Force (N)	--	1731	1334	--	1634	1502	--	1866	1619

Comparison of displacement response due to CO-LQR and PSO-FFT-modified-LQR depicted in Figure 4.7(c) reveals that the proposed controller reduces the displacement more effectively. This reduction in peak values of the relative displacement is by 57% for the first floor, 63% for the second floor and 65% for the third floor as compared with the CO-LQR controller. The inter-story drift is reduced by 72% for the first-second floor and 79% for the second-third floor on applying the proposed control algorithm instead of CO-LQR in the semi active control scheme. Alike, accelerations for the first, second and the third floor are reduced by 41%,43% and 42% respectively as compared with the CO-LQR. The proposed controller attains these reductions in structural responses using 23% lesser force than the CO-LQR controller as

can be seen from Table 4.3 and from the comparison of both the forces as shown in Figure 4.7(d). The variations in the value of **R** are shown in Figure 4.7(e). The comparison of the cumulative energy of the third floor`s displacement response using CO-LQR and the proposed controller is shown in Figure 4.7(f) which shows that displacement response due to the proposed controller has the lesser energy for disruption.

For soft soil, the comparison of the displacement time histories of an uncontrolled and controlled structure employing CO-LQR and proposed control algorithm is shown in Figure 4.8(b) in which the proposed controller mitigates the displacement effectively throughout the earthquake. Comparison of displacement responses due to CO-LQR and the proposed controller is plotted in Figure 4.8(c) which shows that the proposed controller reduced the displacement response more effectively.

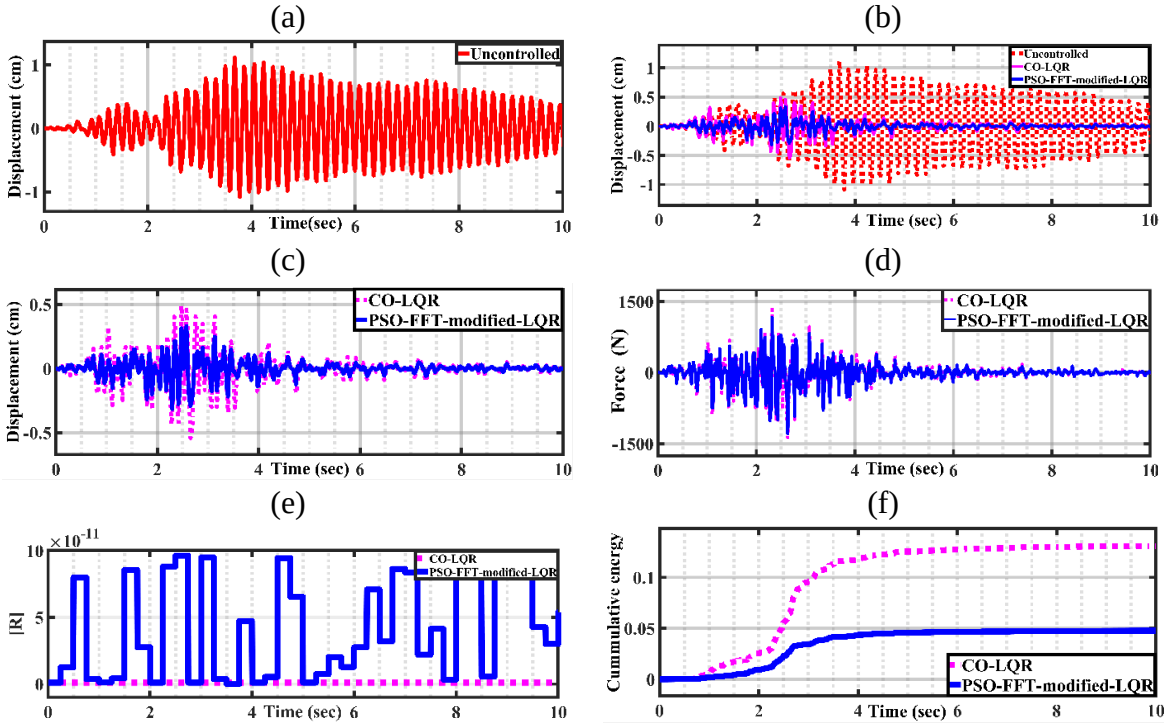

Figure 4.8 Structural responses for the structure subjected to medium soil earthquake (a) displacement response of third floor of uncontrolled structure (b) comparison of controlled responses of third floor using CO-LQR and PSO-FFT-modified-LQR algorithms (c) control forces for the CO-LQR and the PSO-FFT-modified-LQR algorithm (d) variation of **R** with time (e) comparison of cumulative energies of the third floor`s displacement by applying CO-LQR and PSO-FFT-modified-LQR

Observing Table 4.3, the proposed controller achieved a reduction in the displacement by 49%, 41% and 38% for first, second and third floor respectively as compared with the CO-LQR. The interstorey drift between the first-second floor and second third floor are reduced by 25% and 20% more using the proposed controller in place of CO-LQR. Alike, the proposed controller reduced the absolute accelerations for the first, second and the third floor more by 15%,14% and 11% respectively as compared with the CO-LQR. These reductions in structural responses

achieved by the proposed controller using 8% lesser force than the CO-LQR as can be seen in Table 4.3. Variation of the values of the control weighting matrix **R** is shown in Figure 4.8(e). The comparison of the cumulative energies of displacement of the third floor is shown in Figure 4.8(f) which shows that the displacement signal obtained using the proposed controller has the lesser energy for obliteration.

Now the assessment of the proposed controller is carried out by considering the structure is subjected to an earthquake recorded in soft soil. The soft soil works as an amplifier to the intensity of the earthquake hence it becomes difficult to control the structure effectively. Displacement of the third floor of the uncontrolled structure is shown in Figure 4.9(a) which is to be reduced by employing the semi active control scheme. The comparison of the time histories of the displacement response obtained using uncontrolled structure, by employing CO-LQR control algorithm and the proposed control algorithm is shown in Figure 4.9(b). Observing Figure 4.9(b), it can be concluded that effective performance is achieved by both control algorithms as compared to uncontrolled response.

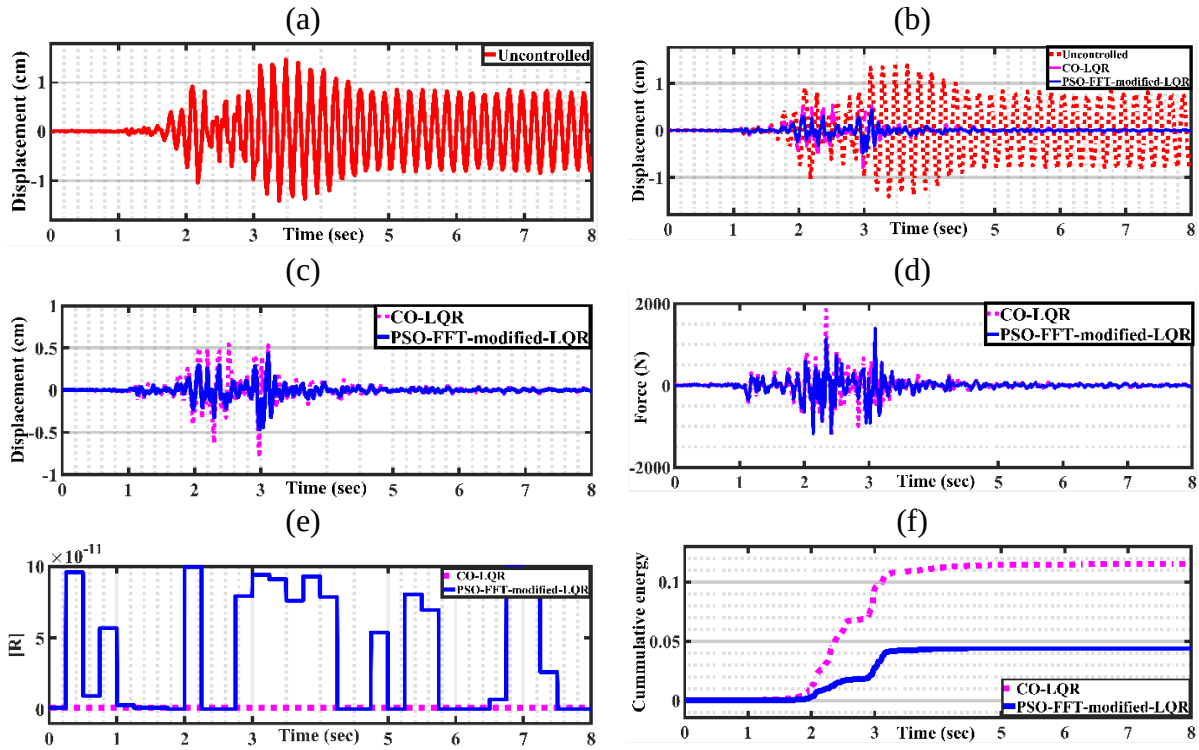

Figure 4.9. Structural responses for the structure subjected to soft soil earthquake (a) displacement response of third floor of uncontrolled structure (b) comparison of controlled responses of third floor using CO-LQR and PSO-FFT-modified-LQR algorithms (c) control forces for the CO-LQR and the PSO-FFT-modified-LQR algorithm (d) variation of **R** with time (e) comparison of cumulative energies of the third floor`s displacement by applying CO-LQR and PSO-FFT-modified-LQR

To estimate the preeminence between the CO-LQR and the proposed controller, the comparison of the third floor`s displacement time histories obtained using CO-LQR and the proposed control algorithm are shown in Figure 4.9(c). it can be concluded in Figure 4.9(c) that the proposed

algorithm demonstrates better displacement reduction capability as compared to the CO-LQR. The same can be verified by observing Table 4.3. The reductions in the peak values of displacement of the first, second and the third floor using the proposed controller are 42%,24% and 46% respectively as compared to the CO-LQR.

Further, the interstorey drift between the first-second floor and second-third floor is reduced respectively by 15% and 59% more using the proposed controller in place of CO-LQR.

Alike, the proposed controller reduced the absolute accelerations for the first, second and the third floor by 9%,17% and 9% respectively as compared with the CO-LQR. These reductions in structural responses achieved by the proposed controller using 13% lesser force than the CO-LQR. This can also be seen in Figure 4.9(d) in which the comparison of the time histories of the CO-LQR and PSO-FFT-modified LQR is demonstrated. Further, the variation of the values of the control weighting matrix **R** is shown in Figure 4.9(e). The comparison of the cumulative energies of the displacement of the third floor is shown in Figure 4.9(f).

Thus, based on the above discussion it can be concluded that the proposed controller gives the better performance over the CO-LQR for a semi active control scheme in hard, medium and soft soil conditions.

(iii) Effect of placing MR damper on different floors

In the present study, an MR damper is being used between the ground and first floor of the prototype three-story structure. Now, the analysis is carried out for PSO-FFT-modified-LQR controller by varying the position of MR damper to find the best location for the damper placement within the structure for attaining maximum performance of the proposed control algorithm in the semi active control scheme. This analysis is carried out by placing the MR damper within the three storey structure at (a) ground floor (b) first floor and, (c) second floor respectively. For each case, the structure is subjected to the three-different earthquake namely El-Centro earthquake, Chi-Chi earthquake and Gebze earthquake for robust numerical testing of the proposed controller.

First, for El-Centro earthquake, the percentage reductions in the peak structural responses (i.e. relative displacement, inter-storey drift, and the absolute acceleration) are shown in Figure 4.10. The percentage reduction in third floor`s relative displacement is 76%,69%, 68% whereas it is 81%,76%,74% in second floor`s displacement and 87%,84%,82% in the first floor`s displacement when damper is kept on the ground, first and second floor respectively.

Observing Figure 4.10(b), the percentage reduction in the inter-storey drift between the first-second floor is 69%, 62% 58% whereas percentage reduction between second-third floor is 49%,34%,27% when the damper is kept on the ground, first and second floor respectively. Because the inter-storey drift of the first floor is equal to relative displacement, therefore, for the first floor, the percentage reduction is 82%,74% and 68% when the damper is kept on the ground, first and second floor respectively.

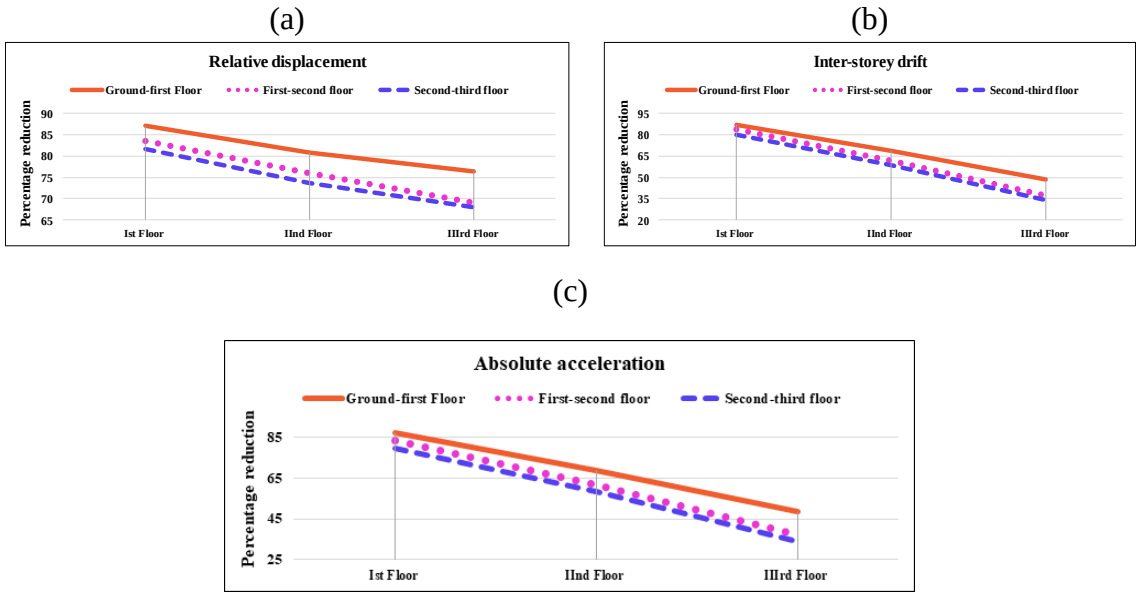

Figure 4.10 Percentage reductions in the structural responses using PSO-FFT-modified-LQR in the structure subjected to El-Centro earthquake by placing MR damper at different floors (a) Relative displacement (b) Inter-storey drift (c) Absolute acceleration

Observations from Figure 4.10(c) reveal that the percentage reduction in the third floor`s absolute acceleration is 62%,56%, 54%, the percentage reduction in the second floor`s absolute acceleration is 57%, 54%,50% and for the first floor, reduction is 69%, 66%, 64% when damper is kept on the ground, first and second floor respectively. For Chi-Chi earthquake time history, the maximum percentage reduction in relative displacement for every floor of the structure is shown in Figure 4.11(a).

The percentage reduction in the third floor`s relative displacement is 85%, 70%, 56%, the percentage reduction in the second floor`s relative displacement is 86%,68%,59% and the percentage reduction in the first floor`s relative displacement is 86%,64%,54% when damper is kept on the ground, first and second floor respectively. the first-second floor is 88%,75%,69% whereas the percentage reduction in the inter-storey drift between second-third floor is 80%,70%, 40% respectively when the damper is kept on the ground first and the second floor respectively. Because relative displacement is equal to the inter-storey drift for the first floor, therefore, for the first floor, it is reduced by 87%, 84% 80% when the damper is kept on the ground, first and

second floor respectively. Figure 4.11(c) reveals that the percentage reduction in the third floor`s absolute acceleration is 70%, 62%, 54%, the percentage reduction in the second floor`s acceleration is 78%, 67%, 62%. and percentage reduction in the first floor`s relative displacement is 80%,75%,69% when the damper is kept on the ground, first and second floor respectively.

To place a MR damper on any floor (i.e. ground, first or second floor) of the three storey structure makes the overall system multiple input single output (MISO). It is easy to design a controller with lesser complexity for the MISO system.

(a)

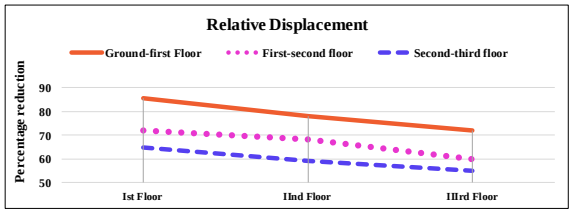

(b)

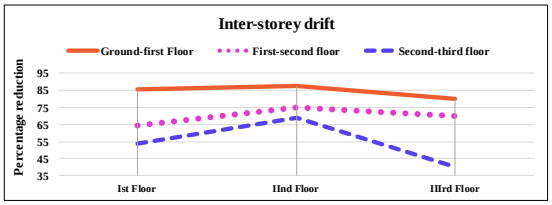

(c)

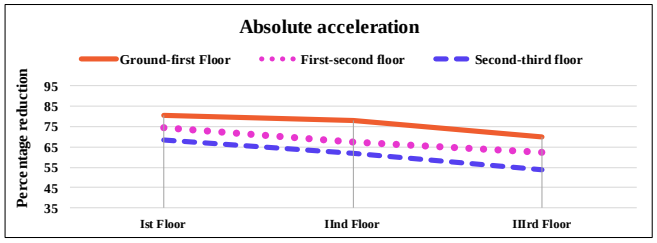

Figure 4.11 Percentage reductions in the structural responses using PSO-FFT-modified-LQR in the structure subjected to Chi-Chi earthquake by placing MR damper at different floors (a) Relative displacement (b) Inter-storey drift (c) Absolute acceleration

For Gebze earthquake, the maximum percentage reduction in relative displacement for every floor of the structure is shown in Figure 4.12(a). The percentage reduction in the third floor`s relative displacement is 64%,57%,48%, for second floor it is 66%,60%,51% and for the first floor the percentage reduction is 73%,66%,60% when the damper is kept on the ground, first and second floor respectively. Observing Figure 4.12(b), the percentage reduction in the inter-storey drift between the first-second floor is 52%,48%,36%, between second-third floor is 55%,45%,32% and for first floor, it is reduced by 73%, 66% 60% when damper is kept on the ground, first and second floor respectively. Figure 4.12(c) reveals that the percentage reduction in the third floor`s absolute acceleration is 41%,27%, 23%, for the second floor it is 55%,46%,39% and for the first floor, percentage reduction is 53%,41%, 32% when damper is kept on the ground, first and second floor respectively. It can be seen from Figure 4.10(a-c), Figure4.11(a-c) and Figure4.12(a-c) that maximum percentage reduction in structural response is achieved by placing MR damper on the ground floor and minimum percentage reduction is attained when MR damper is kept on the second floor. It is substantial to point out here that the

difference between the force applied to the structure in attaining the maximum and minimum percentage reductions in the structural responses is very less.

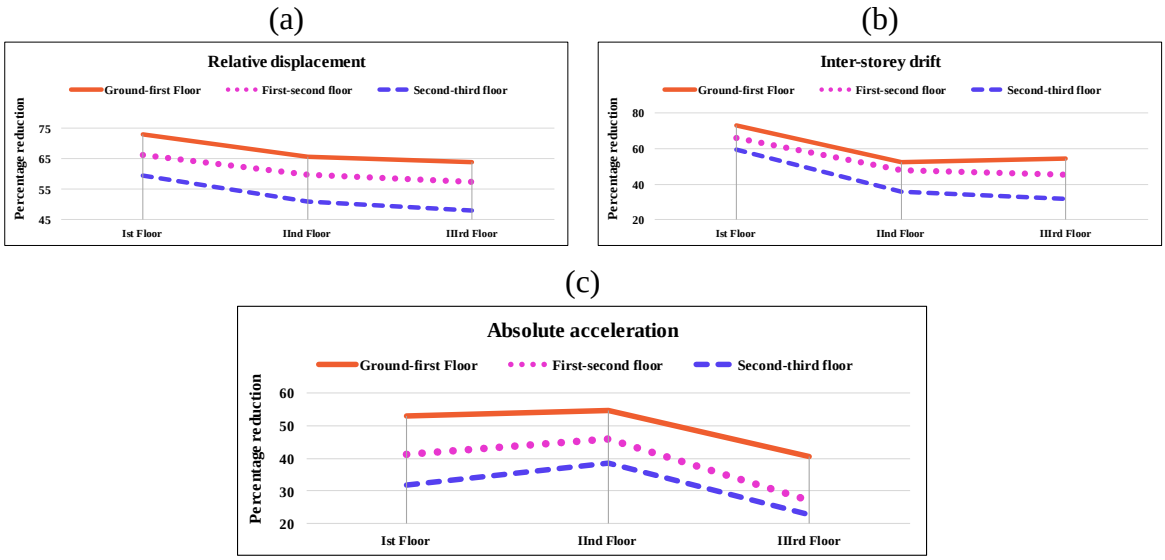

Figure 4.12 Percentage reductions in the structural responses using PSO-FFT-modified-LQR in the structure subjected to Gebze earthquake by placing MR damper at different floors (a) Relative displacement (b) Inter-storey drift (c) Absolute acceleration

the first floor the percentage reduction is 73%,66%,60% when the damper is kept on the ground, first and second floor respectively. Observing Figure 4.12(b), the percentage reduction in the inter-storey drift between the first-second floor is 52%,48%,36%, between second-third floor is 55%,45%,32% and for first floor, it is reduced by 73%, 66% 60% when damper is kept on the ground, first and second floor respectively. Figure 4.12(c) reveals that the percentage reduction in the third floor`s absolute acceleration is 41%,27%, 23%, for the second floor it is 55%,46%,39% and for the first floor, percentage reduction is 53%,41%, 32% when damper is kept on the ground, first and second floor respectively. It can be seen from Figure 4.10(a-c), Figure4.11(a-c) and Figure4.12(a-c) that maximum percentage reduction in structural response is achieved by placing MR damper on the ground floor and minimum percentage reduction is attained when MR damper is kept on the second floor. It is substantial to point out here that the difference between the force applied to the structure in attaining the maximum and minimum percentage reductions in the structural responses is very less.

Moreover, it is observed in Figure 4.10(a), Figure 4.11(a) and Figure 4.12(a) that the percentage reduction in the relative displacement is not very large for all floors irrespective of MR damper placement whereas there is a significant percentage reduction in the other structural responses i.e. inter-storey drift and absolute acceleration with respect to the position of MR damper within the structure. This happens because in three degrees of freedom structure subjected to strong ground motion mainly follows the fundamental mode of vibration.

Consequently, the displacement occurs primarily on the ground floor as compared to the other two floors. This is the main reason, that the maximum percentage reduction in the relative displacement occurs when the MR damper is kept on the ground floor. Therefore, based on the above discussion it is concluded that the optimized location to place single MR damper is the ground floor in a three storey structure to achieve maximum reduction in structural responses.

(iv) Effect of the power cut off at the peak of the earthquake

It is likely that power may trip during the occurrence of an earthquake. A study is carried out here for performance analysis of the suggested PSO-FFT-modified-LQR controller considering the possibility of power loss during the peak of an earthquake time history. The prototype three storey structure fixed with MR damper on the ground floor is subjected to the El-Centro earthquake for the analysis purpose. Principally, any control algorithm shall essentially convert into the passive off controller when power is lost during the earthquake. The responses of a structure employing a semi active control scheme with a passive controller shall be better than the uncontrolled structure. Comparison of the third floor`s relative displacement of uncontrolled structure and the PSO-FFT-modified-LQR controlled structure is shown in Figure 4.13(a) considering the power loss at 2 seconds (sec) of the El-Centro time history.

The power loss at 2 sec is chosen because the energy in the signal is high at this point. The displacement response of the third floor as shown in Figure 4.13(a) is lesser than the uncontrolled structure. A comparison of the third floor`s displacement response of the structure employing the proposed controller before and after 2 sec is shown in Figure 4.13(b). The PSO-FFT-modified-LQR controller converts into passive off controller at 2 sec as can be seen in Figure 4.13 (c). It is to note here that, these results remain same regardless of the controllers used because after the power vanish, any controller essentially converts to the Passive OFF controller. The passive off controller supplies a minimum amount of the counter force at zero volt. Even it may not be sufficient for the structural integrity but it is better than the situation when no counter force is available at all. Therefore, the semi active control scheme employing MR damper performance superior to the other control scheme when no Power is available.

(a)

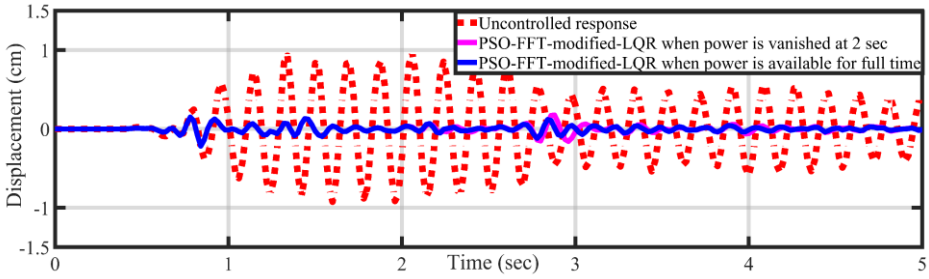

(b)

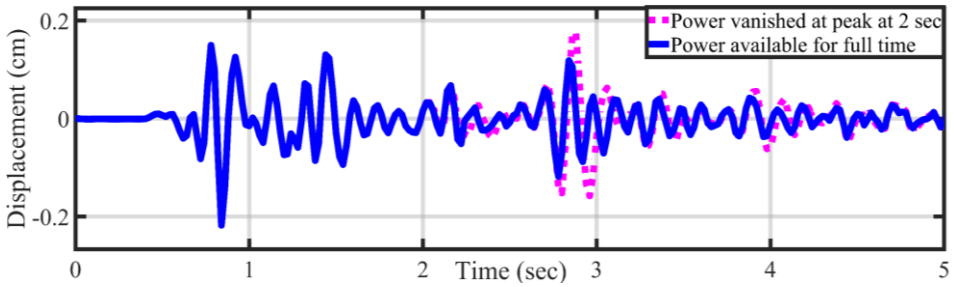

(c)

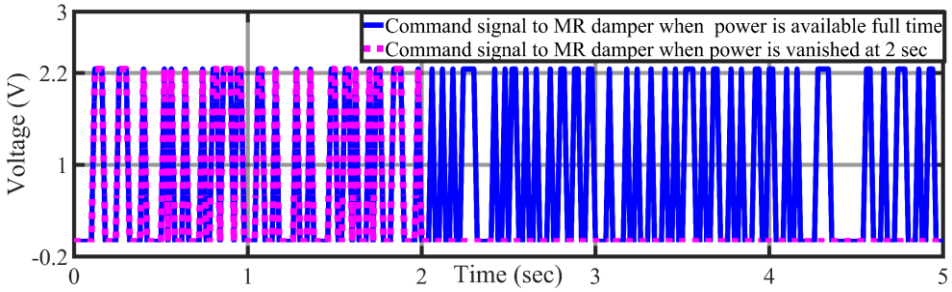

Figure 4.13 Performance analysis of PSO-FFT-modified-LQR for El-Centro time history, considering a situation if power goes off during the peak (at 2 sec) of the earthquake (a) comparison of third floor`s displacement of uncontrolled structure with the PSO-FFT-modified-LQR controlled displacement when power is available for full time and cut off during the peak of the earthquake (b) Comparison of third floor`s displacement of PSO-FFT-modified controlled structure (c) comparison of the voltage to the MR damper when power is available for full time and cut off during the peak of the earthquake

4.2.4 Development of modified LQG controller using PSO-FFT approach (adaptive LQG)

It is assumed in the implementation of the LQR control algorithm, that all the states are available all the time which is practically difficult to ensure in case of an earthquake. Therefore, the LQG controller is advised to employ in the circumstances where uncertainties and noise are present. The combination of the LQR controller and the Kalman filter is known as the Linear Quadratic Gaussian (LQG) controller [136].

Assume an LTI system represented by Eqs. (4.9-4.10)

$$\dot{\boldsymbol{z}}=\mathbf{A}\,\mathbf{z}+\mathbf{B}\,\mathrm{f}+\mathbf{E}\,\mathrm{w} \tag{4.9}$$

$$\mathbf{y}=\mathbf{C}\,\mathbf{z}+\mathbf{D}\,\mathrm{f}+\mathbf{v} \tag{4.10}$$

Where **w** and **v** are the disturbance input and measurement error respectively. Both are assumed as uncorrelated and white Gaussian random process with zero means.

For this system, the cost function is defined as given in Eq. (4.11)

$$\mathrm{J_i}(z,\mathrm{u})=\underset{t\to\infty}{\mathrm{Lim}}\left[\int_0^t \left(z^{\mathrm{T}}\mathbf{Q_i}\,z(t)+u^{\mathrm{T}}\mathbf{R_i}\,u(t)\right)d(t)\right] \tag{4.11}$$

The **Q** is the state weighting matrix and it is semidefinite whereas **R** is the control weighting matrix and it is a positive definite matrix. The LQG controller that solves the LQG control problem is formulated by the Eqs. (4.12-4.13)

$$\dot{\hat{\mathbf{z}}}=\mathbf{A}\,\hat{\boldsymbol{z}}+\mathbf{B}\,\mathrm{u}+\mathbf{L_{Kal}}(\mathbf{y}-\mathbf{C}\hat{\mathbf{z}}-\mathbf{Du}) \tag{4.12}$$

$$\mathbf{u}=-\mathbf{K_{LQR}}\hat{\mathbf{z}} \tag{4.13}$$

Here $\hat{\boldsymbol{z}}$ is the observed state or the next state. As described earlier the LQG controller is the combination of the LQR controller and the Kalman filter, the calculation of the Kalman filter gain $\mathbf{L_{Kal}}$ and the LQR controller gain $\mathbf{K_{LQR}}$ are calculated separately using the algebraic Ricatti equation. These gains are given independently by Eqs. (4.14-4.15).

$$\mathbf{L_{Kal}}=\mathbf{R^{-1}B^{T}P_{LQR}} \tag{4.14}$$

$$\mathbf{K_{LQR}}=\mathbf{P_{Kal}V^{-1}C^{T}} \tag{4.15}$$

The Kalman filter is used to design an observer by measuring the available data. This observer minimizes the spread of the estimate error probability density in the process. The method of determining optimal control weighting matrix to develop an adaptive LQG controller using FFT

and PSO algorithm is similar as described in section 4.1.1 and shown in Figure 4.1 and Figure 4.2. The block diagram for the LQG controller is shown in Figure 4.14.

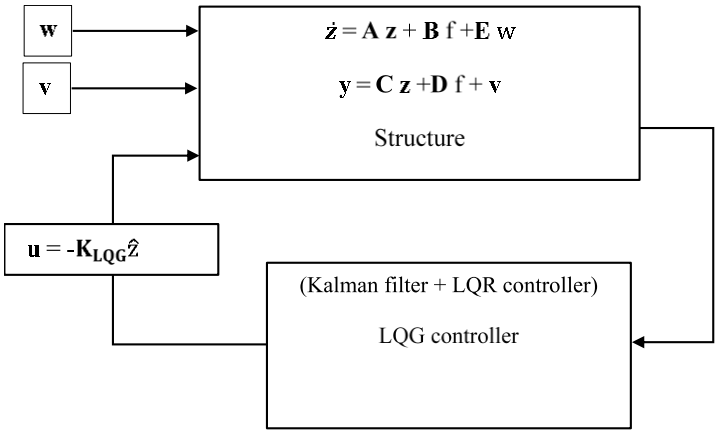

Figure 4.14 The block diagram of LQG controller

The results obtained by employing PSO-FFT-modified-LQG controller for the semi active control scheme in prototype three-storey structure, are discussed in a similar manner as discussed in the section 4.2.3.

4.2.5 Results and discussion on the performance of PSO-FFT-modified-LQG controller

The conditions for the analysis of **PSO**-FFT-modified-LQG (adaptive LQG) controller are similar to those were used in the analysis of adaptive LQR controller. The results for the condition (iii) and (iv) shall remain same for every controller. Therefore, only first two conditions are considered hereafter. These testing conditions are as follows: -

(i) Using different earthquake time histories.

(ii) Using an earthquake recorded in different soil conditions.

There is no need of further analysis for the condition (iii) as the best location for the placement of the MR damper will remain same (i.e. the lowest floor of the structure) always irrespective of the controller. Therefore, it will not be included in the performance analysis now onwards.

(i) Using different earthquake time histories

To assess the effectiveness of the suggested PSO-FFT-modified-LQG controller, the results of the dynamic analysis of the three DOF test structure having an MR damper on the ground floor are discussed. For simulation, the prototype three-storey structure is subjected to the same three earthquake time histories are used which are shown in Figure 4.3(a-c). Referring to Figure 4.15, the displacement response of the uncontrolled structure is shown in Figure 4.15(a) whereas a comparison of the uncontrolled displacement response and response due to CO-LQG and PSO-FFT-modified-LQG controller is shown in Figure 4.15(b).

The visual inspection suggests that the displacement response is reduced. From Table 4.4, this reduction in peak values is 78% using CO-LQG whereas 82% using the PSO-FFT-modified-LQG. Further, the comparison of the third floor`s relative displacement obtained using CO-LQG and PSO-FFT-modified-LQG is demonstrated in Figure 4.15(c). It concludes that third floor`s relative displacement is reduced using the proposed controller throughout the time history.

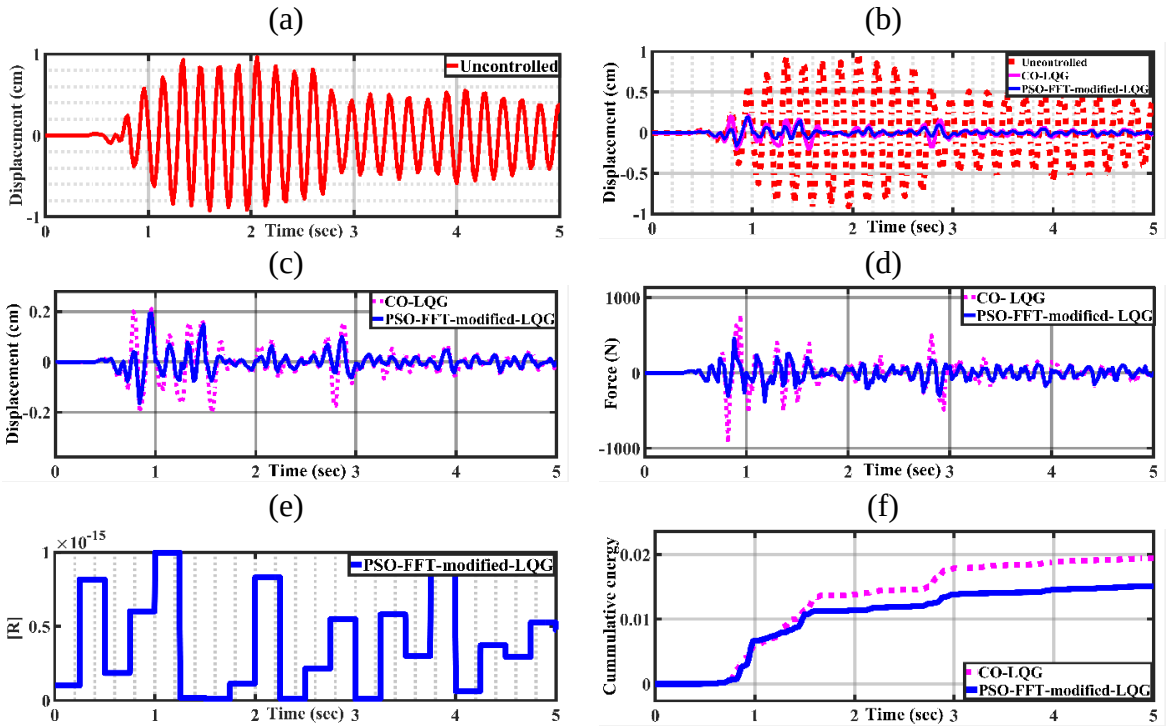

Figure 4.15. Structural responses for the structure subjected to El-Centro earthquake (a) displacement response of third floor of uncontrolled structure (b) comparison of controlled responses of third floor using CO-LQG and PSO-FFT-modified-LQG algorithms (c) control forces for the CO-LQG and the PSO-FFT-modified-LQG algorithm (d) variation of **R** with time (e) comparison of cumulative energies of the third floor`s displacement by applying CO-LQG and PSO-FFT-modified-LQG

From Table 4.4, the reduction in the peak values of relative displacement using the proposed controller is by 15%, 21% and 22% for first, second and the third floor respectively as compared with the CO-LQG. Further, the change in the control weighting matrix **R** is shown in Figure 4.15(e). The value of **R** is changed in real time and determined optimally using the PSO algorithm. In this way, the control force used to mitigate the seismic vibration is used intelligently. For interstorey drift, the proposed controller achieved the reduction of 29% between the first-second floor and 33% between second-third floor as compared with the CO-LQG as can be seen from Table 4.4. Alike, the proposed algorithm can reduce the peak values of absolute acceleration by 28%, 46% and 27% for the first floor, second floor and third floor respectively as compared with the CO-LQG as shown in Table 4.4. This Table 4.4 consists of the peak values of the structural responses of the three-storey structure subjected to EL-Centro, Chi-Chi, and Gebze earthquake. The peak responses are obtained through simulation of the uncontrolled

structure and structure having a semi active control scheme employing the CO-LQR and the proposed controller. The peak values of the applied force to the structure by the MR damper due to the calculation of the controller used is also shown in Table 4.4. All these reductions in the structural responses are achieved using lesser control force as shown in Figure 4.15(d). The proposed controller utilized 24% lesser force (peak value) to achieve the above-mentioned results as compared with the CO-LQG as can be observed from Table 4.4.

Table 4.4: Peak responses of structure using PSO-FFT-modified-LQG and CO-LQG controller for various earthquake time histories.

Control algorithm	El-Centro earthquake			Chi-Chi earthquake			Gebze earthquake		
	Uncontrolled	CO-LQG	PSO-FFT-modified LQG	Uncontrolled	CO-LQG	PSO-FFT-modified LQG	Uncontrolled	CO-LQG	PSO-FFT-modified LQG
Displacement (cm)	0.55	0.12	0.10	0.14	0.02	0.015	0.074	0.0180	0.017
	0.83	0.19	0.15	0.22	0.04	0.031	0.117	0.0353	0.029
	0.97	0.22	0.17	0.27	0.05	0.040	0.138	0.0513	0.040
Inter story drift(i_d) (cm)	0.55	0.12	0.10	0.14	0.02	0.015	0.074	0.018	0.017
	0.29	0.07	0.05	0.08	0.02	0.016	0.042	0.017	0.012
	0.14	0.03	0.02	0.05	0.01	0.009	0.022	0.016	0.011
Acceleration (cm/s^2)	870	733	526	181	98	48	126	91	47
	1070	755	410	268	81	60	150	74	61
	1400	723	525	317	97	84	185	113	101
Force (N)	----	971	736	----	1178	1098	----	1278	1167

Comparison of the energy confined in the signal of the relative displacement of the third floor due to CO-LQG and the proposed controllers is shown in Figure 4.15(f) which confirms that the displacement signal due to the proposed controller has the lesser energy for destruction as compared with the displacement signal due to the CO-LQG.

For Chi-Chi earthquake, it can be seen in Figure 4.16(b) that the relative displacement response is reduced. Comparison of displacement response due to CO-LQG and PSO-FFT-modified-LQG is presented in Figure 4.16(c) for Chi-Chi earthquake whereas the same is presented for Gebze earthquake in Figure 4.17(c). It is concluded from these Figures that the proposed adaptive LQG controller is more effective than the CO-LQG. From Table 4.4, the reduction in the peak values of relative displacement using the proposed controller is 26%, 23% and 22% for first, second and third floor respectively for Chi-Chi earthquake and 6%, 18% and 22% for the first, second and third floor respectively for Gebze earthquake as compared with the CO-LQG. Variations of the control weighting matrix **R** are shown in Figure 4.16(e) for Chi-Chi earthquake whereas for Gebze earthquake these are shown in Figure 4.17(e).

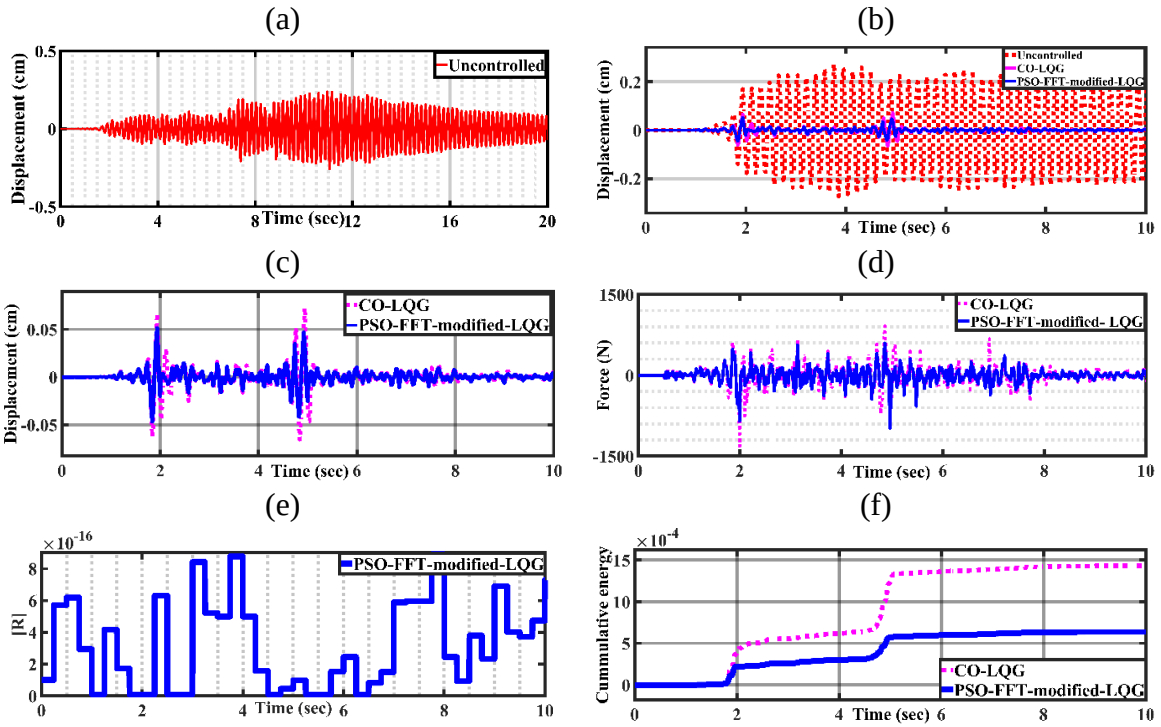

Figure 4.16 Structural responses for the structure subjected to Chi-Chi earthquake (a) displacement response of third floor of uncontrolled structure (b) comparison of controlled responses of third floor using CO-LQG and PSO-FFT-modified-LQG algorithms (c) control forces for the CO-LQG and the PSO-FFT-modified-LQG algorithm (d) variation of **R** with time (e) comparison of cumulative energies of the third floor`s displacement by applying CO-LQG and PSO-FFT-modified-LQG

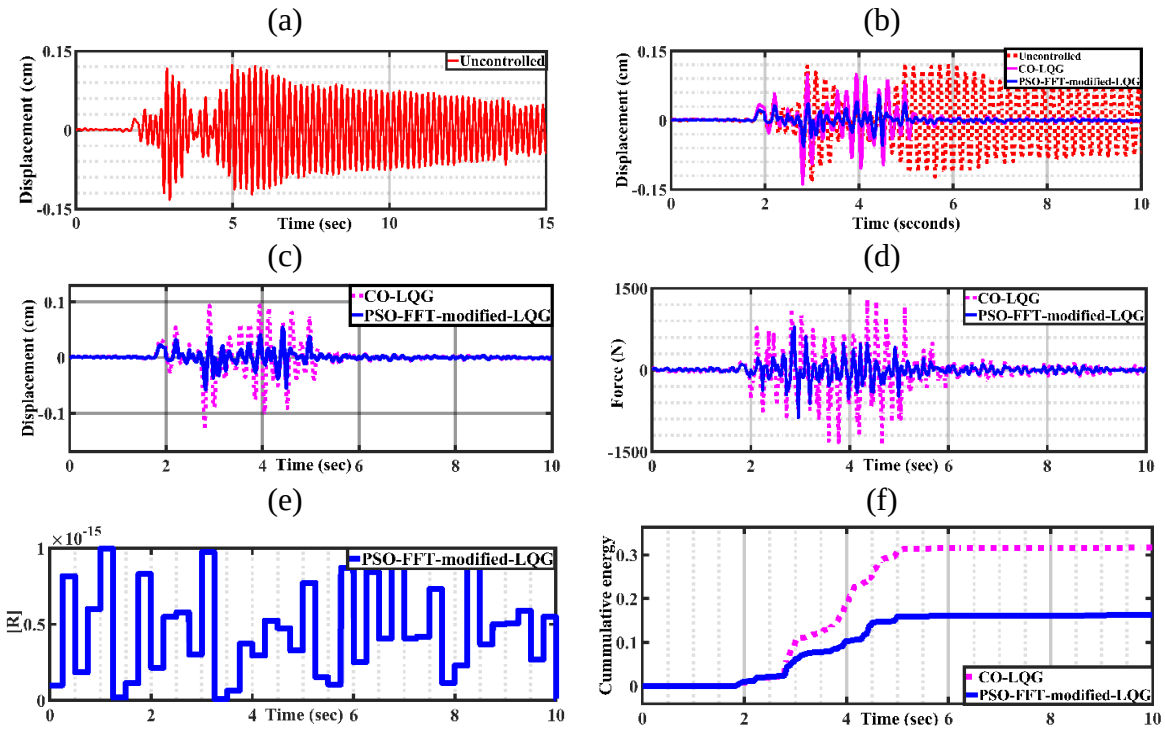

Figure 4.17 Structural responses for the structure subjected to Gebze earthquake (a) displacement response of third floor of uncontrolled structure (b) comparison of controlled responses of third floor using CO-LQG and PSO-FFT-modified-LQG algorithms (c) control forces for the CO-LQG and the PSO-FFT-modified-LQG algorithm (d) variation of **R** with time (e) comparison of cumulative energies of the third floor`s displacement by applying CO-LQG and PSO-FFT-modified-LQG

For Chi-Chi earthquake, it can be seen from Table 4.4 that the proposed controller achieves the reduction in interstorey drift by 20% between the first-second floor and 10% between second-third floor as compared with the CO-LQG. Similarly, for Gebze earthquake, proposed controller achieves the reduction in interstorey drift by 31% between first-second and 31% between second-third floor as compared with CO-LQG.

The observations of Table 4.4 reveal that the proposed algorithm can reduce the peak values of the acceleration by 51%,25%,13% whereas for Gebze earthquake, proposed control algorithm achieved reductions in absolute acceleration by 48%,17%, 10% for first, second and third floor respectively. These reductions in the structural responses are achieved using lesser control force as shown in Figure 4.16(d) for Chi-Chi earthquake and in Figure 4.17(d) for the Gebze earthquake. From Table 4.4, the proposed controller used 7% lesser force (peak value) for Chi-Chi earthquake and 9% lesser force for Gebze earthquake as compared with the CO-LQG. The comparison of the cumulative energies of the third floor`s displacement by applying CO-LQG and the PSO-FFT-modified-LQG is shown in Figure 4.16(f) for Chi-Chi earthquake and in Figure 4.17(f) for Gebze earthquake. These Figures show that the cumulative energy of the third floor`s displacement applying the proposed algorithm is less than that of CO-LQG.

(ii) Using an earthquake recorded in different soil conditions

An analysis is carried out to examine the performance of the proposed controller for an earthquake recorded in different soil conditions (i.e. hard, medium and soft soil).

For an earthquake recorded in hard soil, the effectiveness of the structural control can be seen by the comparison of time histories of third floor`s displacement response of the uncontrolled structure and semi-actively controlled structure using CO-LQG and PSO-FFT-modified-LQG control algorithm is shown in Figure 4.18(b). This Figure shows that the displacement response is effectively reduced through the seismic activity.

It can be seen from Table 4.5, the reduction in the peak value of the displacement response is 72% using CO-LQG and 80% using proposed PSO-FFT-modified-LQG as compared with the uncontrolled structure. Comparison of the displacement response due to CO-LQG and PSO-FFT-modified-LQG is shown in Figure 4.18(c). It can be concluded from the Table 4.5, the proposed controller achieved more reduction by 46%, 33% and 28% for first, the second and third floor in peak values of the relative displacement as compared with the CO-LQG controller. The inter-story drift is reduced by 12% for the first-second floor and 25% for the second-third floor on applying the proposed controller instead of CO-LQG in the semi active control scheme. The reduction in the absolute acceleration using the proposed controller is moderate in hard soil

earthquake as compared with the CO-LQG. The absolute accelerations for the first, second and the third floor are reduced by 4%, 2% and 14% respectively by applying the proposed controller. Further, the proposed controller attains these reductions in structural responses using 20% lesser force than the CO-LQG controller as shown in Figure 4.18(d). Variations in the value of **R** are shown in Figure 4.16(e) and comparison of the cumulative energy of the displacement signal of third floor due to the proposed controller and CO-LQG is shown in Figure 4.18(f) which reveals that cumulative energy is lesser for the proposed controller as compared to that of CO-LQG.

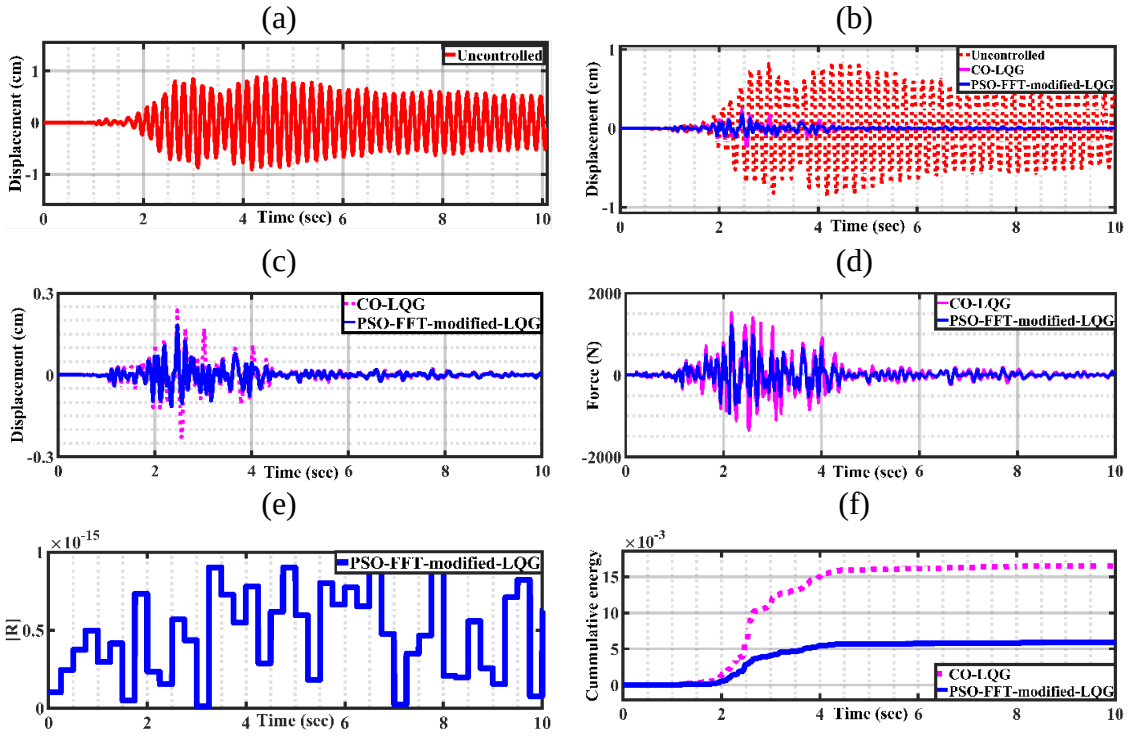

Figure 4.18 Structural responses for the structure subjected to Hard soil earthquake (a) displacement response of third floor of uncontrolled structure (b) comparison of controlled responses of third floor using CO-LQG and PSO-FFT-modified-LQG algorithms (c) control forces for the CO-LQG and the PSO-FFT-modified-LQG algorithm (d) variation of **R** with time (e) comparison of cumulative energies of the third floor`s displacement by applying CO-LQG and PSO-FFT-modified-LQG

For the earthquake recorded in medium soil conditions, the displacement response of the third floor for the uncontrolled structure is shown in Figure 4.19(a). The comparison of displacement response time histories of an uncontrolled and controlled structure employing CO-LQG and proposed control algorithm is shown in Figure 4.19(b) in which the proposed controller mitigates the displacement effectively throughout the earthquake. Comparison of time histories of the displacement responses due to CO-LQG and the proposed controller is plotted in Figure 4.19(c) which shows that the proposed controller reduced the displacement response more effectively than the CO-LQG. This reduction in the displacement response is by 53%,47% and 43% for the first, second and third floor in comparison with CO-LQG as can be seen in Table

4.5. Also, the interstorey drift between the first-second floor and second third floor are reduced by 14% and 17% using the proposed PSO-FFT-modified-LQG controller in place of CO-LQG. Though, there are various factors that affect the behaviour of the structure in different soil structure. However, it is the general observation that the structure located in the relatively soft soil will vibrate more than the structure located in the hard and rocky soil. This is because the soft soil apparently works as an amplifier to the ground motion.

Table 4.5 Peak responses of structure using PSO-FFT-modified-LQG and CO-LQG controller for earthquake recorded in different soil conditions.

Control algorithm	Earthquake (Hard Rock)			Earthquake (Medium soil)			Earthquake (Soft soil)		
	Uncontrolled	CO-LQG	PSO-FFT-modified LQG	Uncontrolled	CO-LQG	PSO-FFT-modified LQG	Uncontrolled	CO-LQG	PSO-FFT-modified LQG
Displacement (cm)	0.66	0.13	0.07	0.60	0.38	0.18	0.99	0.22	0.15
	0.80	0.22	0.15	0.93	0.45	0.24	1.26	0.55	0.39
	0.89	0.25	0.18	1.20	0.51	0.29	1.53	0.76	0.49
Inter story drift(i_d) (cm)	0.66	0.13	0.07	0.60	0.38	0.18	0.99	0.22	0.15
	0.14	0.09	0.08	0.33	0.07	0.06	0.27	0.33	0.24
	0.09	0.04	0.03	0.27	0.06	0.05	0.27	0.21	0.10
Acceleration (cm/s^2)	1167	512	493	830	615	520	852	580	540
	1287	570	561	1018	702	602	1217	770	660
	1356	854	735	1157	970	840	1299	904	814
Force (N)	--	1533	1224	--	1642	1129	--	1690	1367

Alike, the proposed controller reduced the absolute accelerations for the first, second and the third floor by 15%,14% and 13% respectively as compared with the CO-LQG as can be seen in Table 4.5. These reductions in structural responses achieved by the proposed controller using 31% lesser force than the CO-LQG. This can also be seen by observing the comparison of the time histories of the force due to CO-LQG and PSO-FFT-modified LQG in Figure 4.19(d). The variations of the values of the control weighting matrix **R** are shown in Figure 4.19(e). The comparison of cumulative energies of the displacement of t third floor is shown in Figure 4.19(f). Now, the analysis is carried out for the structure subjected to the earthquake recorded in the soft soil. First, the displacement response of the third floor of the uncontrolled structure is shown in Figure 4.20(a) which is to be reduced by employing the semi active control scheme. The comparison of the time histories of the displacement response of the uncontrolled structure, by employing CO-LQG controller and the proposed controller is shown in Figure 4.20(b). Observing Figure 4.20(b), it can be concluded that an effective performance is shown by both control algorithms as compared to the uncontrolled structure. Observing Table 4.5, the proposed

controller achieved a reduction in the displacement by 32%, 29% and 36% for first, second and third floor respectively as compared with the CO-LQG.

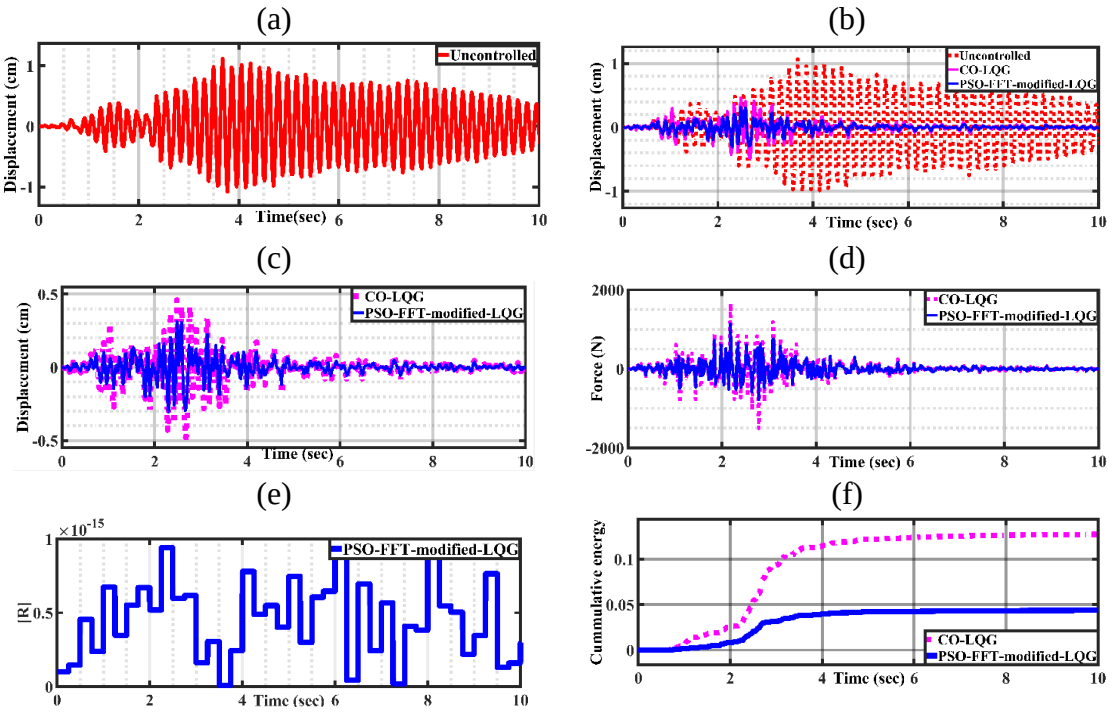

Figure 4.19 Structural responses for the structure subjected to medium soil earthquake (a) displacement response of third floor of uncontrolled structure (b) comparison of controlled responses of third floor using CO-LQG and PSO-FFT-modified-LQG algorithms (c) control forces for the CO-LQG and the PSO-FFT-modified-LQG algorithm (d) variation of **R** with time (e) comparison of cumulative energies of the third floor`s displacement by applying CO-LQG and PSO-FFT-modified-LQG

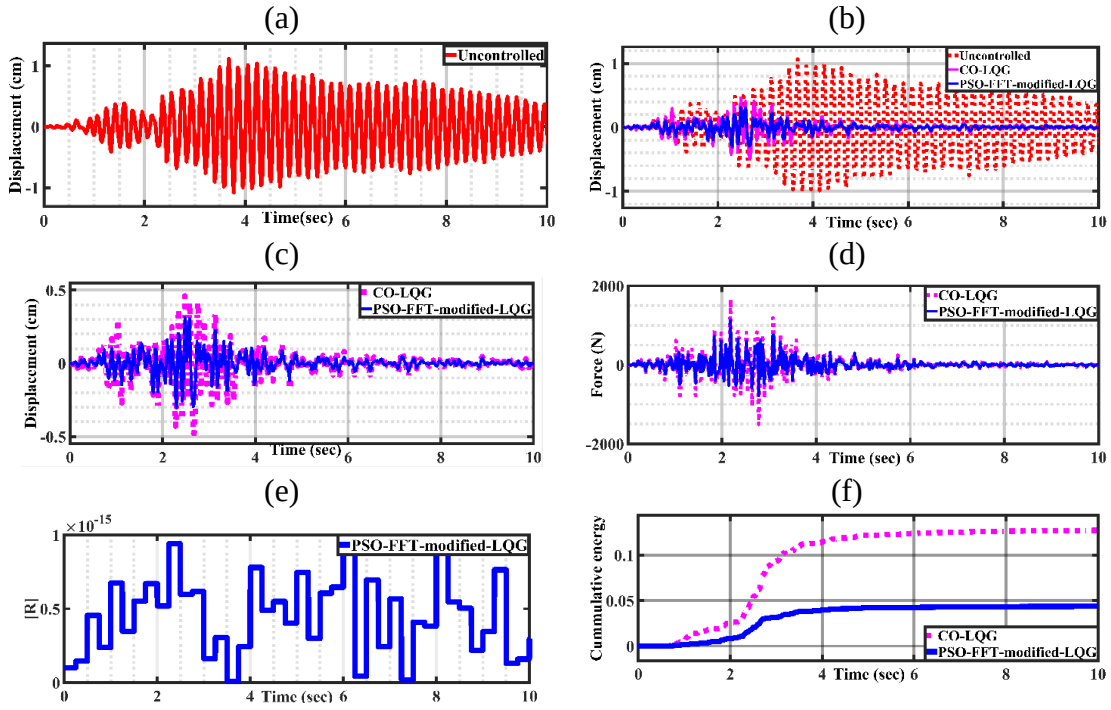

Figure 4.20 Structural responses for the structure subjected to soft soil earthquake (a) displacement response of third floor of uncontrolled structure (b) comparison of controlled responses of third floor using CO-LQG and PSO-FFT-modified-LQG algorithms (c) control forces for the CO-LQG and the PSO-FFT-modified-LQG algorithm (d) variation of **R** with time (e) comparison of cumulative energies of the third floor`s displacement by applying CO-LQG and PSO-FFT-modified-LQG

The interstorey drift between the first-second floor and second third floor are reduced by 27% and 52% more using the proposed controller in place of CO-LQG. Alike, the proposed controller reduces the absolute accelerations for the first, second and the third floor by 7%,14% and 10% respectively as compared with the CO-LQG. These reductions in structural responses achieve by the proposed controller using 19% lesser force than the CO-LQG. This can also be seen by the comparison of the time histories of the control force due to the CO-LQG and PSO-FFT-modified LQG. This is demonstrated in Figure 4.20(d). Variation of the values of the control weighting matrix **R** is shown in Figure 4.20(e). The comparison of the cumulative energies of the displacement of the third floor is shown in Figure 4.20(f).

4.3 Development of modified LQR/LQG controller using PSO- τ_p^{max} approach

In this section, another approach to determine the quasi-resonance between the seismic excitation and the structure is proposed. This is known as time domain approach where the complete system remains in the time domain for the whole duration of the earthquake. It removes the necessity of the analysis of the seismic signal in the frequency domain (FFT) or time-frequency domain (STFT, DWT etc.) for determination of the quasi-resonance. However, the results obtained using this approach are like that of PSO-FFT based approach, but the system becomes inherently fast [137].

4.3.1 Development of adaptive LQR controller using PSO- τ_p^{max} approach

The structure`s response reflects similar properties of the earthquake excitation. So, the entire duration of the response $(0, t_i)$ is divided further into smaller time windows, with the i^{th} window being (t_{i-1}, t_i). Maximum predominant period τ_p^{max} is used to find the dominant frequency for each time window. This keeps the system always in the time domain and thus the system becomes inherently fast. Originally, the idea of the maximum predominant period τ_p was first introduced by Nakamura [138], in order to classify large and small earthquake based on frequency content present in the earthquake signal. The parameter τ_p can be calculated from the acceleration time series for each time step in real time according to the following relations given in Eqs (4.16-4.18).

$$\tau_{p,i}=2\pi\sqrt{\frac{V_i}{A_i}} \tag{4.16}$$

$$V_i=aV_{i-1}+v_i^2 \tag{4.17}$$

$$A_i=aA_{i-1}+\left(\frac{dv}{dt}\right)_i^2 \tag{4.18}$$

Here, v_i is the recorded ground velocity, V_i is the smoothed ground velocity squared, A_i is the smoothed acceleration squared and a is smoothing parameter having a value between 0 to 1. Maximum predominant period τ_p^{max} is the maximum value of τ_p in the selected time window. Thus, maximum dominant frequency of a selected time window can be obtained by Eq. (4.19).

$$f_d=\frac{1}{\tau_p^{max}} \tag{4.19}$$

This dominant frequency determines the quasi-resonance stances where the value of **R** is to be modified. Here, the PSO algorithm is used to find the optimal value of **R** that gives the optimum structural response with lesser control effort. PSO algorithm helps to find weighting matrices **R** on the quasi-resonant bands. The benefit of this specific local optimal solution is that it can

change the estimation of matrix **R** on an odd frequency at which quasi-resonance occurs, unlike the clipped optimal LQR which has a global value of **R** during an earthquake. The cost function to be minimized for this modified LQR problem is formulated by having state weighting matrix [$\mathbf{Q_i}$] and control weighting matrix [$\mathbf{R_i}$] for i^{th} window and is given in Eq. (4.20)

$$J_i(x, u)=\int_0^t \left(x^T Q_i x(t)+u^T R_i u(t)\right) dt \tag{4.20}$$

The result of this modified optimal control problem with cost function J_i leads to a control law given in Eq. (4.21)

$$u = -[G_i]x \tag{4.21}$$

The solution of the Ricatti matrix differential equation for every windowed interval gives the gain matrix [$\mathbf{G_i}$] and the anticipated control force required to counter the effect of quasi-resonance can be found by applying this gain of the i^{th} window. The flow chart of the development of the adaptive LQR controller is shown in Figure 4.21.

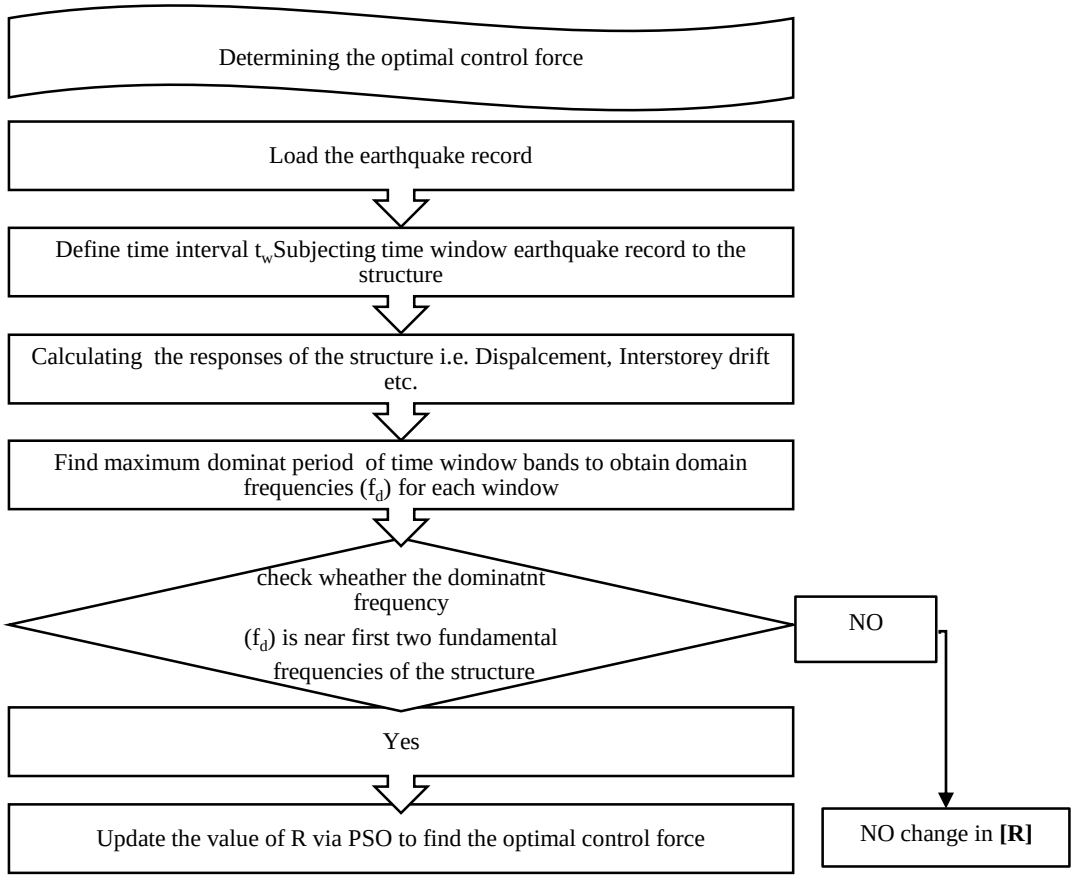

Figure 4.21 Flow chart of the development of adaptive LQR controller using PSO- τ_p^{max}approach [142]

The PSO algorithm used to find the best suitable value of **R** is discussed in section 4.2.2 of this chapter.

4.3.2 Results and discussion on the performance of the adaptive LQR controller (PSO-τ_p^{max}-modified-LQR)

The result and discussion for performance analysis of the newly developed adaptive LQR controller and corresponding conventional clipped optimal LQR controllers are carried out considering the conditions described in section 4.2.5 of this chapter.

(i) Using different earthquake time histories

For the assessment of suggested adaptive LQR (PSO- τ_p^{max}-modified-LQR) controller, the results of the dynamic analysis of the three DOF test structure having an MR damper between ground and first floor are discussed. For simulation analysis, the same three earthquake time histories are used which are shown in Figure 4.3(a-c). As discussed in section 4.1.3, there are two popular methods to show the effect of the proposed controller on the structural responses which are also used here for the performance analysis.

Referring to the Figure 4.22, the displacement response of the uncontrolled structure is shown in Figure 4.22(a) whereas in Figure 4.22(b) a comparison of the uncontrolled displacement response and response due to CO-LQR and PSO- τ_p^{max}-the modified-LQR controller is shown. The visual inspection clearly suggests that the displacement response is reduced. From Table 4.6, this reduction in the peak values is 68% using CO-LQR and 82% using the PSO- τ_p^{max}-modified-LQR. The comparison of the displacement due to CO-LQR and PSO- τ_p^{max}-modified-LQR is depicted in Figure 4.22(c) which concludes that the displacement is reduced using the proposed controller throughout the time history presented.

From Table 4.6, the reduction in the peak values of relative displacement using the proposed controller is 23% for the first floor, 19% for the second floor and 24% for the third floor as compared with the CO-LQR. The change in the control weighting matrix **R** is shown in Figure 4.22(e). The value of **R** for the CO-LQR remains same through the seismic event whereas in the proposed algorithm the variation of **R** for each time window (t_w) is according to the quasi-resonance between the domain frequency and first two fundamental frequency of the structure. The proposed control algorithm achieved the reduction in the inter-storey drift by 15% between the first-second floor and 33% between second-third floor as compared with the CO-LQR. Further, the reduction in peak values of the absolute acceleration is shown in Table 4.6 which reveals that the proposed algorithm can reduce the peak values of the acceleration by 44% for the first floor, 14% for the second floor and 32% for the third floor as compared with the CO-LQR. All these reductions in structural responses of all floors of the three-storey structure are achieved using lesser control force as shown in Figure 4.22(d).

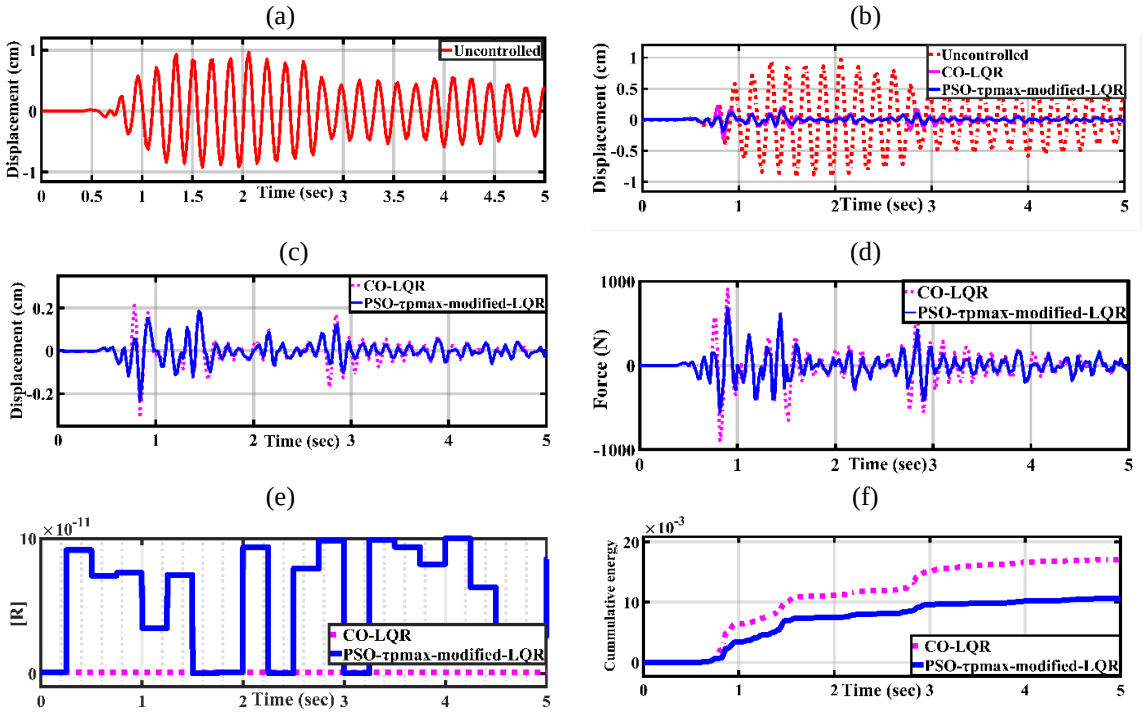

Figure 4.22 Structural responses for the structure subjected to the 1940 El-Centro earthquake (a) displacement response of third floor of uncontrolled structure (b) comparison of controlled responses of third floor using CO-LQR and PSO- τ_p^{max}-modified-LQR algorithms (c) control forces for the CO-LQR and the PSO- τ_p^{max}-modified-LQR algorithm (d) variation of **R** with time (e) comparison of cumulative energies of the third floor`s displacement by applying CO-LQR and PSO- τ_p^{max}-modified-LQR

It can be seen from Table 4.6, the proposed controller utilized 25% lesser force (peak value) to achieve the above-mentioned results as compared with the CO-LQR. The energy confined in the controlled signal of the relative displacement of the third floor due to CO-LQR and the PSO-τ_p^{max}-modified-LQR is shown in Figure 4.22(f).

For Chi-Chi earthquake, the comparison of the displacement response due to CO-LQR and PSO- τ_p^{max}-modified-LQR is presented for the Chi-Chi earthquake in Figure 4.23(c) whereas for Gebze earthquake the same is presented in Figure 4.24(c). These Figures show the displacement is reduced using a proposed controller though out the time history as compared to the CO-LQR. This reduction is 33%,40% and 34% for first, second and third floor respectively for Chi-Chi earthquake and 5%,12% and 17% for first, second and third floor respectively for Gebze earthquake in comparison with the CO-LQR as can be seen from the Table 4.6. The variations of the control weighting matrix **R** are shown in Figure 4.23(e) for Chi-Chi earthquake whereas for Gebze earthquake these are shown in Figure 4.24(e). It can be observed from Table 4.6 the proposed controller achieves the reduction in the inter-storey drift by 50% between the first-second floor and 10% between second-third floor as compared with the CO-LQR for Chi-Chi earthquake. Similarly, for Gebze earthquake, the proposed controller achieved the reduction

in the interstorey drift 43% between the first-second floor and 22% between the second- third floor as compared with the CO-LQR. The reduction in acceleration is achieved moderately by 6% for all floors as compared with the CO-LQR whereas, for Gebze earthquake, the reduction is achieved by 28% 29% and 4% for first, second and third floor respectively.

Table 4.6 Peak responses of structure using PSO- τ_p^{max}-modified-LQR and CO-LQR controller for various earthquake time histories.

Control algorithm	El-Centro earthquake			Chi-Chi earthquake			Gebze earthquake		
	Uncontrolled	CO-LQR	PSO- τ_p^{max}-modified-LQR	Uncontrolled	CO-LQR	PSO- τ_p^{max}-modified-LQR	Uncontrolled	CO-LQR	PSO- τ_p^{max}-modified-LQR
Displacement (x)	0.55	0.09	0.07	0.14	0.03	0.02	0.0741	0.021	0.02
(cm)	0.83	0.20	0.16	0.22	0.05	0.03	0.1165	0.0342	0.03
	0.97	0.31	0.23	0.27	0.06	0.04	0.1381	0.0600	0.05
Inter-story drift (i_d) (cm)	0.55	0.09	0.07	0.14	0.021	0.02	0.074	0.021	0.02
	0.29	0.10	0.09	0.08	0.02	0.01	0.042	0.017	0.01
	0.14	0.11	0.07	0.05	0.011	0.01	0.022	0.026	0.02
Acceleration	870	474	266	181	38	36	126	81	59
(cm/s^2)	1070	540	46	268	63	59	150	95	68
	1400	772	525	317	101	96	185	114	110
Force (N)	0	984	737	0	1398	1190	0	1080	1050

All these reductions in the structural responses are achieved using lesser control force as shown in Figure 4.23(d) for Chi-Chi earthquake and in Figure 4.24(d) for the Gebze earthquake. From Table 4.6, the proposed controller utilized 15% lesser force (peak value) for Chi-Chi earthquake and 3% lesser force for Gebze earthquake to achieve the above-mentioned results as compared with the CO-LQR. The comparison of the cumulative energies of the third floor`s displacement by applying CO-LQR and the PSO- $\tau_p^{max}$-modified-LQR is shown in Figure 4.23(f) for Chi-Chi earthquake and Figure 4.24(f) for Gebze earthquake. It can be concluded by the Figure 4.23(f) and Figure 4.24(f) that the cumulative energy of the third floor`s displacement applying the proposed algorithm is less than that of CO-LQR.

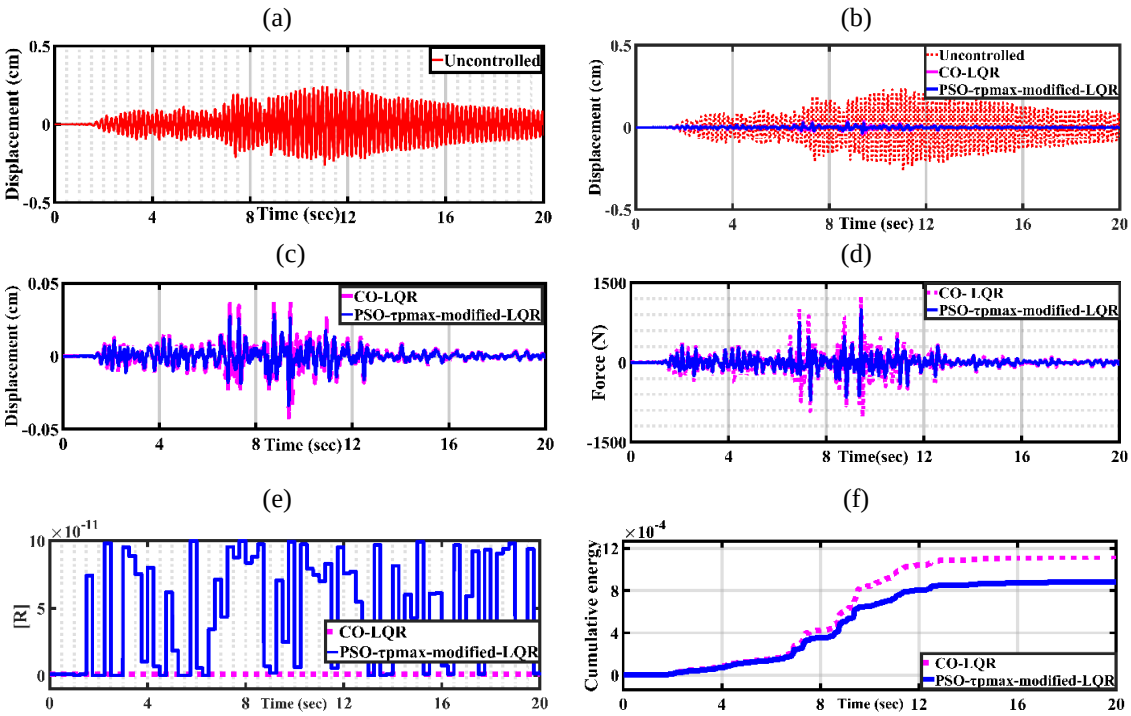

Figure 4.23 Structural responses for the structure subjected to the 1999 Chi-Chi earthquake (a) displacement response of third floor of uncontrolled structure (b) comparison of controlled responses of third floor using CO-LQR and PSO- τ_p^{max}-modified-LQR algorithms (c) control forces for the CO-LQR and the PSO- τ_p^{max}-modified-LQR algorithm (d) variation of **R** with time (e) comparison of cumulative energies of the third floor`s displacement by applying CO-LQR and PSO- τ_p^{max}-modified-LQR

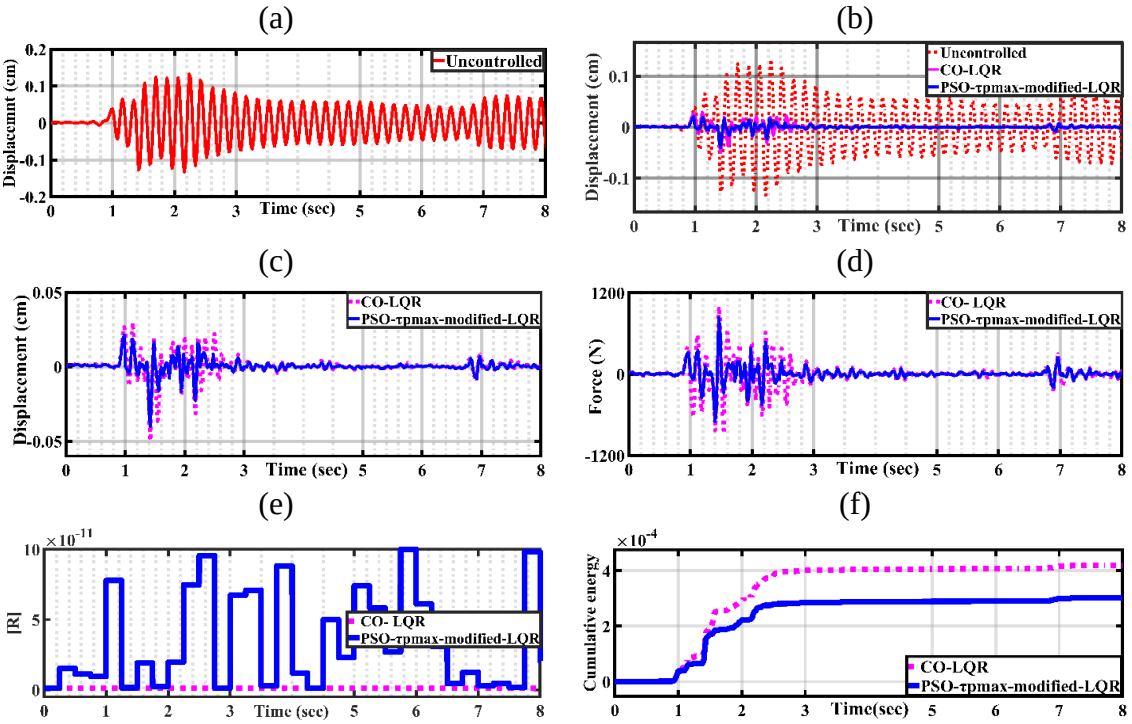

Figure 4.24 Structural responses for the structure subjected to the 1999 Gebze earthquake (a) displacement response of third floor of uncontrolled structure (b) comparison of controlled responses of third floor using CO-LQR and PSO- τ_p^{max}-modified-LQR algorithms (c) control forces for the CO-LQR and the PSO- τ_p^{max}-modified-LQR algorithm (d) variation of **R** with time (e) comparison of cumulative energies of the third floor`s displacement by applying CO-LQR and PSO- τ_p^{max}-modified-LQR

(ii) Using an earthquake recorded in different soil conditions

For the earthquake recorded in hard soil, third floor`s displacement of the uncontrolled structure is shown in Figure 4.25(a). The effectiveness of the structural control can be seen by the comparison of the third floor`s displacement responses of the uncontrolled structure and semi-actively controlled structure using CO-LQR and PSO- τ_p^{max}-the modified-LQR algorithm is shown in Figure 4.25(b). Figure 4.25(b) shows that the displacement is reduced through the seismic event.

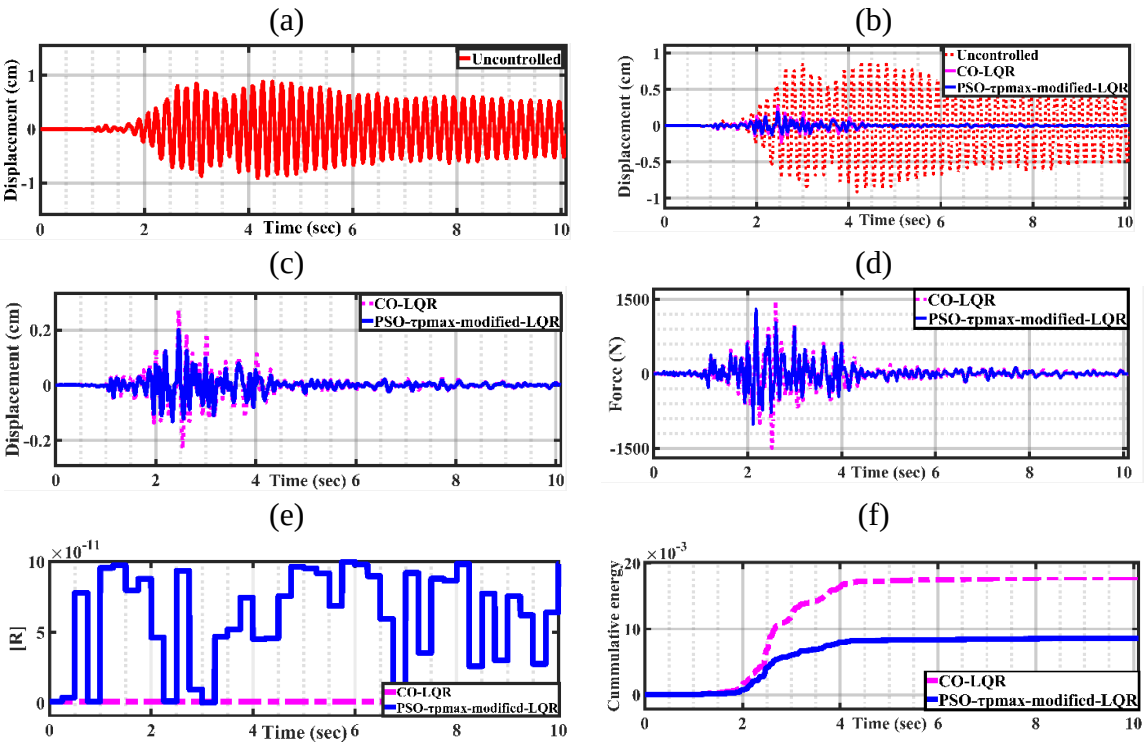

Figure 4.25 Structural responses for the structure subjected to the hard soil earthquake (a) displacement response of third floor of uncontrolled structure (b) comparison of controlled responses of third floor using CO-LQR and PSO- τ_p^{max}-modified-LQR algorithms (c) control forces for the CO-LQR and the PSO- τ_p^{max}-modified-LQR algorithm (d) variation of **R** with time (e) comparison of cumulative energies of the third floor`s displacement by applying CO-LQR and PSO- τ_p^{max}-modified-LQR

The peak values of the structural responses are given in Table 4.7. Comparison of the displacement response due to CO-LQR and PSO- τ_p^{max}-modified-LQR is shown in Figure 4.25(c) which concludes that the displacement obtained by employing the proposed controller is less than that of CO-LQR. For quantitative analysis, observing the Table 4.7, the proposed controller archived more reduction in peak values of the relative displacement by 57% for the first floor, 63% for the second floor and 65% for the third floor as compared with the CO-LQR controller. The inter-story drift is reduced by 72% for the first-second floor and 79% for the second-third floor on applying PSO- τ_p^{max}-modified-LQR control algorithm instead of CO-LQR in the semi

active control scheme. Alike, the absolute accelerations for the first, second and the third floor are reduced by 41%,43% and 42% respectively using the proposed controller. The proposed controller attains these reductions in structural responses using 23% lesser force than the CO-LQR controller. Figure 4.25(d) shows the comparison of the time histories of the forces used by the proposed controller and CO-LQR. The proposed controller can do that because of the variation in the value of the control weighting matrix **R** in real time according to the proposed algorithm. The variations in the value of **R** are shown in Figure 4.25(e). Further, a comparison of the cumulative energies of the displacement signal obtained by employing the proposed controller and the conventional CO-LQR is shown in Figure 4.25(f).

Table 4.7 Peak responses of structure using CO-LQR controller and PSO- τ_p^{max}-modified-LQR controller subjected to earthquake recorded in different soil conditions

Control algorithm	Earthquake (Hard Rock)			Earthquake (Medium soil)			Earthquake (Soft soil)		
	Uncontrol-led	CO-LQR	PSO- τ_p^{max}-modified-LQR	Uncontrol-led	CO-LQR	PSO- τ_p^{max}-modified-LQR	Uncontrol-led	CO-LQR	PSO- τ_p^{max}-modified-LQR
Displacement (cm)	0.66	0.28	0.12	0.60	0.38	0.20	0.99	0.24	0.14
	0.80	0.42	0.16	0.93	0.45	0.27	1.26	0.50	0.38
	0.99	0.56	0.20	1.20	0.50	0.31	1.53	0.87	0.47
Inter story drift(i_d) (cm)	0.66	0.28	0.12	0.60	0.38	0.20	0.99	0.24	0.14
	0.14	0.14	0.04	0.33	0.08	0.06	0.27	0.26	0.22
	0.19	0.14	0.04	0.27	0.05	0.04	0.27	0.27	0.11
Acceleration (cm/s^2)	1167	501	293	830	621	526	852	576	525
	1287	527	304	1018	709	610	1217	757	625
	1356	570	328	1157	986	880	1299	890	806
Force (N)	--	1731	1334	--	1634	1502	--	1866	1619

For the earthquake recorded in the medium soil, the displacement response of the third floor for the uncontrolled structure is shown in Figure 4.26(a). Comparison of the displacement time histories of an uncontrolled and controlled structure employing CO-LQR and proposed control algorithm is shown in Figure 4.26(b). Similarly, comparison of time histories of the displacement responses due to CO-LQR and the proposed controller are shown in Figure 4.26(c) which shows that semi active control scheme employing the proposed controller reduced the displacement response more effectively than the CO-LQR. From Table 4.7, the proposed controller achieved more reduction in the displacement by 49%, 41% and 38% for the first, second and third floor as compared with the CO-LQR. The interstorey drift between the first-second floor and second third floor are reduced by 25% and 20% more using the proposed

controller in place of CO-LQR. Alike, the proposed controller reduced the absolute accelerations for the first, second and the third floor with 15%,14% and 11% respectively as compared with the CO-LQR. These reductions in structural responses achieved by the proposed controller using 8% lesser force than the CO-LQR. The comparison of the time histories of forces due to CO-LQR and PSO- τ_p^{max}-modified-LQR are demonstrated in Figure 4.27(d). The variation of the values of the control weighting matrix **R** is shown in Figure 4.26(e). The comparison of cumulative energies of the displacement of third floor is shown in Figure 4.26(f).

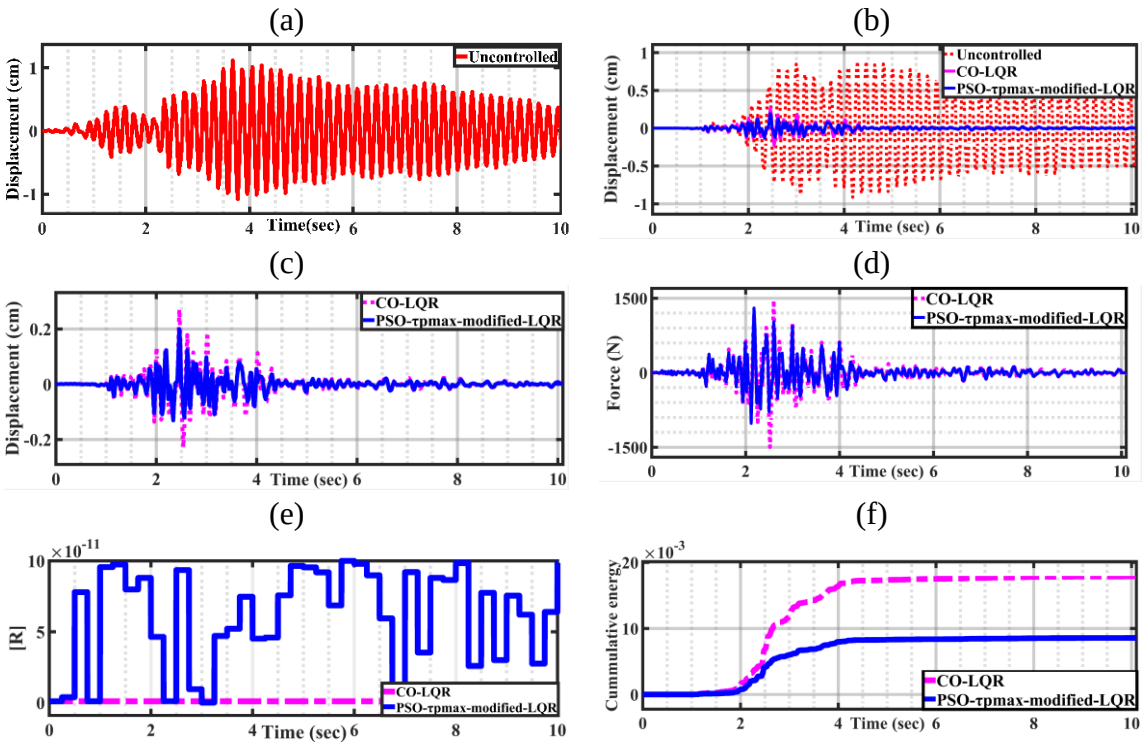

Figure 4.26 Structural responses for the structure subjected to the medium soil earthquake (a) displacement response of third floor of uncontrolled structure (b) comparison of controlled responses of third floor using CO-LQR and PSO- τ_p^{max}-modified-LQR algorithms (c) control forces for the CO-LQR and the PSO- τ_p^{max}-modified-LQR algorithm (d) variation of **R** with time (e) comparison of cumulative energies of the third floor`s displacement by applying CO-LQR and PSO- τ_p^{max}-modified-LQR

For the earthquake recorded in soft soil, the displacement response of the third floor of the uncontrolled structure is shown in Figure 4.27(a) which is to be reduced by employing the semi active control scheme. The comparison of the time histories of the displacement response obtained using uncontrolled structure, by employing CO-LQR control algorithm and the proposed control algorithm is shown in Figure 4.27(b). By inspection of Figure 4.27(b), it can be concluded that an effective performance is achieved by both control algorithms as compared to uncontrolled response. It can be seen in Figure 4.27(c) that the proposed algorithm demonstrates better displacement reduction capability as compared to the CO-LQR. This can also be verified

by observing Table 4.7. The reductions in the displacement of the first, second and the third floor using the proposed controller are 42%,24% and 46% respectively as compared to CO-LQR.

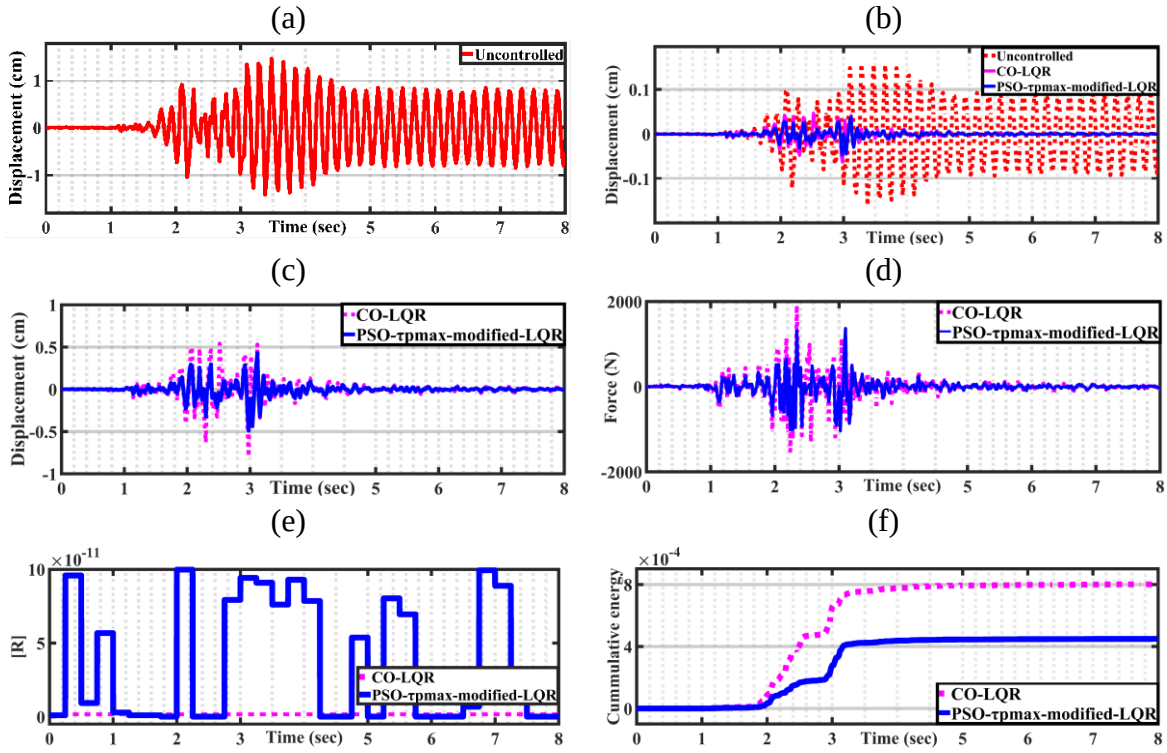

Figure 4.27 Structural responses for the structure subjected to the soft soil earthquake (a) displacement response of third floor of uncontrolled structure (b) comparison of controlled responses of third floor using CO-LQR and PSO- τ_p^{max}-modified-LQR algorithms (c) control forces for the CO-LQR and the PSO- τ_p^{max}-modified-LQR algorithm (d) variation of **R** with time (e) comparison of cumulative energies of the third floor`s displacement by applying CO-LQR and PSO- τ_p^{max}-modified-LQR

From Table 4.7, the interstorey drift between the first-second floor and second third floor are reduced by 15% and 59% more using the proposed controller in place of CO-LQR. The proposed controller reduced the absolute accelerations for the first, second and the third floor by 9%,17% and 9% respectively as compared with the CO-LQR. These reductions in structural responses achieved by the proposed controller using 13% lesser force than the CO-LQR. This can also be seen in the comparison of the force-time histories due to CO-LQR and PSO- τ_p^{max}-modified-LQR demonstrated in Figure 4.27(d). Variation of the control weighting matrix **R** is shown in Figure 4.27(e) and the comparison of the cumulative energies of the displacement of the third floor is shown in Figure 4.27(f) which shows that the displacement signal obtained using the proposed controller has the lesser energy for obliteration. It is challenging to control the response of the structure located in soft soil as this type of soil act as an amplifier to the ground motion. Based on the analysis carried out in the above section, it can be concluded that the proposed controller gives the better performance over the CO-LQR for a semi active control scheme used for structure subjected to the earthquakes recorded in hard, medium and soft soil conditions.

4.3.3 Results and discussion on the performance of the adaptive LQG based on PSO-τ_p^{max}

A performance analysis of the adaptive LQG controller is carried out on the prototype test structure under the various conditions as listed in section 4.2.3 of this chapter.

(i) Using different earthquake time histories

To assess the effectiveness of the suggested PSO-τ_p^{max}-modified-LQG controller, the results of the dynamic analysis of the three DOF test structure having an MR damper on the ground floor are discussed. For simulation, the three different earthquake time histories are used and shown in Figure 4.3(a-c). The displacement response of the uncontrolled structure is shown in Figure 4.28(a) whereas comparison between uncontrolled displacement response and response due to CO-LQG and PSO- τ_p^{max}-modified-LQG controller is shown in Figure 4.28(b). The visual inspection of Figure 4.28(b) suggests that the displacement response is reduced. From Table 4.8, this reduction in the peak values is 78% using CO-LQG and 82% using the PSO- τ_p^{max}-modified-LQG. Further, in Figure 4.28(c), the comparison of the displacement due to CO-LQG and PSO- τ_p^{max}-modified-LQG is presented. Observations from Figure 4.28(c) conclude that the displacement is reduced using the proposed controller throughout the time history presented. From Table 4.8, the reduction in the peak values of relative displacement using the proposed controller is 15% for the first floor, 21% for the second floor and 22% for the third floor as compared with CO-LQG.

Further, the change in the control weighting matrix **R** is shown in Figure 4.28(e). The value of **R** for the CO- LQG remains same through the seismic event whereas in the proposed algorithm there are variations in the values of **R** for each time window (t_w) according to the quasi-resonance between the domain frequency and first two fundamental frequency of the structure. The reduction in the peak values of the inter-storey drift, the proposed control algorithm achieved the reduction of 29% between the first-second floor and 33% between second-third floor as compared with the CO-LQG. The reduction in peak values of the absolute acceleration is shown in Table 4.8. Observations from Table 4.8 reveal that the proposed algorithm can reduce the peak values of absolute acceleration by 28%, 46% and 27% for the first, second and third floor as compared with the CO-LQG. It is necessary to point out here that all these reductions in the structural responses are achieved using lesser control force as shown in Figure 4.28(d).

From Table 4.8, The proposed controller utilized 24% lesser force (peak value) to achieve the above-mentioned results as compared with the CO-LQG. The energy confined in the controlled signal of the relative displacement of the third floor due to CO-LQG and the PSO- τ_p^{max}-modified-LQG is shown in Figure 4.28(f).

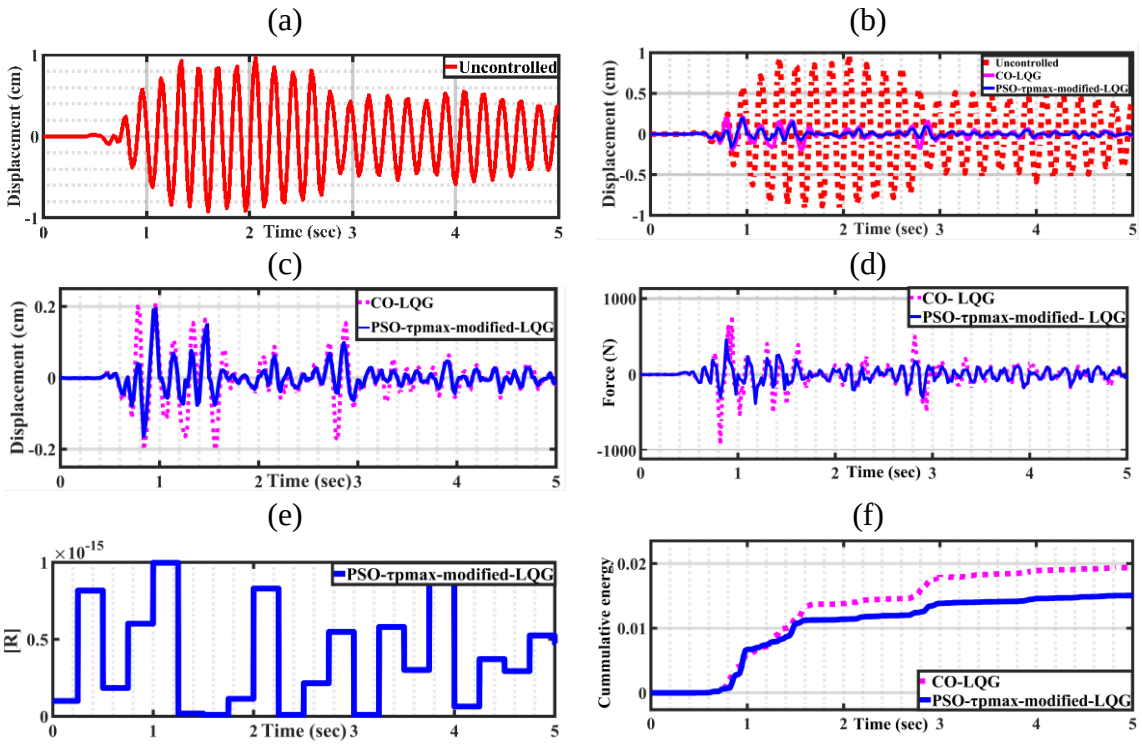

Figure 4.28. Structural responses for the structure subjected to El-Centro earthquake (a) displacement response of third floor of uncontrolled structure (b) comparison of controlled responses of third floor using CO-LQG and PSO- τ_p^{max}-modified-LQG algorithms (c) control forces for the CO-LQG and the PSO- τ_p^{max}-modified-LQG (d) variation of **R** with time (e) comparison of cumulative energies of the third floor`s displacement by applying CO-LQG and PSO- τ_p^{max}-modified-LQG

Similar discussions are presented for the Chi-Chi and Gebze earthquake. For Chi-Chi earthquake, referring to the Figure 4.29, the displacement response of the third floor of the uncontrolled structure is shown in Figure 4.29(a) whereas comparison of uncontrolled displacement response and response due to CO-LQG and PSO- τ_p^{max}-modified -LQG controller is shown in Figure 4.29(b). The visual inspection of Figure 4.29(b) suggests that displacement response is reduced. The comparison of the displacement response due to CO-LQG and PSO-τ_p^{max}-modified-LQG is presented in Figure 4.29(c) for Chi-Chi earthquake whereas the same is presented in Figure 4.30(c) for Gebze earthquake. Observations of these Figures conclude that the displacement is reduced using the proposed controller throughout the time history.

From Table 4.8, the reduction in the peak values of relative displacement using the proposed controller is 26% for the first floor, 23% for the second floor and 20% for the third floor for Chi-Chi earthquake and 6% for the first floor, 18% for the second floor and 22% for the third floor for Gebze earthquake as compared with the CO-LQG. Variations of the control weighting matrix **R** are shown in Figure 4.29(e) for Chi-Chi earthquake whereas for Gebze earthquake it is shown in Figure 4.30(e). The inter-storey drift for Chi-Chi earthquake, from Table 4.8 the proposed control algorithm achieved the reduction of 20% between the first-second

floor and 10% between the second-third floor. For, Chi-Chi earthquake, it is 31% for the both i.e. between the first- second and second-third floor.

Table 4.8 Percentage change in peak responses of structure due to conventional CO-LQG controller and PSO-τ_p^{max}-modified LQG controller

Control algorithm	El-Centro earthquake			Chi-Chi earthquake			Gebze earthquake		
	Uncontrolled	CO-LQG	PSO- τ_p^{max}-modified LQG	Uncontrolled	CO-LQG	PSO- τ_p^{max}-modified LQG	Uncontrolled	CO-LQG	PSO- τ_p^{max}-modified LQG
Displacement (cm)	0.55	0.12	0.10	0.14	0.02	0.015	0.074	0.0180	0.017
	0.83	0.19	0.15	0.22	0.04	0.031	0.117	0.0353	0.029
	0.97	0.22	0.17	0.27	0.05	0.040	0.138	0.0513	0.040
Inter story drift(i_d) (cm)	0.55	0.12	0.10	0.14	0.02	0.015	0.074	0.018	0.017
	0.29	0.07	0.05	0.08	0.02	0.016	0.042	0.017	0.012
	0.14	0.03	0.02	0.05	0.01	0.009	0.022	0.016	0.011
Acceleration (cm/s^2)	870	733	526	181	98	48	126	91	47
	1070	755	410	268	81	60	150	74	61
	1400	723	525	317	97	84	185	113	101
Force (N)	0	971	736	0	1178	1098	0	1278	1167

Similarly, for Gebze earthquake, from Table 4.8, the proposed controller achieved the reduction in the inter-storey drift 31% between the first-second floor and between second-third floor, each as compared to the CO-LQG. The absolute accelerations of all floors of the structure subjected to the Chi-Chi earthquake and Gebze earthquake are also presented in Table 4.8. The observations from Table 4.8 reveal that the proposed algorithm can reduce the peak values of the acceleration by 51% for the first floor, 25% for the second floor and 13% for the third floor as compared with the CO-LQG whereas for Gebze earthquake, 48% for the first floor, 17% for the second floor and 10% reduction for the third floor is achieved by the proposed control algorithm. The comparison of the time histories of the control force due to CO-LQG and the proposed controller are shown in Figure 4.29(d) for Chi-Chi earthquake and in Figure 4.30(d) for the Gebze earthquake. From Table 4.8, the proposed controller utilized lesser force to achieve the above-described results. The comparison of the cumulative energies of the third floor`s displacement by applying CO-LQG and the PSO- τ_p^{max}-modified-LQG is shown in Figure 4.29(f) for Chi-Chi earthquake and Figure 4.30(f) for Gebze earthquake.

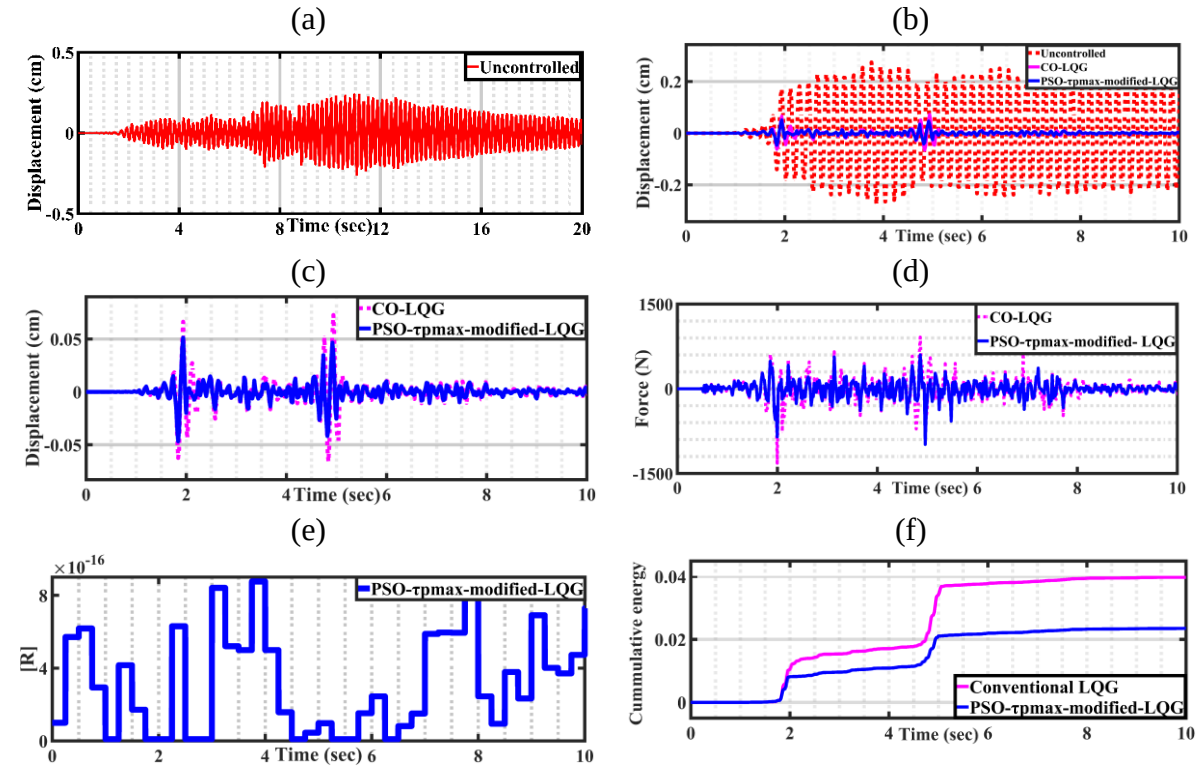

Figure 4.29 Structural responses for the structure subjected to Chi-Chi earthquake (a) displacement response of third floor of uncontrolled structure (b) comparison of controlled responses of third floor using CO-LQG and PSO- τ_p^{max}-modified-LQG algorithms (c) control forces for the CO-LQG and the PSO- τ_p^{max}-modified-LQG (d) variation of **R** with time (e) comparison of cumulative energies of the third floor`s displacement by applying CO-LQG and PSO- τ_p^{max}-modified-LQG

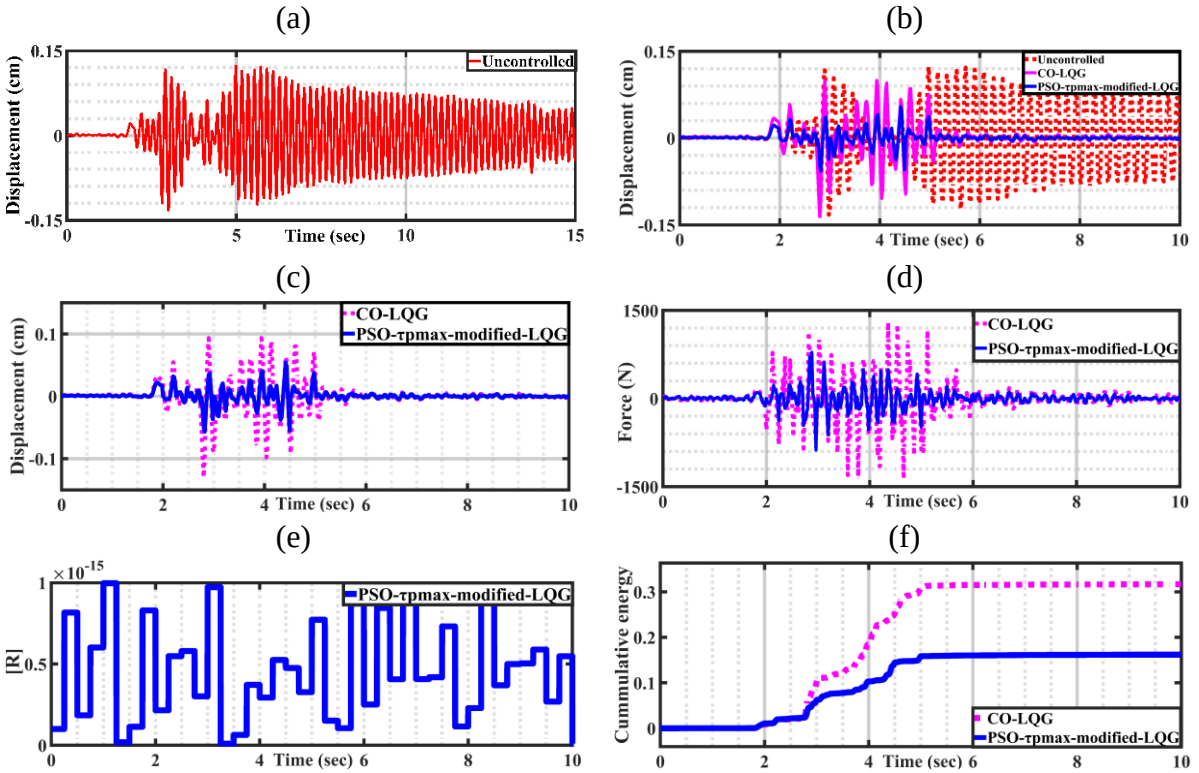

Figure 4.30 Structural responses for the structure subjected to Gebze earthquake (a) displacement response of third floor of uncontrolled structure (b) comparison of controlled responses of third floor using CO-LQG and PSO- τ_p^{max}-modified-LQG algorithms (c) control forces for the CO-LQG and the PSO- τ_p^{max}-modified-LQG (d) variation of **R** with time (e) comparison of cumulative energies of the third floor`s displacement by applying CO-LQG and PSO- τ_p^{max}-modified-LQG

(ii) Using an earthquake recorded in different soil conditions

The performance analysis of the proposed controller is carried for the structure subjected to the hard, medium and soft soil. For the performance assessment in hard soil, the uncontrolled displacement response of the third floor of the structure is considered in the Figure 4.31(a).

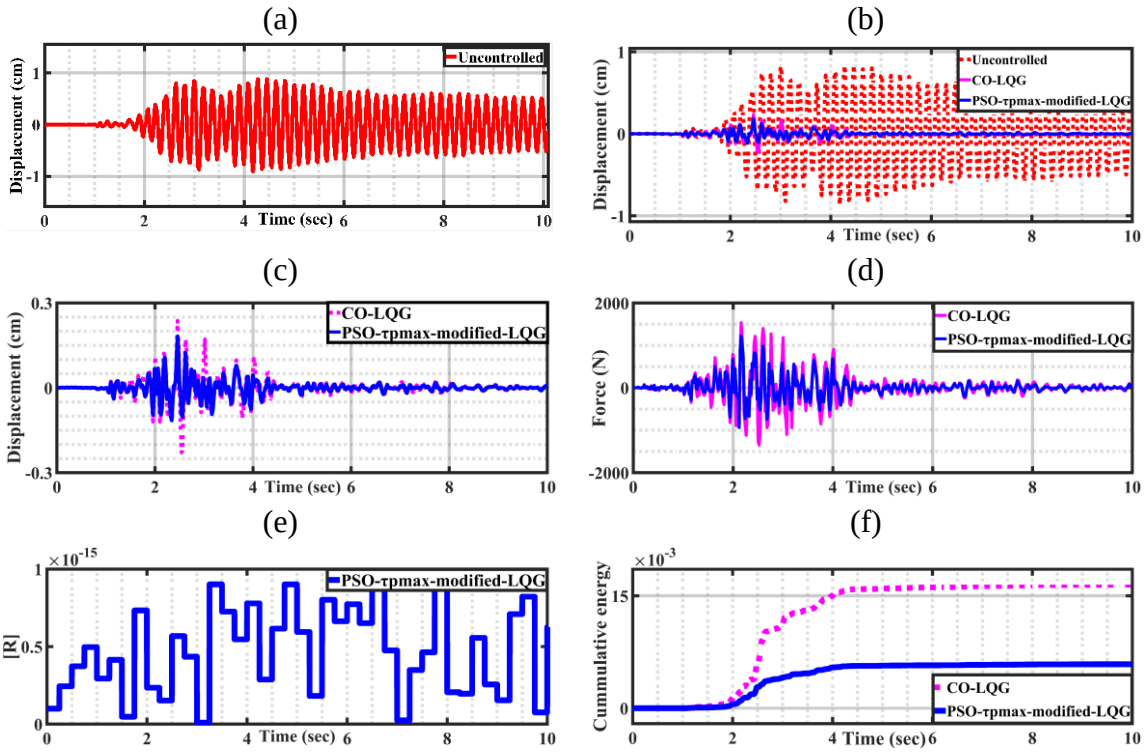

Figure 4.31 Structural responses for the structure subjected to hard soil earthquake (a) displacement response of third floor of uncontrolled structure (b) comparison of controlled responses of third floor using CO-LQG and PSO-τ_p^{max}-modified-LQG algorithms (c) control forces for the CO-LQG and the PSO-τ_p^{max}-modified-LQG algorithm (d) variation of **R** with time (e) comparison of cumulative energies of the third floor`s displacement by applying CO-LQR and PSO-τ_p^{max}-modified-LQG

The comparison of the third floor`s displacement responses of the uncontrolled structure and semi-actively controlled structure using CO-LQG and PSO-τ_p^{max}-modified-LQG control algorithm is shown in Figure 4.31(b). Figure 4.31(b) shows the mitigation of the displacement response through the seismic event. It can be seen from the Table 4.9, the reduction in the peak value of the displacement response is 72% using CO-LQG and 80% using proposed PSO-τ_p^{max}-modified-LQG as compared with the uncontrolled structure. A comparison of the displacement response due to CO-LQG and PSO-τ_p^{max}-modified-LQG is shown in Figure 4.31(c). The Figure shows that the proposed controller is effectively reducing the relative displacement response of the structure. It can also be observed from Table 4.9, the proposed controller achieved more reduction by 46%, 33% and 28% for first, second and third floor in peak values of the relative displacement as compared with the CO-LQG controller. It can be seen from Table 4.9 that the inter-story drift is reduced by 12% for the first-second floor and 25% for the second-third floor

on applying PSO-τ_p^{max}-modified-LQG controller instead of CO-LQG in the semi active control scheme. The reduction in the absolute acceleration using the proposed controller is moderate as compared with the CO-LQG. The absolute accelerations for the first, second and the third floor are reduced by 4%, 2% and 14% respectively by applying the proposed controller.

Table 4.9 Peak responses due to CO-LQG and PSO-FFT-modified LQG for structure the subjected to earthquake recorded in different soil conditions

Control algorithm	Earthquake (Hard Rock)			Earthquake (Medium soil)			Earthquake (Soft soil)		
	Uncontrol-led	CO-LQG	PSO- τ_p^{max}-modified-LQG	Uncontrol-led	CO-LQG	PSO- τ_p^{max}-modified-LQG	Uncontrol-led	CO-LQG	PSO- τ_p^{max}-modified-LQG
Displacement (cm)	0.66	0.13	0.07	0.60	0.38	0.18	0.99	0.22	0.15
	0.80	0.22	0.15	0.93	0.45	0.24	1.26	0.55	0.39
	0.89	0.25	0.18	1.20	0.51	0.29	1.53	0.76	0.49
Inter story drift(i_d) (cm)	0.66	0.13	0.07	0.60	0.38	0.18	0.99	0.22	0.15
	0.14	0.09	0.08	0.33	0.07	0.06	0.27	0.33	0.24
	0.09	0.04	0.03	0.27	0.06	0.05	0.27	0.21	0.10
Acceleration (cm/s^2)	1167	512	493	830	615	520	852	580	540
	1287	570	561	1018	702	602	1217	770	660
	1356	854	735	1157	970	840	1299	904	814
Force (N)	--	1533	1224	--	1642	1129	--	1690	1367

Further, the proposed controller attains these reductions in structural responses using 20% lesser force than the CO-LQG controller. Figure 4.31(d) shows the comparison of the time histories of the forces used by the proposed controller and the CO-LQG. The variations of the control weighting matrix of **R** are shown in Figure 4.31(e) and a comparison of the cumulative energy of the displacement is shown in Figure 4.31(f). This comparison of the cumulative energy concludes that the energy content in the displacement signal of the third floor of the structure is less. Hence the structural integrity is protected.

For earthquake recorded in the medium soil, the comparison of the displacement time histories of an uncontrolled and controlled structure employing CO-LQG and proposed control algorithm are shown in Figure 4.32(b). The preeminence of the proposed control over the CO-LQG can be observed in Figure 4.32(c) in which a comparison of the time histories of the displacement responses due to CO-LQG and the proposed controller is shown. Observing Table 4.9, the proposed controller achieves a reduction in the displacement by 53%, 47% and 43% for first, second and third floor respectively as compared with the CO-LQG. The inter-storey drift

between the first-second floor and second third floor are reduced by 14% and 17% more using the proposed controller in place of CO-LQG. Alike, the proposed controller reduced the absolute accelerations for the first, second and the third floor by 15%,14% and 13% respectively as compared with the CO-LQG. Proposed controller attains these reductions in structural responses using 31% lesser force than the CO-LQG as can be seen in Figure 4.32(d). Variation of the values of the control weighting matrix **R** is shown in Figure 4.32(e). The comparison of the cumulative energies of the displacement of the third floor is shown in Figure 4.32(f) which shows that the displacement signal obtained using the proposed controller has the lesser energy for destruction.

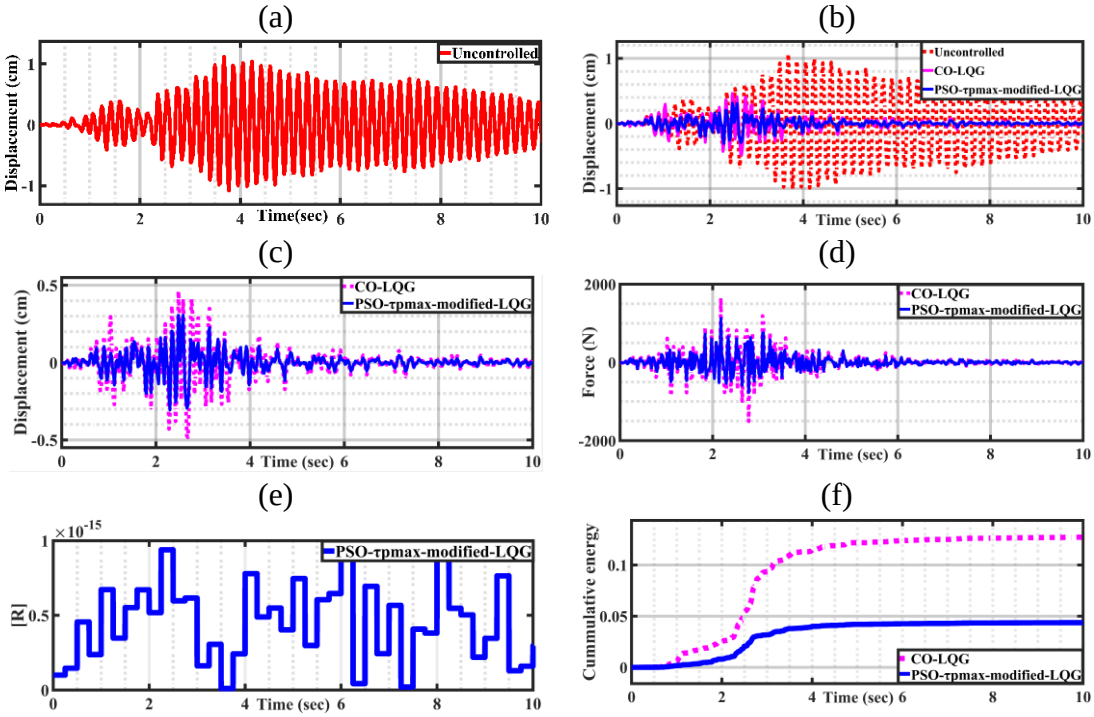

Figure 4.32 Structural responses for the structure subjected to medium soil earthquake (a) displacement response of third floor of uncontrolled structure (b) comparison of controlled responses of third floor using CO-LQG and PSO- τ_p^{max}-modified-LQG algorithms (c) control forces for the CO-LQG and the PSO- τ_p^{max}-modified-LQG algorithm (d) variation of **R** with time (e) comparison of cumulative energies of the third floor`s displacement by applying CO-LQR and PSO- τ_p^{max}-modified-LQG

For earthquake recorded in soft soil, the displacement response of third floor of the uncontrolled structure is shown in Figure 4.33(a) which is to be reduced by employing the semi active control scheme. Comparison of the time histories of the displacement response of uncontrolled structure and obtained by employing CO-LQG and proposed controller is shown in Figure 4.33(b) which shows the effectiveness of the semi active control scheme as compared to the uncontrolled structure. Also, it can be seen from the Table 4.9, the proposed controller achieved a reduction in the displacement by 32% for the first floor, 29% for the second floor and 36% for the third floor as compared with the CO-LQG.

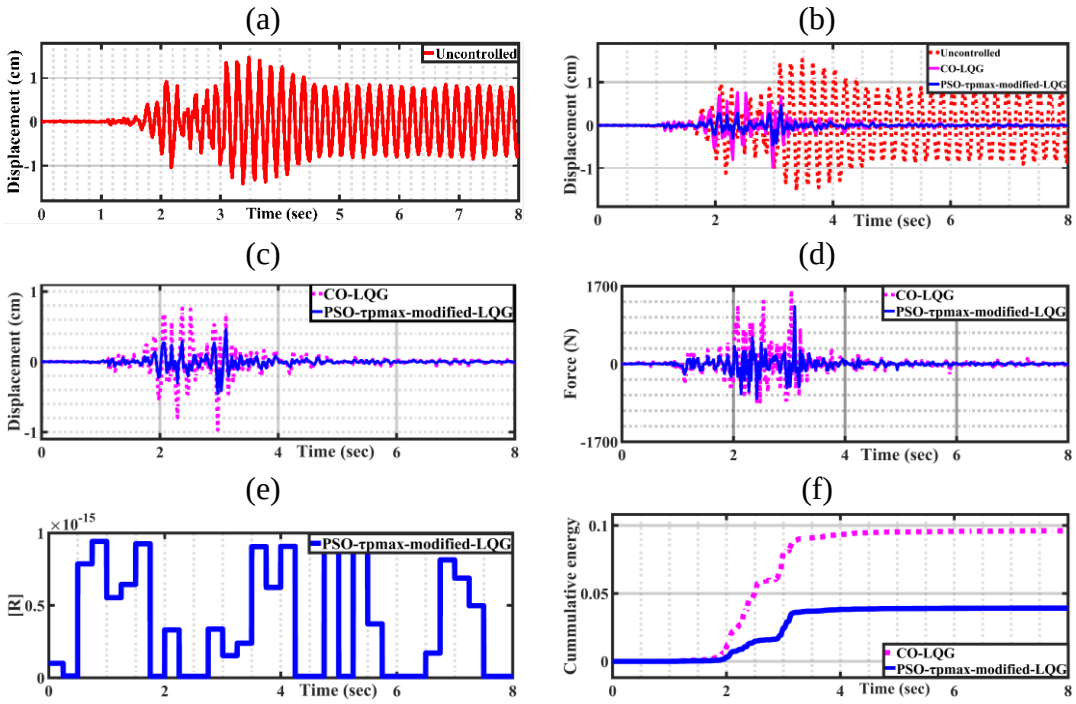

Figure 4.33 Structural responses for the structure subjected to soft soil earthquake (a) displacement response of third floor of uncontrolled structure (b) comparison of controlled responses of third floor using CO-LQG and PSO- τ_p^{max}-modified-LQG algorithms (c) control forces for the CO-LQG and the PSO- τ_p^{max}-modified-LQG algorithm (d) variation of **R** with time (e) comparison of cumulative energies of the third floor`s displacement by applying CO-LQR and PSO- τ_p^{max}-modified-LQG

The inter-storey drifts between the first-second floor and second-third floor are reduced by 27% and 52% as compared to CO-LQG. Alike, the proposed controller reduced the accelerations for the first, second and the third floor by 7%,14% and 10% respectively as compared with the CO-LQG. These reductions in structural responses achieved by the proposed controller using 19% lesser force than the CO-LQG. To validate this fact the comparison of the time histories of the CO-LQG and PSO- τ_p^{max}-modified-LQG is demonstrated in Figure 4.33(d). Further, the variation of the values of the control weighting matrix **R** is shown in Figure 4.33(e). These variations are obtained based on the quasi resonance occurred between the natural frequency of the prototype three storey structure and the dominant frequencies of each time window for the earthquake. In case of quasi resonance, the larger force is required to control the increased vibrations, hence, an appropriate lower value of weighting matrix **R** is determined by PSO algorithm and vice-versa. The comparison of the cumulative energies of the displacement of the third floor is shown in Figure 4.33(f) which shows the cumulative energy content of the displacement signal of the third floor of the structure obtained using the proposed controller. If it is less, there are lesser chances of the damage to the structure and vice-versa. In this way, the proposed controller protects the integrity of the structure. Based on the above discussion it can be concluded that the PSO- τ_p^{max}-modified-LQG performs superior to the conventional CO-LQG for an earthquake recorded in different soils.

4.4 Applicability of the proposed algorithms on a five-storey structure

It is obsered from the discussion by now that the proposed controllers work satisfactorily with the three storey strcutures. To examine the effects of the higher modes on the performance of the semi active control scheme, the proposed controllers are numerically tested on prototype a five-storey structure having 2% damping. The mass and stiffness matrices of the structure are given below.

$$M = \begin{bmatrix} 688 & 0 & 0 & 0 & 0 \\ 0 & 688 & 0 & 0 & 0 \\ 0 & 0 & 688 & 0 & 0 \\ 0 & 0 & 0 & 688 & 0 \\ 0 & 0 & 0 & 0 & 688 \end{bmatrix}$$

$$K = \begin{bmatrix} 8400000 & -4788000 & 0 & 0 & 0 \\ -4788000 & 9576000 & -4788000 & 0 & 0 \\ 0 & -4788000 & 9576000 & -4788000 & 0 \\ 0 & 0 & -4788000 & 9576000 & -4788000 \\ 0 & 0 & 0 & -4788000 & 4788000 \end{bmatrix}$$

The analysis for the adaptive LQR and LQG controllers is carried out based on PSO-FFT and PSO- τ_p^{max} on the five-storey structure having MR damper at ground floor subjected to different earthquake time histories. For remaining conditions used in the analysis of the three-storey, like placing an MR damper at different floors within the structure. The best performance will always be delivered when the MR damper is placed the between the lowest and first floor. However, it is recommended to use multiple MR damper in higher structures to get desired results. Similarly, for assuming the condition, when power is lost at the peak of the earthquake or any other instant during the earthquake, any controller would behave like a passive off controller but still, it shall deliver better performance than the uncontrolled structure.

Again, the performance analysis is carried out for the proposed controller on the five-storey structure by using similar methods as used in the analysis of the proposed controllers on the three storey structure i.e. qualitative analysis and quantitative analysis. In qualitative analysis, the visual inspection of the time histories of the relative displacement responses of fifth floor of the structure using proposed controller and conventional controller is carried out whereas in quantitative analysis, a comparison of the percentage reduction in the peak values of all floors of the structure due to the proposed controller and conventional controller is carried out. Both analysis is required for the critical evaluation of the proposed controllers.

4.4.1 Performance analysis of modified LQR based on the PSO-FFT approach

To assess the effectiveness of the suggested adaptive LQR controller (PSO-FFT-modified-LQR), the results of the dynamic analysis of the five-storey test structure having an MR damper on the ground floor are discussed. For simulation, the following two earthquake time histories listed below are used in the present study and are shown in Figure 4.3(a-b).

(i) 1940 El-Centro Valley earthquake

(ii) 1999 Chi-Chi Nantou County Taiwan earthquake

For visual analysis, only the initial 5 seconds of time histories of structural responses of the third floor of test structure subjected to El-Centro earthquake are shown in Figure 4.34. The reason behind showing only initial 5 seconds of the time histories is that the maximum energy is confined in the initial 5 seconds of the El-Centro earthquake. For a similar reason, the time histories of the structural responses due to Chi-Chi earthquake is shown for an initial 14 seconds in Figure 4.36. The percentage reductions in the peak values of the structural responses are shown in Figure 4.35 for El-Centro earthquake whereas in Figure 4.37 for Chi-Chi earthquake.

For El-Centro earthquake, the relative displacement response of the fifth floor of the uncontrolled structure is shown in Figure 4.34(a). The comparison in the Figure 4.34(b) concludes that the semi active scheme using the CO-LQR and the PSO-FFT-modified-LQR is successful in mitigation of the vibrations. Now, the comparative analysis between the conventional CO-LQR and proposed PSO-FFT-modified-LQR (adaptive LQR) is presented.

Figure 4.34(c) presents the comparison of the time histories of the fifth floor`s displacement response using CO-LQR and the proposed adaptive LQR controller. It can be seen from the Figure 4.34(c) that the proposed controller is more effective in reducing the displacement response. It is notable here that this effective mitigation is achieved by the proposed controller using lesser control force as shown in Figure 4.34(d). These results are due to the real-time variations of the control weighting matrix **R** using the PSO-FFT algorithm. The variations of **R** are shown in Figure 4.34(e). Moreover, cumulative energy of the fifth floor`s displacement signal obtained due to CO-LQR and the proposed controller is shown in Figure 4.34(f). This energy is a measure of the disruptive capability of the displacement signal.

For El-Centro earthquake, it can be observed from Figure 4.35(a), proposed controller delivers approximately 55% more reduction in the peak values of the relative displacement of all floors as compared with the CO-LQR. The inter-storey drift is reduced by 44%,45%,25%,20% and 22% for the first to fifth floor respectively as shown in Figure 4.35(b). The absolute acceleration is

reduced by 44%, 53%,13%,46% and 42 % for first to the fifth floor respectively by using the proposed controller in place of CO-LQR as shown in Figure 4.35(c).

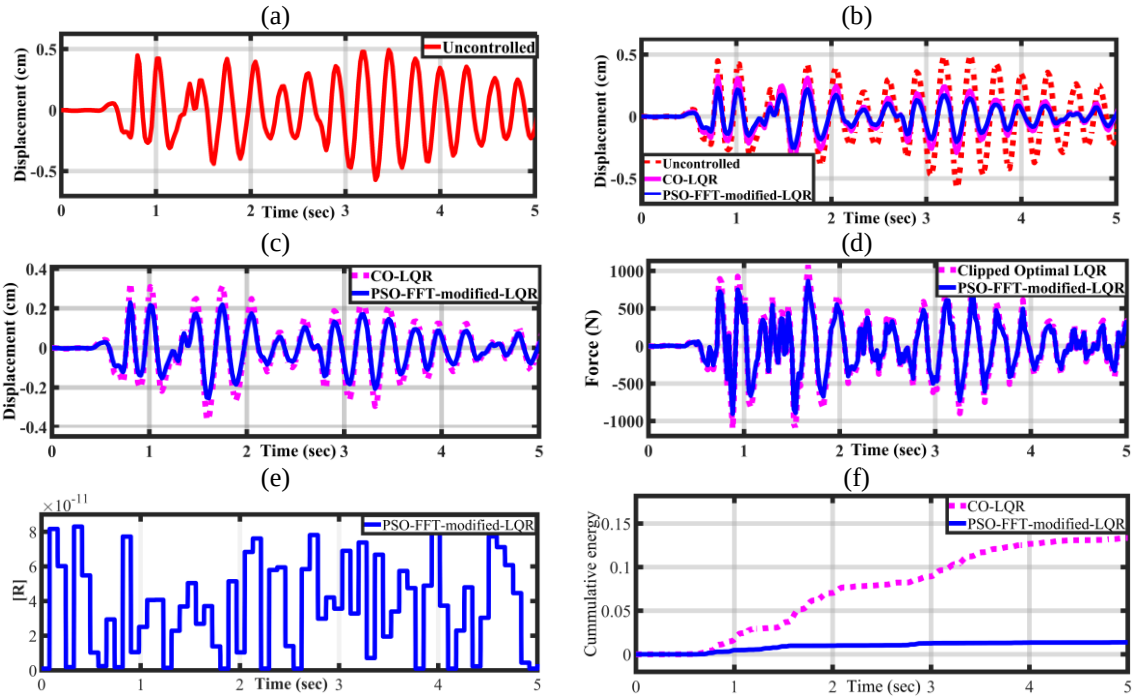

Figure 4.34 Structural responses for five storey structure subjected to the 1940 El-Centro earthquake (a) displacement response of fifth floor of uncontrolled structure (b) comparison of controlled responses of fifth floor using CO-LQR and PSO-FFT-modified-LQR algorithms (c) control forces for the CO-LQR and the PSO-FFT-modified-LQR algorithm (d) variation of **R** with time (e) comparison of cumulative energies of the fifth floor`s displacement by applying CO-LQR and PSO-FFT-modified-LQR

For Chi-Chi earthquake, the displacement response of the fifth floor of uncontrolled structure which is to be reduced by employing the semi active control scheme is shown Figure 4.36(a). The comparison of the time histories of the displacement response obtained using uncontrolled structure by employing CO-LQR control algorithm and the proposed control algorithm is shown in Figure 4.36(b). This Figure shows the effectiveness of the semi active control scheme as compared to the uncontrolled structure. From Figure 4.36(c), the proposed controller achieved a reduction in the displacement as compared with the CO-LQR.This effective mitigation is achieved by the proposed controller using lesser control force as shown in Figure 4.36(d). The variations of **R** are shown in Figure 4.36(e).

These variations in the control weighting matrix **R** occur in real time using the PSO algorithm. The force imparted to the structure by the MR damper follows the variations of control weighting matrix **R**. Further, cumulative energy of the fifth floor`s displacement signal obtained due to CO-LQR and the proposed controller is shown in Figure 4.36(f). This energy is a measure of the disruptive capability of the displacement signal.

(a)

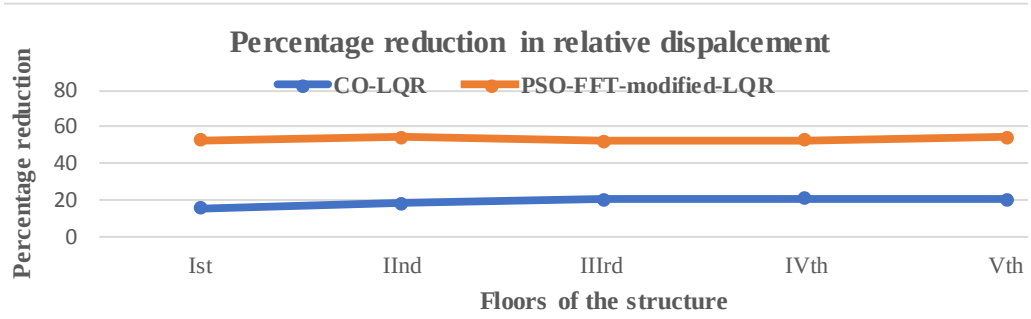

(b)

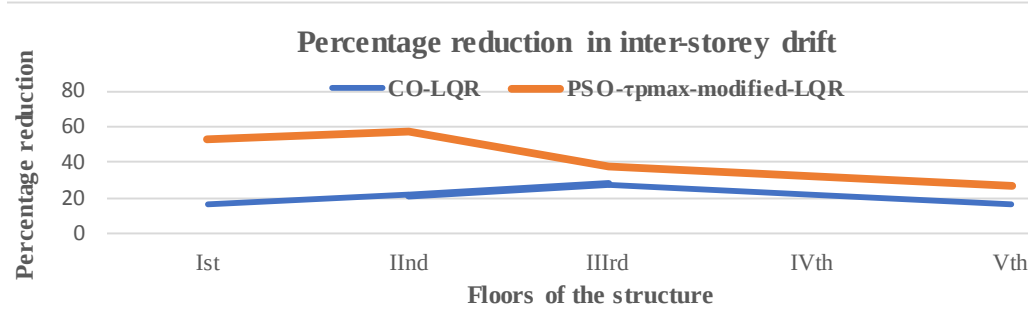

(c)

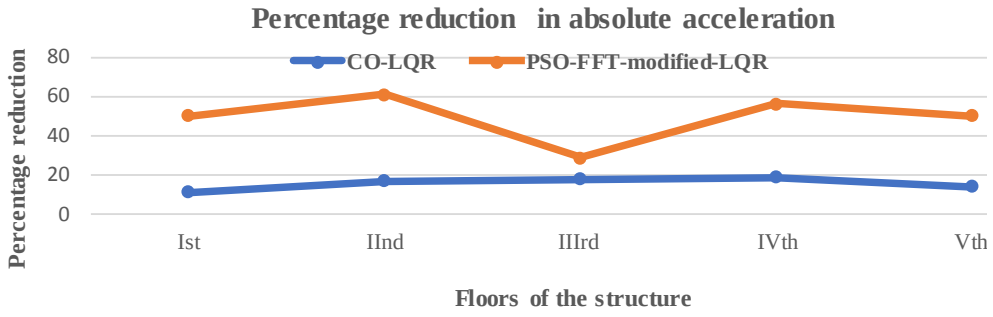

Figure 4.35 Comparison of the percentage reduction in peak values of fifth floor of the structure due to CO-LQR and proposed controller for El-Centro earthquake (a) Displacement (b) Inter-storey drift (c) Acceleration

The comparison in Figure 4.37(e) concludes that the displacement signal obtained due to proposed controller has the lesser energy for disruption. Figure 4.37(a) shows the percentage reduction in relative displacement of all floors using proposed controller and the CO-LQR controller. This reduction is approximately 10% for the first to fifth floor as compared with the CO-LQR. Similarly, the inter-storey drift between the first-second, second-third, third-fourth and fourth-fifth floor is reduced by 17%, 15%, 30% and 2% respectively as shown in Figure 4.37(b). Alike, the proposed controller reduced the accelerations for the first, second, third, fourth and fifth floor by 29%,13%,5%,5% and 20% more respectively as compared with the CO-LQR. This reduction in the structural responses are achieved using 21% lesser force than the conventional LQR controller.

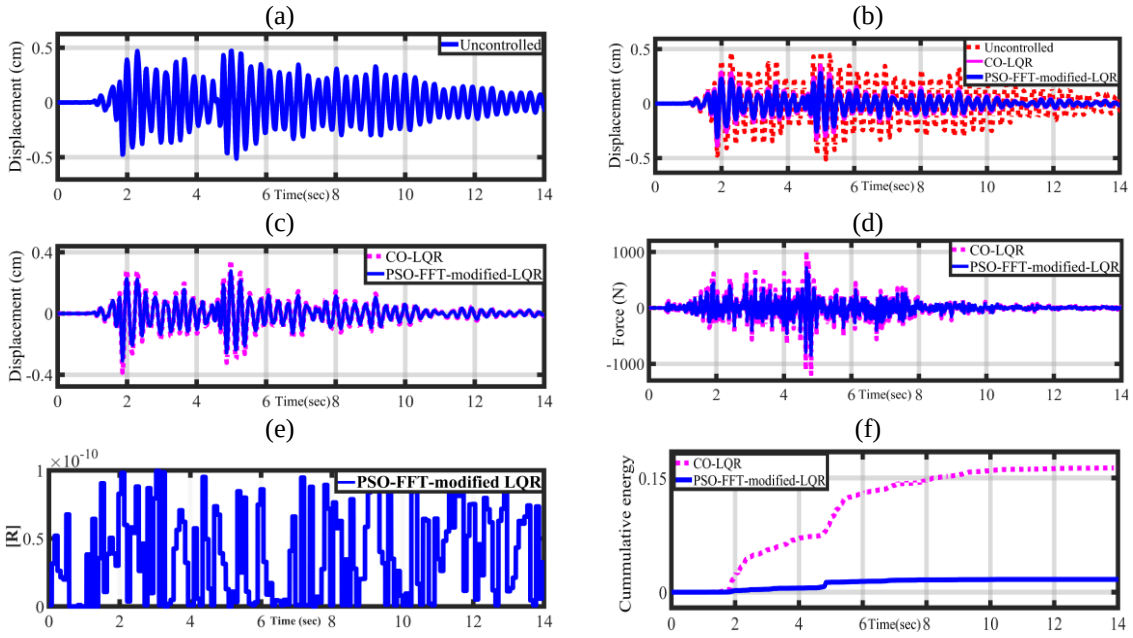

Figure 4.36 Structural responses for five storey structure subjected to the 1999 Chi-Chi earthquake (a) displacement response of fifth floor of uncontrolled structure (b) comparison of controlled responses of fifth floor using CO-LQR and PSO-FFT-modified-LQR algorithms (c) control forces for the CO-LQR and the PSO-FFT-modified-LQR algorithm (d) variation of **R** with time (e) comparison of cumulative energies of the fifth floor`s displacement by applying CO-LQR and PSO-FFT-modified-LQR

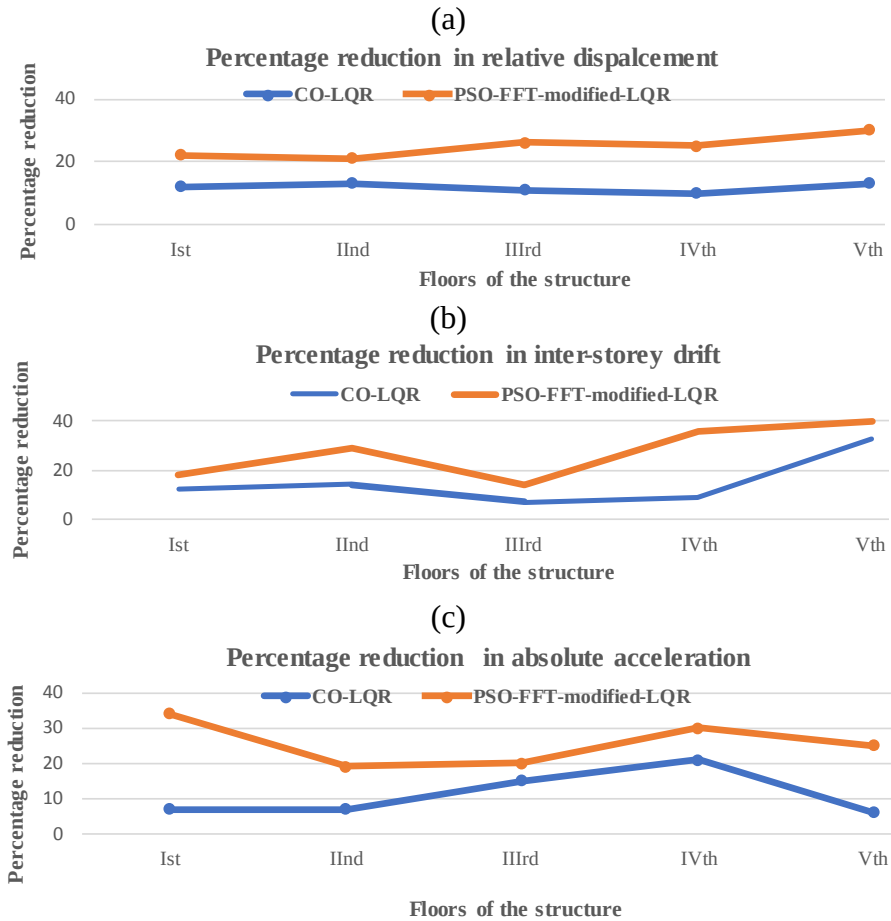

Figure 4.37 Comparison of the percentage reduction in peak values of fifth floor of the structure due to CO-LQR and proposed controller for Chi-Chi earthquake (a) Displacement (b) Inter-storey drift (c) Acceleration

4.4.2 Performance analysis of modified LQG based on PSO-FFT approach

For El-Centro earthquake, the relative displacement response of the fifth floor of the uncontrolled structure is shown in Figure 4.38(a). The comparison in Figure 4.38(b) concludes that the semi active scheme using the CO-LQG and the PSO-FFT-modified-LQG is successful in mitigation of vibrations. Now, the comparative analysis between the conventional CO-LQG and proposed PSO-FFT-modified-LQG (adaptive LQG) is presented.

Figure 4.38(c) presents the comparison of the time histories of the fifth floor`s displacement response using CO-LQG and the proposed adaptive LQG controller. It can be seen from the Figure 4.38 (c), the proposed controller is more effective in reducing the displacement response. It is notable here that this effective mitigation is achieved by the proposed controller using lesser control force as shown in Figure 4.38(d). These results are due the real-time variations of the control weighting matrix **R**. Variations of **R** are shown in Figure 4.38(e). Moreover, cumulative energy of the fifth floor`s displacement signal obtained due to CO-LQG and proposed controller is shown in Figure 4.38(f). This energy is a measure of the disruptive capability of the displacement signal. The comparison in Figure 4.38(f) concludes that displacement signal obtained due to proposed controller has the lesser energy for disruption.

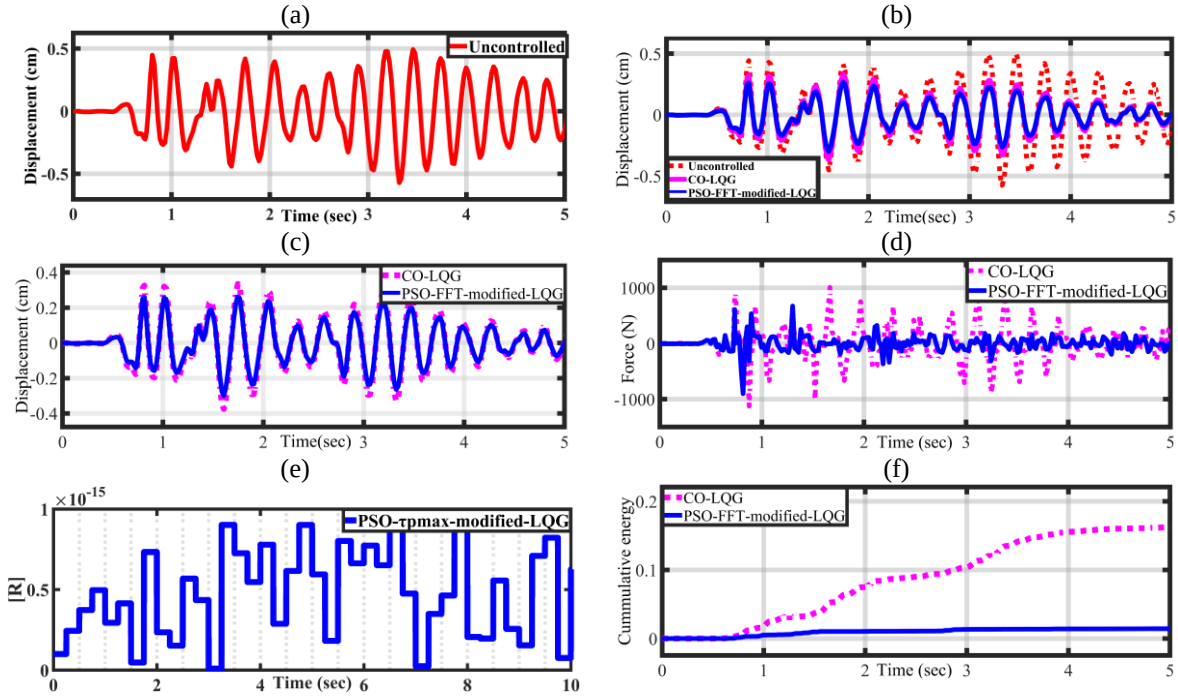

Figure 4.38 Structural responses for five storey structure subjected to the 1940 El-Centro earthquake (a) displacement response of fifth floor of uncontrolled structure (b) comparison of controlled responses of fifth floor using CO-LQG and PSO-FFT-modified-LQG algorithms (c) control forces for the CO-LQG and the PSO-FFT-modified-LQG algorithm (d) variation of **R** with time (e) comparison of cumulative energies of the fifth floor`s displacement by applying CO-LQG and PSO-FFT-modified-LQG

The proposed controller delivers approximately 45% more reduction in the peak values of the relative displacement of all floors as compared with the CO-LQG as can be seen from Figure 4.39(a). Similarly, the inter-storey drift is reduced by 45%,25%,43% and 60% for first-second, second-third, third-fourth and fourth-fifth floor respectively as shown in Figure 4.39(b). The acceleration is reduced by 44%, 53%,13%,46% and 42% for first to the fifth floor respectively by using the proposed controller in place of CO-LQR as shown in Figure 4.39(c).

To achieve these reductions the proposed controller uses 21% lesser force as compared to the CO-LQG. The results discussed above confirms that the proposed controller is more effective in reducing the vibrations as compared with the CO-LQG controller.

(a)

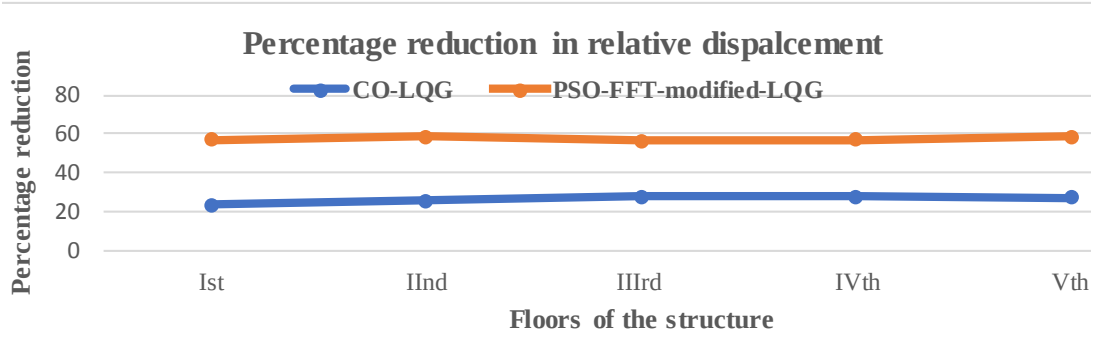

(b)

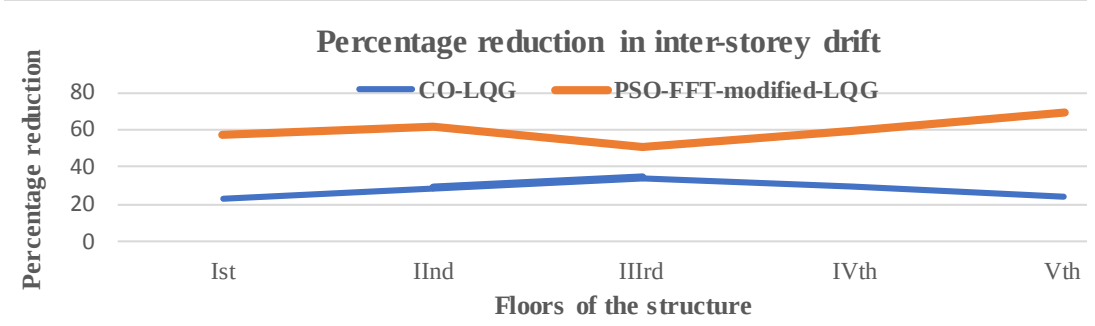

(c)

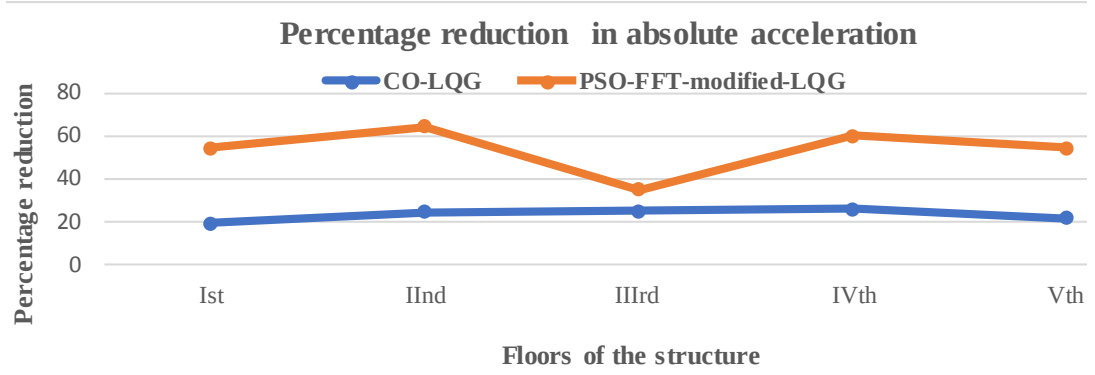

Figure 4.39 Comparison of the percentage reduction in peak values of fifth floor of the structure due to CO-LQG and proposed controller for El-Centro earthquake (a) Displacement (b) Inter-storey drift (c) Acceleration

For Chi-Chi earthquake, displacement response of the fifth floor of uncontrolled structure is shown in Figure 4.40(a). The comparison of the time histories of the displacement response obtained using uncontrolled structure, by employing CO-LQG control algorithm and the proposed control algorithm is shown in Figure 4.40(b). From Figure 4.40(c), proposed controller achieved a reduction in the displacement as compared with the CO-LQG. It is notable here that this effective mitigation is achieved by the proposed controller using lesser control force as shown in Figure 4.40(d).

The variations of **R** are shown in Figure 4.40(e). For, conventional CO-LQG the value of **R** remains unchanged throughout the seismic activity but in case of proposed controller value of **R** changes according to the occurrence of quasi-resonance between earthquake and first two fundamental frequencies of the structure. Whenever quasi-resonance occurs between the structure and the earthquake, the value of **R** goes low and determined for best performance by the PSO algorithm. Further, a comparison of cumulative energies of the fifth floor`s displacement signal obtained due to CO-LQG and the proposed controller is shown in Figure 4.40(f). This energy is a measure of the disruptive capability of the displacement signal. The comparison in Figure 4.41(f) concludes that the energy confined in the displacement signal obtained by employing proposed controller is much lesser than the energy confined in the displacement signal obtained by employing the conventional CO-LQG.

Figure 4.41(a) shows the percentage reduction in relative displacement of all floors using proposed controller and the CO-LQG controller. This reduction is approximately 10% more for the first to the fifth floor as compared with the CO-LQG. This implies that the proposed controller can reduce the displacement response of all floors of the structure efficiently. Similarly, the inter-storey drift between the first-second, second-third, third-fourth and fourth-fifth floor is reduced by 17%, 15%, 30% and 2% respectively as shown in Figure 4.41(b). Alike, the proposed controller reduced the accelerations for the first, second, third, fourth and fifth floor by 29%,13%,5%,5% and 20% respectively as compared with the CO-LQG as shown in Figure 4.41(c). These reductions in structural responses achieved by the proposed controller using 27% lesser force than the CO-LQG. This can also be seen from the comparison of the time histories of the force imparted to the structure due to the proposed controller and the CO-LQG controller. The analysis carried out for the Chi-Chi earthquake in this section on the prototype five storey structure. Based on the above discussion, it is concluded here that the proposed controller shows excellent performance in presence of the higher modes. The displacement, interstorey drift and the absolute acceleration are reduced significantly using the proposed controller.

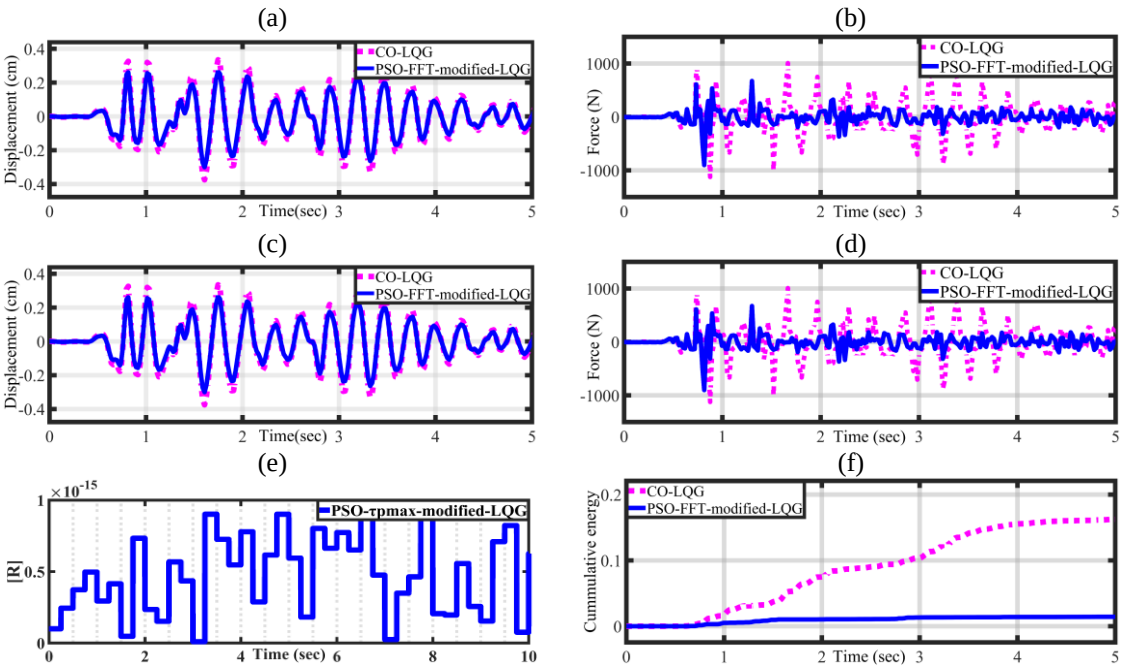

Figure 4.40 Structural responses for five storey structure subjected to the 1940 Chi-Chi earthquake (a) displacement response of fifth floor of uncontrolled structure (b) comparison of controlled responses of fifth floor using CO-LQG and PSO-FFT-modified-LQG algorithms (c) control forces for the CO-LQG and the PSO-FFT-modified-LQG algorithm (d) variation of **R** with time (e) comparison of cumulative energies of the fifth floor`s displacement by applying CO-LQG and PSO-FFT-modified-LQG

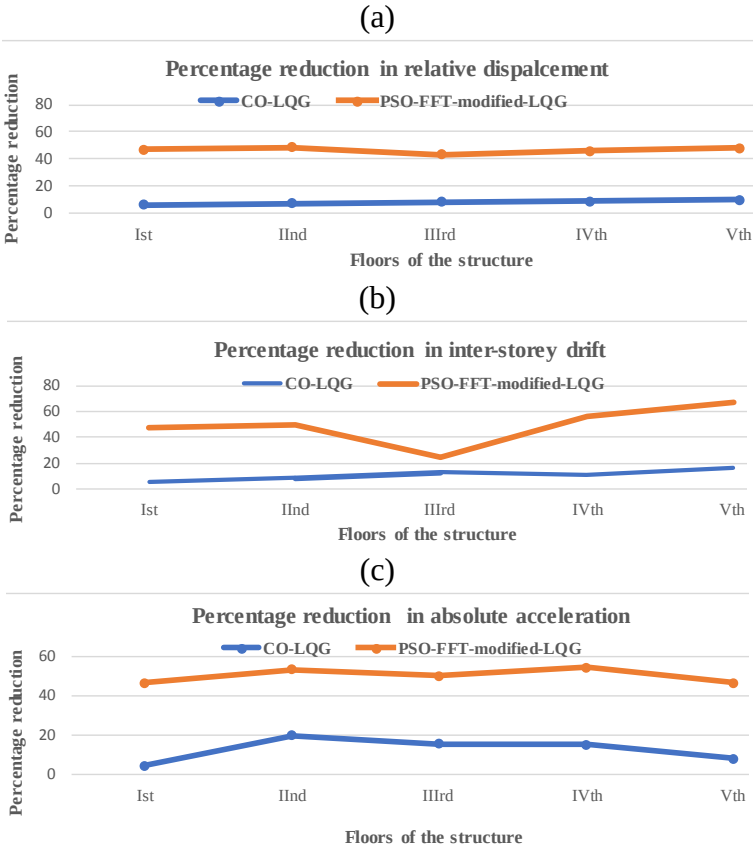

Figure 4.41. Comparison of the percentage reduction in peak values of fifth floor of the structure due to CO-LQG and proposed controller for Chi-Chi earthquake (a) Displacement (b) Inter-storey drift (c) Acceleration

4.4.3 Performance analysis of modified LQR based on PSO- τ_p^{max}approach

For El-Centro earthquake, the relative displacement response of the fifth floor of the uncontrolled structure is shown in Figure 4.42(a). The comparison in Figure 4.42(b) concludes that the semi active scheme using the CO-LQR and the PSO- τ_p^{max}-modified-LQR is successful in mitigation of the vibrations. Now, the comparative analysis between the conventional CO-LQR and proposed PSO- τ_p^{max}-modified-LQR (adaptive LQR) is presented. Figure 4.42(c) presents the comparison of the time histories of the fifth floor`s displacement response using CO-LQR and the proposed adaptive LQR controller. The proposed controller is more effective in reducing the displacement response as can be seen from the Figure 4.42(c).

It is notable here that this effective mitigation is achieved by the proposed controller using lesser control force as shown in Figure 4.42(d). These results are due to the real-time variations of the control weighting matrix **R** using PSO- τ_p^{max} algorithm described in section 4.3.1. of this chapter. The variations of **R** are shown in Figure 4.42(e). Moreover, cumulative energy of the fifth floor`s displacement signal obtained due to CO-LQR and proposed controller is shown in Figure 4.42(f). This energy is measure of disruptive capability of the displacement signal. The comparison in Figure 4.45(f) concludes that displacement signal obtained due to proposed controller has lesser energy for disruption. Figure 4.43(a) shows the percentage reduction in relative displacement of all floors using proposed controller and the CO-LQR controller. This reduction is approximately 10% for first to fifth floor as compared with the CO-LQR. Similarly, the inter-storey drift between the first-second, second-third, third-fourth and fourth-fifth floor is reduced by 17%,15%,30% and 2% respectively as shown in Figure 4.43(b). Alike, the proposed controller reduced the accelerations for the first, second, third, fourth and fifth floor by 29%,13%,5%,5% and 20% more respectively as compared with the CO-LQR. These reductions in structural responses achieved by the proposed controller using 27% lesser force than CO-LQR as can be seen in Figure 4.43(c). The comparison of the time histories of the force due to the CO-LQR and the proposed controller is shown in Figure 4.43(d) is also confirms that these reductions are achieved using the lesser force.

Similarly, for Chi-Chi earthquake, it can be seen from Figure 4.44(a), the displacement response of the fifth floor of uncontrolled structure which is to be reduced by employing the semi active control scheme is shown. The comparison of the time histories of the displacement response obtained using uncontrolled structure, by employing CO-LQR control algorithm and the proposed control algorithm is shown in Figure 4.44(b). The effectiveness of the semi active control scheme as compared to uncontrolled structure is shown in this Figure.

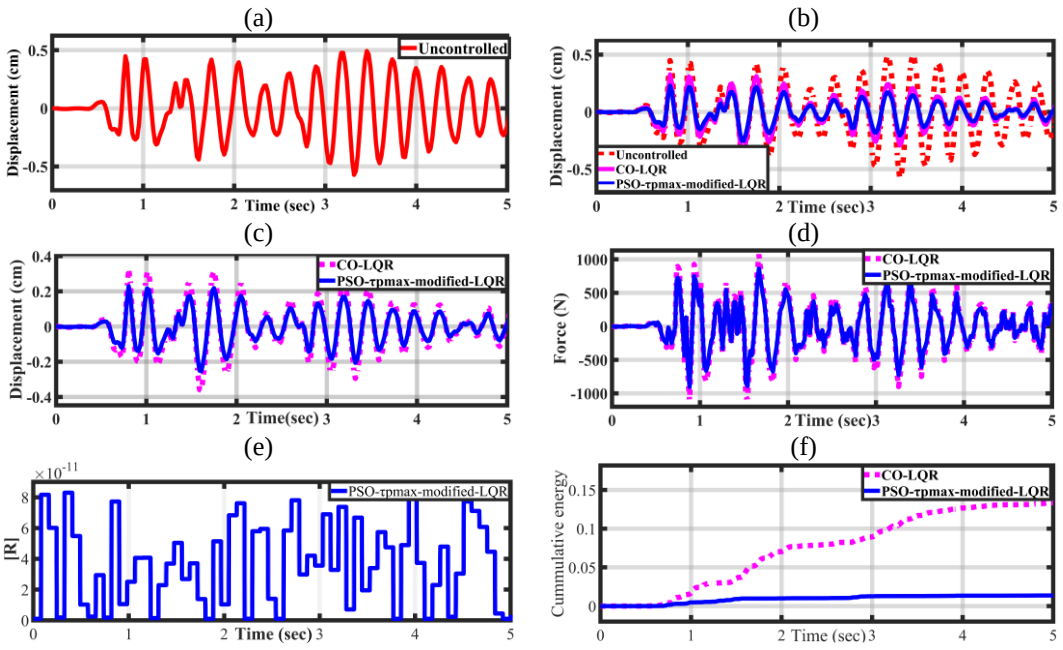

Figure 4.42 Structural responses for five storey structure subjected to the 1940 El-Centro earthquake (a) displacement response of fifth floor of uncontrolled structure (b) comparison of controlled responses of fifth floor using CO-LQR and PSO-τ_p^{max}-modified-LQR algorithms (c) control forces for the CO-LQR and the PSO-τ_p^{max}-modified-LQR algorithm (d) variation of **R** with time (e) comparison of cumulative energies of the fifth floor`s displacement by applying CO-LQR and PSO-τ_p^{max}-modified-LQR

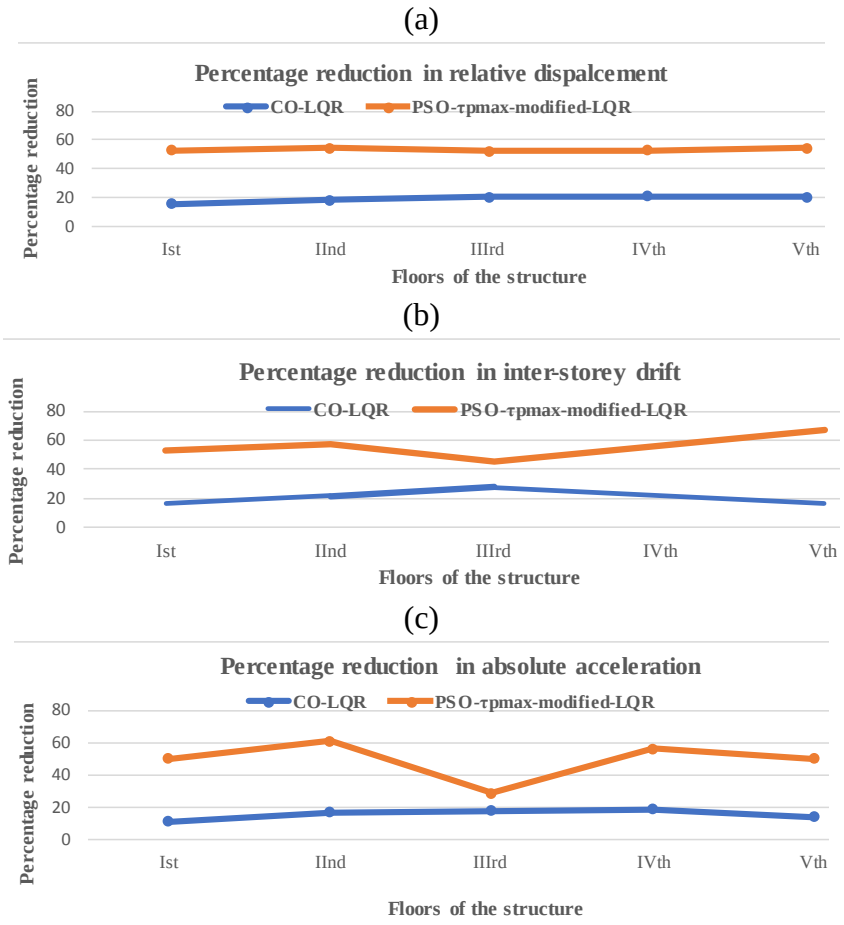

Figure 4.43 Comparison of the percentage reduction in peak values of fifth floor of the structure due to CO- LQR and PSO- τ_p^{max}-modified-LQR for El-Centro earthquake (a) Displacement (b) Inter-storey drift (c) Acceleration

From Figure 4.44(c), proposed controller achieved reduction in the displacement as compared with the CO-LQR. It is notable here that this effective mitigation is achieved by the proposed controller using lesser control force as shown in Figure 4.44(d). It is notable here that this effective mitigation is achieved by the proposed controller using lesser control force as shown in Figure 4.44(d). The variations of **R** are shown in Figure 4.44(e).

For proposed controller value of **R** changes according to the occurrence of quasi-resonance between earthquake and first two fundamental frequencies of the structure. As stated earlier, the lesser value of **R** corresponds to larger force whereas larger value of **R** corresponds to smaller force exerted to the structure. Whenever quasi-resonance occurs between the structure and the earthquake, the value of **R** goes low and determined for best performance by the PSO algorithm. At this quasi-resonance instant, the MR damper exerts a larger force for mitigation of the vibrations. Further, a comparison of cumulative energies of the fifth floor`s displacement signal obtained due to CO-LQR and the proposed controller is shown in Figure 4.44(f). This energy is a measure of the disruptive capability of the displacement signal. The comparison in Figure 4.44(f) concludes that the energy confined in the displacement signal obtained by employing proposed controller is much lesser than that of obtained by employing the conventional CO-LQR.

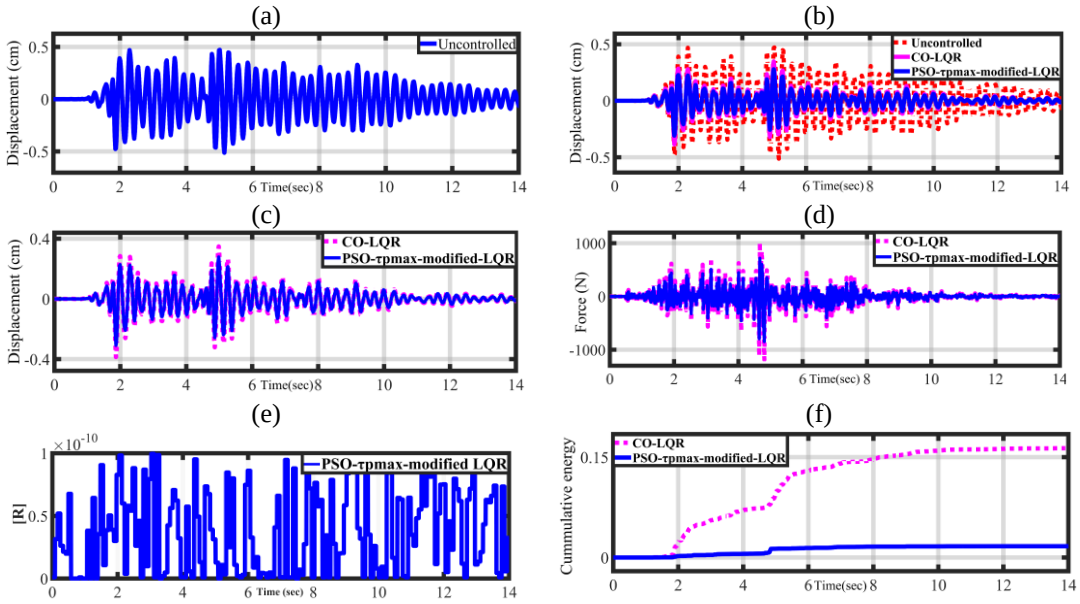

Figure 4.44. Structural responses for five storey structure subjected to the 1999 Chi-Chi earthquake (a) displacement response of fifth floor of uncontrolled structure (b) comparison of controlled responses of fifth floor using CO-LQR and PSO-τ_p^{max}-modified-LQR algorithms (c) control forces for the CO-LQR and the PSO-τ_p^{max}-modified-LQR algorithm (d) variation of **R** with time (e) comparison of cumulative energies of the fifth floor`s displacement by applying CO-LQR and PSO-τ_p^{max}-modified-LQR

Figure 4.45(a) shows the percentage reduction in relative displacement of all floors using proposed controller and the CO-LQR controller. This reduction is approximately 10% for the first to fifth floor as compared with the CO-LQR. Similarly, the inter-storey drift between the first-second, second-third, third-fourth and fourth-fifth floor is reduced by 17%,15%, 30% and 2% respectively as shown in Figure 4.45(b). Alike, the proposed controller reduced the accelerations for the first, second, third, fourth and fifth floor by 29%,13%,5%,5% and 20% more respectively as compared with the CO-LQR. These reductions in structural responses achieved by the proposed controller using 27% lesser force than the CO-LQR as shown in Figure 4.45(c). Based on the analysis presented in this section, it is concluded that the proposed controllers are efficiently reduced the vibrations of the five storey structure.

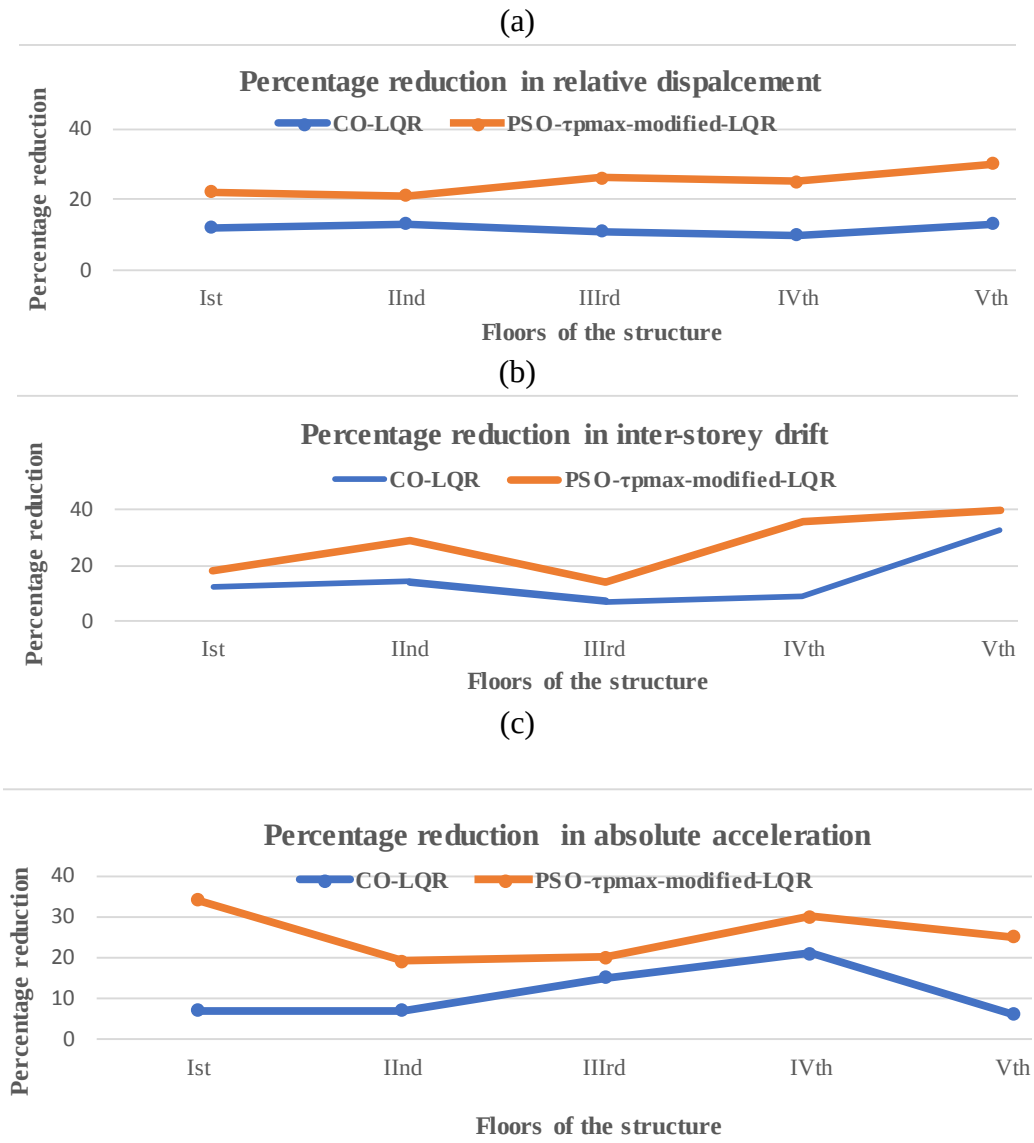

Figure 4.45 Comparison of the percentage reduction in peak values of fifth floor of the structure due to CO-LQG and proposed controller for Chi-Chi earthquake (a) Displacement (b) Inter-storey drift (c) Acceleration

4.4.4 Performance analysis of modified LQG based on PSO- τ_p^{max} approach

For El-Centro earthquake, the relative displacement response of the fifth floor of uncontrolled structure is shown in Figure 4.46(a). The comparison shown in Figure 4.46(b) concludes that the semi active scheme using PSO- τ_p^{max}-modified-LQG is better in the mitigation of the vibrations. Figure 4.46(c) presents the comparison of the time histories of the fifth floor`s displacement response using CO-LQG and the proposed modified LQG controller.

It can be seen from the Figure 4.46(c) that the proposed controller is more effective in reducing the displacement response. It is notable here that this effective mitigation is achieved by the proposed controller using lesser control force as shown in Figure 4.49(d). The variations of **R** are shown in Figure 4.46(e). For, conventional CO-LQG the value of **R** remains unchanged throughout the seismic activity but in case of proposed controller value of **R** changes according to the occurrence of quasi-resonance between the earthquake and first two fundamental frequencies of the structure.

Moreover, cumulative energy of the fifth floor`s displacement signal obtained due to CO-LQG and proposed controller is shown in Figure 4.46(f). The comparison in Figure 4.46(e) concludes that displacement signal obtained due to proposed controller has lesser energy for disruption. The proposed controller delivers approximately 45% more reduction in the peak values of the relative displacement of all floors as compared with the CO-LQG as can be seen from Figure 4.47(a). Similarly, the inter-storey drift is reduced by 45%,25%,43% and 60% for first-second, second-third, third-fourth and fourth-fifth floor respectively as shown in Figure 4.47(b). The absolute acceleration is reduced by 44%,53%,13%,46% and 42% for first to fifth floor respectively by using proposed controller in place of CO-LQR as shown in Figure 4.47(c). To achieve these reductions proposed controller uses 21% lesser force as compared to CO-LQG.

For Chi-Chi earthquake, comparison of displacement response using proposed and CO-LQG is shown in Figure 4.48(c). In Figure 4.49(a), proposed controller reduced displacement response for all floor by approximately 45% employing the proposed controller as compared with the CO-LQG controller. The inter-storey drift is reduced by 45%,14%,50% and 60% for first-second, second-third, third-fourth and fourth-fifth floor respectively as shown in Figure 4.49(b). The absolute acceleration is reduced by 44%, 42%,13%,46% and 42% for first to fifth floor respectively by using proposed controller in place of CO-LQR as shown in Figure 4.49(c).

The comparisons of displacement time histories of uncontrolled structure and the controlled structure shown in 4.46 (b) and 4.48(b) conclude that proposed controller deliver better performance.

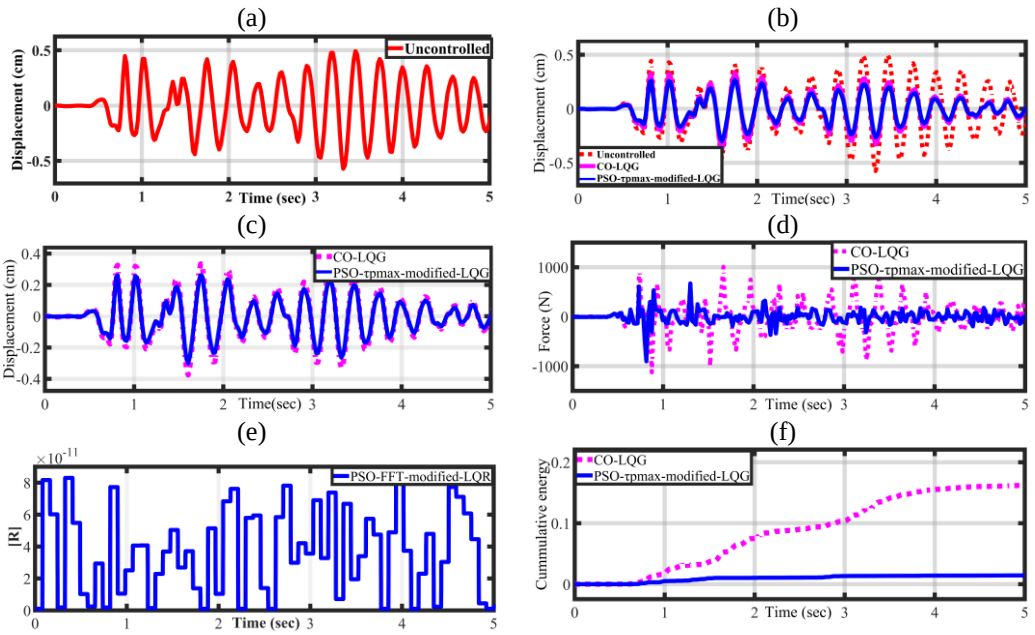

Figure 4.46 Structural responses for five storey structure subjected to the 1940 El-Centro earthquake (a) displacement response of fifth floor of uncontrolled structure (b) comparison of controlled responses of fifth floor using CO-LQG and PSO-τ_p^{max}-modified-LQG algorithms (c) control forces for the CO-LQG and the PSO-τ_p^{max}-modified-LQG algorithm (d) variation of **R** with time (e) comparison of cumulative energies of the fifth floor`s displacement by applying CO-LQG and PSO-τ_p^{max}-modified-LQG

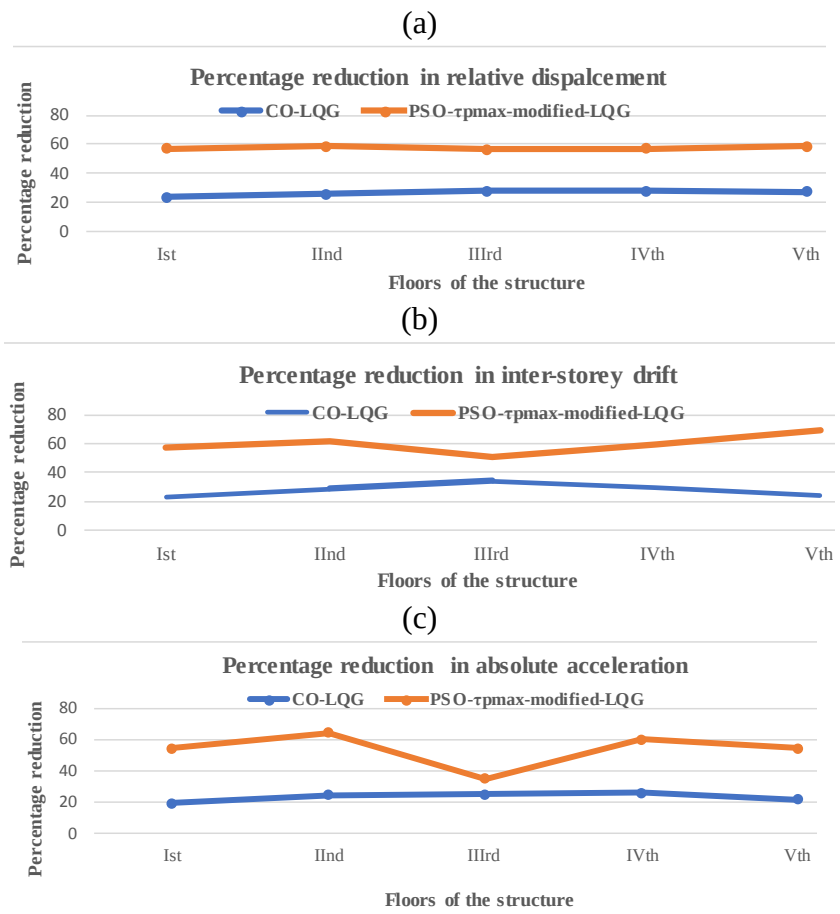

Figure 4.47 Comparison of the percentage reduction in peak values of fifth floor of the structure due to CO-LQG and proposed controller for El-Centro earthquake (a) Displacement (b) Inter-storey drift (c) Acceleration

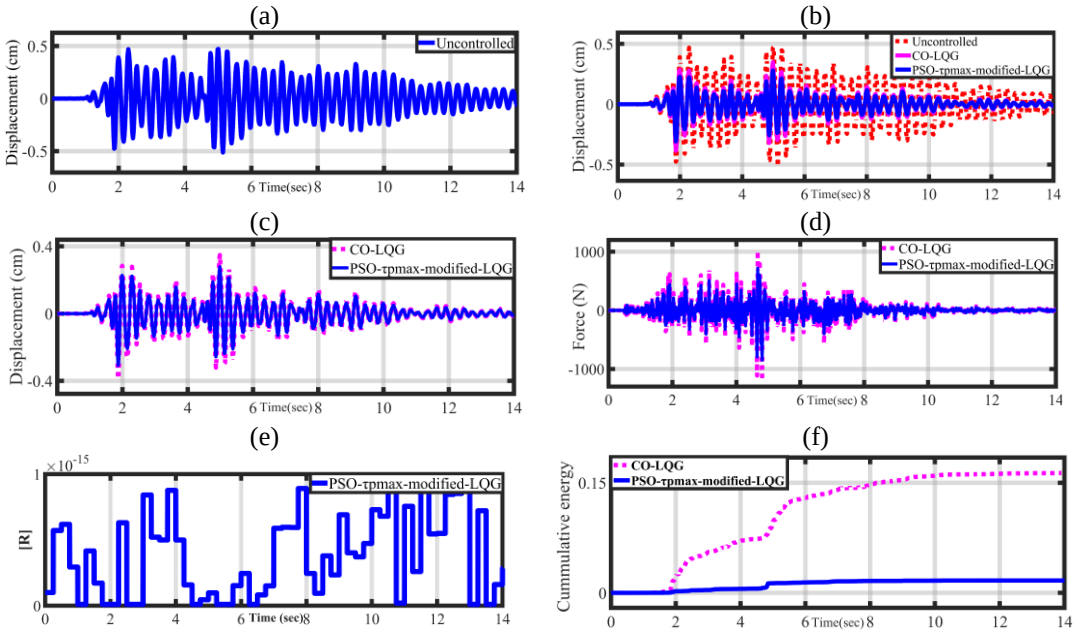

Figure 4.48 Structural responses for five storey structure subjected to the 1999 Chi-Chi earthquake (a) displacement response of fifth floor of uncontrolled structure (b) comparison of controlled responses of fifth floor using CO-LQG and PSO-τ_p^{max}-modified-LQG algorithms (c) control forces for the CO-LQG and the PSO-τ_p^{max}-modified-LQG algorithm (d) variation of **R** with time (e) comparison of cumulative energies of the fifth floor`s displacement by applying CO-LQG and PSO-τ_p^{max}-modified-LQG

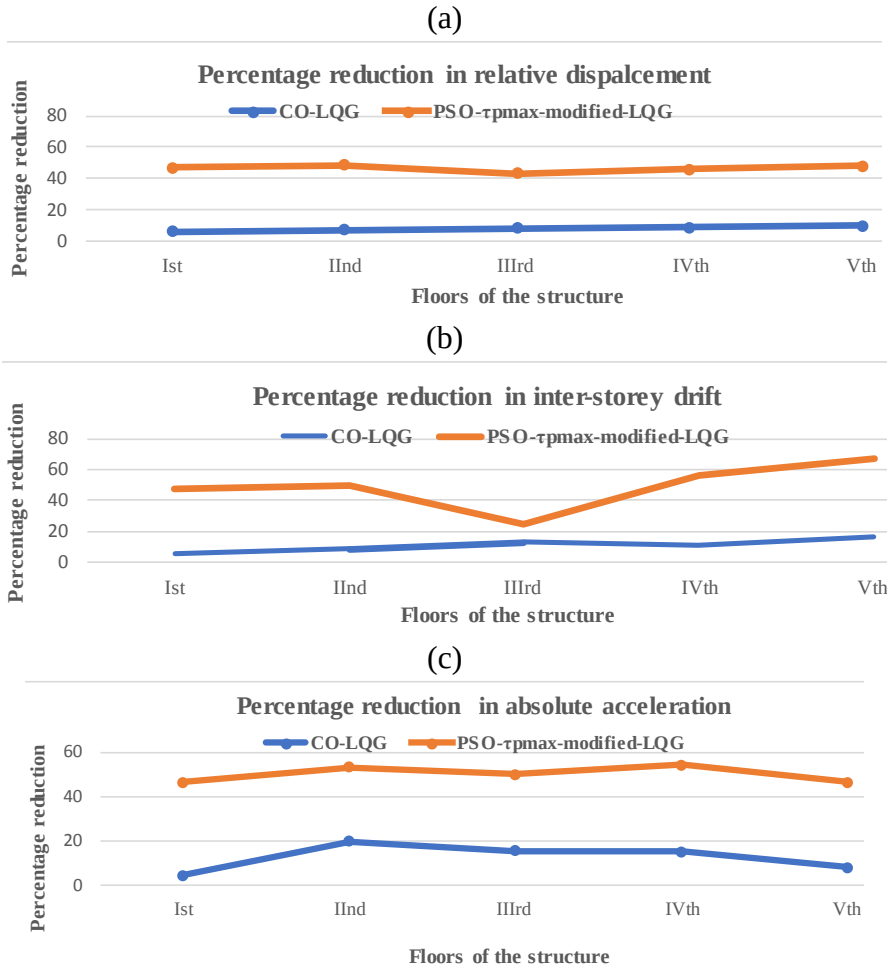

Figure 4.49 Comparison of the percentage reduction in peak values of fifth floor of the structure due to CO-LQG and proposed controller for Chi-Chi earthquake (a) Displacement (b) Inter-storey drift (c) Acceleration

Summary

The methodology to develop PSO-FFT-modified-LQR, PSO-FFT-modified-LQG, PSO-τ_p^{max}-modified-LQR and PSO-τ_p^{max}-modified-LQG controllers is discussed in this chapter. These controllers are developed by changing the ordinary clipped optimal LQR/LQG controller by altering the control weighting matrix $\mathbf{R}_i$ over every small-time window based on PSO-FFT and PSO-τ_p^{max} algorithms as the quasi-resonance occurred. These updated values of components of **R** takes to deliver the desired optimal control force during the earthquake.

In the PSO-FFT algorithm, the signal is analysed in the frequency domain instead of the time-frequency domain such as DWT etc. to determine the quasi-resonance between first two fundamental frequencies and earthquake which results in faster control action. Based on these quasi-resonance occurrences the gain matrices for each time window are ascertained adaptively using PSO algorithm, unlike conventional LQR/LQG controller where the gain matrix remains unaltered. Whereas, in maximum dominant period (τ_p^{max}) approach, the determination of the quasi-resonance instances is done in time domain instead of frequency or time-frequency domain. It is an improvement over the previous studies in which it was essential to analyze the signal in the frequency/time-frequency domain to obtain the dominant frequency for each window. Therefore, the merit of the advised approach is that it remains in the time domain always and the gain matrices are ascertained adaptively by the PSO algorithm.

The proposed PSO-FFT-modified-LQR/LQG and PSO-τ_p^{max}-modified-LQR/LQG controllers have been utilized to get the controlled response of prototype three storey structure with the single MR damper as well as prototype five-storey structure to examine the effects of higher modes on the performance of the proposed controllers. The results exhibit that the proposed controllers perform essentially superior to the clipped optimal LQR/LQG controller to reduce the structural responses (i.e. Relative displacement, inter-story drift as well as the absolute acceleration). Further, the developed controllers are tested numerically on different conditions like subjecting the structure to various earthquakes. Also, studies are carried out to find the best location to put the MR damper within the structure and assuming a condition when power vanishes at the peak of the seismic activity.

The inalienable adaptability in the design of the proposed PSO-FFT/ τ_p^{max}-modified-LQR/LQG controllers to account for the quasi-resonance by the modification of **R** makes these proposed controllers a fascinating choice for the vibration control. Further, the LQR controller is more favoured over LQG for the modification due to its simple design and easy implementation.

CHAPTER 5: DEVELOPMENT OF ADAPTIVE QUASI BANG-BANG CONTROLLER USING PSO

5.1 Introduction

In the quest of design simplicity and performance at par with the clipped optimal LQR/LQG, a particle swarm optimized control algorithm is proposed based on the modified quasi bang-bang control algorithm. The constant output weights used in the modified quasi bang-bang controller are optimized for the best performance in dynamic loading such as earthquake using the particle swarm optimization (PSO). The proposed optimized controller is then applied to a three storey structure fixed with an MR damper. This structure has been subjected to various earthquakes for performance evaluation. The results thus obtained are compared with one of the best performing clipped optimal linear quadratic Gaussian (LQG) controller, quasi bang-bang and modified quasi bang-bang controller. The results establish that the PSO modified quasi bang-bang controller is superior to the other controller in reducing the structural responses i.e. relative displacement, interstorey drift and the absolute accelerations. Further, the voltage comparison shows that the power consumption is less for the proposed controller in attaining better performance[135].

5.2 Evolution of the controller

The development of a controller is a sustained process and the proposed controller is also evolved through this process. The development of the proposed controller is presented in the subsequent sections.

5.2.1 Quasi bang-bang controller

i. If the structure is moving away from the center (i.e. Reference position)

ii. If the structure is moving towards the center

The command voltage is selected as per control law in Eq. (5.1)

$$V_i = \begin{cases} V_{max} & \text{if moving away from the center} \\ 0 & \text{if moving towards the center} \end{cases} \quad (5.1)$$

The major disadvantage of this controller is the undesirable control chattering near the origin of state-space due to high-frequency switching of control force often occurs and great care must be taken against spill over instability at higher modes [139].

5.2.2 Modified quasi bang-bang controller

A modified approach to the quasi bang-bang controller was proposed by A.M. Aly (Aly, 2013) which considers the remaining positions between the reference and the maximum displacements. This is accomplished by assigning constant weights to the output like the fuzzy logic controller (FLC). and chosen randomly in the range of 0 to 1. The control law is given as in Eq. (5.2)

$$V_i = \begin{cases} \alpha_1 V_{max} & (\text{if } \text{sign}(x)=1, \text{sign}(\dot{x})=1) \\ \beta_1 V_{max} & (\text{if } \text{sign}(x)=-1, \text{sign}(\dot{x})=-1) \\ \gamma_1 V_{max} & (\text{if } \text{sign}(x)=1, \text{sign}(\dot{x})=-1) \\ V_{max} & (\text{Otherwise}) \end{cases} \quad (5.2)$$

This random selection does not determine the optimized value of the command signal to the MR damper. It leads to the inferior performance of the controller and semi active control scheme. Further, quasi bang-bang and modified quasi bang-bang controller use the maximum available power which needs to be cut down. Using lesser electrical power is one of the main features of the semi active control method. To find a solution to these prominent problems the authors propose a PSO-modified quasi bang-bang controller based on modified quasi bang-bang control algorithm in which the random weights have been optimized in real time using particle swarm optimization technique to achieve better performance using less power.

5.3 Formulation of the adaptive quasi bang-bang controller using PSO

Particle Swarm Optimization (PSO) is a heuristic calculation system developed by Kennedy and Eberhart in 1995 [4]. The essential of PSO algorithm relies on social conduct illustration as it was intended to reinvent the social demeanour as in a path of flying creatures. PSO introduces a populace of indiscriminately picked up-and-coming solutions. Each emerging solution for the issue is assumed as an individual, called a "particle".

Every particle is considered like a winged creature in the path that modifies its flying way as indicated by its own and its associates' vision of the best area as in the pursuit of sustenance. Subsequently, this algorithm advances particles by collaboration and rivalry among themselves as opposed to the genetic algorithm. For the optimization of any given problem, there is an objective function or cost function based on which every particle in the PSO algorithm has a fitness value or cost. It additionally has a velocity which coordinates the development of the particle with the goal that it can search the pursuit of space. These velocities will be balanced dynamically all together to manage the particles closer and nearer to the solution. the position

and the velocity of the k^{th} the particle may be represented as in Eqs. (5.3-5.4) respectively in the d-dimensional pursuit space[112], [140].

$$q_k = \left[q_{(k,1)}, q_{(k,2),} q_{(k,3),} q_{(k,4),} \ldots\ldots\ldots\ldots q_{(k,d)}\right] \tag{5.3}$$

$$\dot{q}_k = \left[\dot{q}_{(k,1),} \dot{q}_{(k,2),} \dot{q}_{(k,3),} \dot{q}_{(k,4),} \ldots\ldots\ldots\ldots \dot{q}_{(k,d)}\right] \tag{5.4}$$

Here, particle`s velocity and position are demonstrated by $\dot{q}$ and q respectively. There is "$P_{best}$" value for each particle. This is the best arrangement of particle`s position attained by the individual particle up to any point as given in Eq. (5.5).

$$P_{k,j} = \left[p_{(k,1)}, p_{(k,2),} p_{(k,3),} p_{(k,4),} \ldots\ldots p_{(k,d)}\right] \tag{5.5}$$

The other is "G_{best}" or "global best" which is the best arrangement accomplished by any particle in the populace by that instant of time. The particle`s updated velocity is given in Eq.(5.6) [141].

$$\dot{q}_{i,j}(t+1) = \partial \dot{q}_{i,j} + c_1 b_1 \left(P_{k,j} - q_{i,j}(t)\right) + c_2 b_2 \left(G_{best}(t) - q_{i,j}(t)\right) \tag{5.6}$$

The first term on the right-hand side of Eq. (5.6) is the updated velocity where ∂ is the inertia factor. The inertia weight factor plays a significant role in the global optimization. The second term is the "cognitive" term. This contains the knowledge about the particle's own particular experience of the finest path and $P_{k,j}$ being the P_{best} value. The third term is the "social" term which includes the group's knowledge of the best path. Here, c_1 and c_2 are the acceleration coefficient whereas b_1, b_2 are random numbers in the range of 0 to 1. Particle`s position update in each generation is given in Eq. (5.7) [142]

$$q_{i,j}(t+1) = q_{i,j}(t) + \dot{q}_{i,j}(t+1) \tag{5.7}$$

Here, PSO is used to find the most suitable optimal values of the constants α_1 , β_1 and γ_1 for the modified quasi bang-bang controller so that the semi active control method could deliver optimum structural response with smaller and optimum control force. The cost function or the objective function considered here is a function of the relative displacement of the structure. This may be characterized as a function of the relative displacement $x_i(t)$ of the i^{th} floor as given in Eq. (5.8).

$$J_{PSO}= \int_{0}^{t_i} \{x_{i+1}(t)-x_i(t)\}^2 \, dt \tag{5.8}$$

This optimization of weighting constants initiates the lessening of responses using a smaller control force. Therefore, the distinction of the PSO-modified quasi-bang bang controller method is that these weights are computed online as per the need of the system by PSO algorithm, contrasting to those offered in literature [51] in which these constants are decided by trial and error. The flowchart of the PSO algorithm is shown in Figure 4.2 in chapter 4 and the parameters used in this work are given in Table 5.1. This controller is applicable for real-time application. The structure under the seismic loading changes its response constantly and based on the measurement of the sensors the controller determines the appropriate actuating signal (voltage) for the MR damper to produce the control force. Further, the developed controller assumes that all the states are available all the time whereas, in a noisy environment, the states may not be available all the time.

Table 5.1 Parameters used in the particle swarm optimization (PSO) algorithm [135]

Serial number	Parameter`s name	Value
1.	Inertia weight factor ∂	0.6
2.	Acceleration coefficients c_1 and c_2	2
3.	Random number b_1 and b_2	0.3
4.	Iterations	50
5.	Population size	500

5.5 Result analysis and discussion

Performance analysis for the developed controller is carried out by subjecting the three-storey structure to various earthquakes. The simulation results obtained for the purposed controller are compared with the best performing clipped optimal-LQG (CO-LQG), quasi bang-bang controller and modified quasi bang-bang controller visually and quantitively.

For quantitative analysis, the peak values of the relative displacement, interstorey drift, absolute acceleration of all the floors of the structure and the applied force for every controller using different earthquakes are shown in Table 5.2. The parameters X_n (cm), ID_n (cm), A_n (cm/sec^2)

and F(N) represent the peak values of displacement, inter-story drift, and absolute acceleration of the n^{th} floor respectively.

For visual analysis, the comparison of third floor displacement and force time histories using different controllers are shown in Figure 5.1 for El-Centro valley earthquake and in Figure 5.2 for the structure subjected to Hachinohe earthquake. The Figures 5.1(a) and Figure 5.1(c) show the comparison of the time histories of the third-floor displacement and force respectively for first 5 sec and whereas Figures 5.1(b) and Figure 5.1(d) show the enlarged view of same time histories shown in Figure5.1(a) and Figure 5.1(c) respectively for first 2 secs for better visualization of the results.

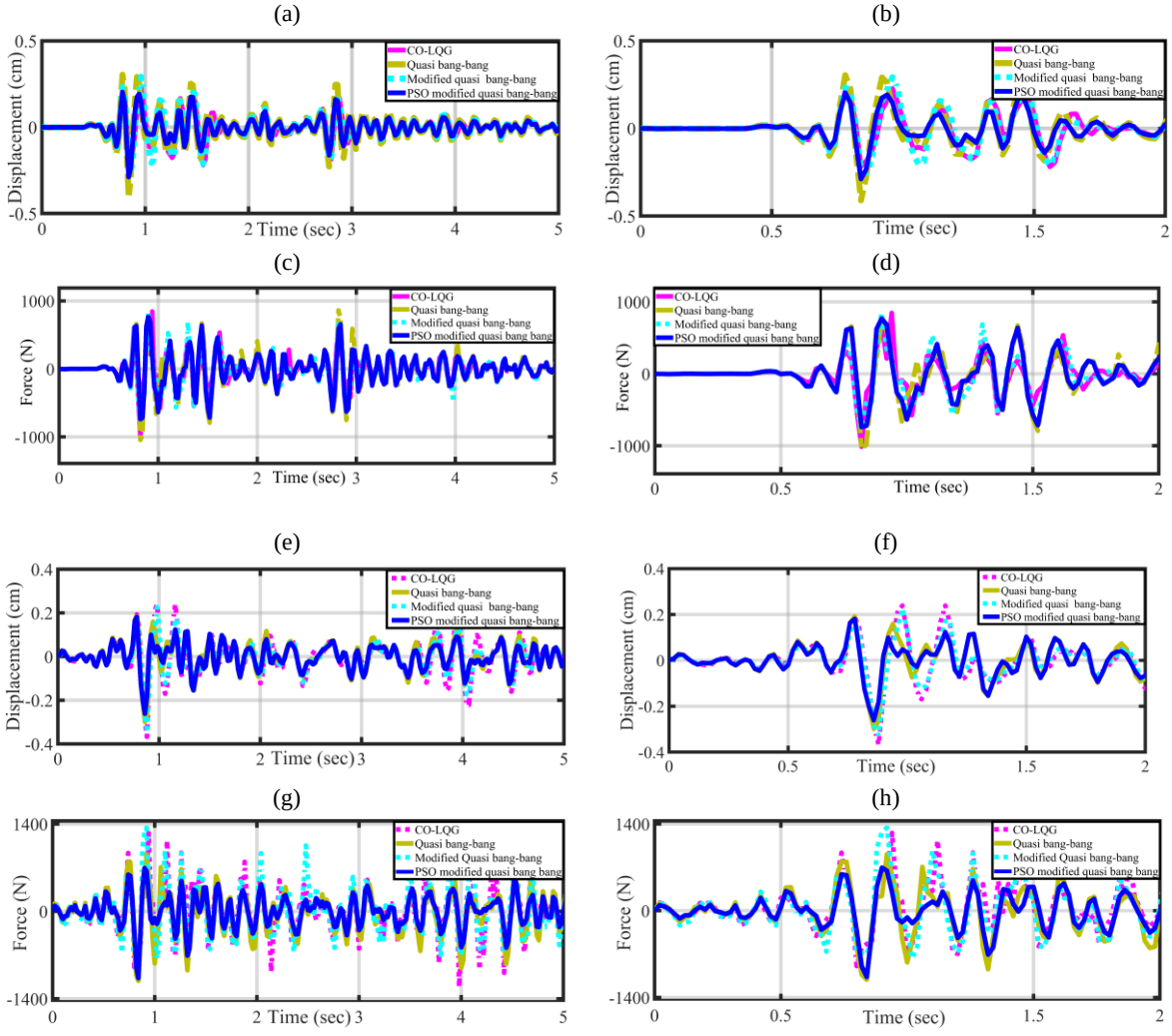

Figure 5.1 Response of the third floor of the structure subjected to El-Centro earthquake time-history (a) Relative displacement time history for 5 sec (b) displacement from 0 to 2 sec (c) Force time history for 0 to 5 sec (d) Force from 0 to 2 sec (e) For Hachinohe earthquake, relative displacement time history for 5 sec (f) displacement from 0 to 2 sec (g) force time history for 5 sec (h) force from 0 to 2 sec.

Similarly, for Hachinohe earthquake Figure 5.1(e) and Figure5.1(g) present the third floor's relative displacement and the force-time history for first 5 secs whereas the Figures 5.1(f)

and Figure 5.1(h) demonstrate the similar time histories for first 2 secs respectively. A careful observation of these Figures(a-h) leads to the conclusion that the suggested PSO-modified quasi bang-bang controller reduces the displacement effectively during the whole-time period using optimized force. The quantitative analysis of the results due to El-Centro earthquake is carried out by the peak values of the displacement, interstorey-drift and acceleration from Table 5.2. It can be observed from Table 5.2, that the third floor's relative displacement is reduced by 27% and 26% over the quasi bang-bang and modified quasi bang-bang controllers respectively and the displacement of all the three floors is substantially lesser about 10-15% using the proposed approach. The PSO modified controller nearly matches the relative displacements of all floors obtained by the best clipped optimal LQG controller. Moreover, the superior results over the CO-LQG controller for the first and second floor also been achieved by using the suggested control algorithm as shown in Table 5.2. The inter-story drift between second-third floor is reduced by 55% and 60% over the quasi bang-bang and modified quasi bang-bang controllers respectively. Similarly, the accelerations of the first, second and third floor are reduced by 46%, 47% and 30% over the clipped optimal-LQG controller. The proposed controller achieves a better reduction in peak absolute acceleration over all other controllers considered for comparison. Further, the analysis is done for Hachinohe earthquake. Referring to Figure 5.1, it can be concluded that the PSO modified controller gives superior results throughout the earthquake time history. The peak values of the responses given in Table 5.2, justify the conclusions just made for El-Centro earthquake.

For Hachinohe earthquake, observing the peak values of the displacement, interstorey-drift, and acceleration from Table 5.2, the third-floor displacement is reduced by 16 % and 26% over the quasi bang-bang and modified quasi bang-bang controllers respectively and the displacement of all floors is substantially lesser about 10-20% using the proposed approach. The PSO modified controller gives superior results for the first, second and third floor by 47%, 36%, and 37% as compared to clipped optimal -LQG controller. The inter-story drift between second-third floor is reduced by 27 %, 37% and 42% over the quasi bang-bang, modified quasi bang-bang and clipped optimal LQG controller respectively. Similarly, the accelerations of the first, second and third floor are reduced by 25%, 4% and 17% over the clipped optimal-LQG controller, 36%, 3% and 12% over the quasi bang-bang controller and 40%,7% and 10% over the clipped optimal LQG controller respectively. Similarly, the accelerations of the first, second and third floor are reduced by 25%, 4% and 17% over the clipped optimal-LQG controller, 36%, 3% and 12% over the quasi bang-bang controller and 40%,7% and 10% over the modified quasi

bang-bang controller. In this way, it can be seen from the observations from the Table 5.2 that the proposed controller is very effective in reducing the seismic vibrations.

Table 5.2 Peak values of the structure subjected to different earthquakes

Controller Name	Earthquake recorded in different soil																			
	El-Centro earthquake				Hachinohe earthquake				Hard Soil				Medium soil				Soft Soil			
	X_n	ID_n	A_n	F	X_n	ID_n	A_n	F	X_n	ID_n	A_n	F	X_n	ID_n	A_n	F	X_n	ID_n	A_n	F
	0.55	0.55	870		0.807	0.81	1138		0.56	0.56	1175		0.27	0.27	624		0.33	0.33	1016	
Uncontrolled	0.83	0.29	1070	0	1.264	0.46	1630	0	0.80	0.24	1340	0	0.42	0.15	720	0	0.43	0.10	1464	0
	0.97	0.14	1400		1.490	0.23	1636		0.92	0.12	1390		0.55	0.12	852		0.51	0.08	1560	
	0.12	0.12	733		0.192	0.19	648		0.13	0.13	490		0.05	0.05	444		0.07	0.07	863	
Clipped optimal-LQG	0.19	0.07	755	900	0.314	0.12	760	1234	0.24	0.11	820	1343	0.11	0.06	552	1032	0.17	0.11	1137	1245
	0.22	0.03	723		0.392	0.08	900		0.29	0.05	840		0.12	0.01	768		0.20	0.03	1260	
	0.13	0.13	521		0.112	0.11	759		0.09	0.09	465		0.05	0.05	492		0.08	0.08	789	
Quasi bang-bang	0.20	0.08	731	1005	0.233	0.12	755	1322	0.20	0.11	570	1402	0.10	0.05	540	1248	0.17	0.09	1170	1560
	0.30	0.10	727		0.295	0.06	850		0.28	0.08	795		0.12	0.02	744		0.20	0.03	1218	
	0.12	0.12	541		0.124	0.12	819		0.10	0.10	520		0.13	0.13	480		0.07	0.07	783	
Modified quasi bang-bang	0.20	0.08	425	851	0.261	0.14	789	1350	0.22	0.12	560	1260	0.10	0.03	528	1164	0.17	0.11	948	1109
	0.29	0.09	510		0.332	0.07	830		0.29	0.07	777		0.12	0.01	696		0.19	0.01	1152	
	0.11	0.11	397		0.100	0.10	487		0.07	0.07	518		0.07	0.07	433		0.06	0.06	756	
PSO modified quasi bang-bang	0.18	0.07	403	785	0.200	0.10	731	1172	0.17	0.10	529	1130	0.09	0.03	487	1050	0.16	0.11	924	1040
	0.22	0.04	504		0.245	0.05	750		0.24	0.07	560		0.11	0.01	660		0.18	0.01	1080	

The Figures 5.2 (a-b) show the third-floor displacement and force time histories respectively for hard soil, Figures 5.2(c-d) and the Figures 5.2(e-f) show the time histories medium soil and soft

soil respectively. A visual inspection of these Figures suggests that the PSO modified quasi bang-bang controller gives excellent performance over other controllers in each soil type. For the earthquake recorded in hard soil, observing the peak values of the displacement, interstorey-drift, and acceleration from Table 5.2, the third-floor displacement is reduced by 15 % and 17% over the quasi bang-bang and modified quasi bang-bang controllers respectively and the displacement of all floors is lesser about 15-25% using the proposed approach. The PSO modified controller reduces the relative displacements for the first, second and third floor by 46%, 31%, and 17% as compared to clipped optimal LQG controller. This is a remarkable achievement because the CO-LQG controller is one of the best performing controllers for the semi active control scheme. The inter-story drift between second-third floor is reduced by 27 %, 37% and 42% over the quasi bang-bang, modified quasi bang-bang and clipped optimal LQG controller respectively. Similarly, the accelerations of the second and third floor are reduced by 25% and 36% over the clipped optimal-LQG controller, 16% and 30% over the quasi bang-bang controller and 12% and 18% over the modified quasi bang-bang controller. The acceleration of the first floor also reduced sufficiently.

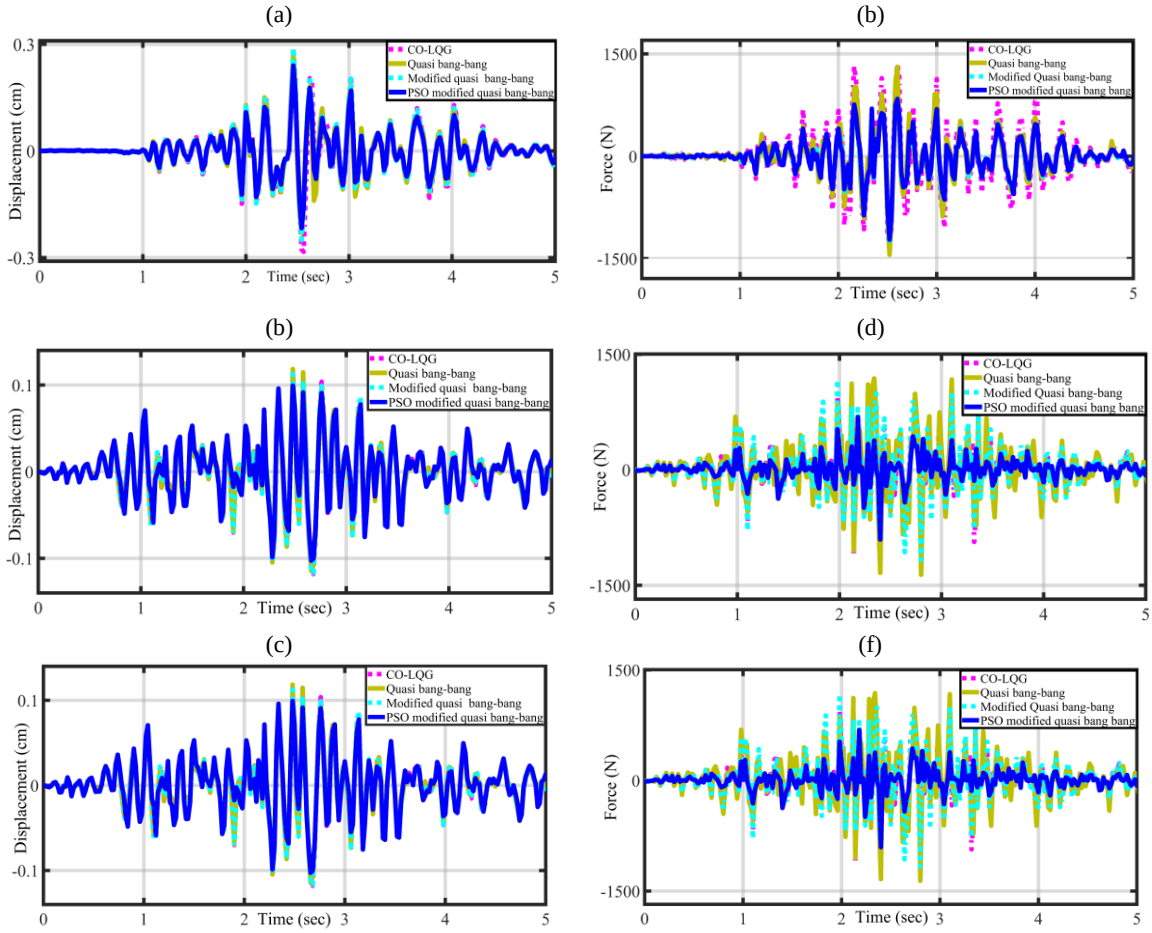

Figure 5.2 Comparison of displacement response of the third floor of the structure subjected to an earthquake recorded in (a) hard soil (b) medium soil (c) soft soil. (d) comparison of force imparted by the controllers when structure subjected to hard soil earthquake. (d) medium soil earthquake (f) soft soil earthquake

Now the analysis is carried out for the structure subjected to an earthquake recorded in different soil conditions i.e. hard, medium and soft soil. For earthquake recorded in medium soil and soft soil, a careful observation the peak values of the displacement, interstorey-drift and acceleration in Table 5.2, advocates superior performance of the suggested control algorithm over all other controllers. Figure 5.3(i-iii) show the force-displacement curve (a) LQG controller (b) Quasi bang-bang (c) Modified quasi bang-bang (d) PSO modified quasi bang-bang controller for hard, medium and soft soil respectively.

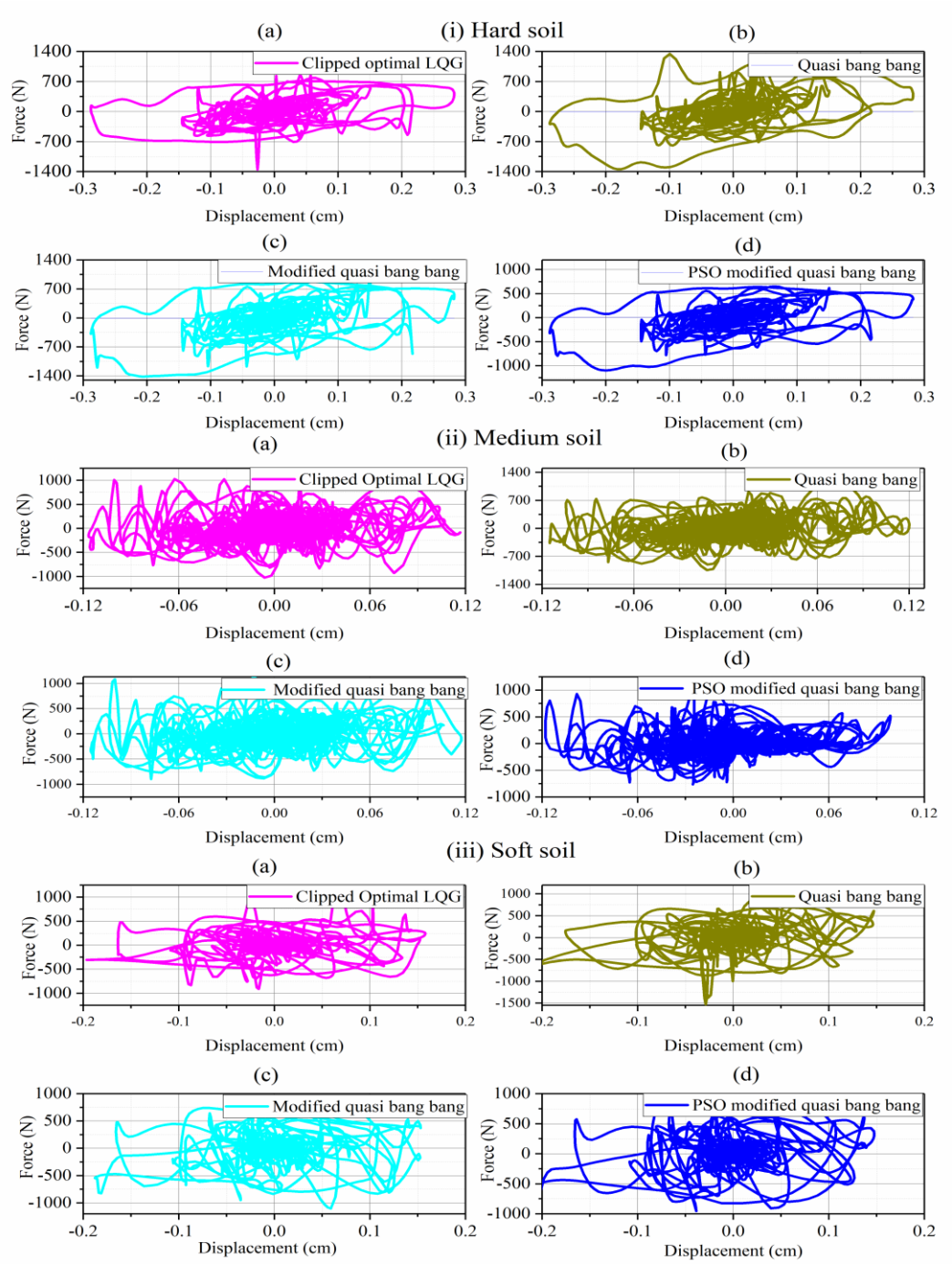

Figure 5.3 Force-displacement curve (i) Hard soil (ii) Medium soil (iii) Soft soil (a) LQG controller (b) Quasi bang-bang controller (c) Modified quasi bang-bang controller (d) PSO-modified quasi bang-bang controller

The input voltage to the MR damper for every controller and for every earthquake considered in the present study is shown in Figure 5.4 (i-v). The voltage is utilized lesser by the proposed controller as can be seen in all the subsections of this Figure 5.4. This is very important feature of the proposed controller as the power is very critical amid the seismic activity.

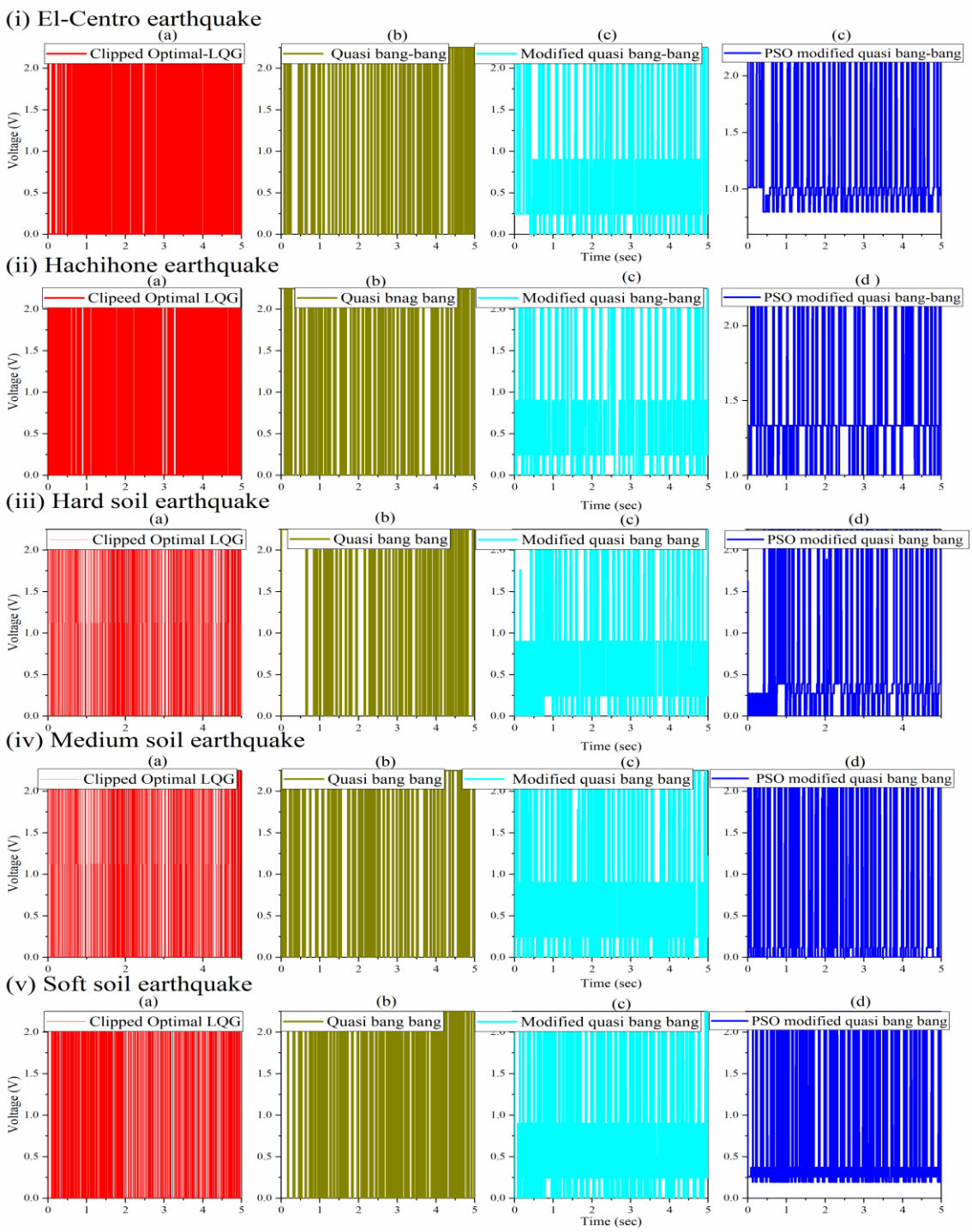

Figure 5.4 Electrical (voltage) signal given to the MR damper by the different controllers when structure subjected to (i) El-Centro-earthquake (ii) Hachinohe Earthquake(iii) Hard Rock (iv) Medium soil (v) Soft soil earthquake

The visual inspection of Figure 5.4 (i) for El-Centro earthquake suggests that the PSO modified bang-bang controller requires lesser voltage to operate. This trend can be observed for every other earthquake considered for simulation in the present study. This is a crucial advantage of

the proposed controller. Figure 5.5 shows the power contained in the displacement signal of the third floor as MSA and RMS displacement amplitude for all controllers for El-Centro earthquake.

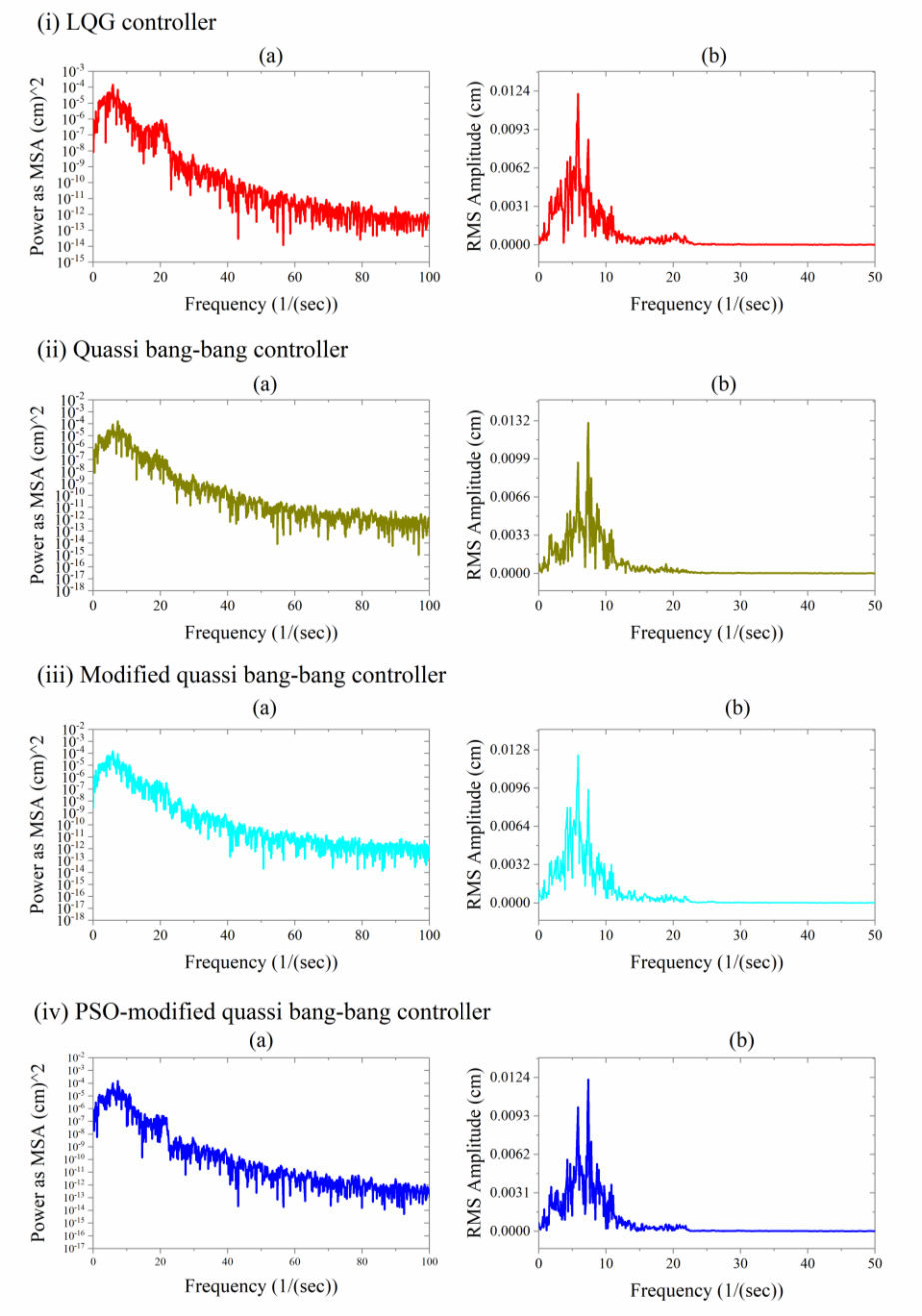

Figure 5.5 Power and response spectra for different controllers for the structure subjected to El-Centro earthquake (i) For CO-LQG controller (ii) Quasi bang-bang (iii) Modified quasi bang-bang (iv) PSO-modified quasi bang-bang controller

This power spectrum clearly shows that PSO-modified controller is the best of all. The RMS value of the displacement is the least for the PSO modified earthquake. Similar comments about the power spectrum and displacement RMS values can be made for other earthquakes time histories considered in this work.

5.6 Development of a prototype hardware and graphic user interface (GUI)

Development of prototype hardware using an ESP32 series microcontroller and three accelerometers (ADXL345) for the demonstration of the working of this PSO optimized controller in semi active control algorithm is explained. Also, A graphic user interface (GUI) is developed for ease of understanding of various controllers used in the semi active control algorithm. The animations of the uncontrolled and controlled structure are developed in the GUI to visualize the effect of the employed controller.

5.6.1 The development of the hardware

A prototype hardware is developed using an ESP32 series microcontroller and three accelerometers (ADXL345) for the demonstration of the working of the proposed controller in the semi active scheme. Three accelerometers are used to record the acceleration of all floors of the prototype three-story structure. The command signal to the MR damper is calculated according to the proposed PSO modified adaptive controller and send in the form of PWM is generated as per the control algorithm and shown on the 0.96" OLED screen in Figure 5.6.

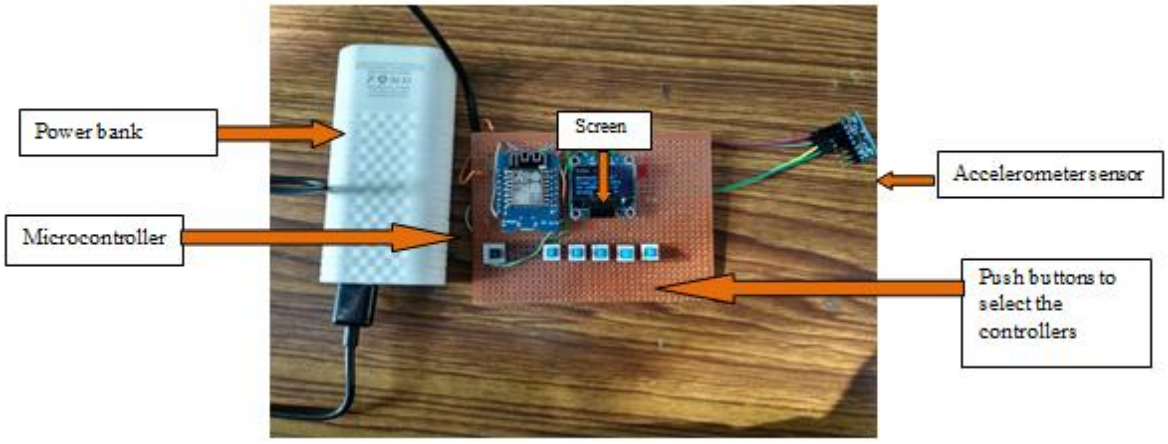

Figure 5.6 Prototype hardware for the proposed controllers

The calibration of the proposed prototype hardware is done on a 50kgf shaker using 5Hz, 8Hz and a 10Hz sinusoidal waveform having amplitude 0.5g. The accelerometer output checked on serial monitor for this purpose. The serial display shows waves like input given through the accelerometer. This prototype hardware is developed for the PSO-modified quasi bang bang controller in this study, however, it can be developed for any controller changing its programming. As can be seen in Figure 5.6, this hardware is a standalone device and can be operated on battery power. Advancement in the DSP technology leads to design power controlling device only on a single silicon chip.

(a) (b)

(c)

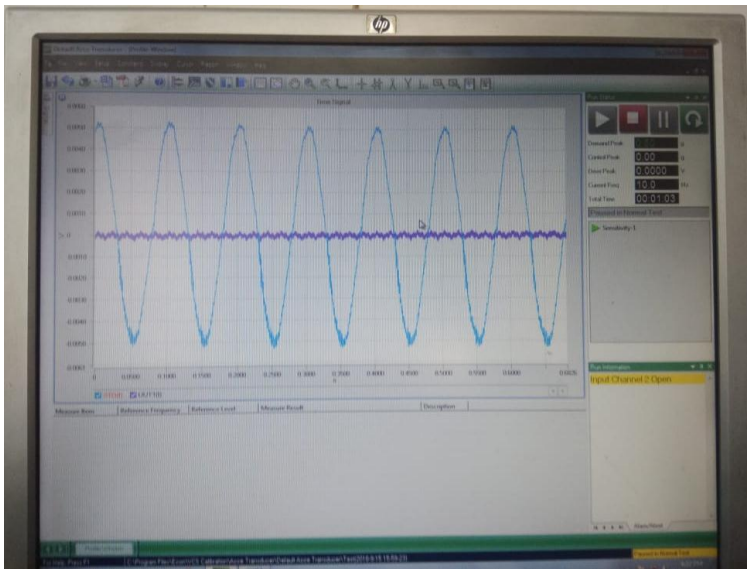

Figure 5.7 Calibration of the prototype hardware using 10 Hz sine wave

5.6.2 Development of graphic user interface (GUI)

A graphic user interface (GUI) is developed for ease of working with the semi active control algorithm. The radio and push buttons are used to select the controllers. A three storey prototype structure having MR damper between ground and the first floor is considered. All controllers studied in this research work can be analyzed with the help of this GUI. The animation of the uncontrolled and controlled structure is developed in the GUI to visualize the effect of the employed controller. For, animations the displacement response of the respective controller and the uncontrolled structure is recorded and arranged. The pictures of the main screen are shown in Figures 5.8(a-b) which gives an idea to use this.

(a)

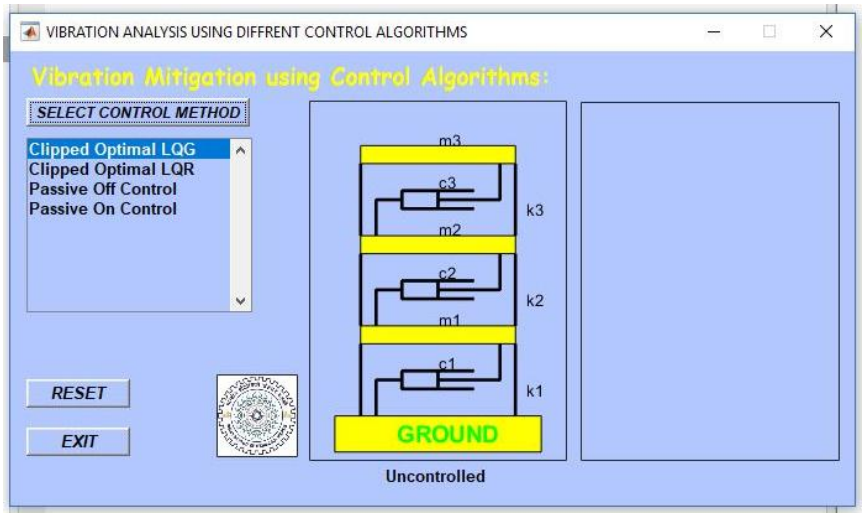

(b)

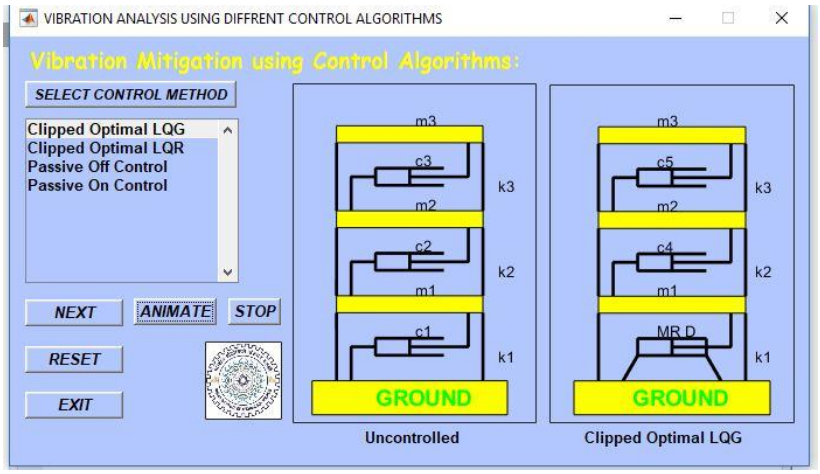

Figure 5.8. Graphic user interface with the (a) List of controllers and uncontrolled structure(b) List of controllers uncontrolled and controlled structure

Summary

A PSO-modified quasi-bang bang controller is presented and evaluated in this chapter. This controller has evolved from the optimization of the ordinary modified quasi bang-bang controller by altering the weights using PSO algorithm. It can generate the optimum control force to diminish structural responses using lesser force utilizing the optimized values of the weights amid the seismic tremor. In this manner, the benefit of the exhorted technique is that the constant weights are found adaptively by the PSO algorithm, unlike modified quasi bang-bang controller.

It utilizes the power intelligently, which is a critical factor in seismic vibration control. The results of the three DOF test structure due to two near-fault earthquake excitation exhibits that the PSO modified quasi bang-bang controller performs superior to other controllers examined in the present work overall. Its simple implementation quality makes this controller an attractive option to control the vibrations.

Though the proposed controller shows commendable performance in various conditions in simulations it`s laboratory testing is highly recommended. Further, the continuous application of high voltage would lead to floor lock-up condition and it could be a perspective field of the research. The study on the issues like non-availability of all states and measurements due to sensor fault during the earthquake may also be interesting problems for further research.

6.1 SUMMARY& CONCLUSIONS

In present work, new controllers for semi-active control scheme are introduced those can take the advantage of the unique features of the MR damper. First, the algorithms for the proposed controllers are described. Through numerical simulations on a scaled three-story and five storey structures, the structural responses produced by the proposed algorithms are investigated. In parallel, the structural response produced by the widely employed LQR/LQG-based clipped-optimal control is introduced and compared. Subsequently, control performance obtained from numerical studies is presented. The details of the work carried out and conclusions drawn from this research work are given below.

A fundamental understanding of the semi-active control scheme is developed through studying its different components such as MR damper, structure and the control law. A suitable mathematical model for the MR damper (modified Bouc-wen model) is chosen that could explore it`s non-linear behaviour fully. The analytical results exhibit that MR damper is an intelligent choice among the various available semi-active control devices. The following conclusions are drawn from this study.

- This study classified controllers into two categories based on their methodology of dispensing command signal to the actuating device (MR damper).
  - First, the controllers those give command signal to the MR damper based on the structural measurements obtained from the sensor without considering the feedback from the MR damper.
  - Second, the controllers those calculate the command signal based on structural measurements as well as feedback from the MR damper.
- This study concludes that controllers which consider the feedback from the actuating device has better control over the MR damper as compared to other class of controllers.
- Based on the parametric study carried out, it is concluded that clipped optimal LQR/LQG controllers are delivering better performance over the other controllers considered in this study.

The clipped optimal LQR/LQG are the optimal controller and has a cost function to be minimized for optimal performance. These controllers have two weighting matrices namely the state weighting

matrix **Q** and the control weighting matrix **R**. These weighting matrices are determined only once while designing the LQR/LQG controller. This makes these controllers perform in the same manner irrespective of the amplitude of the vibrations. This drawback limits their full potential. To overcome this drawback, two new approaches based on fast Fourier transform (FFT) and maximum dominant period approach along with the particle swarm optimization (PSO) are proposed. Two new controllers are developed based on the proposed PSO-FFT approach. Similarly, two new controllers are developed using PSO-τ_p^{max} approach. These controllers are evaluated on a three storey prototype structure for various conditions. Based on the analysis carried out in Chapter 4 the following conclusions can be drawn.

- Two controllers are proposed for the PSO-FFT based approach. These controllers are PSO-FFT-modified-LQR and PSO-FFT-modified-LQG controller
- The PSO-FFT-modified-LQR controller is found superior to the CO-LQR.
- Similarly, the PSO-FFT-modified-LQG controller is found superior to the CO-LQG.
- PSO-FFT-modified-LQR is suggested over PSO-FFT-modified LQG due to its simple design and easy implementation.

Similarly, for the PSO-τ_p^{max} approach, the following conclusions can be made

- Another two new controllers are proposed for the PSO-τ_p^{max} approach. These controllers are PSO-τ_p^{max} -modified-LQR and PSO-τ_p^{max} -modified-LQG controller
- The two proposed controllers (PSO-τ_p^{max} -modified-LQR & PSO-τ_p^{max} -modified-LQG) are found to be superior to the conventional controllers (i.e. CO-LQR & CO-LQG).
- To select between the PSO-τ_p^{max} -modified-LQR and PSO-τ_p^{max} -modified LQG is very difficult. However, the PSO-τ_p^{max} -modified-LQR is preferred due to its simple design and easy implementation.

Further, a parametric study is carried out for the evaluation of the all proposed controllers under several conditions i.e. to observe the effect of soil type, to check suitability to a higher number of stories, to determine the best location for the placement of MR damper, power off conditions. The following conclusions are drawn

- The performance of the proposed controllers is analyzed for an earthquake recorded under different types of soils i.e. (Hard, medium, and soft soil).

- The proposed controllers demonstrate superior performance in reducing the structural responses as compared to conventional CO-LQR/LQG
- All the proposed controllers achieve better performance using lesser control force. Thus, utilize the available power intelligently which is very essential amid the seismic events.
- The comparison of the cumulative energies contained in the top floor`s displacement signal obtained due to the developed controllers and the conventional CO-LQR/LQG shows that displacement signal obtained due to the developed controllers has the lesser capability of the damage. Hence, the structural integrity is protected.
- For the assessment of the suitability of the developed controllers for the higher modes, a study is carried out on the five storey structure under various conditions using the developed controllers.
    - The performance of the developed controllers for the five storey structure is found to be like the responses of the three story structures.
    - From the results, it can be concluded that the developed controllers are applicable to the five storey structure.
- A study is carried out for finding the best location for the placement of MR damper if only one MR damper is available. For this study, the MR damper is placed on the first, second and the third floor sequentially in the three storey structure. For the performance analysis, the structure is subjected to various earthquake time histories for every position of the MR damper. Based on the analysis the following conclusions can be drawn.
- The percentage reduction in the relative displacement is not very large for all floors irrespective of MR damper placement whereas there is a significant percentage reduction in the other structural responses i.e. inter-storey drift and absolute acceleration with respect to the position of MR damper within the structure. This happens because in three degrees of freedom structure subjected to strong ground motion mainly follows the fundamental mode of vibration. Consequently, the displacement occurs primarily in the ground floor as compared to the other two floors. This is the main reason, that the maximum percentage reduction in the relative displacement occurs when the MR damper is kept on the ground floor.
- Similarly, for five storey structure, the damper is placed on the lower floors.
- This study recommends that the MR damper should be placed on the lowest floor for the best results irrespective of the controllers used in the semi active control scheme.

- A study is carried out considering a situation when power vanishes at the peak of the earthquake concludes that any controller including the developed controllers in this work will convert into Passive OFF controller. Passive OFF controller provides better seismic protection over the uncontrolled structure.

Moreover, in the quest of design simplicity and performance at par with the clipped optimal LQR/LQG, a particle swarm optimized control algorithm is proposed based on the modified quasi bang-bang control algorithm. The constant output weights used in the modified quasi bang-bang controller are optimized for the best performance in dynamic loading such as earthquake using the particle swarm optimization (PSO). The proposed optimized controller is then applied to a three storey prototype structure fixed with an MR damper. This structure has been subjected to various earthquakes for performance evaluation. The results thus obtained are compared with the best performing clipped optimal linear quadratic Gaussian (LQG) controller, quasi bang-bang and modified quasi bang-bang controller. The following conclusions can be drawn from this study.

- It utilizes the power intelligently, which is a critical factor in seismic vibration control.
- The results of the three DOF test structure due to two near-fault earthquake excitation exhibits that the PSO modified quasi bang-bang controller performs superior to other controllers examined in this study overall.
- Its simple implementation quality makes this controller an attractive option to control the vibrations.

Finally, the results exhibit that the proposed controllers outperform the conventional LQR/LQG controllers. However, the results obtained for both the approaches are same, but the control action of the controllers developed using PSO-τ_p^{max} approach is quicker because the calculation process for this approach always remains in the time domain. Due to the inalienable adaptability in the design to account for the quasi-resonance by alteration of R, the proposed controllers are recommended as a suitable choice for seismic vibration control. This work provided the seismic performance of semi-active control scheme on structures and showed the strong potential for practical use to mitigate seismic damage.

6.2 Limitation of this research work and future studies

A sincere effort has been made to investigate many aspects related to semi-active control strategies in building structures subjected to earthquake loadings in this dissertation. The structure

considered in this work is assumed to have lumped masses concentrated at the centre but in a real structure, the mass is distributed unevenly in many sections. So, the design consideration of the structure should be considered. Further, the overall system is considered as a linear time-invariant (LTI), and time delay issue is also not considered in this study.

Therefore, some recommendations for future studies still exist, which are outlined below.

- Though the proposed controllers show commendable performance in various conditions in numerical simulations, their laboratory testing is highly recommended.
- Further, the continuous application of high voltage would lead to floor lock-up condition and it could be a perspective field of research. The study on the issues like non-availability of all states and measurements due to sensor fault during the earthquake may also be interesting problems for further research.
- The effectiveness of the modified LQR/LQG controller was shown in this dissertation. However, its seismic performance depended on excitation inputs to a large extent. Therefore, a set of earthquakes recorded in different conditions (tectonic, geophysical, structural etc.) should be considered.
- Generally, it is not easy to model nonlinear structures mathematically. Thus, the proposed simple semi-active control algorithms have a limitation when systems with strong nonlinearity are considered. This can be another field of research for future studies.

Bibliography

[1] S. J. Dyke, B. F. SpencerJr, M. K. Sain, and J. D. Carlson, "Modeling and control of magnetorheological dampers for seismic response reduction," *Smart Mater. Struct.*, vol. 5, no. 5, p. 565, 1996.

[2] G. W. Housner, L. A. Bergman, and B. Spencer, "Structural control: past, present, and future," *J. Eng. Mech.*, vol. 123, no. 9, pp. 897–971, 1997.

[3] H. Sodeyama, K. Sunakoda, H. Fujitani, S. Soda, N. Iwata, and K. Hata, "Dynamic tests and simulation of magneto rheological dampers," *Comput. Civ. Infrastruct. Eng.*, vol. 18, no. 1, pp. 45–57, 2003.

[4] W. Huang, J. Xu, D. Y. Zhu, Y. L. Wu, J. W. Lu, and K. L. Lu, "Semi-active vibration control using a magneto rheological (MR) damper with particle swarm sptimization," *Arab. J. Sci. Eng.*, vol. 40, no. 3, pp. 747–762, 2015.

[5] M. Ashtiani, S. H. Hashemabadi, and A. Ghaffari, "A review on the magnetorheological fluid preparation and stabilization," *J. Magn. Magn. Mater.*, vol. 374, pp. 716–730, 2015.

[6] R. Kandasamy, F. Cui, and N. Townsend, "A review of vibration control methods for marine offshore structures," *Ocean Eng.*, vol. 127, pp. 279–297, 2016.

[7] M. M. Zafarani and A. M. Halabian, "Supervisory adaptive nonlinear control for seismic alleviation of inelastic asymmetric buildings equipped with MR dampers," *Eng. Struct.*, vol. 176, pp. 849–858, 2018.

[8] R. Ceravolo, M. L. Pecorelli, and L. Zanotti Fragonara, "Comparison of semi-active control strategies for rocking objects under pulse and harmonic excitations," *Mech. Syst. Signal Process.*, vol. 90, pp. 175–188, 2017.

[9] L. M. Jansen and S. J. Dyke, "Semiactive Control Strategies for MR Dampers: Comparative Study," *J. Eng. Mech.*, vol. 126, no. 8, pp. 795–803, 2000.

[10] Y. Fu, S. J. Dyke, J. M. Caicedo, and J. D. Carlson, "Experimental verification of multiinput seismic control strategies for smart dampers," *J. Eng. Mech.*, vol. 127, no. 11, pp. 1152–1164, 2001.

[11] T. E. Saaed, G. Nikolakopoulos, J. E. Jonasson, and H. Hedlund, "A state-of-the-art review of structural control systems," *J. Vib. Control*, vol. 21, no. 5, pp. 919–937, 2015.

[12] T. T. Soong and B. F. Spencer, "Supplemental energy dissipation: State-of-the-art and state-of-the-practice," *Eng. Struct.*, 2002.

[13] L. L. Sun, C. H. Hansen, and C. Doolan, "Evaluation of the performance of a passive-active vibration isolation system," *Mech. Syst. Signal Process.*, vol. 50–51, pp. 480–497, 2015.

[14] R. S. Jangid and J. M. Kelly, "Base isolation for near-fault motions," *Earthq. Eng. Struct. Dyn.*, vol. 30, no. 5, pp. 691–707, 2001.

[15] A. Sharma and R. S. Jangid, "Seismic response of base-isolated benchmark building with variable sliding isolators," *J. Earthq. Eng.*, vol. 14, no. 7, pp. 1063–1091, 2010.

[16] R. S. Jangid, "Response of SDOF system to non-stationary earthquake excitation," *Earthq. Eng. Struct. Dyn.*, vol. 33, no. 15, pp. 1417–1428, 2004.

[17] S. Narasimhan, S. Nagarajaiah, H. P. Gavin, and E. A. Johnson, *Smart base isolated benchmark building. part I: Problem definition*, vol. 13, no. 2–3. 2006.

[18] A. K. Singh and P. C. Pandey, "An implicit integration algorithm for plane stress damage coupled elastoplasticity," *Mech. Res. Commun.*, vol. 26, no. 6, pp. 693–700, 1999.

[19] J. N. Yang., J. C. Wu., and A. K. Agrawal., "Sliding mode control for nonlinear and hysteretic structures," *J. Eng. Mech.*, vol. 121, no. 12, pp. 1330–1339, 1995.

[20] W. Yu and S. Thenozhi, *Active structural control with stable fuzzy PID techniques*. Springer international publishing, 2016.

[21] A. Oveisi and M. Gudarzi, "Robust active vibration control of smart structures; a comparison between two approaches: μ-synthesis & amp; LMI-based design," *Int. J. Aerosp. Sci.*, vol. 1, no. 5, pp. 116–127, 2013.

[22] H. Yazici and R. Güçlü, "Active vibration control of seismic excited structural system using LMI-based mixed H2/H ∞ state feedback controller," *Turkish J. Electr. Eng. Comput. Sci.*, vol. 19, no. 6, pp. 839–849, 2011.

[23] P. Tan and A. K. Agrawal, "Benchmark structural control problem for a seismically excited

highway bridge-Part II: Phase I sample control designs," *Struct. Control Heal. Monit.*, vol. 16, no. 5, pp. 530–548, 2009.

[24] T. K. Datta, "A state-of-the-art review on active control of structures," *ISET J. Earthq. Technol.*, vol. 40, no. 1, pp. 1–17, 2003.

[25] S. Moheimani, "A survey of recent innovations in vibration damping and control using shunted piezoelectric transducers," *IEEE Trans. Control Syst. Technol.*, vol. 11, no. 4, pp. 482–494, 2003.

[26] T. T. Soong, "Experimental simulation of degrading structures through active control," *Earthq. Eng. Struct. Dyn.*, vol. 27, no. 2, pp. 143–154, 1998.

[27] A. Kumar, B. Poonam, and V. Sehgal, "Active vibration control of structures against earthquakes using modern control theory," *Asian J. Civ. Eng.*, vol. 3, no. 2007, pp. 283–299, 2007.

[28] O. Llane-santiago and M. Rfos-bolfvar, "Active control of mechanical vibrations using dynamic variable structure control," in *Proceedings of the International Conference on Control Applications*, 2002, pp. 316–320.

[29] M. Davoodi, M. Ebrahimnejad, and J. Vaseghi-Amiri, "Active vibration control of smart building frames by feedback controllers," *Comput. Methods Civ. Eng.*, vol. 1, no. 1, pp. 63–73, 2010.

[30] S. N. Mahmoodi, M. J. Craft, S. C. Southward, and M. Ahmadian, "Active vibration control using optimized modified acceleration feedback with adaptive line enhancer for frequency tracking," *J. Sound Vib.*, vol. 330, no. 7, pp. 1300–1311, 2011.

[31] L. V. Pradeesh and S. F. Ali, "Active vibration control of thin plate using optimal dynamic inversion technique," *IFAC-PapersOnLine*, vol. 49, no. 1, pp. 326–331, 2016.

[32] B. Karimpour, A. Keyhani, and J. Alamatian, "New active control method based on using multiactuators and sensors considering uncertainty of parameters," *Adv. Civ. Eng.*, vol. 2014, p. 10, 2014.

[33] T. T. Soong, S. F. Masri, and G. W. Housner, "An overview of active structural control under seismic loads," *Earthq. Spectra*, vol. 7, no. 3, pp. 483–505, 1991.

[34] T. T. Soong and B. F. Spencer, “Active, semi-active and hybrid control of structures,” *Bull. New Zeal. Natl. Soc. Earthq. Eng.*, vol. 33, no. 3, pp. 387–402, 2000.

[35] B. Spencer and T. Soong, “New applications and development of active, semi-active and hybrid control techniques for seismic and non-seismic vibration in the USA,” in *Proceedings of International Post-SMiRT Conference Seminar on Seismic Isolation, Passive Energy Dissipation and Active Control of Vibration of Structures*, 1999, vol. 1994, pp. 23–25.

[36] H. Cheol Cho, S. Fadali, M. Saiid, and K. Soon Lee, “Neural network active control of structures with earthquake excitation,” *Int. J. Control. Autom. Syst.*, vol. 3, no. 2, pp. 202–210, 2005.

[37] S. Korkmaz, “A review of active structural control: challenges for engineering informatics,” *Comput. Struct.*, vol. 89, no. 23, pp. 2113–2132, 2011.

[38] B. F. Spencer and S. Nagarajaiah, “State of the art of structural control,” *J. Struct. Eng.*, vol. 129, no. 7, pp. 845–856, 2003.

[39] X. Zhu, X. Jing, and L. Cheng, “Magnetorheological fluid dampers: A review on structure design and analysis,” *J. Intell. Mater. Syst. Struct.*, vol. 23, no. 8, pp. 839–873, 2012.

[40] D. Zhao and Y. Li, “Fuzzy control for seismic protection of semiactive base-isolated structures subjected to near-fault earthquakes,” *Math. Probl. Eng.*, vol. 2015, 2015.

[41] F. Casciati, J. Rodellar, and U. Yildirim, “Active and semi-active control of structures – theory and applications: A review of recent advances,” *J. Intell. Mater. Syst. Struct.*, vol. 23, no. 11, pp. 1181–1195, 2012.

[42] R. E. Christenson and B. F. Spencer, “Semiactive control of civil structures for natural hazard mitigation: analytical and experimental studies,” Department of Civil Engineering and Geological Sciences.University of Notre Dame, 2001.

[43] H. Davorin, B. Pinhas, and R. Michael, “Semi- Active versus Passive or Active Tuned Mass Dampers for Structural Control,” *J. Eng. Mech.*, vol. 109, no. 3, pp. 691–705, Jun. 1983.

[44] Y. Si, “Structural Control Strategies for Load Reduction of Floating Wind Turbines,” 2015.

[45] Z. D. Xu, Y. P. Shen, and Y. Q. Guo, “Semi-active control of structures incorporated with magnetorheological dampers using neural networks,” *Smart Mater. Struct.*, vol. 12, no. 1, p. 80, 2003.

[46] R. Villamizar, N. Luo, S. J. Dyke, and J. Vehí, “Experimental verification of backstepping controllers for magnetorheological MR dampers in structural control,” in *Proceedings of the 20th IEEE International Symposium on Intelligent Control, ISIC ’05 and the 13th Mediterranean Conference on Control and Automation, MED ’05*, 2005, vol. 2005, pp. 316–321.

[47] Y. J. Cha, A. Agrawal, and A. Friedman, “Performance validations of semiactive controllers on large-scale moment-resisting frame equipped with 200-kN MR damper using real-time hybrid simulations,” *J. Struct. Eng.*, vol. 140, no. 10, p. 4014066, 2014.

[48] S. B. Choi, W. Li, M. Yu, H. Du, J. Fu, and P. X. Do, “State of the art of control schemes for smart systems featuring magneto-rheological materials,” *Smart Mater. Struct.*, vol. 25, no. 4, p. 43001, 2016.

[49] S. J. Dyke and B. F. Spencer, “A comparison of semi-active control strategies for the MR damper,” in *Proceedings Intelligent Information Systems. IIS’97*, 1997, pp. 580–584.

[50] M. Bikdash, V. Kunchithapadam, K. Ragunathan, and A. Homaifar, “Comparison of quasi bang-bang and sliding mode controls for a DC shunt motor with time delay,” *Nonlinear Dyn.*, vol. 23, no. 1, pp. 87–102, 2000.

[51] A. M. Aly, “Vibration control of buildings using magnetorheological damper: A new control algorithm,” *J. Eng.*, vol. 2013, pp. 1–10, 2013.

[52] J. M. Madsen, L. S. Shieh, and S. M. Guo, “State-space digital PID controller design for multivariable analog systems with multiple time delays,” *Asian J. Control*, vol. 8, no. 2, pp. 161–173, 2008.

[53] Y. Li, X. Wang, R. Huang, and Z. Qiu, “Active vibration and noise control of vibro-acoustic system by using PID controller,” *J. Sound Vib.*, vol. 348, pp. 57–70, 2015.

[54] R. Guclu, “Sliding mode and PID control of a structural system against earthquake,” *Math. Comput. Model.*, vol. 44, no. 1, pp. 210–217, 2006.

[55] S. Y. Zhang and X. M. Wang, “Study of Fuzzy-PID control in MATLAB for two-phase hybrid stepping motor,” in *Energy Research and Power Engineering*, 2013, vol. 341, pp. 664–667.

[56] A. C. Nerves and R. Krishnan, “Active control strategies for tall civil structures,” in *Proceedings of IECON ’95 - 21st Annual Conference on IEEE Industrial Electronics*, 1995, vol. 2, pp. 962–967 vol.2.

[57] R. Guclu and H. Yazici, “Vibration control of a structure with ATMD against earthquake using fuzzy logic controllers,” *J. Sound Vib.*, vol. 318, no. 1, pp. 36–49, 2008.

[58] T. L. Teng, C. P. Peng, and C. Chuang, “A study on the application of fuzzy theory to structural active control,” *Comput. Methods Appl. Mech. Eng.*, vol. 189, no. 2, pp. 439–448, 2000.

[59] G. Zames, “Feedback and optimal sensitivity: model reference transformation, multiplicative semiforms and approximate inverse,” *IEEE Trans. Automat. Contr.*, vol. 26, no. 2, pp. 301–320, 1981.

[60] J. Gadewadikar, A. Bhilegaonkar, F. Lewis, and O. Kuljaca, *Technological Developments in Education and Automation*. Springer Science & Business Media, 2010.

[61] W. Park, K. S. Park, and H. M. Koh, “Active control of large structures using a bilinear pole-shifting transform with H∞ control method,” *Eng. Struct.*, vol. 30, no. 11, pp. 3336–3344, 2008.

[62] J. C. Wu, J. N. Yang, and W. E. Schmitendorf, “Reduced-order H∞ and LQR control for wind-excited tall buildings,” *Eng. Struct.*, vol. 20, no. 3, pp. 222–236, 1998.

[63] R. Saragih, “Designing active vibration control with minimum order for flexible structure,” in *2010 8th IEEE International Conference on Control and Automation, ICCA 2010*, 2010, pp. 450–453.

[64] A. Boccia and R. Vinter, “The maximum principle for optimal control problems with time delays,” *SIAM J. Control Optim.*, vol. 55, no. 5, pp. 2905–2935, 2017.

[65] J. N. Yang, A. Akbarpour, and G. Askar, “Effect of time delay on control of seismic-excited buildings,” *J. Struct. Eng.*, vol. 116, no. 10, pp. 2801–2814, 1991.

[66] L. Chi Chang, C. Chang Ching, and C. Huang Lin, “Optimal H∞ output feedback control systems with time delay,” *J. Eng. Mech.*, vol. 132, no. 10, pp. 1096–1105, 2006.

[67] H. Du and N. Zhang, “H∞ control for buildings with time delay in control via linear matrix inequalities and genetic algorithms,” *Eng. Struct.*, vol. 30, no. 1, pp. 81–92, 2008.

[68] K. Liu, L. Chen, and G. Cai, “H∞ control of a building structure with time-varying delay,” *Adv. Struct. Eng.*, vol. 18, no. 5, pp. 643–657, 2015.

[69] V. Utkin, “Variable structure systems with sliding modes,” *IEEE Trans. Automat. Contr.*, vol. 22, no. 2, pp. 212–222, 1977.

[70] R. Adhikari, H. Yamaguchi, and T. Yamazaki, “Modal space sliding-mode control of structures,” *Earthq. Eng. Struct. Dyn.*, vol. 27, no. 11, pp. 1303–1314, 1998.

[71] B. Zhao, X. Lu, M. Wu, and Z. Mei, “Sliding mode control of buildings with base-isolation hybrid protective system,” *Earthq. Eng. Struct. Dyn.*, vol. 29, no. 3, pp. 315–326, 2000.

[72] M. Allen, F. Bernelli-Zazzera, and R. Scattolini, “Sliding mode control of a large flexible space structure,” *Control Eng. Pract.*, vol. 8, no. 8, pp. 861–871, 2000.

[73] S. Monajemi-Nezhad and F. R. Rofooei, “Decentralized sliding mode control of multistory buildings,” *Struct. Des. Tall Spec. Build.*, vol. 16, no. 2, pp. 181–204, 2007.

[74] X. Xiang, C. Liu, H. Su, and Q. Zhang, “On decentralized adaptive full-order sliding mode control of multiple UAVs,” *ISA Trans.*, vol. 71, pp. 196–205, 2017.

[75] O. Yakut and H. Alli, “Neural based sliding-mode control with moving sliding surface for the seismic isolation of structures,” *J. Vib. Control*, vol. 17, no. 14, pp. 2103–2116, 2011.

[76] Z. Li, Z. Deng, and Z. Gu, “New sliding mode control of building structure using RBF neural networks,” in *2010 Chinese Control and Decision Conference*, 2010, pp. 2820–2825.

[77] H. Alli and O. Yakut, “Fuzzy sliding-mode control of structures,” *Eng. Struct.*, vol. 27, no. 2, pp. 277–284, 2005.

[78] L. Zhou, C. Chang, and L. X. Wang, “Adaptive fuzzy control for nonlinear building-magnetorheological damper system,” *J. Struct. Eng.*, vol. 129, no. 7, pp. 905–913, 2003.

[79] S. A. Chen, J. C. Wang, M. Yao, and Y. B. Kim, “Improved optimal sliding mode control

for a non-linear vehicle active suspension system," *J. Sound Vib.*, vol. 395, pp. 1–25, 2017.

[80] Y. K. Wan, J. Ghaboussi, P. Venini, and K. Nikzad, "Control of structures using neural networks," *Smart Mater. Struct.*, vol. 4, no. 1A, p. A149, 1995.

[81] G. Jamshid and J. Abdolreza, "Active control of structures using neural networks," *J. Eng. Mech.*, vol. 121, no. 4, pp. 555–567, 1995.

[82] M. Zapateiro, N. Luo, H. R. Karimi, and J. Vehí, "Vibration control of a class of semiactive suspension system using neural network and backstepping techniques," *Mech. Syst. Signal Process.*, vol. 23, no. 6, pp. 1946–1953, 2009.

[83] A. Madan, "Vibration control of building structures using self-organizing and self-learning neural networks," *J. Sound Vib.*, vol. 287, no. 4, pp. 759–784, 2005.

[84] A. K. Bledzki and W. Zhang, "Dynamic mechanical properties of natural fiber-reinforced epoxy foams," *J. Reinf. Plast. Compos.*, vol. 20, no. 14–15, pp. 1263–1274, 2001.

[85] J. Kim, J. Jung, and I. Lee, "Optimal structural control using neural networks," *J. Eng. Mech.*, vol. 126, no. 2, pp. 201–205, 2000.

[86] S. Hidaka, Y. K. Ahn, and S. Morishita, "Adaptive vibration control by a variable-damping dynamic absorber using ER fluid," *J. Vib. Acoust.*, vol. 121, no. 3, pp. 373–378, 1999.

[87] S. Laflamme and J. J. Connor, "Application of self-tuning Gaussian networks for control of civil structures equipped with magnetorheological dampers," in *SPIE Smart Structures and Materials Nondestructive Evaluation and Health Monitoring*, 2009, vol. 7288, p. 72880M–7288–12.

[88] S. Laflamme, J. J. E. Slotine, and J. J. Connor, "Wavelet network for semi-active control," *J. Eng. Mech.*, vol. 137, no. 7, pp. 462–474, 2011.

[89] R. Abbasi-ghalehtaki, H. Khotanlou, and M. Esmaeilpour, "Fuzzy evolutionary cellular learning automata model for text summarization," *Swarm Evol. Comput.*, vol. 30, pp. 11–26, 2016.

[90] E. H. Mamdani, "Application of fuzzy algorithms for control of simple dynamic plant," *Proc. Inst. Electr. Eng.*, vol. 121, no. 12, p. 1585–1588(3), 1974.

[91] A. Ahlawat and A. Ramaswamy, “Multiobjective optimal structural vibration control using fuzzy logic control system,” *J. Struct. Eng.*, vol. 127, no. 11, pp. 1330–1337, 2001.

[92] K. M. Choi, S. W. Cho, H. J. Jung, and I. W. Lee, “Semi-active fuzzy control for seismic response reduction using magnetorheological dampers,” *Earthq. Eng. Struct. Dyn.*, vol. 33, no. 6, pp. 723–736, 2004.

[93] S. F. Ali and A. Ramaswamy, “GA-optimized FLC-driven semi-active control for phase-II smart nonlinear base-isolated benchmark building,” *Struct. Control Heal. Monit.*, vol. 15, no. 5, pp. 797–820, 2008.

[94] S. F. Ali and A. Ramaswamy, “Optimal fuzzy logic control for MDOF structural systems using evolutionary algorithms,” *Eng. Appl. Artif. Intell.*, vol. 22, no. 3, pp. 407–419, 2009.

[95] A. Rama Mohan Rao and K. Sivasubramanian, “Multi-objective optimal design of fuzzy logic controller using a self configurable swarm intelligence algorithm,” *Comput. Struct.*, vol. 86, no. 23–24, pp. 2141–2154, 2008.

[96] K. Park, H. Koh, and S. Ok, “Active control of earthquake excited structures using fuzzy supervisory technique,” *Adv. Eng. Softw.*, vol. 33, no. 11, pp. 761–768, 2002.

[97] K. M. Choi, S. W. Cho, D. O. Kim, and I. W. Lee, “Active control for seismic response reduction using modal-fuzzy approach,” *Int. J. Solids Struct.*, vol. 42, no. 16–17, pp. 4779–4794, 2005.

[98] D. Das, T. K. Datta, and A. Madan, “Semiactive fuzzy control of the seismic response of building frames with MR dampers,” *Earthq. Eng. Struct. Dyn.*, vol. 41, no. 1, pp. 99–118, 2012.

[99] F. A. Shirazi, J. Mohammadpour, K. M. Grigoriadis, and G. Song, “Identification and control of an MR damper with stiction effect and its application in structural vibration mitigation,” *IEEE Trans. Control Syst. Technol.*, vol. 20, no. 5, pp. 1285–1301, 2012.

[100] J. L. Wu, “A simultaneous mixed LQR/H∞ control approach to the design of reliable active suspension controllers,” *Asian J. Control*, vol. 19, no. 2, pp. 415–427, 2017.

[101] A. Shafieezadeh, K. Ryan, and Y. Chen, “Fractional order filter enhanced LQR for seismic protection of civil structures,” *J. Comput. Nonlinear Dyn.*, vol. 3, no. 2, pp. 21404–21407,

2008.

[102] C. S. Chang and T. S. Liu, “LQG controller for active vibration absorber in optical Disk drive,” *IEEE Trans. Magn.*, vol. 43, no. 2, pp. 799–801, 2007.

[103] S. B. Choi, S. R. Hong, K. G. Sung, and J. W. Sohn, “Optimal control of structural vibrations using a mixed-mode magnetorheological fluid mount,” *Int. J. Mech. Sci.*, vol. 50, no. 3, pp. 559–568, 2008.

[104] A. Barkefors, M. Sternad, and L. J. Brännmark, “Design and analysis of Linear Quadratic Gaussian feedforward controllers for active noise control,” *IEEE/ACM Trans. Audio Speech Lang. Process.*, vol. 22, no. 12, pp. 1777–1791, 2014.

[105] E. G. Collins and M. F. Selekwa, “A fuzzy logic approach to LQG design with variance constraints,” *IEEE Trans. Control Syst. Technol.*, vol. 10, no. 1, pp. 32–42, 2002.

[106] L. M. Jansen and S. J. Dyke, “Semiactive control strategies for MR dampers: comparative study,” *J. Eng. Mech.*, vol. 126, no. 8, pp. 795–803, 2000.

[107] G. F. Panariello, R. Betti, and R. W. Longman, “Optimal structural control via training on ensemble of earthquakes,” *J. Eng. Mech.*, vol. 123, no. 11, pp. 1170–1179, 1997.

[108] A. Alavinasab, H. Moharrami, and A. Khajepour, “Active control of structures using energy-based LQR method,” *Comput. Civ. Infrastruct. Eng.*, vol. 21, no. 8, pp. 605–611, 2006.

[109] Y. Li, J. Liu, and Y. Wang, “Design approach of weighting matrices for LQR based on multi-objective evolution algorithm,” in *2008 International Conference on Information and Automation*, 2008, pp. 1188–1192.

[110] B. Basu and S. Nagarajaiah, “Multiscale wavelet-LQR controller for linear time varying systems,” *J. Eng. Mech.*, vol. 136, no. 9, pp. 1143–1151, 2010.

[111] B. Basu and S. Nagarajaiah, “A wavelet-based time-varying adaptive LQR algorithm for structural control,” *Eng. Struct.*, vol. 30, pp. 2470–2477, 2008.

[112] F. Amini, N. K. Hazaveh, and A. A. Rad, “Wavelet PSO-based LQR algorithm for optimal structural control using active tuned mass dampers,” *Comput. Civ. Infrastruct. Eng.*, vol. 28,

no. 7, pp. 542–557, 2013.

[113] C. Wongsathan and C. Sirima, “Application of GA to design LQR controller for an inverted pendulum system,” in *IEEE International Conference on Robotics and Biomimetics, ROBIO*, 2008, no. 2, pp. 951–954.

[114] S. J. Dyke, B. F. Spencer Jr, P. Quast, M. K. Sain, D. C. Kaspari, and T. T. Soong, “Acceleration feedback control of MDOF structures,” *J. Eng. Mech.*, vol. 122, no. 9, pp. 907–918, 1996.

[115] D. Das, “ANN-cum-fuzzy control of seismic response using MR dampers,” in *15th World Conference on Earthquake Engineering, Lisbon Portugal*, 2012.

[116] S. F. Ali and A. Ramaswamy, “Testing and modeling of MR damper and its application to SDOF systems using integral backstepping technique,” *J. Dyn. Syst. Meas. Control*, vol. 131, no. 2, pp. 21009–21011, 2009.

[117] B. F. Spencer, S. J. Dyke, M. K. Sain, and J. D. Carlson, “Phenomenological model for magnetorheological dampers,” *J. Eng. Mech.*, vol. 123, no. 3, pp. 230–238, 1997.

[118] A. Dominguez, R. Sedaghati, and I. Stiharu, “Modeling and application of MR dampers in semi-adaptive structures,” *Comput. Struct.*, vol. 86, no. 3–5, pp. 407–415, 2008.

[119] Y. F. Liu, T. K. Lin, and K. C. Chang, “Analytical and experimental studies on building mass damper system with semi-active control device,” *Struct. Control Heal. Monit.*, vol. 25, no. 6, p. e2154, 2018.

[120] R. Ahamed, S. B. Choi, and M. M. Ferdaus, “A state of art on magneto-rheological materials and their potential applications,” *J. Intell. Mater. Syst. Struct.*, vol. 29, no. 10, pp. 2051–2095, 2018.

[121] G. Yang, B. F. SpencerJr., and H. J. Jung, “Dynamic modeling of large-scale magnetorheological damper systems for civil engineering applications,” *J. Eng. Mech.*, vol. 130, no. 9, pp. 1107–1114, 2004.

[122] F. Weber, “Semi-active vibration absorber based on real-time controlled MR damper,” *Mech. Syst. Signal Process.*, vol. 46, no. 2, pp. 272–288, 2014.

[123] Q. P. Ha, M. T. Nguyen, J. Li, and N. M. Kwok, “Smart structures with current-driven MR dampers: modeling and second-order sliding mode control,” *IEEE/ASME Trans. Mechatronics*, vol. 18, no. 6, pp. 1702–1712, 2013.

[124] Z. Jiang and R. E. Christenson, “A fully dynamic magneto-rheological fluid damper model,” *Smart Mater. Struct.*, vol. 21, no. 6, p. 65002, 2012.

[125] S. Talatahari, A. Kaveh, and N. Mohajer Rahbari, “Parameter identification of Bouc-Wen model for MR fluid dampers using adaptive charged system search optimization,” *J. Mech. Sci. Technol.*, vol. 26, no. 8, pp. 2523–2534, Aug. 2012.

[126] I. H. Vadtala, D. P. Soni, and D. G. Panchal, “Semi-active control of a benchmark building using neuro-inverse dynamics of MR damper,” *Procedia Eng.*, vol. 51, pp. 45–54, 2013.

[127] M. Ismail, F. Ikhouane, and J. Rodellar, “The hysteresis Bouc-Wen model, a survey,” *Arch. Comput. Methods Eng.*, vol. 16, no. 2, pp. 161–188, 2009.

[128] F. Ma, “An improved fuzzy PID control algorithm applied in liquid mixing system,” in *IEEE International Conference on Information and Automation (ICIA)*, 2014, pp. 587–591.

[129] S. Jafarzadeh, R. Mirheidari, M. R. J. Motlagh, and M. Barkhordari, “Designing PID and BELBIC controllers in path tracking problem,” *Int. J. Comput. Commun. Control*, vol. 3, no. spl. issue, pp. 343–348, 2008.

[130] H. R. Koofigar and S. Amelian, “Active vibration suppression in smart structures subjected to model uncertainties and environmental disturbances: an adaptive approach,” *J. Vib. Control*, vol. 19, no. 13, pp. 2046–2053, 2013.

[131] H. Garrido, O. Curadelli, and D. Ambrosini, “A straightforward method for tuning of Lyapunov-based controllers in semi-active vibration control applications,” *J. Sound Vib.*, vol. 333, no. 4, pp. 1119–1131, 2014.

[132] P. C. Fourie and A. A. Groenwold, “The particle swarm optimization algorithm in size and shape optimization,” *Struct. Multidiscip. Optim.*, vol. 23, no. 4, pp. 259–267, 2002.

[133] S. Das, A. Abraham, and A. Konar, “Particle swarm optimization and differential evolution algorithms: technical analysis, applications and hybridization perspectives,” in *Advances of Computational Intelligence in Industrial Systems*, Berlin Heidelberg: Springer, 2008, pp. 1–

38.

[134] G. G. Amiri, A. Abdolahi Rad, S. Aghajari, and N. Khanmohamadi Hazaveh, “Generation of near-field artificial ground motions compatible with median-predicted spectra using PSO-based neural network and wavelet analysis,” *Comput. Civ. Infrastruct. Eng.*, vol. 27, no. 9, pp. 711–730, 2012.

[135] G. Kumar, A. Kumar, and R. S. Jakka, “The particle swarm modified quasi bang-bang controller for seismic vibration control,” *Ocean Eng.*, vol. 166, pp. 105–116, 2018.

[136] H. J. Lee, H. J. Jung, S. W. Cho, and I. W. Lee, “An experimental study of semiactive modal neuro-control scheme using MR damper for building structure,” *J. Intell. Mater. Syst. Struct.*, vol. 19, no. 9, pp. 1005–1015, 2008.

[137] G. Kumar, A. Kumar, and R. S. Jakka, “An adaptive LQR controller based on PSO and maximum predominant frequency approach for semi-active control scheme using MR damper,” *Mech. Ind.*, vol. 19, no. 1, p. 109, 2018.

[138] Y. Nakamura and J. Saita, “UrEDAS, the earthquake warning system: today and tomorrow,” in *Earthquake Early Warning Systems*, Berlin, Heidelberg: Springer, 2007, pp. 249–281.

[139] C. W. Lim, T. Y. Chung, and S. J. Moon, “Adaptive bang-bang control for the vibration control of structures under earthquakes,” *Earthq. Eng. Struct. Dyn.*, vol. 32, no. 13, pp. 1977–1994, 2003.

[140] R. Hassan, B. Cohanim, O. de Weck, and G. Venter, “A comparison of particle swarm optimization and the genetic algorithm,” in *46th AIAA/ASME/ASCE/AHS/ASC Structures, Structural Dynamics and Materials Conference*, 2005, p. 1897.

[141] G. Kumar and A. Kumar, “Fourier transform and particle swarm optimization based modified LQR algorithm for mitigation of vibrations using magnetorheological dampers,” *Smart Mater. Struct.*, vol. 26, no. 11, p. 115013, 2017.

[142] V. Plevris and M. Papadrakakis, “A hybrid particle swarm-gradient algorithm for global structural optimization,” *Comput. Civ. Infrastruct. Eng.*, vol. 26, no. 1, pp. 48–68, 2011.

LIST OF PUBLICATIONS FROM THE THESIS WORK

List of Publications

1. Gaurav Kumar and Ashok Kumar (2017), "Fourier transform, and particle swarm optimization based modified LQR algorithm for mitigation of the vibrations using magnetorheological dampers," Smart Mater. Struct. (IOP science), 26 115013. https//doi:10.1088/1361- 665X/aa8681

2. Gaurav Kumar, Ashok Kumar and Ravi. S. Jakka (2018), " The particle swarm modified quasi bang-bang controller for seismic vibration control," Ocean Engineering, Volume 166, 15 October 2018, Pages 105-116 https://doi.org/10.1016/j.oceaneng.2018.08.002

3. Gauarv Kumar, Ashok Kumar and Ravi. S. Jakka (2018), "An adaptive LQR controller based on PSO and maximum predominant frequency approach for semi-active control scheme, "Mechanics & Industry, EDP Sciences 2018. DOI: https://doi.org/10.1051/meca/2018018

4. Gaurav Kumar, Ashok Kumar and Ravi. S. Jakka (2018), " Adaptive LQG controller based on the maximum predominant period approach for five storey structures," Soil dynamics and structure, Elsevier publications (Under review)

5. Gaurav Kumar, Ashok Kumar and Ravi. S. Jakka (2018), " Semi active control scheme: a state of art survey," Journal of sound and vibrations, Elsevier publications (Under review)